

**STUDY ON SOME NITROGEN CONTAINING DRUG
MOLECULES FOR METALLIC CORROSION
INHIBITION IN ACIDIC MEDIUM**

Thesis

Submitted for the Award of the Degree of

DOCTOR OF PHILOSOPHY

in

(CHEMISTRY)

By

Shveta Sharma

(41800668)

Supervised By

Dr Ashish Kumar



L OVELY
P ROFESSIONAL
U NIVERSITY

Transforming Education Transforming India

**LOVELY PROFESSIONAL UNIVERSITY
PUNJAB
2022**

Dedicated
To
My Daughter

(Ms. Jwala Sharma)

for her unconditional love, support and understanding.

DECLARATION

I declare that the thesis entitled “**Study on Some Nitrogen Containing Drug Molecules for Metallic Corrosion Inhibition in Acidic Medium**” has been prepared by me under the guidance of Dr. Ashish Kumar, Professor (HOD), Department of Chemistry, School of Chemical Engineering and Physical Sciences, Lovely Professional University, Phagwara, Punjab, and as per the requirement for the award of the degree of Doctor of Philosophy (Ph.D.) in Chemistry is entirely an authentic record of my own research work and ideas and references are duly acknowledged. It is further certified that the results incorporated in this thesis have not been submitted, in part or full, to any other university or institution for the award of any degree or diploma.



Shveta Sharma

Reg. No- 41800668

Department of Chemistry

School of Chemical Engineering and Physical Sciences


Lovely Professional University

Phagwara, Punjab, India

CERTIFICATE

It is hereby certified that thesis entitled, "**Study on Some Nitrogen Containing Drug Molecules for Metallic Corrosion Inhibition in Acidic Medium**", being submitted by **Ms. Shveta Sharma**, in Department of Chemistry, School of Chemical Engineering and Physical Sciences, Lovely Professional University, Punjab, to award the degree of Doctor of Philosophy in Chemistry is a record of bonafide research work carried out by her. **Ms. Shveta Sharma** has worked under my supervision and guidance and has fulfilled all the requirements for the submission of the thesis. It is further certified that the results incorporated in this thesis have not been submitted, in part or full, to any other university or institution for the award of any degree or diploma.

Supervised By


16464
Dr. Ashish Kumar

Professor

Department of Chemistry

School of Chemical Engineering and

Physical Sciences

Lovely Professional University, Punjab.

ABSTRACT

Corrosion is described as the degradation of materials over a period of time. Corrosion occurs in all materials, including metals, polymers, and wood, as a result of their reaction with the surroundings. Corrosion involves two processes, one when metal gets converted in to its ionic form because of chemical reaction and second is movement of ejected electrons towards another sites and this metal corrosion is caused by the loss of these valence electrons of metal. Corrosion is affecting our life in many ways, like threat to human safety, loss of energy, loss of time and economic loss is also there. It is a significant problem that cannot be entirely eradicated. It is more practicable to use a preventative strategy rather than attempting to eradicate, which is nearly impossible. Corrosion can be reduced by number of ways, but the use of corrosion inhibitors is becoming increasingly prevalent as a strategy that is safe, appropriate and monetarily acceptable. The current study comprises the application of drug molecules as corrosion inhibitors for mild steel in an acidic medium. The compounds studied are Baclofen, Betahistine dihydrochloride, Isoxsuprine hydrochloride, Panthenol, Naphazoline, Dicyclomine hydrochloride.

The aims and objectives of the present investigations are:

- Selection of nitrogen containing drug molecules as corrosion inhibitors.
- To determine inhibition efficiency of the selected molecules for corrosion inhibition.
- To study various adsorption isotherms to identify the mechanism of corrosion.
- To calculate thermodynamic parameters like Enthalpy, Entropy, Gibbs Free Energy and Activation Energy.
- To validate the above observed parameters by using quantum chemical calculations.

The following methods were used to investigate the inhibitors' efficacy:

- Weight Loss Measurements.
- Study of Thermodynamics and Kinetics Parameters.
- Electrochemical Impedance Spectroscopy.

- Potentiodynamic Polarization Studies.
- Scanning Electron Microscopy.
- Atomic Force Microscopy.
- Computational Studies (Quantum Chemical Analysis and Molecular Dynamics Simulations).

The following are the chapters that make up this thesis.

Chapter 1: Introduction

This chapter contains fundamental information on corrosion. It discusses the concept of corrosion, including its types and consequences, as well as measurement and control approaches, as well as the need of ongoing research into corrosion control and prevention. Finally, this chapter provides an overview of the extent of the research being conducted.

Chapter 2: Review of Literature

Throughout this chapter, a comprehensive overview of the inhibitory activity of pharmaceuticals on the corrosion of metal in acidic media has been provided. The structure and properties of inhibitors are summarized in this chapter. It describes the electrochemistry of mild steel corrosion in an acidic media and provides the theoretical underpinnings of the current investigation.

Chapter 3: Experimental Section

This section contains a description of the experimental protocols that were used in the current investigation. It describes the experimental setups, apparatus, and chemicals that were used for all of the techniques, which include weight loss studies, electrochemical impedance spectroscopy, potentiodynamic polarization, scanning electron microscopy, atomic force microscopy, and theoretical studies, which include quantum chemical and molecular dynamics simulations.

Chapter 4: Results and Discussion

In accordance with the findings of preliminary investigations and literature review, inhibitors were chosen for extensive corrosion inhibition study for mild steel in acidic

medium. Weight loss study is a very basic and precise way to investigate the corrosion inhibition efficiency of the drugs. In this technique the metal samples were exposed to particular environment (acid with and without the presence of different drug molecules) and are weighed before and after the exposure. The tests were carried out at various inhibitor doses and at a temperature of 298 K. Inhibition efficiency, surface coverage, corrosion rate were then calculated with further measurements of kinetic and thermodynamic data, which validated the adsorption of drug molecules along with the probable ways of adsorption adopted by different drugs as inhibitor.

An electrochemical workstation was used to carry out electrochemical impedance spectroscopy (EIS) and potentiodynamic polarization studies (PDP). The Nyquist, bode plot from EIS and Tafel plots from PDP were obtained along with various parameters like charge transfer resistance (R_{ct}), double layer capacitance (C_{dl}), corrosion current density (j_{corr}) corrosion potential (E_{corr}) were calculated. These calculated parameters (R_{ct} and j_{corr}) were then utilized to find out the value of inhibition efficiency, and further confirms the corrosion mitigation by drug molecules.

Theoretical study including quantum calculations and molecular dynamics simulations studies was also performed by employing the material studio version 7.0 software. Various quantum chemical parameters were calculated in order to validate the experimental results.

Scanning electron microscopy and atomic force microscopy are the two surface morphological techniques employed in the current study to know more about the inhibition process. Scanning electron microscopy gives two dimensional images of sample and atomic force microscopy provides three dimensional topographs along with roughness data. Both the techniques provide the information about the corroded surface in pure acid solution and reduction of corrosion when drugs are used as inhibitors, which confirmed the formation of protective layer on the metal.

Chapter 5: Conclusions

In this chapter the findings mentioned in the previous chapters are described and the results discussed in the previous chapters are summarized.

ACKNOWLEDGMENT

Thanks to “**Ashtbhuja Ma**” for the countless blessings you have offered me.

I wish to extend my sincere regards and gratitude to my esteemed supervisor, **Dr. Ashish Kumar** for his invaluable guidance and constant encouragement, throughout the research work. I am extremely grateful to him for all the useful discussion, constant clarifications, and suggestions. His excellence and knowledge of the subject matter steered me through this research. His passion and commitment towards research always motivated me to conduct quality work. I shall be forever obliged for his guidance and support. This work could not have been successfully completed without his effective and meaningful contribution at every step.

I am like to express my sincere gratitude and appreciation to **Dr. Sourav Kumar Saha** for their insightful comments and suggestions. In spite of his busy schedule he always managed to help me in research articles with his valuable suggestions. I am also thankful to **Ms. Richika Ganjoo**, for her unconditional support. I would like to express my gratitude to **my family**, without their tremendous understanding and encouragement, it would be impossible for me to complete my study. “**My Parents**” Your prayer for me was what sustained me this far. Finally, my daughter “**Jwala**” whose contribution in my Ph.D., cannot be expressed in words. She literally sacrificed her time for my study, I am forever in your debt little angel.

Shveta Sharma

TABLE OF CONTENTS

<i>Title</i>	<i>i</i>
<i>Dedication</i>	<i>ii</i>
<i>Declaration</i>	<i>iii</i>
<i>Certificate</i>	<i>iv</i>
<i>Abstract</i>	<i>v</i>
<i>Acknowledgement</i>	<i>viii</i>
<i>Table of Contents</i>	<i>ix</i>
<i>List of Tables</i>	<i>xv</i>
<i>List of Figures</i>	<i>xix</i>
<i>List of Abbreviation</i>	<i>xxvi</i>

Table of Contents

S.no	Content	Pages
CHAPTER 1: INTRODUCTION		
1	Introduction	2
1.1	Forms of corrosion	3
1.2	Corrosion chemistry	7
1.3	Factors influencing corrosion	8
1.4	Chemistry involved in corrosion	8
1.5	Importance of corrosion mitigation	9
1.6	Impact and cost of corrosion damage	9
1.7	Methods of corrosion inhibition	11
1.8	Disadvantages of different corrosion inhibition methods	12
1.9	Corrosion inhibitors	12
CHAPTER 2: REVIEW OF LITERATURE		
2.1	A succinct overview of inhibitors	15
2.2	Effect of acid on steel	16
2.3	Drugs as inhibitor for corrosion retardation	18
2.4	Review of literature	18
2.5	The objectives of present study	27
2.6	Techniques determining the corrosion inhibition	27
CHAPTER 3: MATERIALS AND METHODS		
3	Experimental techniques	31
3.1	Materials	31
3.2	Electrochemical cell	33
3.2.1	Working electrode	34
3.2.2	Reference Electrode	34
3.2.3	Counter electrode	35
3.3	Instrumentation	35
3.4	Experimental procedure	35

CHAPTER: 4 RESULTS AND DISCUSSIONS

	Section 4.1 Weight loss measurements	39
4.1.1	Determination of weight loss measurements for the MS corrosion at different concentrations of acid	40
4.1.2	Measurements of weight loss in 1M HCl for the estimation of corrosion parameters for MS, by employing Baclofen as inhibitor	40
4.1.3	Measurements of weight loss in 1M HCl for the estimation of corrosion parameters for MS, by employing Betahistine dihydrochloride as inhibitor	43
4.1.4	4.1.4 Measurements of weight loss in 1M HCl for the estimation of corrosion parameters for MS, by employing Isoxsuprine hydrochloride as inhibitor	46
4.1.5	Measurements of weight loss in 1M HCl for the estimation of corrosion parameters for MS, by employing Panthenol as inhibitor	49
4.1.6	Measurements of weight loss in 1M HCl for the estimation of corrosion parameters for MS, by employing Naphazoline as inhibitor	51
4.1.7	Measurements of weight loss in 1M HCl for the estimation of corrosion parameters for MS, by employing Dicyclomine hydrochloride as inhibitor	54
4.1.8	Conclusions	57
	Section 4.2 Adsorption and kinetic study of corrosion	
4.2.1	Adsorption isotherm	58
4.2.2	Calculation of thermodynamic and kinetic parameters from adsorption study	62
4.2.3	Estimation of kinetic and adsorption variables for MS using Baclofen	64
4.2.4	Estimation of kinetic and adsorption variables for MS using Betahistine dihydrochloride as inhibitor.	66
4.2.5	Estimation of kinetic and adsorption variables for MS using Isoxsuprine hydrochloride as inhibitor	67

4.2.6	Estimation of kinetic and adsorption variables for MS using Panthenol as corrosion inhibitor.	69
4.2.7	Estimation of kinetic and adsorption variables for MS using Naphazoline as corrosion inhibitor.	71
4.2.8	Estimation of kinetic and adsorption variables for MS using Dicyclomine hydrochloride as corrosion inhibitor.	72
4.2.9	Conclusions	75
Section 4.3 Electrochemical impedance spectroscopy		
4.3.1	Electrochemical impedance spectroscopic (EIS) measurements	78
4.3.2	EIS investigations of corrosion inhibition properties of Baclofen for MS in acidic medium	79
4.3.3	EIS investigations of corrosion inhibition properties of Betahistine dihydrochloride for MS in acidic medium	82
4.3.4	EIS investigations of corrosion inhibition properties of Isoxsuprine hydrochloride for MS in acidic medium	84
4.3.5	EIS investigations of corrosion inhibition properties of Panthenol for MS in acidic medium	86
4.3.6	EIS investigations of corrosion inhibition properties of Naphazoline for MS in acidic medium	88
4.3.7	EIS investigations of corrosion inhibition properties of Dicyclomine hydrochloride for MS in acidic medium	90
4.3.8	Conclusions	93
Section 4.4 Potentiodynamic Polarization		
4.4.1	Potentiodynamic polarization investigation of MS in presence of 1M HCl	95
4.4.2	Potentiodynamic polarization study of corrosion reducing tendency for MS in 1M HCl by using Baclofen as inhibitor	96
4.4.3	Potentiodynamic polarization study of corrosion reducing tendency for MS in 1M HCl by using Betahistine dihydrochloride as inhibitor	97

4.4.4	Potentiodynamic polarization study of corrosion reducing tendency for MS in 1M HCl by using Isoxsuprine hydrochloride as inhibitor	99
4.4.5	Potentiodynamic polarization study of corrosion reducing tendency for MS in 1M HCl by using Panthenol as inhibitor	101
4.4.6	Potentiodynamic polarization study of corrosion reducing tendency for MS in 1M HCl by using Naphazoline as inhibitor	102
4.4.7	Potentiodynamic polarization study of corrosion reducing tendency for MS in 1M HCl by using Dicyclomine hydrochloride as inhibitor	104
4.4.8	Conclusions	106
Section 4.5 Scanning electron microscopy		
4.5.1	Application of SEM in the present study	107
4.5.2	Scanning electron microscopy analysis for Baclofen as inhibitor	108
4.5.3	Scanning electron microscopy analysis for Betahistine dihydrochloride as inhibitor	109
4.5.4	Scanning electron microscopy analysis for Isoxsuprine hydrochloride as inhibitor	110
4.5.5	Scanning electron microscopy analysis for Panthenol as inhibitor	111
4.5.6	Scanning electron microscopy analysis for Naphazoline as inhibitor	112
4.5.7	Scanning electron microscopy analysis for Dicyclomine hydrochloride as inhibitor	113
4.5.8	Conclusions	114
Section 4.6 Atomic force microscopy		
4.6.1	Principle	115
4.6.2	The AFM's operational modes	116
4.6.3	Application of AFM in the Present Study	117
4.6.4	AFM examinations evaluating the application of Baclofen for the reduction of corrosion of MS in 1 M HCl	119
4.6.5	AFM examinations evaluating the application of Betahistine dihydrochloride for the mitigation of MS corrosion in 1 M HCl	120

4.6.6	AFM examinations evaluating the application of Isoxsuprine hydrochloride to prevent corrosion of MS in 1 M HCl	121
4.6.7	AFM examinations evaluating the application of Panthenol to prevent corrosion of MS in 1 M HCl	122
4.6.8	AFM examinations evaluating the application of Naphazoline to prevent corrosion of MS in 1 M HCl	123
4.6.9	AFM examinations evaluating the application of Dicyclomine hydrochloride to prevent corrosion of MS in 1 M HCl	124
4.6.10	Conclusions	125
Section 4.7 Computational Study		
4.7.1	Quantum chemical analysis	126
4.7.2	Fukui functions	133
4.7.3	Molecular dynamic simulation	141
4.7.4	Conclusions	146
CHAPTER 5 SUMMARY AND CONCLUSION		
5	Summary and conclusions	148
REFERENCES		153
LIST OF PUBLICATIONS		191
LIST OF CONFERENCES/ SHORT TERM COURSES ATTENDED		202

LIST OF TABLES

S.NO	CAPTION	PAGE
CHAPTER 1: INTRODUCTION		
Table 1.1	Annual expenditure of different countries in different years on corrosion.	10
CHAPTER 2: REVIEW OF LITERATURE		
Table 2.1	List of selected Drug molecules.	26
CHAPTER: 4 RESULTS AND DISCUSSIONS		
Section 4.1 Weight loss measurements		
Table 4.1.1	Calculation of MS corrosion rate at varying acid concentrations.	40
Table 4.1.2	Effect of variation of Baclofen concentration.	41
Table 4.1.3	Effect of immersion time on inhibition efficiency of Baclofen as inhibitor for MS.	42
Table 4.1.4	Effect of temperature on corrosion inhibition of MS using Baclofen.	42
Table 4.1.5	Effect of variation of Betahistine dihydrochloride concentration.	44
Table 4.1.6	Effect of immersion time on inhibition efficiency of Betahistine dihydrochloride as inhibitor for MS.	44
Table 4.1.7	Effect of temperature variation using Betahistine dihydrochloride as an inhibitor.	45
Table 4.1.8	Effect of variation of Isoxsuprine hydrochloride concentration	47
Table 4.1.9	Effect of immersion time on inhibition efficiency of Isoxsuprine hydrochloride as inhibitor for MS.	47
Table 4.1.10	Effect of temperature variation using Isoxsuprine hydrochloride as an inhibitor	48
Table 4.1.11	Effect of variation of Panthenol concentration.	49
Table 4.1.12	Effect of immersion time on inhibition efficiency of Panthenol as inhibitor for MS.	50

Table 4.1.13	Effect of temperature variation using Panthenol as an inhibitor.	50
Table 4.1.14	Effect of variation of Naphazoline concentration.	52
Table 4.1.15	Effect of immersion time on inhibition efficiency of Naphazoline as inhibitor for MS.	52
Table 4.1.16	Effect of temperature variation using Naphazoline as an inhibitor.	53
Table 4.1.17	Effect of variation of Dicyclomine hydrochloride concentration.	54
Table 4.1.18	Effect of immersion time on inhibition efficiency of Dicyclomine hydrochloride as inhibitor for MS.	55
Table 4.1.19	Effect of temperature variation using Dicyclomine hydrochloride as an inhibitor.	55
Section 4.2 Adsorption and kinetic study of corrosion		
Table 4.2.1	Thermodynamic parameters calculated for Baclofen as inhibitor in MS corrosion.	65
Table 4.2.2	Thermodynamic parameters calculated for Betahistine dihydrochloride.	67
Table 4.2.3	Thermodynamic parameters for Isoxsuprine hydrochloride investigation.	68
Table 4.2.4	Thermodynamic parameters for Panthenol used as inhibitor.	70
Table 4.2.5	Thermodynamic parameters for Naphazoline used as inhibitor.	71
Table 4.2.6	Thermodynamic and kinetic parameters for Dicyclomine hydrochloride used as inhibitor.	73
Section 4.3 Electrochemical impedance spectroscopy		
Table 4.3.1	Electrochemical parameters calculated for varied concentration of Baclofen.	80
Table 4.3.2	Impedance parameters for mild steel soaked in varying amounts of Betahistine as an inhibitor.	84

Table 4.3.3	Parameters identified for varied concentration of Isoxsuprine hydrochloride with electrochemical analysis.	85
Table 4.3.4	Parameters calculated from EIS for MS sample and Panthenol as inhibiting molecule.	88
Table 4.3.5	Parameters calculated from EIS for MS sample and Naphazoline as inhibiting molecule.	89
Table 4.3.6	Parameters calculated from EIS for MS sample and Dicyclomine as inhibiting molecule.	92
Section 4.4 Potentiodynamic Polarization		
Table 4.4.1	Potentiodynamic parameters for MS when Baclofen was employed as inhibitor.	96
Table 4.4.2	Potentiodynamic parameters for MS using Betahistine dihydrochloride as a corrosion inhibiting molecule.	98
Table 4.4.3	Computed Tafel parameters for corrosion of MS when Isoxsuprine hydrochloride inhibitor is introduced.	100
Table 4.4.4	Computed Tafel parameters for corrosion of MS when Panthenol inhibitor is introduced.	102
Table 4.4.5	Computed Tafel parameters for corrosion of MS when Naphazoline inhibitor is introduced.	103
Table 4.4.6	Computed Tafel parameters for corrosion of MS when Dicyclomine hydrochloride inhibitor is introduced.	105
Section 4.6 Atomic force microscopy		
Table 4.6.1	Roughness data calculated from AFM investigation	118
Section 4.7 Computational Study		
Table 4.7.1	Quantum chemical parameters of the investigated Drug molecules	129
Table 4.7.2	Calculated Fukui indices of the Baclofen inhibitor.	135
Table 4.7.3	Fukui indices of Betahistine as inhibiting molecule.	136
Table 4.7.4	Fukui indices for Isoxsuprine hydrochloride.	137

Table 4.7.5	Fukui indices for Panthenol.	138
Table 4.7.6	Fukui indices for Naphazoline.	139
Table 4.7.7	Fukui indices for Dicyclomine hydrochloride.	140
Table 4.7.8	Energy values calculated from MD simulation on Fe (110) surface when Baclofen is adsorbed.	143

LIST OF FIGURES

S.NO	CAPTION	PAGE
CHAPTER 1: INTRODUCTION		
Figure 1.1	Cause of corrosion	3
Figure 1.2	Uniform corrosion	4
Figure 1.3	Galvanic corrosion	4
Figure 1.4	Crevice corrosion	5
Figure 1.5	Pitting corrosion	5
Figure 1.6	Intergranular corrosion	6
Figure 1.7	Erosion corrosion	6
Figure 1.8	Stress corrosion	6
Figure 1.9	Methods of corrosion protection	12
CHAPTER 2: REVIEW OF LITERATURE		
Figure 2.1	Classification of corrosion inhibitors.	16
Figure 2.2	Pictorial presentation of various techniques employed for corrosion inhibition study.	27
CHAPTER 3: MATERIALS AND METHODS		
Figure 3.1	Working electrodes of selected sample with epoxy resin as additive	34
Figure 3.2	Representation of (a) analytical balance (b) electrochemical workstation (c) scanning electron microscope.	36
CHAPTER: 4 RESULTS AND DISCUSSIONS		
Section 4.1 Weight loss measurements		
Figure 4.1.1	Percentage deviation of inhibition efficiency with Concentration, Time, and temperature.	43
Figure 4.1.2	(a) Plot of concentration variation vs inhibition efficiency (b) Time vs inhibition efficiency and (c) temperature vs inhibition efficiency.	45

Figure 4.1.3	(a) Plot of concentration variation vs inhibition efficiency (b) Time vs inhibition efficiency and (c) temperature vs inhibition efficiency.	48
Figure 4.1.4	(a) Plot of concentration variation vs inhibition efficiency (b) Time vs inhibition efficiency and (c) temperature vs inhibition efficiency.	51
Figure 4.1.5	(a) Plot of concentration variation vs inhibition efficiency (b) Time vs inhibition efficiency and (c) temperature vs inhibition efficiency.	53
Figure 4.1.6	(a) Plot of concentration variation vs inhibition efficiency (b) Time vs inhibition efficiency and (c) temperature vs inhibition efficiency.	56
Section 4.2 Adsorption and kinetic study of corrosion		
Figure 4.2.1	Adsorption Isotherms	59
Figure 4.2.2	Graphical presentation of (a) Langmuir isotherm, (b) plot between $1/T$ vs $\log CR$ (c) plot between $\log K_{ads}$ vs $1/T$, (d) plot of ΔG_{ads} vs T .	65
Figure 4.2.3	Graphical presentation of (a) Langmuir isotherm, (b) plot between $1/T$ vs $\log CR$ (c) plot between $\log K_{ads}$ vs $1/T$, (d) plot of ΔG_{ads} vs T .	66
Figure 4.2.4	Graphical presentation of (a) Langmuir isotherm, (b) plot between $1/T$ vs $\log CR$ (c) plot between $\log K_{ads}$ vs $1/T$, (d) plot of ΔG_{ads} vs T .	69
Figure 4.2.5	Graphical presentation of (a) Langmuir isotherm, (b) plot between $1/T$ vs $\log CR$ (c) plot of ΔG_{ads} vs T (d) plot between $\log K_{ads}$ vs $1/T$.	70
Figure 4.2.6	Graphical presentation of (a) Langmuir isotherm, (b) plot between $1/T$ vs $\log CR$ (c) plot of ΔG_{ads} vs T (d) plot between $\log K_{ads}$ vs $1/T$.	72

Figure 4.2.7	Graphical presentation of (a) Langmuir isotherm, (b) plot between $1/T$ vs $\log CR$ (c) plot of ΔG_{ads} vs T (d) plot between $\log K_{ads}$ vs $1/T$.	74
Section 4.3 Electrochemical impedance spectroscopy		
Figure 4.3.1	Current and voltage waves as a function of time.	76
Figure 4.3.2	Nyquist Plot	77
Figure 4.3.3	Simplest circuit diagram.	78
Figure 4.3.4	Pictorial presentation of Bode Plots.	78
Figure 4.3.5	(a) Nyquist impedance diagram for metal in acid with different amount of Baclofen. (b) Electrical equivalent circuit.	81
Figure 4.3.6	(a) Bode Phase angle and (b) Bode modulus plots for metallic sample in acidic solution in the varied amount of Baclofen.	81
Figure 4.3.7	(a) Nyquist plots for metallic sample in acid solution with different amount of Betahistine dihydrochloride (b) Equivalent electrochemical circuit diagram.	83
Figure 4.3.8	(a) Bode Phase angle and (b) Bode modulus plots for metallic sample in acidic solution in the varied amount of Betahistine dihydrochloride	83
Figure 4.3.9	(a) Graphical presentation of Nyquist plot for MS with Isoxsuprine as corrosion inhibitor. (b) Equivalent circuit for electrochemical study	85
Figure 4.3.10	(a,b) Bode graphs for metal under study in HCl containing Isoxsuprine hydrochloride (0 to 2000 ppm) as inhibitor.	86
Figure 4.3.11	(a) Representation of Nyquist Plot with varied amount of Panthenol as inhibitor and (b) Equivalent circuit diagram.	87
Figure 4.3.12	(a, b) Bode graphs for metal under study in HCl containing Panthenol (0 to 400 ppm) as inhibitor.	87

Figure 4.3.13	(a) Representation of Nyquist Plot with varied amount of Naphazoline as inhibitor and (b) Equivalent circuit diagram.	89
Figure 4.3.14	(a, b) Bode graphs for metal under study in HCl containing Naphazoline (0 - 1500 ppm) as inhibitor	90
Figure 4.3.15	(a) Representation of Nyquist Plot with varied amount of Dicyclomine hydrochloride as inhibitor and (b) Equivalent circuit diagram.	91
Figure 4.3.16	(a, b) Bode graphs for metal under study in HCl containing Dicyclomine hydrochloride (0 - 800 ppm) as inhibitor	91

Section 4.4 Potentiodynamic Polarization

Figure 4.4.1	Tafel plot.	94
Figure 4.4.2	Tafel plots with varied concentration of Baclofen containing in acid solution.	97
Figure 4.4.3	Representation of Tafel plot with varying concentrations of Betahistine dihydrochloride as inhibitor.	98
Figure 4.4.4	Potentiodynamic polarization plots for metallic samples submerged in the 1M HCl solution with the varied concentration of Isoxsuprine hydrochloride from 0 to 2000 ppm.	100
Figure 4.4.5	Potentiodynamic polarization plots for metallic samples submerged in the 1M HCl solution with the varied concentration of panthenol	101
Figure 4.4.6	Potentiodynamic polarization plots for metallic samples submerged in the 1M HCl solution with the varied concentration of Naphazoline.	103
Figure 4.4.7	Potentiodynamic polarization plots for metallic samples submerged in the 1M HCl solution with the varied concentration of dicyclomine hydrochloride from 0 to 1500 ppm	104

Section 4.5 Scanning electron microscopy

- Figure 4.5.1** SEM images of (a) polished metallic sample (b) sample submerged in 1M HCl (c) sample submerged in 1 M HCl with an optimized concentration of Baclofen.. **108**
- Figure 4.5.2** SEM Micrograph: (a) Clear MS sample (b) Without Inhibitor (c) with Betahistine dihydrochloride as corrosion inhibitor. **109**
- Figure 4.5.3** SEM pictures of (a) steel sample without any exposure (b) sample treated with acidic solution (c) sample expose to acidic solution with 2000 ppm of Isoxsuprine hydrochloride. **110**
- Figure 4.5.4** SEM pictures of (a) steel sample without any exposure (b) sample treated with acidic solution (c) sample expose to acidic solution with 400 ppm of Panthenol. **111**
- Figure 4.5.5** SEM pictures of (a) steel sample without any exposure (b) sample treated with acidic solution (c) sample immersed in acidic solution with 1500 ppm of Naphazoline. **112**
- Figure 4.5.6** SEM pictures of (a) steel sample without any exposure (b) sample treated with acidic solution (c) sample dipped in acid with 1500 ppm of Dicyclomine hydrochloride. **113**

Section 4.6 Atomic force microscopy

- Figure 4.6.1** Surface morphology (a) plain and unexposed metal sample (b) metal surface soaked in test solution (c) metal kept in acid with 2000 ppm Baclofen. **119**
- Figure 4.6.2** Surface morphology (a) of polished sample surface (b) metal dipped in acid (c) metal in acidic with 1500 ppm Betahistine dihydrochloride. **120**
- Figure 4.6.3** Surface morphology (a) polished surface (b) metal submerged in acid (c) metal in acid containing 2000 ppm of ppm Isoxsuprine hydrochloride. **121**
-

Figure 4.6.4	Surface morphology (a) clean metal (b) surface morphology of metal soaked in acid solution (c) surface morphology of metal soaked in Panthenol contained acid solution.	122
Figure 4.6.5	Surface morphology of (a) clean metal (b) surface morphology of metal soaked in acid solution (c) surface morphology of metal soaked in Naphazoline contained acid solution	123
Figure 4.6.6	Surface morphology of (a) clean metal (b) surface morphology of metal soaked in acid solution (c) surface morphology of metal soaked in Dicyclomine hydrochloride contained acid solution.	124
Section 4.7 Computational Study		
Figure 4.7.1	Pictorial presentation of (a) optimized structure, (b) HOMO and (c) LUMO of Baclofen.	130
Figure 4.7.2	Representation of (a) optimized geometry (b) HOMO and (c) LUMO of Betahistine.	131
Figure 4.7.3	Representation of (a) optimized structure, (b) HOMO and (c) LUMO of Isoxsuprine.	131
Figure 4.7.4	Representation of (a) optimized structure, (b) HOMO and (c) LUMO of Panthenol.	132
Figure 4.7.5	Representation of (a) optimized structure, (b) HOMO and (c) LUMO of Naphazoline.	132
Figure 4.7.6	Representation of (a) optimized structure, (b) HOMO and (c) LUMO of Dicyclomine.	133
Figure 4.7.7	Equilibrium adsorption configuration of Baclofen inhibitor on the Fe (110) plane. (a,c) side view and (b) top view.	143
Figure 4.7.8	Stable low energy equilibrium configuration, (a and c) representing side view, (b) showing top view of Betahistine interacting on the surface of Fe (110)	144

Figure 4.7.9	Low energy configuration of Isoxsuprine on Fe (110) surface obtained by MD simulations. (a & c) side view, (b) top view.	144
Figure 4.7.10	Low energy configurations of Panthenol on Fe (110) surface obtained by MD simulations. (a & c) side view, (b) top view.	145
Figure 4.7.11	Low energy configurations of Naphazoline on Fe (110) surface obtained by MD simulations. (a & c) side view, (b) top view.	145
Figure 4.7.12	Adsorption configurations of Dicyclomine hydrochloride (low energy) on Fe (110) surface obtained by MD simulations. (a & c) side view, (b) top view.	146

LIST OF ABBREVIATIONS

MS	Mild Steel
WE	Working Electrode
OCP	Open Circuit Potential
SEM	Scanning Electron Microscopy
AFM	Atomic Force Microscopy
HOMO	Highest Occupied Molecular Orbital
LUMO	Lowest Unoccupied Molecular Orbital
ppm	Parts Per Million
M	Molar
In	Inhibitor
Ads	Adsorption
j_{corr}	Corrosion Current Density
b_a	Anodic Slope
b_c	Cathodic Slope
E_{corr}	Corrosion Potential
IE%	Inhibition Efficiency
θ	Surface Coverage
CR	Corrosion Rate
R_{ct}	Charge Transfer Resistance
C_{dl}	Double Layer Capacitance
C	Concentration
T	Temperature (K)

K	Kelvin
ΔG	Free Energy Change
ΔH	Enthalpy change
ΔS	Entropy change
Ea	Activation Energy
R _a	Average roughness
R _v	Root mean square roughness

CHAPTER 1
INTRODUCTION

1 Introduction

Corrosion means destruction of substance by chemical reaction with its environment. Few years back corrosion was related to only metals and alloys but now the term corrosion is wrapping up all natural as well as synthetic materials. For example, decay of plastic, wood etc. is also corrosion but generally it refers to metals (Nasab et al., 2019). It is impossible to avoid the corrosive effects of the surrounding environment on any kind of material. When a material's corrosion rate is low and it lasts for several years before collapsing due to corrosion, such material is most valuable (Tait, 2018). When the metal comes in contact with its surroundings, the main cause by which metal decays is always corrosion. In general, metals degrade when they react with moisture, acids, bases, salt, chemicals like ammonia and hydrogen sulphide (Raja et al., 2016). So, while discussing about corrosion one cannot ignore environmental conditions. Metals just as gold and platinum are not affected but metals like iron, copper etc. deteriorates. Metals on exposure to surroundings changes to their oxides, carbonates and sulphides etc. Different definitions of corrosion are given some of them are following:

- The surface wastage and damage caused by metals being exposed to a reactive environment is corrosion.
- Corrosion is a type of degradation that occurs as a result of a material's exposure and reaction to its environment.
- Corrosion is an electrochemical reaction between the metal and the surrounding environment. (Ahmad, 2006; Kadhim et al., 2021)

Metals are generally get deteriorated due to corrosion and to understand the basic cause of corrosion, we need to understand how metals exist in our surroundings. Commonly two forms are there in which metals are present, one is native and another is combined form. Few metals in free state are most stable and least prone to corrosion but maximum of metals found in combined state are very much susceptible to corrosion, they react with the surrounding environment and form compounds of oxides, sulphides etc. and every element has the tendency to attain the state of minimum energy and maximum stability and these compounds of metals (called as ores) are more stable as compare to

free metals. Therefore, metals form various compounds as shown in Figure 1.1 to attain the stability and this process is called as corrosion.

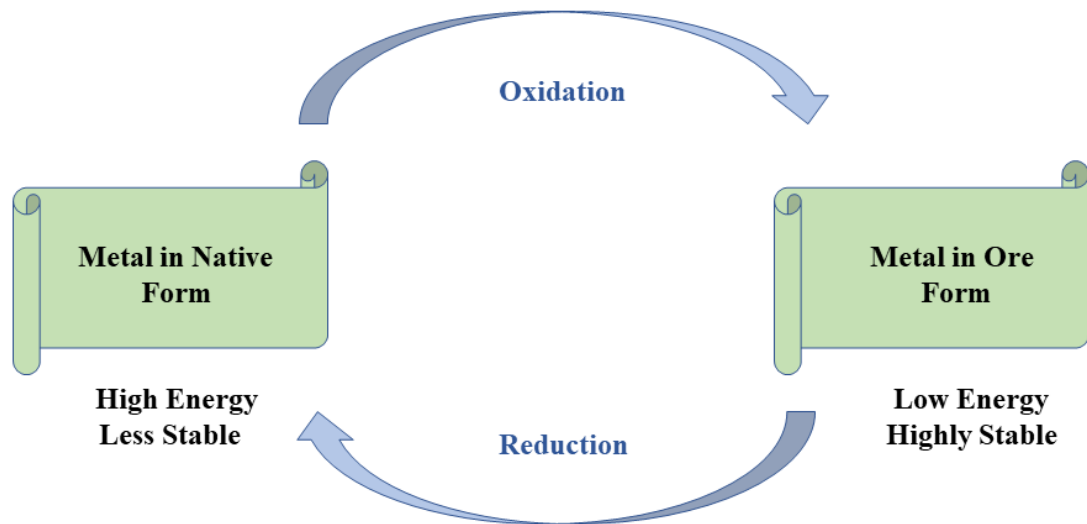


Figure 1.1 Cause of corrosion

Corrosion is broadly categorised in to dry and wet corrosion. The term "dry corrosion" refers to the type of corrosion that happens in the absence of water and only gases or air is present. This type of corrosion takes place at high temperature. Oxidation of silver is example of dry corrosion. Wet corrosion on the other hand is the deterioration of metal in the presence of water. In this type oxidation of metal and reduction of other species in solution takes place at different places. Corrosion of steel in water is the most seen example of wet corrosion (Zarras & Stenger Smith, 2015). Out of these types one which is most common is wet corrosion.

1.1 Forms of corrosion

On the basis of physical appearance of metal because of corrosion in wet environment it is further divided in to eight types. Knowing about these forms, cause and prevention can be easily understood. Following are the main types of corrosion: (Landolt, 2007)

1.1a Uniform corrosion

In this corrosion material is lost uniformly over the whole Surface (as shown in Figure1.2). This type of corrosion is visible with the naked eyes. The reaction starts over the whole surface with same rate. Tarnishing of silver is its example.



Figure 1.2 Uniform corrosion

1.1b Galvanic corrosion

In an electrolyte, two metals combine to form an electrochemical cell (Figure 1.3), which causes this phenomenon. Therefore, bimetallic corrosion is another term used to describe this form of corrosion. When two metals or alloys are joined together in the presence of electrolyte, due to the difference in electrode potential, ions start moving from less noble metal. Galvanized iron is its example.

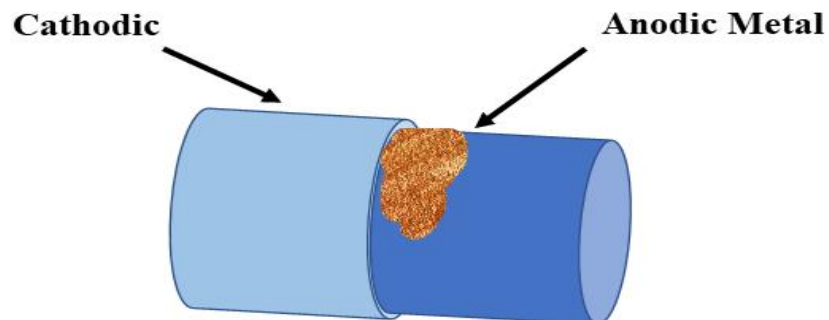


Figure 1.3 Galvanic corrosion

1.1c Crevice corrosion

This type of corrosion occurs in very small areas where access of attacking reagent is very less. It occurs in the gap of micrometres. The crevice corrosion is caused by active galvanic cells that build on metal surface. It occurs under the protective film or covered area on any metal but in crevices. Main cause of this type of corrosion is variation in concentration. For example, covered area of any metal will have lesser supply of

oxygen as compared to uncovered area, therefore concentration cell will set up and resulted in the deterioration of unexposed area (illustrated in Figure 1.4).

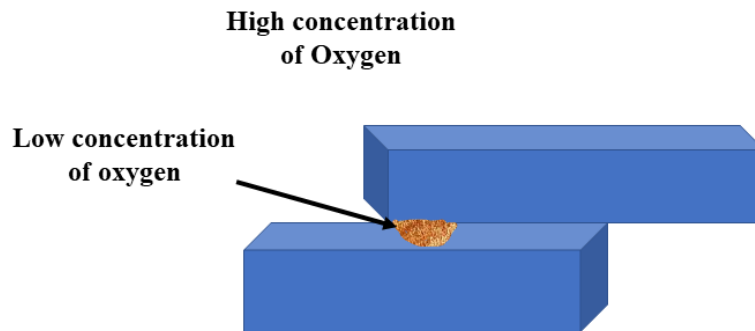


Figure 1.4 Crevice corrosion

1.1d Pitting corrosion

It is referred to as localised corrosion because it occurs only at a single location on the metal, with the rest of the metal remaining undamaged (Figure 1.5). It is noticed on metals when certain anions are present. Cavities in the tens of micrometres range are created using this method. It is an autocatalytic process. Corrosion under the applied protective layer on metal but on the plane, surface is an example of pitting corrosion.

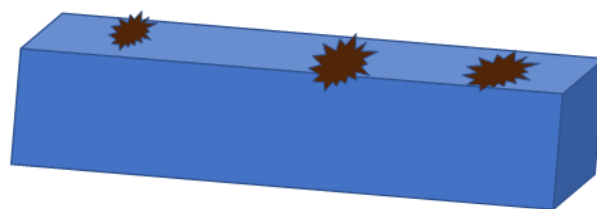


Figure 1.5 Pitting corrosion

1.1e Intergranular corrosion

Microscopically the metals are having granular boundaries and when deterioration occurs at these grain boundaries and bulk remains unaffected, it is called granular corrosion (given in Figure 1.6). It affects mechanical strength of metal. It occurs when there is local difference in composition because of high temperature. Weld decay of

stain less steel is its example or in steel sometimes chromium and carbon react and form chromium carbide at the grain boundaries.



Figure 1.6 Intergranular corrosion

1.1f Erosion corrosion

There is increase in rate of deterioration on a metal surface because flowing liquid and the metal surface are associated and it is the combination of an electrochemical reaction and mechanical wear that led to the destruction of material (as given in Figure 1.7). Water pipes are the best example of erosion corrosion.



Figure 1.7 Erosion corrosion

1.1g Stress corrosion

In stress corrosion (Figure 1.8) cracks appeared as a result of the two factors. One is caused by corrosion, whereas the other is caused by mechanical force or stress. Its example is dezincification of brass.



Figure 1.8 Stress corrosion

1.2 Corrosion chemistry

It is generally agreed that corrosion of metals in water comprises two processes: a chemical reaction that transforms metal atoms into metal ions and the shift of metallic valence electrons to some other molecule in its surrounding electrochemically so metal corrosion in wet environment is called as electrochemical corrosion (Kutz, 2018).

In case of corrosion metal lose its electron or gets oxidised. After oxidation metal ion leave metal surface. This oxidation of metal is called anodic half-cell and when reduction of electrolyte or electrochemically active substance takes place, it is called cathodic half reaction. Anodic and cathodic processes are required for the onset and continuation of metallic corrosion. Mechanism of electrochemical corrosion can be better understood with the help of iron as corroding metal.

Anodic electrochemical equation (oxidation)



Cathodic half reaction (reduction)

Cathodic reactions depend upon pH of solution.

In acidic and deaerated solution



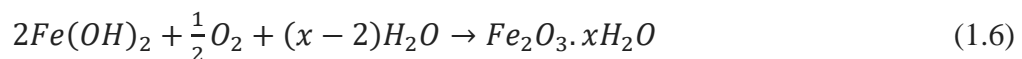
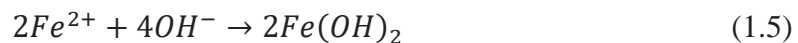
In neutral solution



In neutral solution



Metal ion formed at anode combines with hydroxyl ion and form iron hydroxide, which further oxidised to hydrated ferric oxide.



Clearly, removing one of the half cells will prevent corrosion from developing (Glass et al.,1991).

1.3 Factors influencing corrosion

Corrosion is influenced by the nature of the metal or alloy as well as the surrounding environment, and this is accomplished by chemical or electrochemical changes. Some of the environmental variables which can influence corrosion rate are: (Stansbury & Buchanan, 2000)

- **Nature of the metal:** The type of metal affects the corrosion rate. Metals having low reduction potential have high reactivity and are more susceptible to corrosion.
- **pH:** Lower the pH of the corrosion medium, higher is the corrosion rate. If the $\text{pH} < 3$, corrosion can occur in absence of air due to evolution of hydrogen at cathode region.
- **Temperature:** Generally, with increase in temperature, the rate of chemical reaction increases which result in an increased corrosion.
- **Impurities:** Impurities in atmosphere set voltaic cell and thus corrosion rate increase due to conducting species in atmosphere.
- **Humidity:** Generally, at low humidity, the speed of corrosion is low. With the increase in humidity rate of corrosion also increases.

1.4 Chemistry involved in corrosion reactions

1.4a Thermodynamics of corrosion

We can find out whether corrosion is going to take place or not with the help of free energy considerations. Free energy with negative value means a sudden reaction, whereas a positive value of free energy means that the reaction is not going to proceed. That means $\Delta G < 0$, reaction is spontaneous (Elayaperumal & Raja, 2015).

The free energy change for corrosion reaction can be calculated if we know the value of cell potential.

$$\Delta G = -nEF \quad (1.7)$$

Where n - number of moles of electrons in an electrochemical reaction,

F - Faraday's constant

E - Cell potential (V).

1.4b Kinetics of corrosion

Kinetics of corrosion generally relates with the rate with which corrosion takes place and can be measured by different methods. Different parameters are calculated from different methods, which ultimately used to find out the corrosion rate. For example, most common used methods are weight loss, electrochemical method etc. Corrosion rate can be evaluated with the help of weight change during the corrosion process in case of weight loss study and corrosion current densities are used to find out the rate of corrosion in electrochemical analysis (Olasunkanmi, 2021).

1.5 Importance of corrosion mitigation

Corrosion is needed to control in consideration of safety and economy. It has effect on small screw to large machineries in day-to-day life. Estimates place the cost of corrosion at approximately 4% of the nation's gross national product (Latanision,1987).

- To avoid personal injury because of any type of machinery failure.
- Replacing of corroded part of machine cause financial loss.
- Even only repair can be a costly affair.
- To limit the risk of life-threatening incidents, such as the release of poisonous or explosive gases from pressure vessels or piping systems.
- Corrosion also brings about mechanical loss like breaking of large machinery etc.
- Wastage of time, loss of production and profit.

Corrosion mitigation can be achieved by preventive measures rather than opting maintenance. Deep and serious study should be done to check corrosion prevention measures. Timely and routine inspection should be there.

1.6 Impact and cost of corrosion damage

Corrosion is inevitable and we can only plan to deal with it. Corrosion control techniques are very necessary on one hand but on the other hand they consume a lot of

money (in the form of payments, expenditure on machinery), Labour, energy loss etc. Every nation has to spend a lot on maintenance, different measures, and inventions. A study was published in 1978 in U.S. by National Bureau of standards (National Institute of Standard and Technology) and Battelle Columbus laboratories in which total cost of \$ 82 billion, which was 4.95% of GNP. After twenty years report was updated corrosion cost on the basis of documented data a total loss due to corrosion was \$276 billion in the U.S. which was about 3.1 % of GNP (Roberge & Eng, 2005). The total cost including undocumented data was about \$552 billion which was 6 % of the GNP. In United Kingdom in 1969 a 25-member committee was framed to study corrosion cost and it came out to be \$ 3.2 billion, which was 3.5% of GNP. In Germany it was documented in 1968-1969 and cost was six billion American dollars which was 3% of GNP. Sweden mentioned it in 1964, Finland in 1965, Soviet Union in 1969. Similarly, Australia, Japan and India in 1973, 1977, 1960-1961 documented the corrosion cost. Loss of different countries is mentioned in table 1 and it is clear that different countries are spending a huge amount on corrosion (Kruger, 2011). In 2013 various organizations dealing with corrosion like NACE International, CORCON and GAIL India and Outokumpu Institute gave a study “Impact India-Cost of Corrosion Study of India”. In this study global cost of corrosion 2.5 trillion was give which was 3.4% of world GDP and in India it was 4.25% of total GDP.

Table 1.1 Annual expenditure of different countries in different years on corrosion.

Countries	Total Corrosion Cost in US Dollars (Annually)	GNP (%)
India	\$320 million	1.54%
USA	276 billion	2.1%
UK	3.2 billion	3.5%
Germany	6.0 billion	3 %
USSR	6.7 billion	4.2%
Australia	550 million	1.5%
Japan	9.2 billion	1.8%
Finland	47-62 million	-
Sweden	58-77 million	-

1.7 Methods of corrosion inhibition

Environmental modification, design enhancement, potential change, coating and plating are five basic approaches for protecting metals and alloys from corrosion. Figure 1.9 illustrates a variety of corrosion-prevention methods (Rajeswari et al., 2017). First and foremost is the design selection, because metals may have different standard electrode potential, therefore the contact of metal should be avoided in order to prevent the corrosion of more active metal. Weld should be replaced with bolts, proper flow of air should be there, accumulation of dust should be avoided and extra stress should not be there on machinery. Potential change comprises of cathodic and anodic protection. Cathodic protection further classified as sacrificial anode and impressed current. A wide variety of surface coatings can be used to protect a metal surface from corrosion. Coating and plating can be done by various ways like inorganic, organic coatings. Hot dipping, electroplating etc. can also be used. The eradication of corrosion causing reagents such as the removal of dissolved oxygen accomplished by the addition of hydrazine, neutralization is the process of removing acidity. And use of desiccants, such as silica gel, are used to reduce humidity etc. are few examples that comes under environment modification. Addition of corrosion reducing agents may also be preferred in order to retard the corrosion. In the present study, corrosion inhibitors have been selected to investigate their corrosion retardation tendency (Walsh,1993).

|

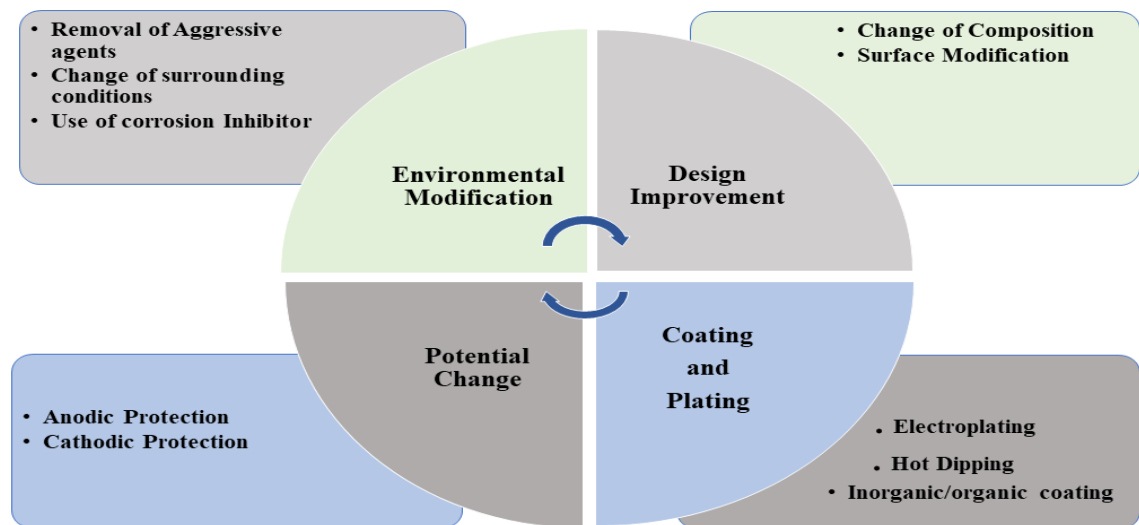


Figure 1.9 Methods of corrosion protection

1.8 Disadvantages of different corrosion inhibition methods

Common methods employed for corrosion inhibition are very advantageous but having few drawbacks. Few examples are like while doing the design improvement or alloying, material can have difference in their potential resulting in deterioration of machinery. Use of paints to protect the metal can cause pollution and chemicals added are harmful even to humans. Cathodic protection is costly and needs regular maintenance. Impressed current cathodic protection is not cost effective. In anodic protection sometimes anodic current becomes uncontrollable. Acid pickling may cause the surface roughness and cracking due to acid used. Corrosion inhibitors are the most opted and successful to inhibit corrosion because of their high inhibition efficiencies.

1.9 Corrosion inhibitors

Corrosion inhibitors are chemicals that, when employed in modest concentrations and in a corrosive condition, can avert or mitigate corrosion. There are many ways through which an inhibitor protects the metal. The inhibitor is adsorbed on to the surface of the metal, resulting in the formation of a compound by forming the chemical bonds and a protective thin coating that has an inhibitory effect is formed. The inhibitor may also

cause the growth of a film on the base metal which resulted in the oxide protection or the inhibitor reacts with potential corrosive reagents present in aqueous media, resulting in the formation of complex. If molecule which is behaving as inhibitor gets adsorbed, its adsorption depends upon the nature of the metal, the adsorption mode, the chemical structure of the inhibitor molecules, and the kind of electrolyte solution. Steel corrosion in acidic media can be prevented by using an inhibitor, which is one of the growing techniques of doing so currently available. (Dariva & Galio, 2014; Negm, 2012; Popova, 2007; Qiu et al., 2008; Lukovits et al., 2001). When it comes to inhibitors, they can be either organic or inorganic, and they are frequently dissolved in aqueous conditions (Palanisamy, 2019). Organic substances with double bond and heteroatoms as well as inorganic compounds such as chromate, dichromate etc. are the most potent and efficacious inhibitors (Gece, 2008; Gece, 2011; Lece et al., 2008; Obot, 2009a; Samiento-Bustos, 2008). However, due to the numerous harmful consequences that these conventional compounds have had on the environment, the use of these compounds has recently been called into question. As a result, the discovery of novel corrosion inhibitors of natural origin and of the non-toxic type has been deemed to be more vital and desirable and these characteristics of pharmacological molecules make them desirable as corrosion-reducing agents in the future (Broussard et al., 1997; Gece, 2011; Newman & Cragg, 2007; Raja & Sethuraman, 2008; Struck et al., 2008). When selecting an inhibitor, however, there are a number of things to take into consideration (Faltermeier, 1999).

- The inhibitor's price should not be too exorbitant.
- It is important to keep toxicity levels in mind while selecting a product as the inhibitor's toxicity can have a negative impact on humans and animals.
- Selecting an inhibitor is influenced by how easily it may be procured.
- The inhibitor must be safe for the environment.
- The solubility of the inhibitor is a necessary aspect in its effectiveness. The solvent in which the inhibitor is dissolved should be affordable, non-toxic, and not detrimental to the environment.

CHAPTER 2
REVIEW OF LITERATURE

2 Literature survey

Throughout this chapter, a brief literature overview is presented, in which the theoretical approach about corrosion inhibitors, behaviour of mild steel (MS) in different environments, selected techniques for the present study are explored. The previous corrosion-related researches have been studied and the results are documented with special reference to the corrosion of MS and the inhibitors used to mitigate corrosion in acidic medium.

2.1. A succinct overview of inhibitors

2.1.1 Corrosion inhibitors

Considering the detrimental effects of corrosion on quality of human life it becomes of crucial necessity to minimize the corrosion process. Corrosion can't be totally eliminated, but it can be slowed down and halted from continuing. By knowing about corrosion and taking appropriate steps to reduce it, are the only two ways to somehow reduce the loss caused by corrosion. Use of the corrosion inhibitors is an efficient method of keeping corrosion under control. Over the year, a large number of corrosion inhibitors have been explored and developed. A corrosion inhibitor is a chemical that is introduced in to the corrosive medium in order to slow down the rate of corrosion. On the basis of mechanism inhibitors are broadly divided in to cathodic, anodic and mixed type of inhibitors as mentioned in Figure 2.1.

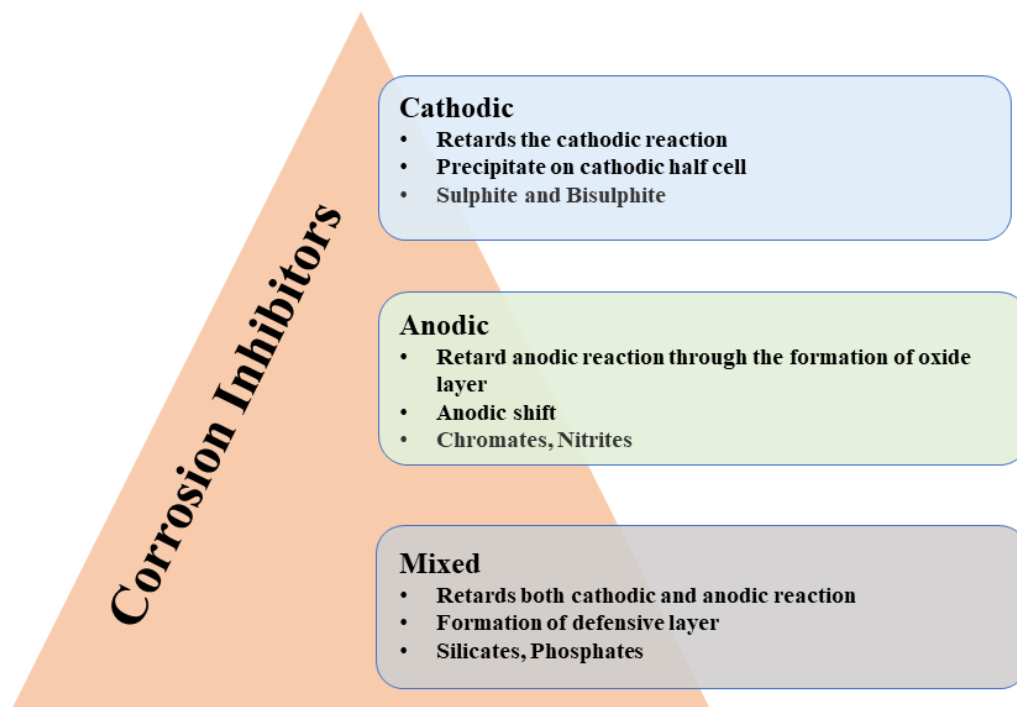


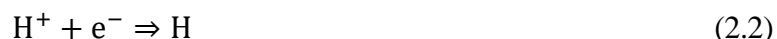
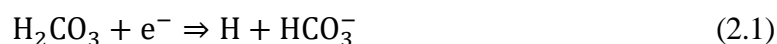
Figure 2.1 Classification of corrosion inhibitors.

Further the inhibitors can also be classified on the basis of environment and their mode of saving the metals. On the basis of way of protection, they are classified as chemical passivators, Vapour phase inhibitors, precipitators, synergistic, adsorption film forming and inhibitors safe to environment and acidic, alkaline and neutral inhibiting molecules classification base on environment is also there (Obot et al., 2009b).

2.2 Effect of acids on steel

Variety of steel depends upon percentage of carbon present in the composition, and various mechanical properties of steel like strength, ductility etc. depends upon the carbon percentage. Depending upon the mechanical properties steel is used in a variety of residential and commercial constructions, such as bridges, automobiles trains, ships and storage tanks etc. Along with this usage of steel is also very important in oil and gas industry (Dwivedi et al., 2017). There are numerous industrial procedures where acid is employed, including descaling, oil-well acidizing, and acid pickling (Chauhan & Gunasekaran, 2007; Prabhu et al., 2008; Shiva kumar & Mohana, 2012; Quraishi et al., 2010). In the literature various examples were there explaining the effect of acids and

other reagents on the steel samples. Presently the effect of carbonic acid and acetic acid on MS extracted from the literature has been briefly discussed. Water molecules and carbon dioxide reacted and form carbonic acid. At cathodic half- cell of corrosion cell on metallic surface two reactions occurred (George & Nestic, 2007).



At anode



Similarly for the corrosion that takes place in the acetic acid as corrosive medium, at the anodic half-cell metal loose its electrons and changes into its ionic form and at cathode acetic acid reduced and both the reactions are mentioned below: (Tran et al.,2014)

Cathodic reaction



Anodic reaction



Use of corrosion inhibitors is an effective way among other several corrosion protections measures. Any substance when added in small quantity and it inhibited the corrosion, is termed as corrosion inhibitor. A number of chemicals like inorganic complexes, organic molecules, natural products and rare earth elements were proved as excellent corrosion inhibitors (Raja et al., 2016). Notably, since the nineteenth century, corrosion inhibitors have been employed. Even in 1948 article about the inhibitors was published in which different inhibitors, types of corrosion and different theories were explained (Hackerman, 1948). Intensive work has already been done on surfactants, polymers, inorganic compounds and organic compound as inhibitors (Arthur et al., 2013; Singh et al., 2012; Sayin & Karakaş, 2013; Zhu et al., 2017). Various agencies from different parts of world restricted the application of toxic chemicals as corrosion

mitigating agents and therefore environmentally friendly green compounds are increasingly being favoured as inhibitors these days (El-Enin & Amin,2015; Zaferani et al.,2013). Corrosion mitigation involves the adsorption of the molecule (with inhibiting capability) on the metallic surface (Nmai, 2004; Popova et al., 2007; Tebbji et al., 2005). As a result, understanding of the adsorption phenomena is critical to comprehending the process of corrosion inhibition (Chetouani et al.,2006). It was also proved in the previous studies that the presence of heteroatoms, unsaturated bonds and length of an alkyl chain in inhibitors have an inhibitory impact on metal dissolution and due to that protecting efficiency was also boosted (Ai.J.et al., 2006). Literature also confirmed the higher efficiency of inhibitors with heteroatoms and heterocyclic rings in retarding the corrosion (Popova et al., 2003).

2.3 Drugs as inhibitor for corrosion retardation

In light of other hazardous inhibitors' detrimental effects on environmental health, scientists around the world began looking at other compounds as potential corrosion inhibitors. The hetero atoms, ring structure, and double bonds included in organic compounds along with their low cost, which make them particularly useful in corrosion mitigation, but environmental hazards make them unsuitable for this use. Alternatively, the usage of ecologically friendly and benign inhibitors is being preferred in the recent past. Commercial corrosion inhibitors and drug molecules are shown to share significant chemical similarities. Because of their structural similarity, eco-friendly nature medicines can be employed as a non-toxic substitute for corrosion inhibitors. The cost and accessibility of drugs make them the primary choice of researchers. Also due to the cheap raw ingredients, the presence of heteroatoms, the aromatic ring and long chain, high water solubility and the easy manufacturability and purification of pharmaceuticals, the use of drugs as corrosion inhibitors can be made more viable (Gece, 2011; Shamnamol et al., 2020).

2.4 Review of literature

The use of medicines as inhibitors of metallic corrosion has received a great deal of research interest in the last few decades and therefore a brief about the usage of drug molecules as corrosion inhibitor in acidic solution has been discussed below.

El- Haddad and Fouda (2021) investigated Curam drug for its inhibitive properties in acidic medium by employing various methods like weight loss, electrochemical and surface analysis and study also demonstrated that the outcomes of all the methods were in agreement.

Hameed et al. (2021) studied Expired Megavit for steel in acidic solution and confirmed effectiveness of inhibitor increases with the rise in drug concentrations, reaching 91.7% at 300 ppm.

Geethamani et al. (2019) investigated efficacy of expired Ambroxol drug to retard the metallic corrosion in hydrochloric acid. Techniques employed were weight loss, electrochemical measurements and various surface morphological investigation techniques. Result revealed that adsorption obeyed Langmuir's and Temkin adsorption isotherm. Polarization studies confirmed the suppression of both anodic and cathodic reactions. The efficacy raised with the rise in concentration and exposure time.

Raghavendra (2019a) studied Amitriptyline for its corrosion reducing properties for MS in acidic solution by employing potentiodynamic polarization, atomic absorption spectroscopy techniques and scanning electron microscopy technique. Results depicted rise in the corrosion inhibition efficiency with the rise in concentration of inhibitors. Inhibitor suppressed both cathodic and anodic reactions and adsorption followed Langmuir adsorption isotherm.

El- Haddad et al. (2019) investigated Cephapirin for its corrosion reducing tendency for steel samples in acidic solution. Various electrochemical methods and surface morphological techniques were employed for investigation. Result revealed that inhibition efficiency increased with the rise in concentration and showed a dip with the increased temperature. Cephapirin suppressed both cathodic as well as anodic reactions. Adsorption was in accordance to Temkin adsorption isotherm.

Mohammadinejad et al. (2020) studied role of Metoprolol in retarding the steel corrosion by employing various techniques and maximum inhibition was at 300 ppm and inhibitor showed mixed type of inhibition.

Raghavendra (2019b) studied expired Lorazepam as inhibitor for MS in 0.5 M hydrochloric acid and 3M hydrochloric acid. Methods employed were weight loss and electrochemical. Result depicted drugs behaved as excellent corrosion inhibitor. Inhibition efficiency showed a rise with increased concentration and decreased

temperature. The adsorption was in accordance to Langmuir isotherm. Potentiodynamic polarization experiments revealed that expired Lorazepam inhibited corrosion by reducing both the electrode reactions.

Elabbasy and Gadow (2021) investigated Tenoxicam and confirmed its corrosion mitigating capacity 81%, which further enhanced to 91.3% after the addition of KI. Temkin isotherm was obeyed and inhibition efficacy increased with the increased amount of inhibitor.

Abeng et al. (2021) studied steel corrosion mitigation by employing Levofloxacin, Moxifloxacin, Metolazone, and Nifedipine with the help of techniques like SEM, AFM and electrochemical methods along with theoretical study and the results demonstrated exceptional efficiency, and outcomes were agreed upon for all of the procedures.

Singh et al. (2019) studied modified Dapsone drug molecule for steel corrosion in acidic solution by employing various experimental and theoretical studies and confirmed the excellent inhibition efficiency, and even after modification done by the addition of potassium iodide further enhanced the inhibition efficacy.

Maduelosi and Iroha (2021) investigated Spironolactone for steel sample in HCl and mixed type of inhibition was proved with electrochemical study and the efficiency of about 98% was confirmed with the help of weight loss technique. SEM and theoretical study also proved the presence of drug on the metallic surface.

Hameed et al. (2020) explored the corrosion mitigation capacity of expired Indomethacin by utilizing electrochemical, weight loss and SEM technologies and proved the rise in efficiency with the increased concentration of drug and maximum efficiency was 83% at 500 ppm.

Farahati et al. (2020) proved the D-penicillamine (PA) drug and Cysteine as excellent inhibitors for retarding the MS corrosion, in acidic medium with the help of weight loss, EIS, PDP and SEM techniques. Results revealed the retardation of both electrode reactions and further theoretical study verified the experimental work.

Qiang et al. (2021) investigated the behaviour of Losartan potassium for corrosion mitigation of MS in acidic medium, by employing the experiments like electrochemical and molecular dynamics along with density functional theory. Results revealed the hike in inhibition efficiency with increased temperature. Surface study confirmed the protection of metal, and presence of both physical and chemical adsorption was also confirmed.

Fouda et al. (2021) performed research on Niclosamide and Dichlorphenamide drugs for their capacity to inhibit the steel corrosion in acidic medium and proved the efficiency of 99% and 98.8% respectively at 50 μM concentration and mixed inhibition was also confirmed.

Bashir et al. (2019) investigated the corrosion mitigation capacity of Venlafaxine by employing electrochemical, computational, surface morphological techniques. Drug molecule proved to be excellent inhibitor with 86% of maximum corrosion mitigating capacity at 4000 ppm and successfully reduced the corrosion rate of both anodic and cathodic reactions.

Bashir et al. (2020) by utilising electrochemical, computational, and surface morphological approaches, explored the corrosion abatement capacity of Acarbose. At 4000 ppm, a maximum inhibitory effectiveness of 96 % was observed. The application of computational computations allowed for the acquisition of detailed theoretical understanding.

Bashir et al. (2018) evaluated the corrosion mitigation capacity of Analgin using electrochemical, and surface morphological techniques. In order to gain detailed theoretical insights, computational studies were used. Analgin demonstrated 96.1 % inhibitory efficiency at 4000 ppm and adsorption was in accordance to Langmuir isotherm.

Singh et al. (2013) analysed the Phenobarbital for its effective ness to reduce the steel corrosion in acidic medium by employing the weight loss and quantum chemical methods and proved the 95% efficiency at 2000 ppm.

Kumar and Bashir (2016) explored the Ethambutol on steel for its corrosion inhibiting capacity by using weight loss, quantum chemical analysis and proved the 91.3% efficiency, also the inhibition capacity increased with the increased amount and showed a dip with the rise in temperature.

Bashir et al. (2019) used Phenylephrine drug molecule to search for the corrosion reducing tendency on steel sample in the acid and the drug molecule proved to be an excellent inhibitor with 88% efficiency.

Anaee et al. (2019) reported the extraordinary corrosion reducing tendency of Etoricoxib and proved the 80.62 % of inhibition efficacy at 225 ppm and process was predominantly anodic in nature. A good agreement was also seen in experimental and theoretical data.

Anadebe et al. (2020) documented the exceptional corrosion reduction capability of Dexamethasone drug by employing weight loss, electrochemical and MD simulation methods and revealed the 80% of efficiency and retardation of both anodic and cathodic reactions.

Fajobi et al. (2019) documented the significant corrosion control ability of Ibuprofen drug when experiment was carried out with weight loss and electrochemical methods. Efficiency increased with the increased amount of drug and was maximum 60 % was achieved.

Gholamhosseinzadeh et al. (2019) demonstrated the corrosion inhibition of Rosuvastatin drug for MS in acidic medium by using various methods and 92% of efficiency was achieved at 600 ppm. Adsorption was in accordance to Langmuir.

G. Vengatesh and M. Sundaravadivelu (2019) studied Bisacodyl drug molecule in acid for steel corrosion inhibition properties by employing various techniques. SEM, EDX and AFM verified the formation of layer made up of drug molecule on metallic surface and PDP confirmed the retardation of both anodic as well as cathodic reactions. Adsorption followed both Langmuir and Temkin isotherms.

Singh et al. (2017) worked on expired Atorvastatin for its anti- corrosive properties with the help of weight loss, electrochemical and surface morphological techniques and confirmed the increased charge transfer resistance with increased concentration of inhibitor, along with protection of metallic surface through the adsorption of drug by forming layer on the surface. Even the drug shown a excellent efficiency at 150 ppm.

Gupta et al. (2017) proved corrosion mitigating capacity of expired Atenolol and Nifedipine. Results revealed 91.30 % and 93.91% at 200 ppm of Atenolol and Nifedipine respectively. Mixed type of behaviour along with increased polarization resistance with the increased drug concentration was also confirmed. Further surface study technique like SEM and theoretical study also validated the experimental results.

Xu et al. (2017) investigated anti- corrosion property of Biotin drug by utilizing weight loss, PDP, EIS and surface study techniques like SEM, contact angle, AFM etc. along with quantum chemical study. There was excellent agreement between the experimental and theoretical findings. Inhibiting molecule successfully reduce the corrosion rate with the efficiency of 95.3% at 500 ppm with weight loss investigations.

Naseri et al. (2018) reported the anti- corrosion property of Clopidogrel drug in acidic solution for metallic corrosion. Results depicted the replacement of water molecule by inhibitor, presence of both physical and chemical adsorption.

Abd and Ali (2018) investigated Ery- thromycin and proved the physical adsorption of drug molecule on the steel sample under study and inhibitor molecule showed mixed behaviour with anodic predominance. Techniques employed were EIS, PDP along with various surface morphological investigations.

Ayoola et al. (2018) reported the drug Chloramphenicol in corrosion inhibition study, and proved effective inhibition of corrosion by the use of gravimetry, open circuit potential study and linear polarization study.

Fouda et al. (2017) reported the corrosion reducing property of Modazur in their study and proved the successful mitigation of corrosion by employing the various experimental techniques like weight loss, electrochemical and surface morphological

methods. Maximum efficiency came out to be 92.3% at 300 ppm and inhibition efficacy increased with the rise in the concentration and dip was there with the increased temperature.

Dohare et al. (2017) studied in their investigation that expired Tramadol has corrosion-reducing properties, and they demonstrated these properties through the use of numerous experimental methodologies, such as weight loss, electrochemical, theoretical and surface morphological methods. Results revealed the rise in inhibition efficacy with the increased drug concentration.

Srivastava et al. (2017) studied the Irbesartan for metallic corrosion inhibition in acidic solution by employing various electrochemical techniques. Results depicted that adsorption obeyed Langmuir isotherm with suppression of both cathodic and anodic reactions. Formation of thin layer of inhibitor on the surface of metal under investigation was also validated by the SEM investigation.

Chitra and Anand (2017) studied Tetracycline and Neomycin tri sulphate by using weight loss, SEM and FTIR. The outcomes demonstrated; use of these drugs provided corrosion protection for the sample under investigation.

Vengatesh et al. (2017) reported the corrosion inhibition tendency of Ondansetron hydrochloride by using weight loss, electrochemical study, SEM, EDX, AFM, FT-IR spectroscopy. Results confirmed the protection of metallic sample by the adsorption of ondansetron on the top of sample.

Fouda et al. (2018) investigated Ciprofloxacin drug molecule for its corrosion inhibition property and maximum efficiency came out to be 91% at 300 ppm of drug concentration. Techniques employed were various chemical, electrochemical and surface morphological techniques. Suppression of both anodic and cathodic reactions were confirmed. Protective layer formation because of adsorption was also confirmed.

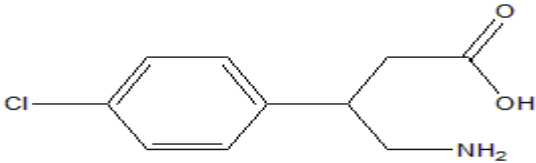
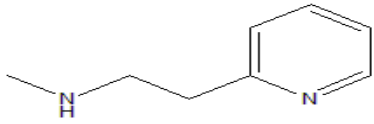
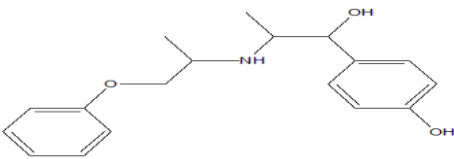
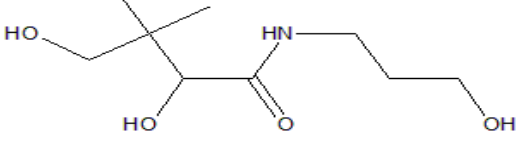
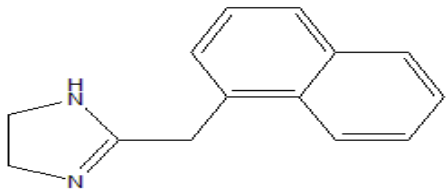
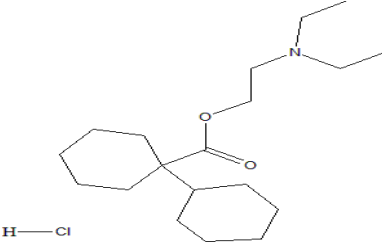
Singh et al. (2019) performed the systematic study to find out the anti-corrosive properties of Cefdinir drug for steel corrosion, by using the weight loss, surface study methods, electrochemical analysis and theoretical analysis. Retardation of both

cathodic and anodic reactions from PDP study, donor -acceptor interactions from theoretical analysis and thin layer formation from surface study were verified.

Addoun et al. (2019) reported the piroxicam as corrosion inhibitor for steel corrosion retardation with the maximum efficiency of 86.90 % at 600 ppm by using weight loss, SEM and DFT study. Results further revealed adsorption of drug obeyed Langmuir adsorption isotherm and physical adsorption was more prevailed.

In the past, a lot of work has already been done on organic, inorganic compounds, and surfactants etc. Imidazolines, amides, amines, dimeric and trimeric acids, quaternary amines, and surfactants are some examples of the types of corrosion inhibitors that are frequently utilised in industrial settings. But all these compounds have a number of significant drawbacks, including high prices, difficult synthesis, and high levels of toxicity. Researchers have looked into many environmentally friendlier alternatives that might be employed as corrosion inhibitors e.g. drugs, plant extracts, ionic liquids etc. Therefore, it was decided to work on active pharmaceutical ingredients (API's) of new drugs and to check the extent to which they will be successful to inhibit the corrosion. As the drugs are environmentally friendly inhibitors, for MS corrosion inhibition with drug molecules in acidic medium is explored in this work, which makes use of a metal environment modification method to achieve corrosion inhibition of MS. The drugs used for this study consist of the active pharmaceutical ingredients (API's) and these drugs also have heteroatoms. The drugs that were employed in the current research are listed below in Table 2.1.

Table 2.1 List of selected Drug molecules

S.No.	Name	Structure of Drug Molecule
1	Baclofen	 <p>4-amino-3-(4-chlorophenyl)butanoic acid</p>
2	Betahistine dihydrochloride	 <p>HCl HCl</p> <p><i>N</i>-methyl-2-(pyridin-2-yl)ethanamine dihydrochloride</p>
3	Isoxsuprine hydrochloride	 <p>4-[1-hydroxy-2-(1-phenoxypropan-2-ylamino)propyl]phenol hydrochloride</p>
4	Panthenol	 <p>2,4-dihydroxy-N-(3-hydroxypropyl)-3,3-dimethylbutanamide</p>
5	Naphazoline	 <p>2-(naphthalen-1-ylmethyl)-4,5-dihydro-1H-imidazole</p>
6	Dicyclomine hydrochloride	 <p>H—Cl</p> <p>2-(diethylamino)ethyl 1-cyclohexylcyclohexane-1-carboxylate hydrochloride</p>

2.5 The objectives of the present study

- Selection of nitrogen containing drug molecules as corrosion inhibitors.
- To determine inhibition efficiency of the selected molecules for corrosion inhibition.
- To study various adsorption isotherms to identify the mechanism of corrosion.
- To calculate thermodynamic parameters like Enthalpy, Entropy, Gibbs Free Energy and Activation Energy.
- To validate the above observed parameters by using quantum chemical calculations.

2.6 Techniques determining the corrosion inhibition

Main techniques employed for corrosion study includes weight loss, electrochemical analysis, surface morphological techniques and computational methods (as given in Figure 2.2), a brief about these techniques is discussed as follows

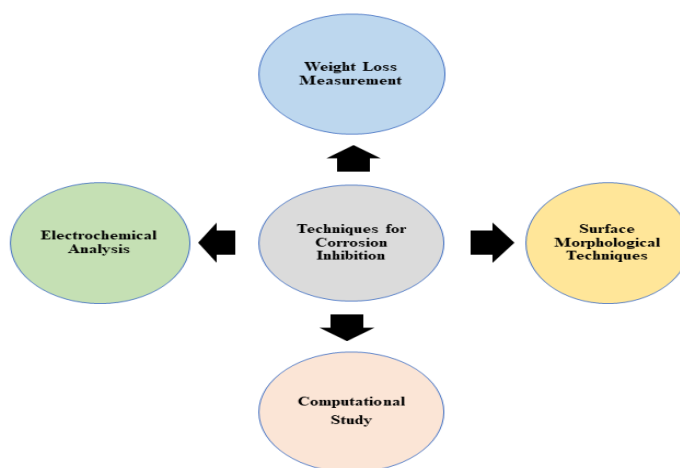


Figure 2.2 Pictorial presentation of various techniques employed for corrosion inhibition study.

2.6a Weight loss method

This is the most fundamental, widely used, and inexpensive technology for determining the corrosion efficiencies and corrosion rates of inhibitors. The samples were weighed by keeping them in 1 M HCl solution without and with varying amounts of the inhibitor. It is necessary to remove any solid reaction products from the samples prior to weighing in order to acquire reliable outcomes from this procedure. (Geece,2011; Usman & Okoro, 2015).

2.6b Electrochemical methods

When electrons from atoms on the metal's surface are transported to a suitable electron acceptor in the presence of any medium, electrochemical corrosion occurs. To investigate the electrochemical corrosion, researchers use electrochemical analysis techniques, in which potentiostat is generally employed to get thorough knowledge of corrosion process, also these electrochemical techniques are precise, fast, and reliable. These are the techniques, where currents are measured as a function of changing voltages over time.

2.6c Potentiodynamic polarization methods

These methods involve potentiodynamic polarization, potentiostatic staircase, and cyclic voltammetry, all of these approaches can be used for corrosion analysis, and they are thoroughly explained in the scientific literature. Three types of polarization can take place, anodic polarization, cathodic polarization and cyclic polarization. In anodic type, potential is allowed to change at anode towards positive side, resulted in emission of electrons and cathodic polarization involves addition of electrons causing movement of polarization towards more negative side. In cyclic polarization both anodic and cathodic polarization takes place in cyclic fashion. In the present study potentiodynamic polarization has been used to get the data, in this technique potential of a particular range is given to the corrosion cell, causing a oxidation or reduction process to occur on the metal surface and, as a result, an appropriate current to be produced on the electrode surface. Polarization curve is drawn in which potential is the function of log of current value. From these measurements, the E_{corr} and j_{corr} values can be calculated (Telegdi et al., 2018).

2.6d Electrochemical impedance spectroscopy

EIS is quantitative method for assessing inhibitor anti-corrosion efficacy in a short period of time and it measure impedance in a circuit. The alterations at the steel/solution interface were investigated using the electrochemical impedance spectroscopy. A small signal excitation (function of frequency) is applied to investigate the changes in the sample and solution interface and impedance response is also measured (Hernandez et al. 2020; Magar et al., 2021)

2.6e Surface morphological techniques

Surface morphology approaches for MS surfaces under corrosive conditions are used to determine surface changes and prove metal shielding through the development of thin layers of corrosion inhibitors. Scanning electron microscopy (SEM) and atomic force microscopy (AFM) were employed in the present study to investigate the surface changes. SEM provides two dimensional pictures and AFM gives three dimensional pictures along with roughness data (Sharma & Kumar, 2021).

2.6f Computational study

A theoretical investigation was conducted to compare the experimental findings with the inhibitor's molecular structure and electronic characteristics (Dagdag et al., 2020). Studies of corrosion inhibition processes utilising computational methods save time because they don't require the use of laboratory tests. Quantum chemical calculations, Fukui indices and Molecular dynamic simulations were employed in the present study to understand the role of inhibitor compounds in inhibition mechanism (Sharma & Kumar, 2021).

CHAPTER 3
MATERIAL AND METHODS

3 Experimental techniques

This chapter comprises all the approaches used to study the corrosion-inhibiting characteristics of selected drugs for MS. In this chapter, everything from solution preparation to types of electrodes employed and a theoretical detail of the inhibitors employed in this study are briefly described.

The first section focuses on the preparation of the solution and the preparation of metal samples. The second section discusses the different types of electrodes and how they are used in electrochemical procedures. After that the techniques and instrumentation that were employed have been explored in detail in the third section.

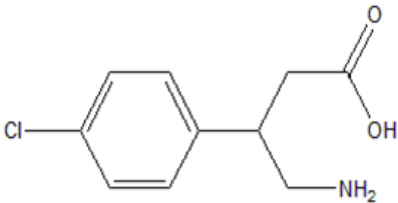
3.1 Materials

3.1.1. Preparation of solution

All of the reagents used were from CDH fine chemicals, including hydrochloric acid (HCl). Here HCl was employed as test solution (exposed to air at 298K) and the double distilled water was used throughout for all the solution preparation. Selected concentration of acid for all the measurements was 1M HCl. The inhibitors that were used in the present study are drugs purchased from different suppliers like Yarrow Chem Products (Baclofen, Panthenol, Naphazoline) Enal Drug Pvt. Ltd. (Betahistine dihydrochloride), Jayco Chemical Industries (Isoxsuprine hydrochloride), Shreepati Pharmaceutical Pvt. Ltd. (Dicyclomine hydrochloride) whose different properties including name, molecular weight, structures are summed as follows

- **Baclofen**

Baclofen	
Molecular formula	C₁₀H₁₂ClNO₂
Molecular weight	213.66 g/mol
Assay	98.7%
CAS NO.	1134-47-0
Physical state	Solid
Solubility in water	Soluble


Clc1ccc(cc1)C2CCCC(N)C2=O

- **Betahistine dihydrochloride**

Betahistine dihydrochloride	
Molecular formula	C₈H₁₄Cl₂N₂
Molecular weight	209.11 g/mol
Assay	98.5%
CAS NO.	5579-84-0
Physical state	Solid
Solubility in water	Soluble

- **Isoxsuprine hydrochloride**

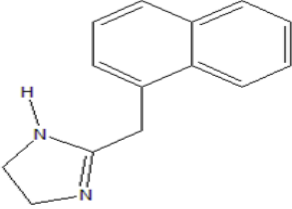
Isoxsuprine hydrochloride	
Molecular formula	C₁₈H₂₄ClNO₃
Molecular weight	337.8 g/mol
Assay	99.5%
CAS NO.	579-56-6
Physical state	Solid
Solubility in water	Soluble

- **Panthenol**

Panthenol	
Molecular formula	C₉H₁₉NO₄
Molecular weight	205.25 g/mol
Assay	98%
CAS NO.	16485-10-2
Physical state	Solid
Solubility in water	Soluble

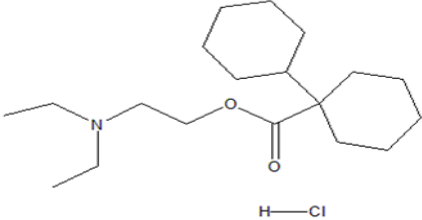
- **Naphazoline**

Naphazoline	
Molecular formula	C₁₄H₁₄N₂
Molecular weight	210.27 g/mol
Assay	>98%
CAS NO.	835-31-4
Physical state	Solid
Solubility in water	Soluble



- **Dicyclomine hydrochloride**

Dicyclomine hydrochloride	
Molecular formula	C₁₉H₃₆ClNO₂
Molecular weight	345.9 g/mol
Assay	99.65%
CAS NO.	67-92-5
Physical state	Solid
Solubility in water	Soluble



For the preparation of varied concentrations of inhibitors in 1 M HCl for investigating the corrosion mitigation property for MS corrosion, stock solution of the amount 1000 ml was taken and from the stock solution other required concentrations of inhibitors were prepared by diluting the stock solution.

3.2 Electrochemical Cell

For electrochemical study, a three-electrode assembly consisting of a counter electrode, working electrode and reference electrode was used. Working electrode was made up of the material selected for study (MS), counter electrode was constructed with platinum, and the selected reference electrode was Ag|AgCl|3 M KCl. Volume of the solution taken for analysis was 100 ml in order to avoid any alterations caused by

corrosion in the results (ASTM G 31– 72 (2004) standards) (ASTM,2004). Here the potentiostat mode is used in which the potential is controlled, the potential difference between working and reference is measured, and current response between counter and working electrode is measured.

3.2.1 Working electrode

MS was selected for analysis, therefore working electrodes (given in Figure 3.1) were formed with MS and the composition of chosen MS is iron as major constituent along with other constituents C (0.17%), Mn (0.46%), Si (0.26%), P (0.019%), S (0.017%) in small quantities (Sharma et al., 2022). Basically, the working electrode is the electrode on which the half redox reaction of interest is taking place at the time of measurement. When constructing the working electrodes for electrochemical measurements, metallic rods of dimension 5 X 1 X 1 cm (l X b X h) were combined with a adhesive (epoxy resin) to produce a surface area of roughly 1 cm² on the electrode surface. After that emery papers with grades ranging from 100 to 2000 were used to scarp the surface of these WE's to achieve a homogeneous shinny surface. After degreasing the electrodes with acetone, they were washed with double distilled water to remove any remaining residue.



Figure 3.1 Working electrodes of selected sample with epoxy resin as additive.

3.2.2 Reference electrode

The reference electrode is an electrode that has a consistent and known electrode potential. It is used as a point of reference in the electrochemical cell to control and measure the potential of the cell. The current that flows through the reference electrode

is kept as near to zero as possible. In the present system the Ag|AgCl|3 M KCl was taken as reference electrode (Eco 8, 2011).

3.2.3 Counter electrode

The counter electrode (also known as auxiliary electrode), is an electrode which is used to close the current circuit in the electrochemical cell. It is usually made of an inert material, here platinum was used for electrode preparation and second half reaction occurs here, and current is measured between auxiliary and working electrode (Eco 8, 2011).

3.3 Instrumentation

The weight loss technique was used to discover the corrosion mitigation study of MS, and the measurements were carried out with the use of an analytical weighing machine of brand ALN 220. Further, electrochemical analysis was performed by employing Autolab equipment Metrohum model (PGSTAT 204) attached with software Nova 2.1 (Farahati et al., 2020; Gracia et al., 2013). Surface morphology for the present study includes scanning electron microscopy (SEM) and atomic force microscopy (AFM). SEM analysis was performed by using JEOL SEM instrument and gave two dimensional pictorial presentations and AFM was performed by utilizing multimode 8, make Bruker instrument, which gave three dimensional topographs. Figure 3.2 (a-c) represents here the various instruments used in the study. Theoretical investigations which include quantum chemical calculation and molecular dynamics (MD) simulation were performed with the help of BIOVIA Material Studio software (version 7.0).

3.4 Experimental procedures

The measurements of weight loss were carried out in accordance with the standard technique defined by the American Society for Testing and Materials (ASTM G1-03(2017) e1 standard). Sample coupons were cut in to small pieces of dimensions 2 X 2 cm². The experiment began with scraping the metal coupons with emery papers (100-2000 grades), followed by degreasing, washing and air drying the metal samples. Using an analytical balance, the MS samples were weighed twice: once before and once after being exposed to test solution (1 M HCl), which included a variable amount (in ppm)

of selected drug molecules as an inhibitor, respectively. The tests of weight loss were carried out with varied concentration of inhibitors, by varying exposure time, and at various temperature ranges. Experimentation was conducted out at optimal conditions, which were room temperature (298 ± 2 K) and for two hours, with the thermostat set to maintain the desired temperature. In order to obtain credible results, triplicate tests were averaged (Sharma et al., 2021; Sharma et al., 2022).

Prior to beginning of electrochemical experimentation, the working electrode was scraped with various types of emery sheets to ensure that it was free of contaminants (corrosion products). In order to establish open circuit potential, it was retained for half an hour in the test solution. Quantitative measurements were carried out utilizing electrochemical impedance spectroscopy (EIS) at a frequency ranging from 10^5 to 0.1 Hz with respect to open circuit potential (OCP) with an amplitude of 0.005 V. PDP study was carried out in the potential ranging between ± 250 mV with respect to OCP with particular scan rate. Corrosion current density values and charge transfer resistance values extracted from PDP and EIS respectively, were then employed for the calculation of inhibition efficacy (Sharma et al., 2021; Sharma et al., 2022).

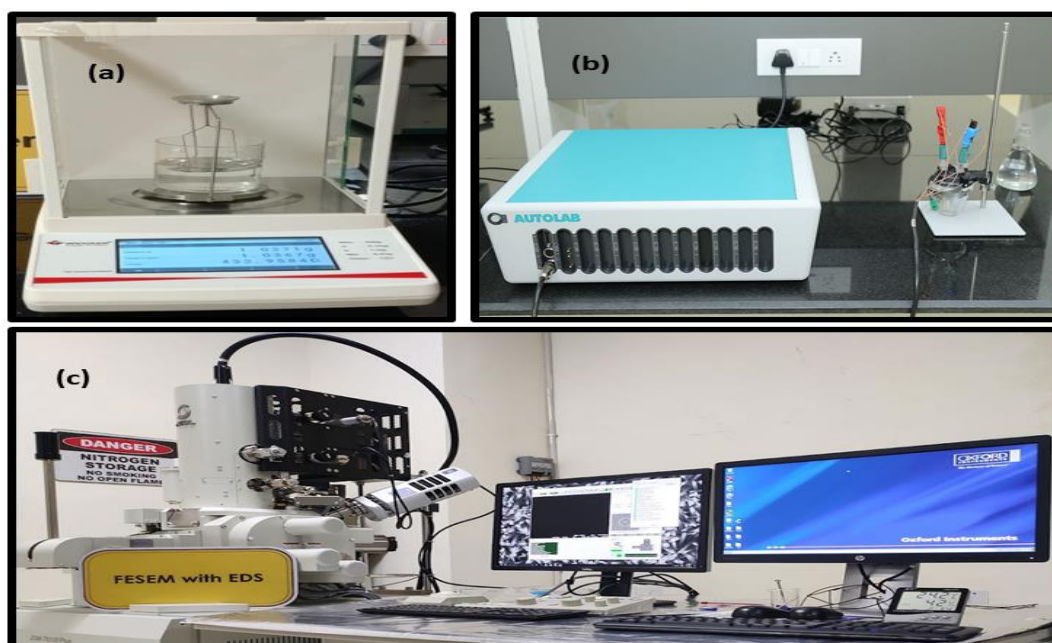


Figure 3.2 (a-c) Representation of (a) analytical balance (b) electrochemical workstation (c) scanning electron microscope.

In the current investigation, surface modifications were analysed using JEOL make scanning electron microscopy (SEM) instrument and atomic force microscopy (AFM), (multimode 8, make Bruker) respectively. In scanning electron microscopy (SEM), an electron beam is permitted to fall on the specific region of the sample that is being investigated. In some instances, these electrons are responsible for dissociating the atoms that make up the sample, which results in the release of electrons from the sample. These electrons are called as secondary electrons and further studied. In case of AFM, A cantilever with a sharp tip makes contact with the surface of the sample, which enables the tip to feel the forces that are exerted between the surface of the metal and the molecules of the tip. BIOVIA Material Studio software (version 7.0) was used for theoretical investigation. Module employed was DMol³, which optimized the geometry to get the lowest energy state the approximation (GGA) with Becke- Lee- Yang- Parr (BLYP), double numeric basis sets plus polarization (DNP) were decided for further calculations (Cao et al., 2014; Ciezak & Trevino, 2006). Fukui indices were also kept in to consideration in order to get an idea about the role of different parts of inhibitor molecule in donation or acceptance of electrons (Alibakhshi et al., 2018).

CHAPTER 4
RESULTS AND DISCUSSION

A total of six distinct inhibitors (Baclofen, Betahistine dihydrochloride, Isoxsuprine hydrochloride, Panthenol, Naphazoline and Dicyclomine hydrochloride) were chosen for comprehensive corrosion inhibition and adsorption investigations by employing weight loss measurements for MS. All the findings are addressed in the following sections.

Section 4.1: Weight loss measurements

Weight loss measurement is one of the oldest, very basic and the most convenient method for determining corrosion parameters. The present study incorporates three types of studies, including variations in temperature, variations in immersion time, and variations in the concentration of the selected inhibitor, and the inhibitory efficiency from each type of investigation determined in turn. Various plots and tables have also been presented in the chapter to find out the relation of inhibition efficiency with concentration (which was taken in ppm), immersion time (From one hour to four hours) and temperature (four different temperatures 298-328 K) respectively. Weight loss measurements were carried out in accordance with standard protocol prescribed by the American Society for Testing and Materials (ASTM G1-03(2017) e1 standard) (Bashir et al., 2020; Garcia et al., 2013). Testing was done on MS coupons with the selected dimension of 2 X 2 cm², and for each MS sample, we performed two weight checks: one before and one after they were exposed to test solution under various experimental conditions applied like changing the concentrations of selected inhibitors, at different dipping time and at different temperatures. All the Experiments were thermostatically controlled and carried out at optimized conditions of room temperature (298 ± 2 K) and two hours. In order to ensure the validity of the data, the results of three separate tests were averaged together. Corrosion-reducing capacity, surface coverage, and corrosion rate were all calculated using the equations 4.1.1-4.1.3 listed below: (Bashir et al., 2017; Bashir et al., 2019; Sharma & Kumar, 2021)

$$I.E. (\%) = \frac{W_0 - W_i}{W_0} \times 100 \quad (4.1.1)$$

$$\theta = \frac{W_0 - W_i}{W_0} \quad (4.1.2)$$

$$CR = \frac{87.6W}{DAT} \quad (4.1.3)$$

In the present investigation W_0 , W_i denotes the reduction in weight of metal sample with no inhibitor is in solution and with an inhibitor in the test solution respectively and θ indicates the surface coverage (Ji et al.,2015). CR , W , and D denote corrosion rate (mmpy), weight loss (g), density of coupon (g cm⁻³), respectively. A and T denote the area of coupon(cm²) and dipping time (hours), respectively. (Singh et al., 2020)

4.1.1 Determination of weight loss measurements for the MS corrosion at different concentrations of acid

The weight loss of metal samples was calculated by varying concentrations of HCl ranged from 1M to 4 M for MS. The purpose of this experiment was to determine the acid content that would serve as an optimized concentration for all subsequent tests. All the results were computed using equation 4.1.3 and are tabulated in Table 4.1.1. Results depicted that 1M HCl has an effective corrosion rate, thus it was used as an optimized concentration of acid for MS corrosion.

Table 4.1.1 Calculation of MS corrosion rate by varying acid concentrations.

Conc.	W ₀ (g)	W _i (g)	W ₀ -W _i (g)	CR (mm/y)
1M	1.28	0.40	0.88	2.45
2M	1.30	0.33	0.97	2.70
3M	1.28	0.15	1.13	3.15
4M	1.29	0.10	1.19	3.32

4.1.2 Measurements of weight loss in 1M HCl for the estimation of corrosion parameters for MS, by employing Baclofen as inhibitor

Table 4.1.2-4.1.4 summarizes the results of the weight loss experiment using equations 4.1.1-4.1.3 to calculate inhibitory efficacy, surface coverage and corrosion rate. Figure 4.1.1(a-c) shows several graphs based on these data, including concentration vs. inhibitory efficacy, time vs. inhibitory efficacy, and temperature vs. inhibitory efficacy. According to the results, inhibitory efficiency in 1M HCl improved with increasing

concentrations of Baclofen from 0 to 2000 ppm, with a peak of 96.71 % at 2000 ppm of Baclofen as an inhibitor. The increased efficiency and reduces corrosion rate may be attributed to the prevalence of heteroatom and ring structure in Baclofen, which established a bonding with the metallic sample (Bashir et al., 2018). The various calculated corrosion parameters by varying the concentration of Baclofen (0 to 2000 ppm) outlined in Table 4.1.2 and Figure 4.1.1(a) depicted the increased trend of efficacy with concentration and for the optimal concentration of 2000 ppm of Baclofen as an corrosion suppressor in a solution of 1M HCl at 298 K, the variation in inhibition efficacy with time was also investigated (vide Table 4.1.3 and Figure 4.1.1b) and results confirmed when the time period was extended from one to two hours, the inhibition efficacy increased; however, as the temperature rose, the inhibition efficacy decreased. Another investigation was carried out under optimum conditions, and an increase in temperature from 298K to 328K (vide Table 4.1.4 and Figure 4.1.1c) resulted in a decrease in inhibitory efficiency. The desorption of Baclofen from the sample, which resulted in greater accessibility of MS surface to corrosive medium, may account for the drop in inhibitory efficacy observed with increasing temperature (Abdallah et al., 2019).

Table 4.1.2 Effect of variation of Baclofen concentration.

Inhibitor	Inhibitor Concentration (ppm)	Surface Coverage (θ)	Inhibition Efficiency (%)	Corrosion Rate (CR) (mmy^{-1})
	Blank			2.12
Baclofen	100	0.77	76.97	0.49
	500	0.83	82.89	0.38
	1000	0.87	86.84	0.28
	1500	0.92	92.10	0.17
	2000	0.97	96.71	0.07

Table 4.1.3 Effect of immersion time on inhibition efficiency of Baclofen as inhibitor for MS.

Inhibitor	Time of Immersion (Hours)	Concentration	Corrosion Rate (mmy⁻¹)	Surface Coverage (θ)	Inhibition Efficiency (%)
Baclofen	1	Blank (1M HCl)	4.07		
		2000 ppm	0.25	0.94	93.83
	2	Blank (1M HCl)	2.04		
		2000 ppm	0.07	0.96	96.57
	3	Blank (1M HCl)	1.36		
		2000 ppm	0.10	0.92	92.46
	4	Blank (1M HCl)	1.02		
		2000 ppm	0.10	0.90	89.72

Table 4.1.4 Effect of temperature on corrosion inhibition of MS using Baclofen.

Inhibitor	Temperature of Immersion (K)	Concentration	Corrosion Rate (mmpy)	Surface Coverage (θ)	Inhibition Efficiency (%)
Baclofen	298	Blank (1M HCl)	2.07		
		2000 ppm	0.06	0.97	96.64
	308	Blank (1M HCl)	2.09		
		2000 ppm	0.13	0.93	93.28
	318	Blank (1M HCl)	2.06		
		2000 ppm	0.23	0.88	88.59
	328	Blank (1M HCl)	2.07		
		2000 ppm	0.34	0.83	83.22

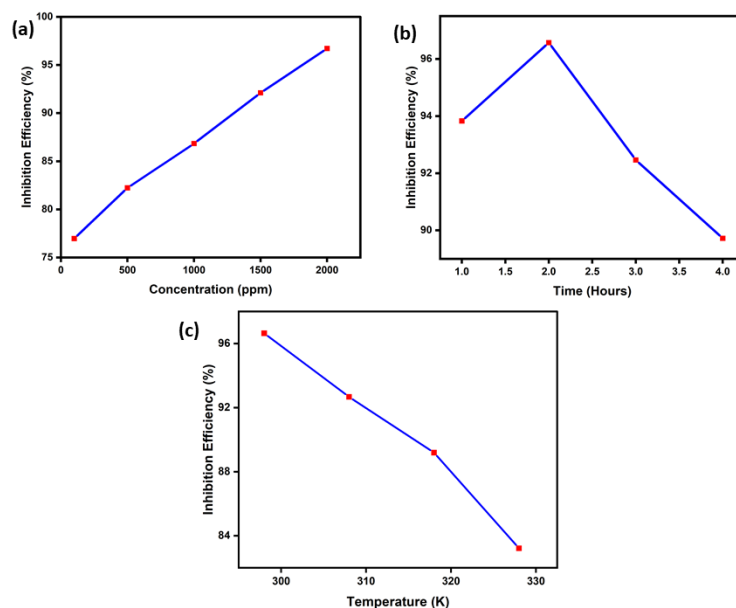


Figure 4.1.1(a-c) Percentage deviation of inhibition efficiency with concentration, time, and temperature.

4.1.3 Measurements of weight loss in 1M HCl for the estimation of corrosion parameters for MS, by employing Betahistine dihydrochloride as inhibitor

Betahistine dihydrochloride was analysed for its corrosion inhibition properties and the for determining the effect of concentration on efficiency was investigated for the concentration ranging from 50 to 1500 ppm. The results showed that increasing concentration of Betahistine dihydrochloride had an effect on the corrosion inhibition efficiency, which raised to 96.36 % at 1500 ppm of the inhibitor molecule (Fouda et al.,2016). All the measured variables are tabulated in Table 4.1.5 and Figure 4.1.2a shows the plot between inhibition efficiency and concentration of Betahistine dihydrochloride dissolved in test solution. The effects of changing the dipping time were investigated and reported in Table 4.1.6 using a 1500 ppm concentration of Betahistine as an inhibitor in an acidic solution (of concentration 1M) at 298 K, and graph (Figure 4.1.2b) was plotted to analyse the result as shown in the results. It was found that the efficiency of inhibition decreased as immersion time grew above 2 hours, and was maximum when dipping time reached 2 hours. Further, Table 4.1.7 and Figure

4.1.2c summarise the results of testing 1500 ppm of Betahistine dihydrochloride in 1M HCl at temperatures ranging from 298K to 328K to see the influence of the temperature has on inhibitory efficacy and confirmed the reduced effectiveness of the inhibitor as the temperature was raised because adsorption process was altering and also proved physical adsorption was dominating (Fouda & Badawy, 2019).

Table 4.1.5 Effect of variation of Betahistine dihydrochloride concentration.

Inhibitor	Inhibitor Concentration (ppm)	Surface Coverage (θ)	Inhibition Efficiency (%)	Corrosion Rate (CR) (mmpy^{-1})
Betahistine dihydrochloride	Blank			1.53
	50	0.77	77.27	0.33
	100	0.83	82.72	0.27
	500	0.87	87.27	0.20
	1000	0.92	91.82	0.13
	1500	0.96	96.36	0.06

Table 4.1.6 Effect of immersion time on inhibition efficiency of Betahistine dihydrochloride.

Inhibitor	Time of Immersion (Hours)	Concentration	Corrosion Rate (mmpy)	Surface Coverage (θ)	Inhibition Efficiency (%)	
Betahistine dihydrochloride	1	Blank (1M HCl)	1.56			
		1500 ppm	.08	0.95	94.64	
	2	Blank (1M HCl)	1.56			
		1500 ppm	.05	0.96	96.42	
	3	Blank (1M HCl)	.90			
		1500 ppm	.05	0.94	93.81	
	4	Blank (1M HCl)	.77			
		1500 ppm	.06	0.92	91.82	

Table 4.1.7 Effect of temperature variation using Betahistine dihydrochloride as an inhibitor.

Inhibitor	Temperature (K)	Concentration	Corrosion Rate (mmpy)	Surface Coverage (θ)	Inhibition Efficiency (%)
Betahistine dihydrochloride	298	Blank (1M HCl)	1.04		
		1500 ppm	0.04	0.96	96.00
	308	Blank (1M HCl)	0.99		
		1500 ppm	0.06	0.93	93.00
	318	Blank (1M HCl)	1.04		
		1500 ppm	0.11	0.89	89.33
	328	Blank (1M HCl)	0.91		
		1500 ppm	0.13	0.85	84.62

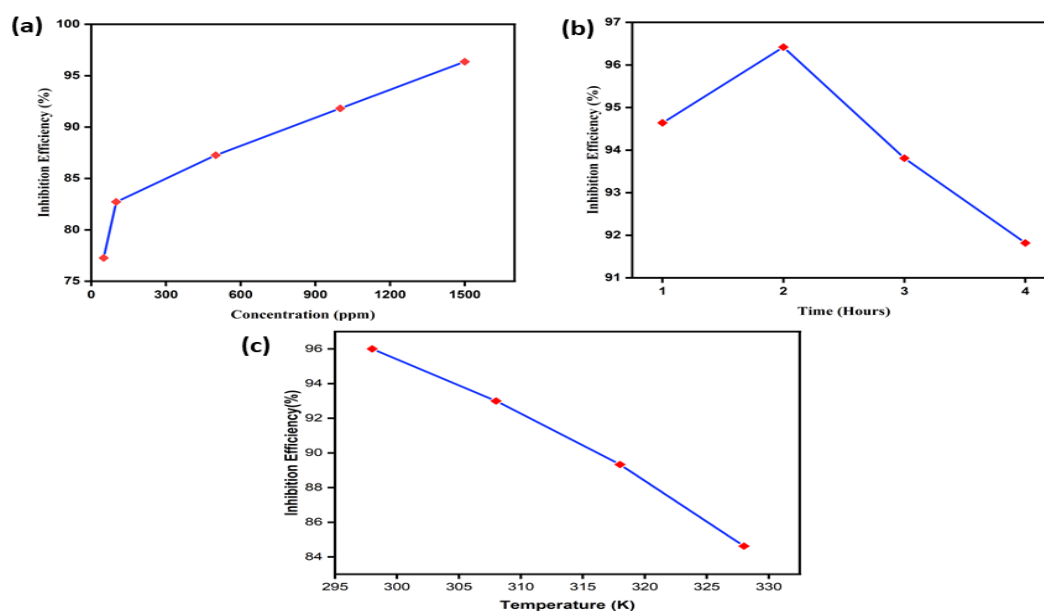


Figure 4.1.2 (a) Plot of concentration variation vs inhibition efficiency (b) time vs inhibition efficiency and (c) temperature vs inhibition efficiency.

4.1.4 Measurements of weight loss in 1M HCl for the estimation of corrosion parameters for MS, by employing Isoxsuprine hydrochloride as inhibitor

Weight loss analyses for metal coupons were carried out using a 1M HCl solution and with different experimental conditions like by varying concentrations of Isoxsuprine hydrochloride ranging from 0 to 2000 ppm, at different immersion times ranging from 1 hour to 4 hours at different temperatures, the values of inhibitory efficiency, corrosion rate, and surface coverage were calculated and tabulated in Tables 4.1.8- 4.1.10, and all the variations were graphically represented in Figure 4.1.3a- c. At a concentration of 2000 ppm of Isoxsuprine hydrochloride, there was a significant rise in inhibitory efficiency and the maximum level of inhibition efficiency and corrosion retardation was obtained. Heteroatoms, electron clouds, and rings may all be present, increasing the adsorption of Isoxsuprine hydrochloride on the sample, which could explain the observed retardation (Berdimurodov et al., 2021). Further time variation studies and temperature variation studies for selected samples dipped in 1.0 M HCl with dissolved 2000 ppm of Isoxsuprine hydrochloride as corrosion inhibitor confirmed that the inhibition efficacy was maximum upon two hours of immersion time and also that the maximum inhibitory efficiency was achieved at 298 K, and that the inhibitory efficiency reduced as the temperature was further increased. Because of desorption of adsorbed Isoxsuprine hydrochloride inhibitor particles from the metal surface, the inhibition efficiency has decreased, which has resulted in higher corrosion rates (Dhaundiyal et al., 2019). The enhanced adsorption and surface coverage of the inhibitor at a certain temperature (298K) resulted in higher inhibition efficiency.

Table 4.1.8 Effect of variation of Isoxsuprine hydrochloride concentration.

Inhibitor	Inhibitor Concentration (ppm)	Surface Coverage (θ)	Inhibition Efficiency (%)	Corrosion Rate (CR) (mmy^{-1})
	Blank			1.66
Isoxsuprine hydrochloride	100	0.86	85.71	0.24
	500	0.89	89.07	0.18
	1000	0.92	92.44	0.12
	1500	0.95	94.96	0.08
	2000	0.97	97.48	0.04

Table 4.1.9 Effect of immersion time on inhibition efficiency of Isoxsuprine hydrochloride as inhibitor for MS.

Inhibitor	Time of Immersion (Hours)	Concentration	Corrosion Rate (mmpy)	Surface Coverage (θ)	Inhibition Efficiency (%)
Isoxsuprine hydrochloride	1	Blank (1M HCl)	2.15		
		2000 ppm	0.22	0.90	89.61
	2	Blank (1M HCl)	0.98		
		2000 ppm	0.04	0.96	95.71
	3	Blank (1M HCl)	0.66		
		2000 ppm	0.06	0.90	90.14
	4	Blank (1M HCl)	0.42		
		2000 ppm	0.06	0.85	85.24

Table 4.1.10 Effect of temperature variation using Isoxsuprine hydrochloride as an inhibitor.

Inhibitor	Temperature (K)	Concentration	Corrosion Rate (mmy^{-1})	Surface Coverage (θ)	Inhibition Efficiency (%)
Isoxsuprine hydrochloride	298	Blank (1M HCl)	1.39		
		2000 ppm	0.04	0.97	97.00
	308	Blank (1M HCl)	1.37		
		2000 ppm	0.05	0.94	94.00
	318	Blank (1M HCl)	1.35		
		2000 ppm	0.12	0.91	90.67
	328	Blank (1M HCl)	1.08		
		2000 ppm	1.5	0.86	85.90

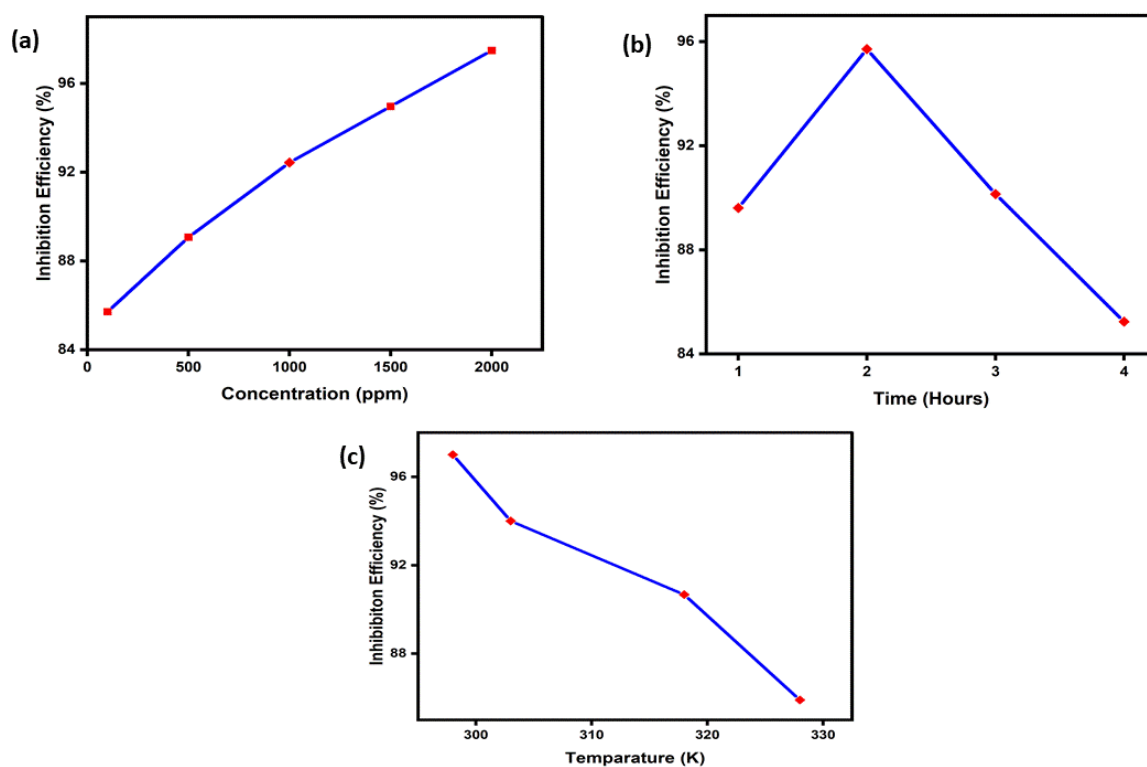


Figure 4.1.3 (a) Plot of concentration variation vs inhibition efficiency (b) time vs inhibition efficiency and (c) temperature vs inhibition efficiency.

4.1.5 Measurements of weight loss in 1M HCl for the estimation of corrosion parameters for MS, by employing Panthenol as inhibitor

Weight loss investigations were carried out by selecting the Panthenol as a new corrosion inhibitor and different experimental conditions were applied to see the behaviour of Panthenol. First investigation was by changing the amount of panthenol from 0 to 400 ppm and all the results were compiled in Table 4.1.11 and Figure 4.1.4a. A clear increase in inhibition efficacy and reduction in corrosion rate was there with the rise in the concentration and 90.71 % was the highest inhibition efficiency at 400 ppm of Panthenol (Idris et al.,2013). Further, two more studies were performed by changing the dipping time of metal coupons and by altering the temperature conditions, all the data was summarized in Tables 4.1.12 and 4.1.13 along with plots showing the trend of inhibitor efficacy in the Figure 4.1.4b,c. With the increase in immersion time beyond two hours, corrosion rate increased and results depicted that inhibitor adsorbed to metal surfaces lose inhibitory efficacy when the temperature raised and this indicated that the adsorption–desorption equilibria has shifted toward desorption (Sovizi et al., 2020; Umoren et al., 2007)

Table 4.1.11 Effect of variation of Panthenol concentration.

Inhibitor	Inhibitor Concentration (ppm)	Surface Coverage (θ)	Inhibition Efficiency (%)	Corrosion Rate (CR) (mmy⁻¹)
Panthenol	Blank			0.75
	100	0.67	66.91	0.25
	200	0.74	74.72	0.19
	300	0.83	82.90	0.13
	400	0.95	90.71	0.07

Table 4.1.12 Effect of immersion time on inhibition efficiency of Panthenol as inhibitor.

Inhibitor	Time of Immersion (Hours)	Concentration	Corrosion Rate (mmpy)	Surface Coverage (θ)	Inhibition Efficiency (%)
Panthenol	1	Blank (1M HCl)	0.16		
		400 ppm	0.03	0.83	83.33
	2	Blank (1M HCl)	0.49		
		400 ppm	0.05	0.90	90.28
	3	Blank (1M HCl)	0.38		
		400 ppm	0.06	0.84	84.15
	4	Blank (1M HCl)	0.39		
		400 ppm	0.08	0.78	78.57

Table 4.1.13 Effect of temperature variation using Panthenol as an inhibitor.

Inhibitor	Temperature (K)	Concentration	Corrosion Rate (mmy⁻¹)	Surface Coverage (θ)	Inhibition Efficiency (%)
Panthenol	298	Blank (1M HCl)	0.47		
		400 ppm	0.04	0.91	91.00
	308	Blank (1M HCl)	0.85		
		400 ppm	0.12	0.85	85.00
	318	Blank (1M HCl)	1.29		
		400 ppm	0.30	0.76	76.34
	328	Blank (1M HCl)	1.38		
		400 ppm	0.40	0.71	70.71

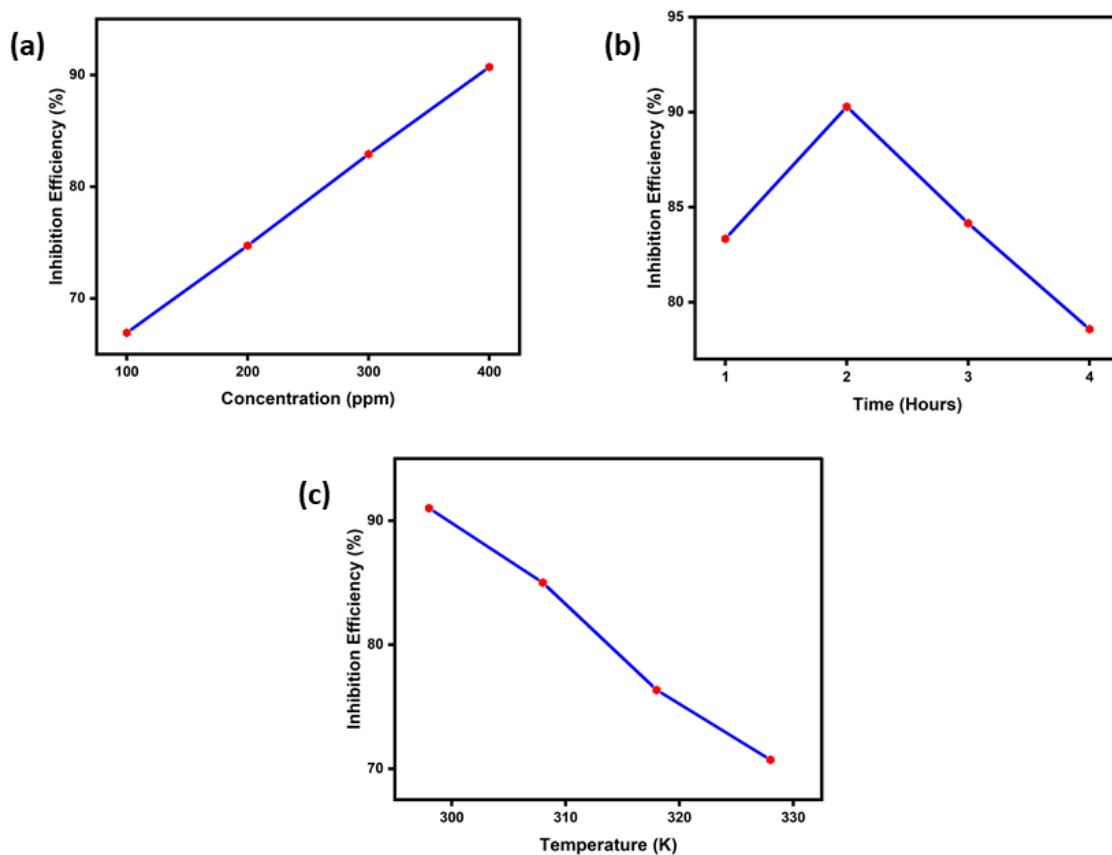


Figure 4.1.4 (a) Plot of concentration variation vs inhibition efficiency (b) time vs inhibition efficiency and (c) temperature vs inhibition efficiency.

4.1.6 Measurements of weight loss in 1M HCl for the estimation of corrosion parameters for MS, by employing Naphazoline as inhibitor

Weight loss investigations with Naphazoline as corrosion inhibitor for MS were carried out and corrosion parameters were summarised in Tables 4.1.14- 4.1.16 and trends were plotted in Figure 4.1.5a-c. Results claimed the increased inhibition efficacy and reduced corrosion rate values with the rise in the concentration of Naphazoline (Attia, 2015) and came out to be highest with the value 90.76% at 1500 ppm of Naphazoline, and experimented again at different temperature and by varying time of exposure. As the temperature rises, the protective film of Naphazoline formed on the metallic surface becomes less stable because of desorption of some adsorbed drug molecules from the surface at higher temperatures, exposing a larger area of the metal to the acidic

environment, resulting in a decrease in inhibition efficiency (Al-Shafey et al.,2014; Hameed et al., 2015).

Table 4.1.14 Effect of variation of Naphazoline concentration.

Inhibitor	Inhibitor Concentration (ppm)	Surface Coverage (θ)	Inhibition Efficiency (%)	Corrosion Rate (CR) (mmy^{-1})
Naphazoline	Blank			1.66
	100	0.73	73.95	0.43
	500	0.77	77.31	0.38
	1000	0.84	84.03	0.26
	1500	0.91	90.76	0.15

Table 4.1.15 Effect of immersion time on inhibition efficiency of Naphazoline as inhibitor for MS.

Inhibitor	Time of Immersion (Hours)	Concentration	Corrosion Rate (mmy^{-1})	Surface Coverage (θ)	Inhibition Efficiency (%)	
Naphazoline	1	Blank (1M HCl)	2.15			
		1500 ppm	0.31	0.86	85.71	
	2	Blank (1M HCl)	0.75			
		1500 ppm	.07	0.91	90.74	
	3	Blank (1M HCl)	.66			
		1500 ppm	.11	0.83	83.09	
	4	Blank (1M HCl)	.42			
		1500 ppm	.09	0.77	77.05	

Table 4.1.16 Effect of temperature variation using Naphazoline as an inhibitor.

Inhibitor	Temperature (K)	Concentration	Corrosion Rate (mmpy)	Surface Coverage (θ)	Inhibition Efficiency (%)
Naphazoline	298	Blank (1M HCl)	0.96		
		1500 ppm	0.08	0.91	91.00
	308	Blank (1M HCl)	0.92		
		1500 ppm	0.14	0.85	85.00
	318	Blank (1M HCl)	1.03		
		1500 ppm	0.19	0.81	81.08
328	Blank (1M HCl)	0.91			
	1500 ppm	0.21	0.77	76.92	

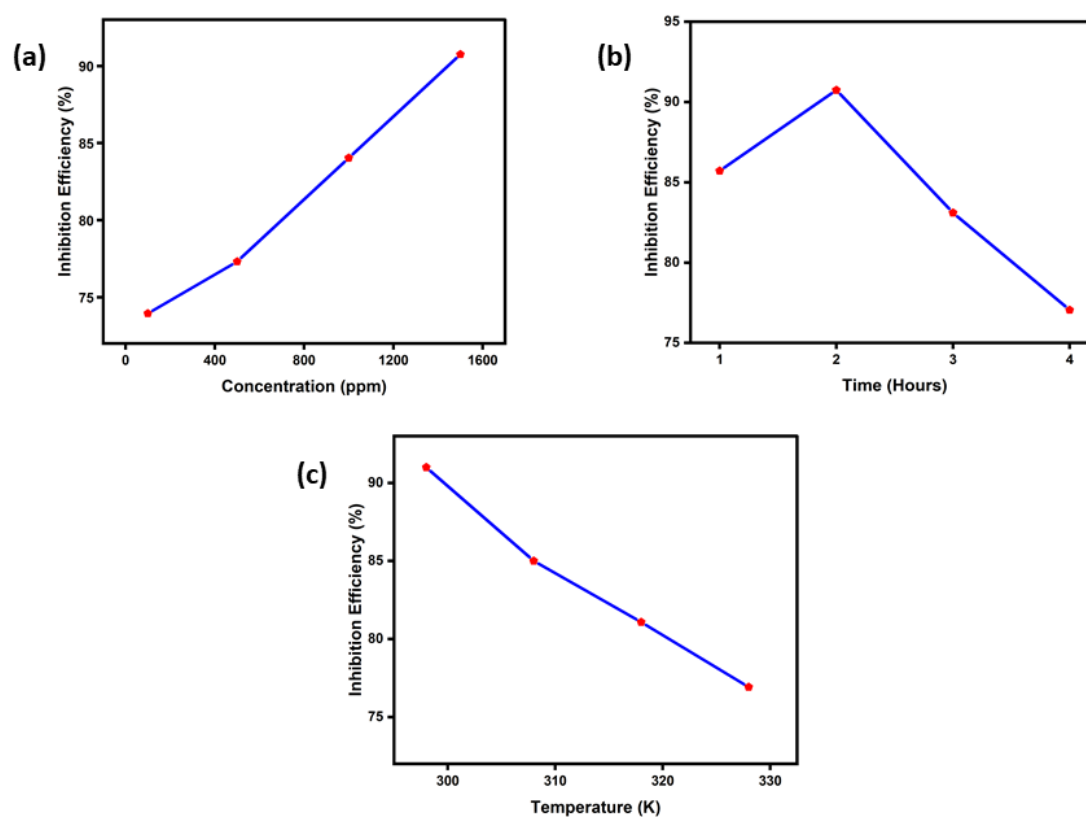


Figure 4.1.5 (a) Plot of concentration variation vs inhibition efficiency (b) time vs inhibition efficiency and (c) temperature vs inhibition efficiency.

4.1.7 Measurements of weight loss in 1M HCl for the estimation of corrosion parameters for MS, by employing Dicyclomine hydrochloride as inhibitor

Corrosion parameters like surface coverage, corrosion rate, inhibition efficacy were calculated with the change in Dicyclomine concentration, with the change in immersion time and with the variation in temperature conditions. All the measured values were tabulated in the Tables 4.1.17- 4.1.19 and plotted graphs are shown in Figure 4.1.6a-c. While investigating effect of concentration, results revealed increased inhibition efficiency with enhancing drug concentration and efficiency was about 95.04% at 800 ppm of dicyclomine hydrochloride and this rise attributed to adsorption of drug molecule on sample, the drug forms a barrier that keeps the metal's surface safe from corrosion (Ameh & Sani, 2015), but while investigating the effect of temperature, results confirmed the decreased inhibition efficiency with the rise in temperature as the desorption of dicyclomine has started (Chaubey et al., 2017; Diki et al., 2018). Immersion time investigations also depicted the highest inhibition efficacy at two hours and it started falling beyond two hours of dipping time.

Table 4.1.17 Effect of variation of Dicyclomine hydrochloride concentration.

Inhibitor	Inhibitor Concentration (ppm)	Surface Coverage (θ)	Inhibition Efficiency (%)	Corrosion Rate (CR) (mmy^{-1})
	Blank			0.51
	200	0.82	82.09	0.09
Dicyclomine hydrochloride	400	0.87	86.78	0.07
	600	0.90	90.08	0.05
	800	0.95	95.04	0.02

Table 4.1.18 Effect of immersion time on inhibition efficiency of Dicyclomine hydrochloride as inhibitor for MS.

Inhibitor	Time of Immersion (Hours)	Concentration	Corrosion Rate (mmpy)	Surface Coverage (θ)	Inhibition Efficiency (%)
Dicyclomine hydrochloride	1	Blank (1M HCl)	2.26		
		800 ppm	0.22	0.90	90.12
	2	Blank (1M HCl)	0.95		
		800 ppm	.04	0.95	95.59
	3	Blank (1M HCl)	.66		
		800 ppm	.07	0.89	88.73
	4	Blank (1M HCl)	.42		
		800 ppm	.07	0.84	83.61

Table 4.1.19 Effect of temperature variation using Dicyclomine hydrochloride as an inhibitor.

Inhibitor	Temperature (K)	Concentration	Corrosion Rate (mmy^{-1})	Surface Coverage (θ)	Inhibition Efficiency (%)
Dicyclomine hydrochloride	298	Blank (1M HCl)	1.05		
		800 ppm	0.05	0.95	95.00
	308	Blank (1M HCl)	1.05		
		800 ppm	0.11	0.89	89.00
	318	Blank (1M HCl)	1.05		
		800 ppm	0.17	0.84	84.00
	328	Blank (1M HCl)	1.09		
		800 ppm	0.21	0.81	80.77

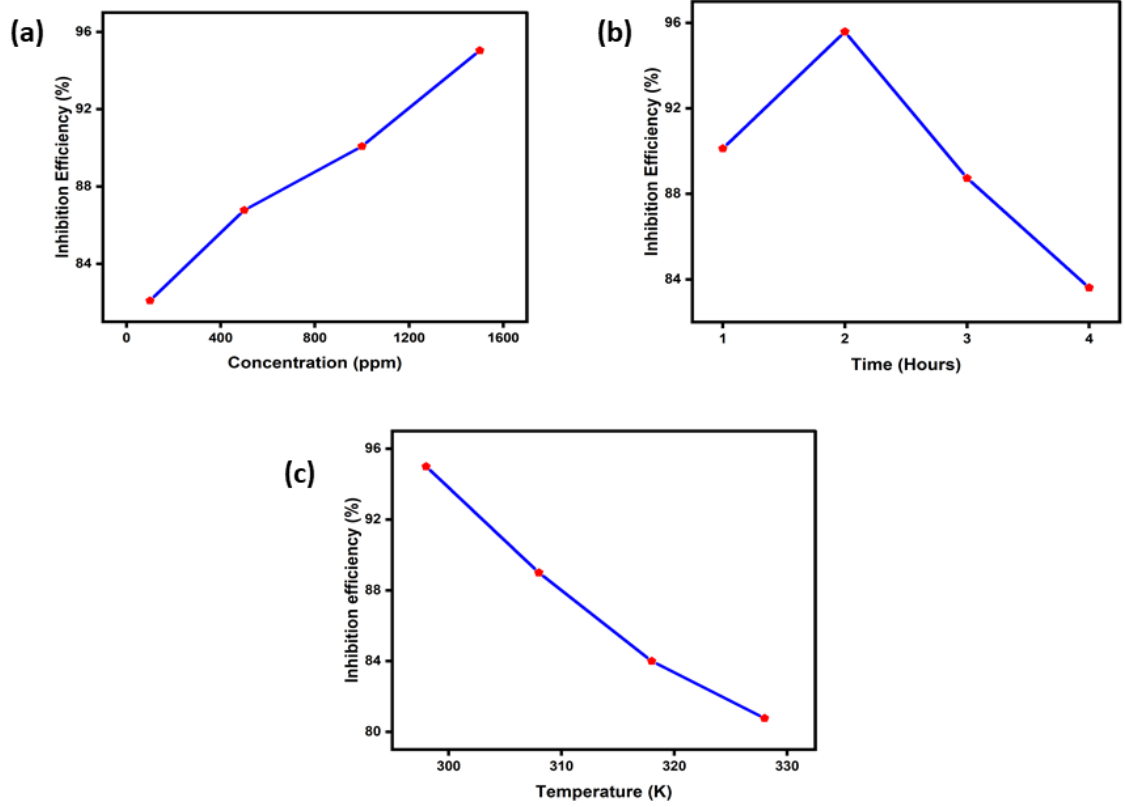


Figure 4.1.6 (a) Plot of concentration variation vs inhibition efficiency (b) time vs inhibition efficiency and (c) temperature vs inhibition efficiency.

4.1.8. Conclusions

- This research adopted several inhibitors, all of which inhibited MS corrosion quite effectively.
- The corrosion inhibition efficiency of the examined inhibitors for MS at their greatest concentration and 298K are as follows:
Isoxsuprine hydrochloride > Baclofen > Betahistine dihydrochloride > Dicyclomine hydrochloride > Panthenol > Naphazoline.
- All investigated inhibitors showed a significant increase in inhibitory efficiency as the concentration of the inhibitor was raised.
- Temperature lowered the effectiveness of all the drugs as inhibitor used in present study.
- As the immersion time increases, the inhibition efficiency decreases and it was maximum up to two hours of immersion time beyond which inhibition efficacy falls, which suggested the adsorption was maximum at two hours of dipping time.

4.2 Adsorption and kinetic study of corrosion

This chapter focuses on the assessment of several kinetic and adsorption parameters that are important in corrosion process. Thermodynamic and kinetic parameters are necessary to understand the mode by which the inhibitor is adsorbed on the surface of metal in order to achieve corrosion mitigation, and adsorption isotherms are used to gather information on the mechanism of adsorption in order to achieve corrosion mitigation (Ateya et al., 1984; Bockris, & Yang, 1999; Behpour et al., 2008; Dabrowski, 2001; Emregul & Hayvali 2006; Noble et al., 2004; Mohammed et al., 2012; Peme et al., 2015). The different types of adsorption isotherms that can be used for the current investigations are discussed briefly in this chapter. Correlation has been established between the parameters acquired from thermodynamic research and corrosion inhibition properties in order to explain how inhibitors' inhibitory capabilities are influenced by these factors. Adsorption is described as accumulation of adsorbate substances on the surface of adsorbent, and the reason for adsorption is solid surface have unsaturated forces capable of adhering to adsorbates and basically the adsorption process occurs at the interface of every system undergoing adsorption (Dabrowski, 2001; Iskandar & Selim, 1999; Ismadji et al., 2015; Noble et al., 2004). The various types of forces present on the solute surface balances the unsaturated forces present on the surface, leading to greater concentration of molecules of solute in nearby proximity of solid surface (Kanellopoulos, 2016; Negi & Anand, 1985). Adsorption of any molecule may be of two types physical adsorption and chemical adsorption and to put it simply, the binding forces between the adsorbate and its host are weaker dipole-dipole or Van der Waal forces in case of physical adsorption and strong chemical bonds are involved in chemical adsorption (Bouklah et al., 2006; Mortimer et al., 2009). This distribution of adsorbate and adsorbent on a surface can be explained by certain models of adsorption, which are briefly explained as follows:

4.2.1 Adsorption isotherms

Adsorption isotherms can help us better understand the corrosion process. Adsorption isotherms provide insight into the equilibrium between adsorbed and bulk inhibitors (Ituen et al., 2017). In the study of the sample-inhibitor interaction, adsorption isotherms are an important tool. Adsorption is validated if the surface coverage statistics

fit in any isotherm (Awe et al., 2015; Gouy,1910). The isotherm should be illustrated as a straight line on a graph and the regression coefficient should be unity, further adsorption equilibrium constant (K_{ads}) can be interpreted from the intercept of adsorption isotherm which is employed to find out the value of free energy (Akinbulumo et al.,2020). The general form of all isotherm is given below

$$f(\theta, x) \exp(-2a\theta) = KC \quad (4.2.1)$$

Here $f(\theta, x)$ represents configurational factor, θ and C defines surface coverage and inhibitor concentration respectively, x denotes size ration, a refers to molecular interaction and K defines equilibrium constant of the adsorption process (Oguzie,2006; Umoren et al., 2008). Above mentioned equation is the basic equation from which all other isotherms utilized for the study of mechanism in corrosion process are derived. Important Isotherms (vide Figure 4.2.1) which can be effectively employed for corrosion studies, are as follows (Oguzie,2007).

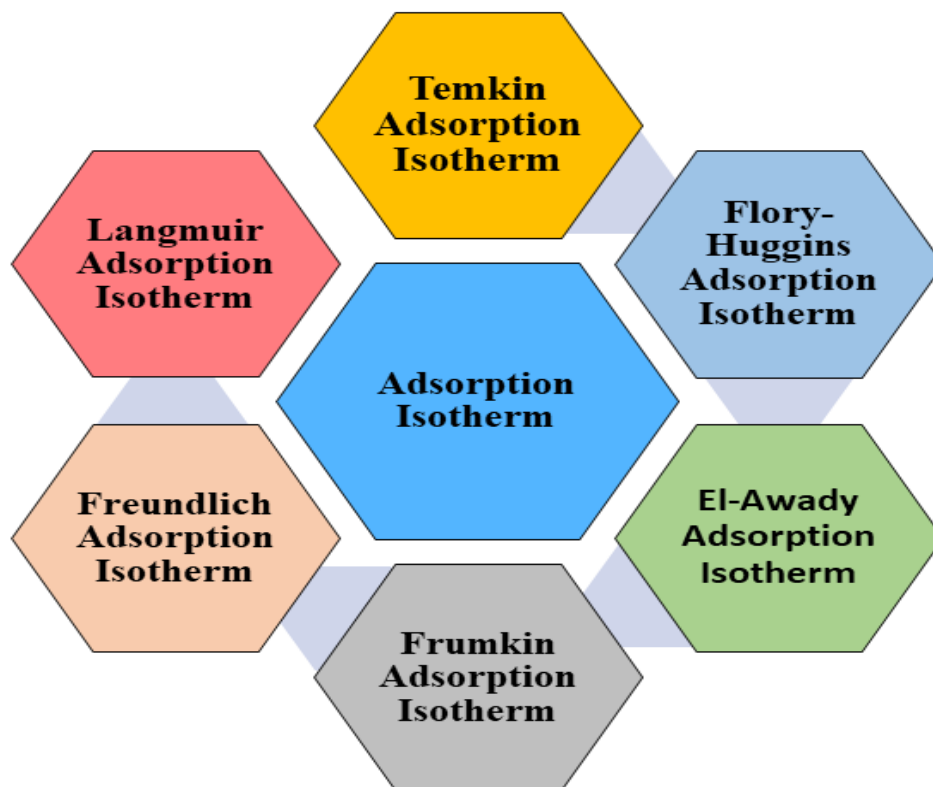


Figure 4.2.1 Adsorption Isotherms

4.2.1a Langmuir adsorption isotherm

In 1916, Irving Langmuir presented adsorption isotherm which explained relationship of adsorption with pressure. It gives the idea about the dynamic equilibrium that exist between inhibitor (adsorbate) and metal surface (adsorbent). Main assumptions of this isotherm are as follows (Atkin et al., 2018).

A particular number of adsorption sites with same size are present on the surface of adsorbent. Only one molecule is allowed to adsorb and constant heat liberation is there. Equilibrium is supposed to be dynamic in nature.

Langmuir suggested a quantitative relationship between the fractional surface coverage (θ) and inhibitor (adsorbate) concentration (C) as a result of a dynamic equilibrium pertaining between adsorption and desorption processes between surface of metal and the inhibitor molecules (Liu et al., 2019). and is given by the equation

$$C_{inh}/\theta = 1/K_{ads} + C_{inh} \quad (4.2.2)$$

' K_{ads} ' here refers to equilibrium constant in the adsorption process (El-Etre et al., 2016). Graph is plotted between $\log C/\theta$ versus $\log C$ and if adsorption obeyed Langmuir isotherm, it should give a straight line with unity value regression coefficient (R^2) (Abdallah et al., 2016; Fouda et al., 2016; Hegazy et al., 2013; Yadav et al., 2016).

4.2.1b Freundlich adsorption isotherm

Heterogeneous adsorption can be characterised by the Freundlich adsorption isotherm, which was first suggested by Freundlich in 1906. And in this isotherm concentrations of adsorbed inhibitor and inhibitor presented in solution are compared. Following equation can be used to express it mathematically (Abdallah et al., 2016; Bockris et al., 1998; John & Joseph, 2012; liu et al., 2019; Oguzie, 1998; Singh et al., 2019; Singh et al., 2019; Shalabi et al., 2014; Timbola et al., 2007; Valek & Martinez 2007).

$$\theta = K_{ads} \cdot C^{\frac{1}{n}} \quad (4.2.3)$$

Here, n should be between 0 and 1, further K_{ads} , θ and C denotes equilibrium constant, surface coverage and concentration respectively. Equation on taking log can be written as

$$\log \theta = \log K_{ads} + \frac{1}{n \log C} \quad (4.2.4)$$

Graph is drawn between $\log \theta$ vs $\log C$ and should be straight line with correlation coefficient (R^2) near to 1, if adsorption has to be in accordance with Freundlich adsorption isotherm.

4.2.1c Frumkin adsorption isotherm

It is one of the oldest isotherms that deals with lateral interactions between the adsorbed species and can be expressed as

$$\theta/1 - \theta \exp(-2a\theta) = K_{ads} \cdot C \quad (4.2.5)$$

Here ‘ a ’ is a term expressing interaction and can also measure steepness for adsorption isotherm. Adsorption will obey only if graph gave a straight line (plot between $\log(\theta/C \cdot (1 - \theta))$ and θ), with near to unity correlation coefficient value (Christov & Popova, 2004; El-Awady et al., 1992; Hosseini et al., 2003; Martinez & Stern, 2002; Abd El-Rehim et al., 2001; Volkova-Gugeshashvili et al., 2006; Yurt et al., 2004).

4.2.1d Temkin adsorption isotherm

Temkin isotherm divides the whole surface under investigation in to small patches and then Langmuir adsorption isotherm was obeyed at each part if applied also it is applicable on heterogeneous surface with no interactions are supposed to exist. Temkin adsorption isotherm is expressed with the help of following equation

$$\text{Exp}(-2a\theta) = K_{ads} C \quad (4.2.6)$$

Where ‘ a ’ signifies inhomogeneity factor; K_{ads} is adsorption equilibrium constant. Equation can also be written as

$$\theta = -2.303(\log C)/2a - 2.303(\log K_{ads})/2a \quad (4.2.7)$$

Adsorption followed this isotherm if the plot between θ vs $\log C$ resulted into a straight line with R^2 value equal to one (Bansal & Goyal, 2005; Durnie et al., 2001; Horsman et al., 2013; Khamis et al., 1991; Petchiammal et al., 2012; Abd El-Rehim et al., 2001).

4.2.1e Flory-Huggins adsorption isotherm

In this isotherm the size of the ions and dispersion forces has significant effect along with the assumption that water molecules are replaced with inhibitor present in the solution and is given by the expression as follows

$$\theta/C = K_{FH} (1-\theta)^{\chi^{FH}} \quad (4.2.8)$$

Where θ indicates coverage value, C refers to concentration; K_{FH} defines equilibrium adsorption constant and χ^{FH} signifies number of desorbed water molecules. Another form of isotherm can be written as

$$\text{Log } \theta/C = \text{log } K_{FH} + X_{FH} \text{log}(1-\theta) \quad (4.2.9)$$

Straight line with R^2 equal to one, confirmed the adsorption of inhibitor obeyed follow Flory-Huggins adsorption isotherm (Abdel-Gober et al.2009; El-Awady et al., 1992; Karthikaiselvi & Subhashini, 2014; Oguzie et al.2004; Omotosho et al., 2016).

4.2.1f El-Awady adsorption isotherm

The Langmuir isotherm was modified and was named as El-Awady adsorption isotherm and can be expressed as

$$\text{Log } \theta/(1-\theta) = \text{log } K + Y \text{log } C \quad (4.2.10)$$

Where Y refers to adsorbed inhibitor molecules, θ and C signifies coverage and concentration respectively and K denotes equilibrium constant (Bentiss et al., 2005; Flis & Zakroczymski, 1996; Obot et al., 2009; Shriver et al., 1994).

4.2.2 Calculation of thermodynamic and kinetic parameters from adsorption study

Adsorption studies can be used to estimate thermodynamic and kinetic parameters. Parameters that are calculated in this study are Enthalpy of Adsorption (ΔH^0_{ads}), Gibbs Free Energy of Adsorption (ΔG^0_{ads}), and Entropy of Adsorption (ΔS^0_{ads}) and the Activation Energy (E_a) etc. First the behaviour of inhibitor molecule is estimated by using various adsorption isotherm. Surface coverage measurements were used to

determine the adsorption of inhibitors on the sample surface. Then the isotherm with straight line and with regression coefficient nearly equal to zero is selected as best fit isotherm.

4.2.2a Equilibrium constant of adsorption

Equilibrium constant of adsorption (K_{ads}) can also be calculated from the surface coverage data as follows

$$K_{ads} = \frac{\theta}{(1-\theta)c} \quad (4.2.11)$$

Here θ refers to surface coverage and C refers to concentration (Chaudhari & Patel, 2019; Eddy & Ebenso, 2010; Karthikeyan & Jeeva, 2019).

4.2.2b Gibbs free energy of Adsorption

The value of Gibbs free energy has a direct impact on adsorption, as well. The formula to calculate the Gibbs free energy has been given as follows

$$\Delta G_{ads}^0 = -RT \ln (55.5K_{ads}) \quad (4.2.12)$$

where 55.5 M refers as molar concentration of water in the solution, R is gas constant and T denote temperature (Ameh & Sani, 2015; Bashir et al., 2018).

4.2.2c Calculation of activation energy

Activation energy by employing the Arrhenius equation

$$\log CR = \frac{-E_a}{2.303RT} + \log A \quad (4.2.13)$$

Where CR and E_a signifies corrosion rate and activation energy respectively, R and A are the constants (gas and Arrhenius constant respectively) (Bashir et al., 2020; Desai et al., 2015; Vinutha et al., 2018).

4.2.2d Enthalpy of the Adsorption

Enthalpy of the adsorption (ΔH_{ads}^0) was determined by utilizing Van't Hoff equation, which is as follows

$$d \ln K_{ads} / dT = \Delta H_{ads}^0 / RT^2 \quad (4.2.14)$$

Equation can also be rewritten after taking the log as follows

$$\log K_{ads} = -\Delta H^0_{ads}/2.303RT + D \quad (4.2.15)$$

Here, D denote disintegration constant, T and R refers to absolute temperature and gas constant (8.314J/K/mol) respectively. The plot of $\log K_{ads}$ vs $1/T$ with straight line and slope is equal to $\Delta H/2.303R$, and from the value of slope enthalpy is calculated.

4.2.2e Entropy of Adsorption

Entropy values are calculated by using the following equation

$$\Delta G_{ads} = \Delta H_{ads} - T\Delta S_{ads} \quad (4.2.16)$$

Here ΔG_{ads} , ΔH_{ads} , are the free energy of adsorption and enthalpy (Bashir et al., 2020; Desai et al., 2015; Vinutha et al., 2018).

4.2.3 Estimation of kinetic and adsorption variables for MS using Baclofen

Baclofen was employed as corrosion inhibitor and various thermodynamic and kinetic parameters were measured by utilizing equations from 4.2.2- 4.2.16 and measured values are summed up in Table 4.2.1 and various graphs were represented in Figure 4.2.2(a-d). Surface coverage data extracted from weight loss investigations was used and various isotherm were checked to investigate adsorption of Baclofen on the surface of the sample and results revealed that the adsorption was best fitted in Langmuir adsorption isotherm ($\log (C/\theta)$ vs. $\log C$, vide Figure 4.2.2a) as straight line with slope 0.93 and regression coefficient (R^2) 0.99 was obtained. It was mentioned in the literature that if the values of $\Delta G^0_{ads} < -20$ kJ/mol, the inhibitor is supposed to be physically adsorbed on sample and if value lies higher than - 40 kJ/mol, inhibitor follows chemisorption (Kumar et al., 2021; Obot et al., 2010). ΔG^0_{ads} measured in the study of corrosion inhibitive property of Baclofen revealed the chances of physical adsorption and the negative sign of ΔG^0_{ads} confirmed the spontaneity of reaction (Abdallah et al., 2019; Chen et al., 2021). Langmuir fit also indicated the chances of physical adsorption and the negative enthalpy values validates the exothermic nature of the reaction (Abdallah et al., 2019). Baclofen inhibited solutions had the largest

activation energy compared to the blank solution, which proved the presence of Baclofen on the MS sample, which was reducing corrosion.

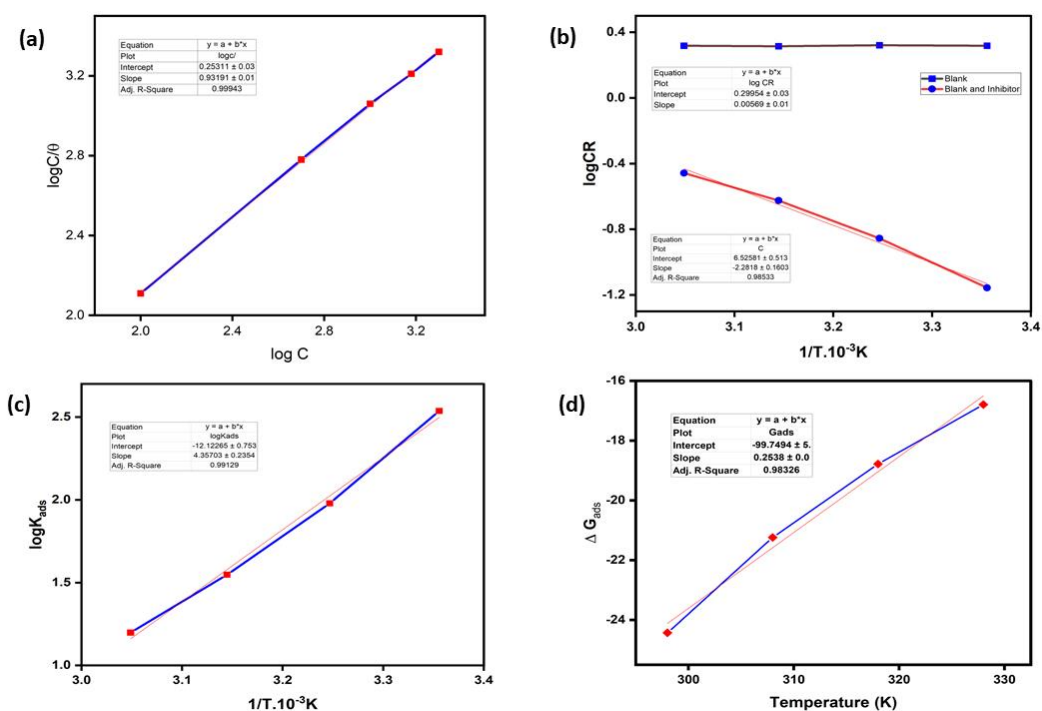


Figure 4.2.2 (a- d) Graphical presentation of (a) Langmuir isotherm, (b) plot between $1/T$ vs $\log CR$ (c) plot between $\log K_{ads}$ vs $1/T$, (d) plot of ΔG_{ads} vs T .

Table 4.2.1 Thermodynamic parameters calculated for Baclofen as inhibitor in MS corrosion.

Metal	Inhibitor	Temp.	K_{ads}	ΔG_{ads}^0	ΔH_{ads}	E_a	ΔS_{ads}
	Conc. (ppm)	(K)		$KJmol^{-1}$	$KJmol^{-1}$	$KJ mol^{-1}$	$KJ mol^{-1} K^{-1}$
mild steel	Blank					0.1	
		298	344.10	-24.43			0.25
	2000 ppm	308	95.24	-21.24	-0.04	43.66	
		318	35.30	-18.78			
		328	15.78	-16.79			

4.2.4 Estimation of kinetic and adsorption variables for MS using Betahistine dihydrochloride as inhibitor.

Betahistine dihydrochloride was used as an inhibitor, and adsorption isotherms were used to study the interaction between metal and the inhibitor. Isotherms given in Figure 4.2.3a, were constructed using weight loss data (surface coverage) and proved to be in accordance with the Langmuir isotherm with the regression coefficient (R^2) value 0.999 and slope value 0.942 which are almost unity (Shukla et al., 2009). Other calculated variables and graphical presentations are mentioned in Table 4.2.2 and Figure 4.2.3.(b-d).

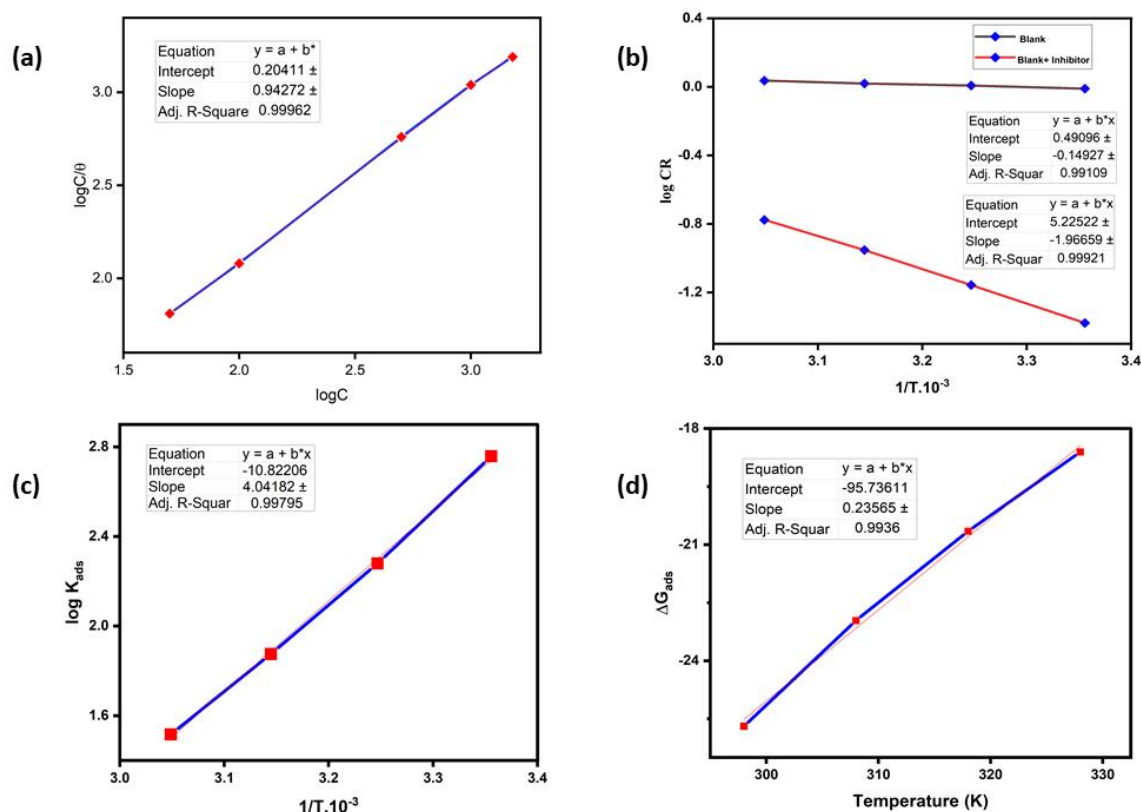


Figure 4.2.3 (a- d) Graphical presentation of (a) Langmuir isotherm, (b) plot between $1/T$ vs $\log CR$ (c) plot between $\log K_{ads}$ vs $1/T$, (d) plot of ΔG_{ads} vs T .

Negative ΔG_{ads}^0 relates to the spontaneity of adsorption and as the value of free energy of adsorption lies between -20 to -40 KJ/mol, presence of both physical and chemical

adsorption but with the dominance of physical adsorption was confirmed (Hussin & Kasim, 2011; Odewunmi et al., 2015a, b). In this study, both types are present but the physical adsorption dominated the nature of adsorption. A rise in solvent entropy was validated when the entropy value was found to be positive. Physical adsorption of Betahistine dihydrochloride on the sample is indicated by the higher activation energy of the inhibited solution compared to the blank solution (Chaudhari & Patel, 2019).

Table 4.2.2 Thermodynamic parameters calculated for Betahistine dihydrochloride.

Metal	Inhibitor Conc. (ppm)	Temp. (K)	K_{ads}	ΔG^0_{ads} KJmol⁻¹	ΔH_{ads} KJmol⁻¹	E_a KJ mol⁻¹	ΔS_{ads} KJ mol⁻¹ K⁻¹
mild steel	Blank	298	573.52	-25.69		2.68	
	1500 ppm	308	190.49	-22.96	- 0.03	37.72	0.23
		318	75.02	-20.65			
		328	32.87	-18.61			

4.2.5 Estimation of kinetic and adsorption variables for MS using Isoxsuprine hydrochloride as inhibitor.

Various calculated parameters when Isoxsuprine hydrochloride was used as inhibitor are summed up in Table 4.2.3 and Figure 4.2.4 (a-d). Adsorption isotherms were used to evaluate how Isoxsuprine hydrochloride interacted with MS (Zhang et al., 2020). Adsorption was according to Langmuir adsorption isotherms with regression coefficient value (R^2) 0.999 and slope value 0.959. Value of K_{ads} decreased with the rising temperature and was maximum at at 298 K, which depicted the high corrosion reducing tendency of Isoxsuprine hydrochloride at (Albrimi et al.,2015; Dehghani et

al.,2019; El- Deeb et al., 2018; Singh et al., 2013; Verma et al., 2019; Zheng et al., 2018). At 298 K value of ΔG_{ads}^0 confirmed the presence of both physical and chemical adsorption. Further the negative value of enthalpy and positive entropy value confirmed the exothermic and increased entropy respectively due adsorption of Isoxsuprine hydrochloride (Popova, 2007). Increased activation energy value on the addition of drug molecule also confirmed the slowing down of corrosion process.

Table 4.2.3 Thermodynamic parameters for Isoxsuprine hydrochloride investigation.

Sample	Isoxsuprine Conc. (ppm)	Temp. (K)	K_{ads}	ΔG_{ads}^0 KJmol ⁻¹	ΔH_{ads} KJmol ⁻¹	E_a KJ mol ⁻¹	ΔS_{ads} KJ mol ⁻¹ K ⁻¹
mild steel	Blank	298	772.65	-26.43	- 0.03	-3.45 36.0	0.23
		308	280.78	-23.92			
	2000 ppm	318	99.52	-21.35			
		328	44.32	-19.35			

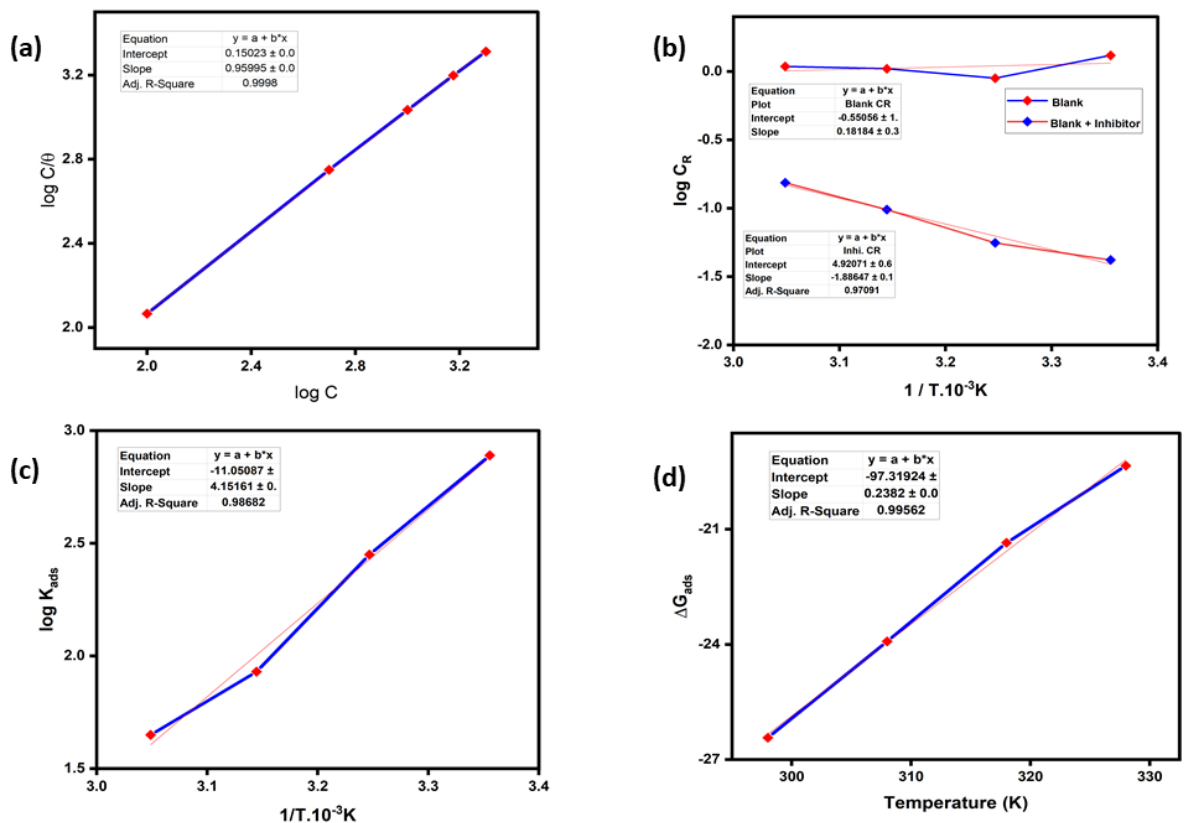


Figure 4.2.4 (a- d) Graphical presentation of (a) Langmuir isotherm, (b) plot between $1/T$ vs $\log C_R$ (c) plot between $\log K_{ads}$ vs $1/T$, (d) plot of ΔG_{ads} vs T .

4.2.6 Estimation of kinetic and adsorption variables for MS using Panthenol as corrosion inhibitor.

Study was performed by using Panthenol as corrosion reducing agent in order to find out the thermodynamic and kinetic parameters and all the calculated variables are summed up in Table 4.2.4 and pictorial presentations are given in Figure 4.2.5 (a-d). Adsorption was best fitted in Langmuir adsorption isotherm, which was confirmed from the regression coefficient and slope value (Hossam et al.,2021) Further, the Value of K_{ads} was highest at 298 K, which showed that on increasing the temperature the corrosion mitigation capacity of Panthenol showed a downfall (Yadav et al., 2016). Further negative value of ΔG_{ads}^0 and negative value of ΔH_{ads} confirmed the spontaneous and exothermic nature (Abdallah et al., 2021; Cao et al., 2019). Value of activation energy calculated for acid and optimized concentration of Panthenol was higher than

the value calculated for pure acid solution, which claimed the successful mitigation of corrosion.

Table 4.2.4 Thermodynamic parameters for Panthenol used as inhibitor.

Metal	Inhibitor Conc. (ppm)	Temp. (K)	K_{ads}	ΔG^0_{ads} KJmol ⁻¹	ΔH_{ads} KJmol ⁻¹	E_a KJ mol ⁻¹	ΔS_{ads} KJ mol ⁻¹ K ⁻¹
mild steel	Blank					29.67	
		298	241.62	-23.55			
	400 ppm	308	45.14	-20.04	- 0.05	62.99	0.26
		318	10.51	-16.84			
		328	5.97	-15.83			

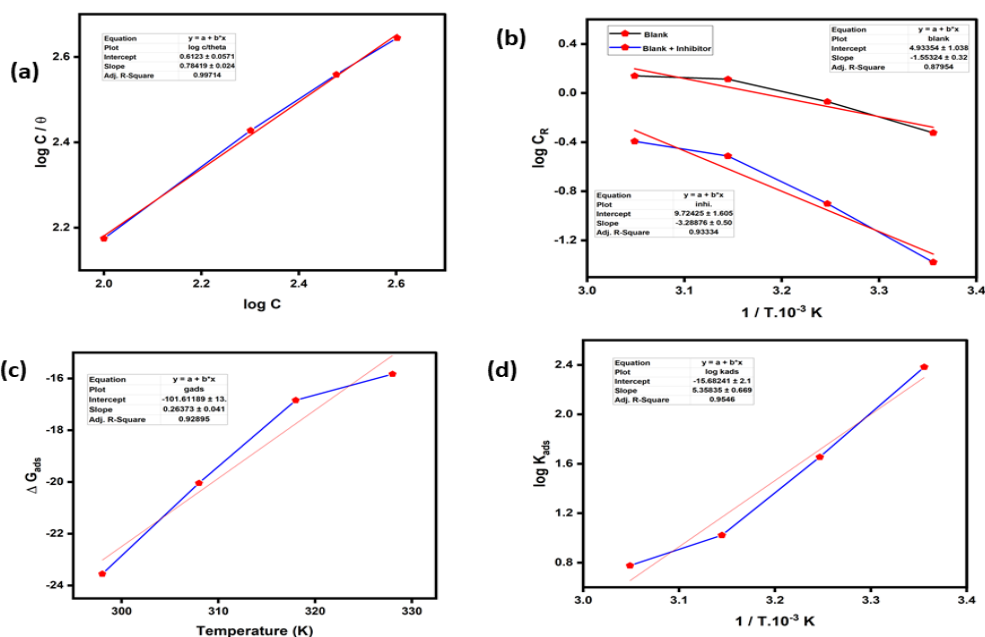


Figure 4.2.5 (a- d) Graphical presentation of (a) Langmuir isotherm, (b) plot between $1/T$ vs $\log C_R$ (c) plot of ΔG_{ads} vs T (d) plot between $\log K_{ads}$ vs $1/T$.

4.2.7 Estimation of kinetic and adsorption variables for MS using Naphazoline as corrosion inhibitor.

Fifth drug molecule investigated for the corrosion inhibition properties was Naphazoline and all the thermodynamic and kinetic parameter are summed up in Table 4.2.5 and graphically presented in Figure 4.2.6 (a-d). Adsorption was best fitted in Langmuir isotherm with R^2 value of 0.99 and slope 0.93 (Tan et al. 2020). Further, Values of K_{ads} showed a dip with the increased temperature, which depicted the decreased inhibition efficacy with the increased temperature. Again, by using the value of K_{ads} , the free energy values were calculated and at all the selected temperatures, the values came out to be negative, which validated the spontaneous nature and also the negative value of enthalpy of adsorption confirmed the exothermic nature (Abdallah et al., 2021; Tasic et al., 2021). Further, the value of ΔG_{ads}^0 at 298 K lies between -20KJ/mol to -40 KJ /mol, that confirmed that the naphazoline adsorbed on metallic surface both physically and chemically. Arrhenius equation was employed to find out the value of activation energy, which came out to be higher in case of Naphazoline dissolved in the test solution as compare to the activation energy value of pure acid solution. This showed the formation of layer of Naphazoline on the top of metal, which mitigates the corrosion of sample.

Table 4.2.5 Thermodynamic parameters for Naphazoline used as inhibitor.

Metal	Inhibitor Conc. (ppm)	Temp. (K)	K_{ads}	ΔG_{ads}^0 KJmol⁻¹	ΔH_{ads} KJmol⁻¹	E_a KJ mol⁻¹	ΔS_{ads} KJ mol⁻¹ K⁻¹
mild steel	Blank	298	386.33	-24.71		-0.48	
	1500 ppm	308	112.31	-22.38	- 0.02	25.27	0.14
		318	49.76	-20.95			
		328	32.50	-20.44			

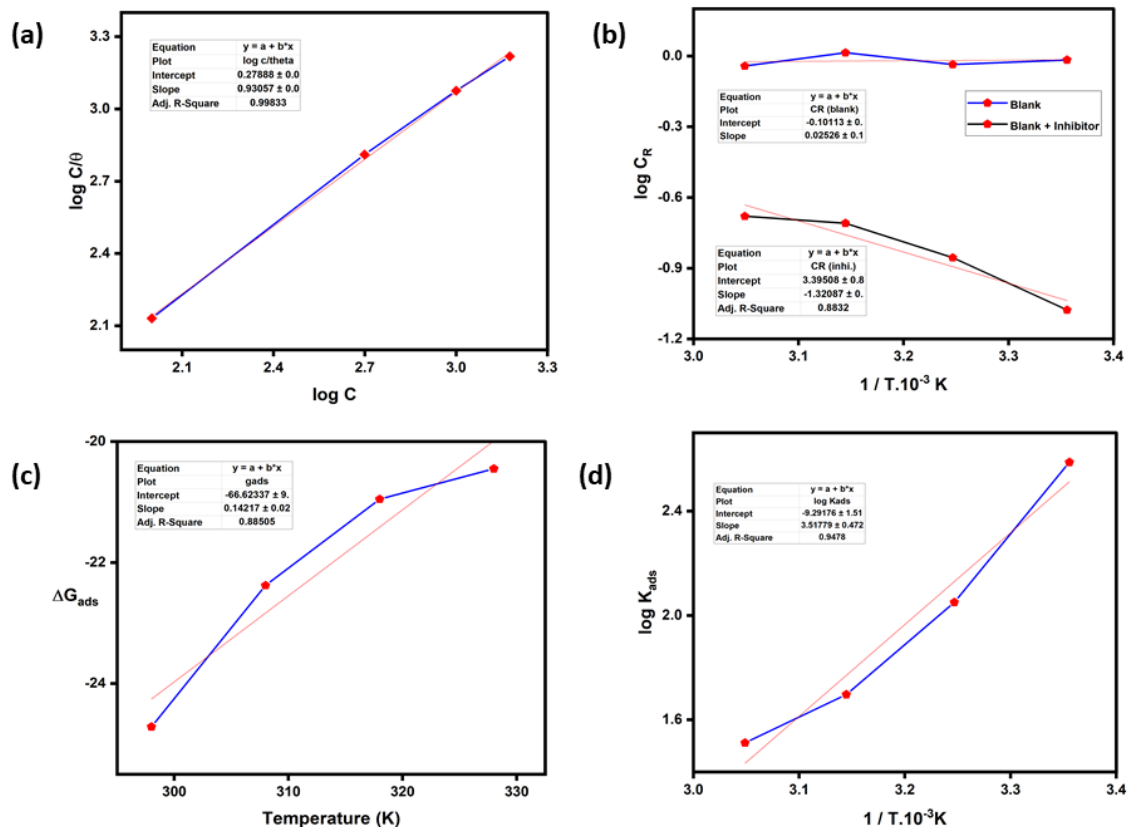


Figure 4.2.6 (a- d) Graphical presentation of (a) Langmuir isotherm, (b) plot between $1/T$ vs $\log CR$ (c) plot of ΔG_{ads} vs T (d) plot between $\log K_{ads}$ vs $1/T$.

4.2.8 Estimation of kinetic and adsorption variables for MS using Dicyclomine hydrochloride as corrosion inhibitor.

Dicyclomine was selected as inhibitor molecule to investigate its capacity to mitigate the corrosion of MS. Adsorption of Dicyclomine hydrochloride was according to Langmuir adsorption isotherm as regression coefficient value (0.99) was nearly equal to unity (Guo et al., 2019). All the calculated parameters are summed up in Table 4.2.6 and graphs are shown in Figure 4.2.7 (a-d). Further K_{ads} value was highest at 298 K and decreased with the rise in temperature, it confirmed the decreased inhibition efficacy

with the increase in temperature. Also, on the basis of K_{ads} , free energy values were calculated, the value was -26.12 KJ /mol, which confirmed that Dicyclomine hydrochloride was present on the metal through physical forces as well as chemical forces. Further negative free energy value, negative enthalpy of adsorption value, and positive entropy value confirmed the spontaneity, exothermic nature and increased entropy respectively (Popova, 2007). Activation energy calculations depicted the high value of inhibitor containing solution, which confirmed the formation of thin layer of Dicyclomine hydrochloride on the metal, resulted in excellent reduction in corrosion (Chaudhari & Patel,2019).

Table-4.2.6 Thermodynamic and kinetic parameters for Dicyclomine hydrochloride used as inhibitor.

Metal	Inhibitor Conc. (ppm)	Temp. (K)	K_{ads}	ΔG^0_{ads} KJmol⁻¹	ΔH_{ads} KJmol⁻¹	E_a KJ mol⁻¹	ΔS_{ads} KJ mol⁻¹ K⁻¹
mild steel	Blank	298	681.75	-26.12		0.76	
	1500 ppm	308	140.39	-22.95	- 0.03	39.63	0.18
		318	58.06	-21.36			
		328	32.50	-20.44			

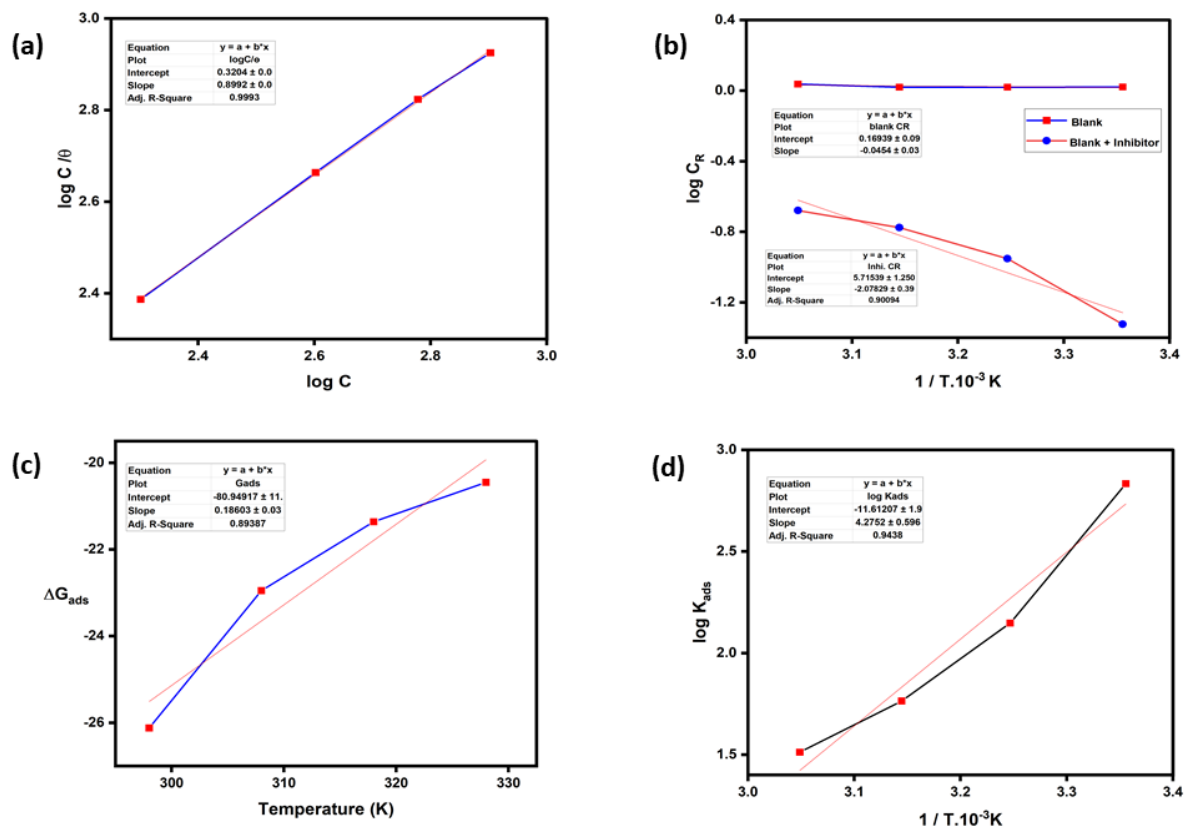


Figure 4.2.7 (a- d) Graphical presentation of (a) Langmuir isotherm, (b) plot between $1/T$ vs $\log C_R$ (c) plot of ΔG_{ads} vs T (d) plot between $\log K_{\text{ads}}$ vs $1/T$.

4.2.9 Conclusions

. The conclusions that can be drawn from the above discussion are as follows

- Langmuir isotherm was obeyed by adsorption of all the six investigated drug molecules. A straight line with the regression coefficient almost equal to unity which shows the formation of monolayer on metal surface.
- High values of K_{ads} gave an idea about strong interaction between sample under investigation and inhibitor molecules, which resulted in high corrosion mitigation of sample.
- ΔG^0_{ads} values suggest that almost all the inhibitor molecules adsorbed physically as well as chemically on the metallic surface; their negative sign depicted the spontaneity of process.
- Enthalpy value came out to be negative, which suggested the exothermic nature of adsorption.
- The adsorption of all the six inhibitors on metal surface is favoured by entropy (positive value). Therefore, spike in system randomness is caused by the adsorption of inhibitor molecules onto metal surfaces as well as desorption of water from metal surfaces.
- Higher activation energy values suggest the when inhibitors are there in the test solution, confirmed rise in energy barrier formation, therefore more energy will be required in order to continue the corrosion.

4.3 Electrochemical Impedance Spectroscopy

Electrochemical impedance spectroscopy (EIS) is one of the most potent techniques for assessing the electrical characteristics of metallic materials. In this chapter main parameters like charge transfer resistance, double layer capacitance are evaluated by employing EIS and were used to find out the inhibition efficiency of the selected inhibitors. A comprehensive explanation of the overall electrochemical mechanism involved in the process of corrosion of metals is provided in this chapter.

EIS is a very effective, non-destructive measurement technique to find out the electric nature of sample under study by applying the low amplitude AC voltage (which is a function of frequency). Therefore, the basic principle of EIS is that external potential is applied to check the behaviour of electrochemical cell under investigation. Three electrode assembly is used which includes working, counter and reference electrodes, and voltage is applied, after that quantitative data produced is then used to get insight in to mechanism of the process (Barsoukov& Macdonald,2018; Lasia, 2002; Prakash et al., 2006). Based on the following postulates, Impedance explains the complicated nature of working electrode (Magar et al., 2021)

- It is not possible to apply Ohm's law at all voltages and currents.
- Impedance is the frequency dependent resistance value.
- Impedance is the proportionality factor between AC current and voltage signals.

Current produce after the application of AC voltage, is again comes in the form of sinusoidal wave (vide Figure 4.3.1) of same frequency but the phase and amplitude may vary (Fliu,2020).

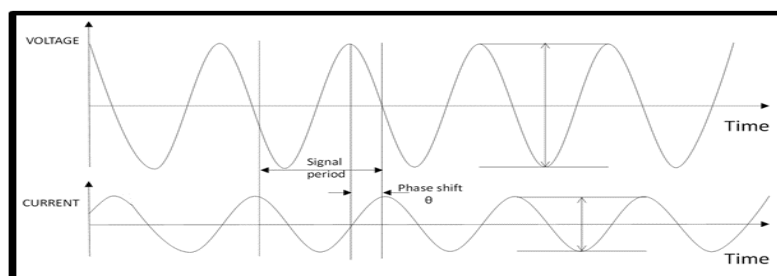


Figure 4.3.1 Current and voltage waves as a function of time. Source: Adapted from the reference (Fliu, 2020).

The excitation signals are given as follows

$$E_t = E_0 \sin(\omega t) \quad (4.3.1)$$

$$\omega = 2\pi f \quad (4.3.2)$$

$$I_t = I_0 \sin(\omega t + \phi) \quad (4.3.3)$$

Where E_t refers to potential at time t , E_0 define amplitude, ω and f refers to radial frequency and frequency. I_t is current shifted to phase (ϕ) with amplitude, I_0 .

Further, Impedance which is a complex number and is calculated as follows

$$Z(\omega) = \frac{E}{I} = Z_0 \exp(j\phi) = Z_0(\cos \phi + j \sin \phi) \quad (4.3.4)$$

Here equation 4.3.4 comprises of real and imaginary parts and when real part is taken on x-axis and imaginary part is taken on y-axis for a plot (as given in Figure 4.3.2), then this plot is called as Nyquist Plot (Ins, 2007).

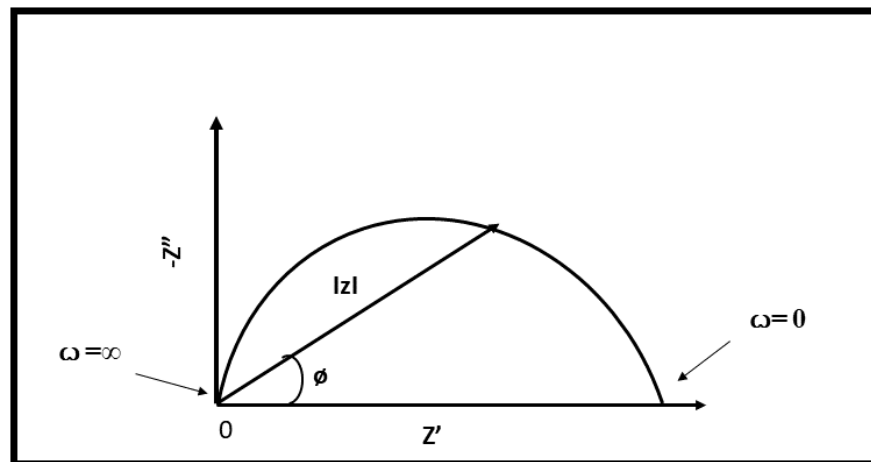


Figure 4.3.2 Nyquist Plot

Unavoidably, there is a flaw in Nyquist plots. There is no way to tell by looking at the plot which frequency was applied to record any particular data point. The data obtained is then fitted in to the electric circuit as mentioned in Figure 4.3.3.

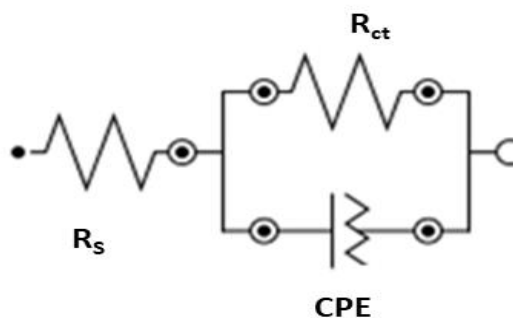


Figure 4.3.3 Simplest circuit diagram.

In order to overcome the limitation of Nyquist plot, another type of plots can be drawn and that are called as Bode plot. In the Bode plots the frequency is taken on the x-axis and $\log |Z|$ on the y-axis and second time phase angle on the y-axis as given in the Figure 4.3.4 (a-b) (Ins,2007).

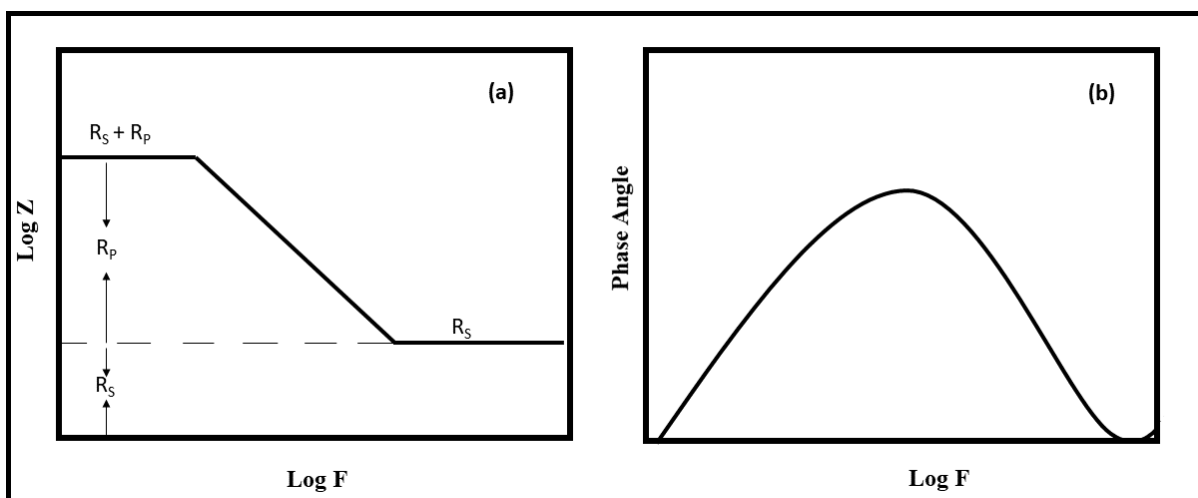


Figure 4.3.4 (a-b) Pictorial presentation of Bode Plots.

4.3.1 Electrochemical impedance spectroscopic (EIS) measurements

Electrochemical impedance spectroscopy is important technique while executing electrochemical operations and examining the adsorption of chemicals on metal coupons (Baig et al., 2019). EIS Plots of various drug molecules study (Baclofen, Betahistine dihydrochloride, Isoxsuprine hydrochloride, Panthenol, Naphazoline, Dicyclomine hydrochloride) used in the present are explained below. The EIS may be used to quantify corrosion kinetics characteristics including charge transfer resistance

and double-layer capacitance and the charge transfer resistance value can be substituted in equation 4.3.5 to evaluate corrosion mitigation capacity.

$$IE(\%) = \frac{R'_{ct} - R_{ct}}{R_{ct}} \times 100 \quad (4.3.5)$$

where R'_{ct} and R_{ct} are the charge transfer resistance when selected inhibitor is mixed with test solution and when selected inhibitor is not present in the test solution respectively (Bedir et al., 2021; Kumar et al., 2018). Double layer capacitance of every investigation including different drug molecules as inhibitors can be measured with the help of following equation 4.3.6.

$$C_{dl} = 1/2\pi f_{max} R_{ct} \quad (4.3.6)$$

Here, C_{dl} , R_{ct} , f_{max} specify double-layer capacitance and charge transfer resistance and frequency value when imaginary impedance is at its maximum respectively (Fouda et al. 2019).

4.3.2 EIS investigations of corrosion inhibition properties of Baclofen for MS in acidic medium

Figure 4.3.5 displays the Nyquist plots, which were obtained with regard to the OCP, at 298 K with varied amounts (0-2000 ppm) of Baclofen in 1M HCl, and the data derived from the measurement was then fitted in the simple Randel's circuit (Figure 4.3.5b) (Ahamad and Quaraiishi, 2010). The plots show that the concentration of 2000 ppm of Baclofen expanded the capacitive loop's diameter to its maximum, validating the sample's surface protection and it also confirmed increased Baclofen deposition layer's thickness on the MS surface (Fouda et al., 2018). Furthermore, even with the increasing amount of inhibitory molecules, semi-circular loops of the same type were present, confirming that the reaction's mechanism remained unchanged and only impedance increased and values of increased impedance are given in Table 4.3.1(Khaled & Amin, 2009). It was also visible in the diagram that semi-circular loops are not proper and are bit depressed, because of the roughness and inhomogeneity of electrode surface, which resulted in an inaccurate double layer therefore, constant phase

element (CPE) is inserted in place of double layer capacitance in the circuit diagram given in Figure 4.3.5b (Edison et al., 2018). Value of CPE/ C_{dl} (C_{dl} calculated by employing equation 4.3.6) showed a dip in the values with the enhanced concentration of Baclofen due of the MS's good adsorption of the inhibitory drug molecule (Singh et al., 2020). It is seen from Table 4.3.1 that inhibition efficiency (calculated by employing equation 4.3.5) increased with increased amount of Baclofen in selected acidic medium and was maximum 97.12% at 2000 ppm (Khaled,2008). Figure 4.3.6 (a,b) shows that phase angle and impedance rise with increasing inhibitor concentration, confirming the corrosion mitigation of MS with increased Baclofen concentration (Elabbasy & Gadow.2021).

Table 4.3.1 Electrochemical parameters calculated for varied concentration of Baclofen.

Inhibitor	Inhibitor Concentration (ppm)	CPE.Y₀ (μF cm⁻²)	CPE ,N	C_{dl} (μF cm⁻²)	R_{ct} (Ω cm²)	R_s (Ω cm²)	χ²	IE (%)
Baclofen	Acid without inhibitor	1010	0.80	393.11	12.77	1.18	0.18	
	100	720	0.79	200.66	31.59	1.41	0.14	59.57
	500	460	0.82	190.27	41.95	2.02	0.09	69.56
	1000	250	0.85	90.91	69.73	2.10	0.15	81.68
	1500	340	0.79	98.86	127.93	1.85	0.19	90.01
	2000	120	0.80	56.88	443.66	3.93	0.62	97.12

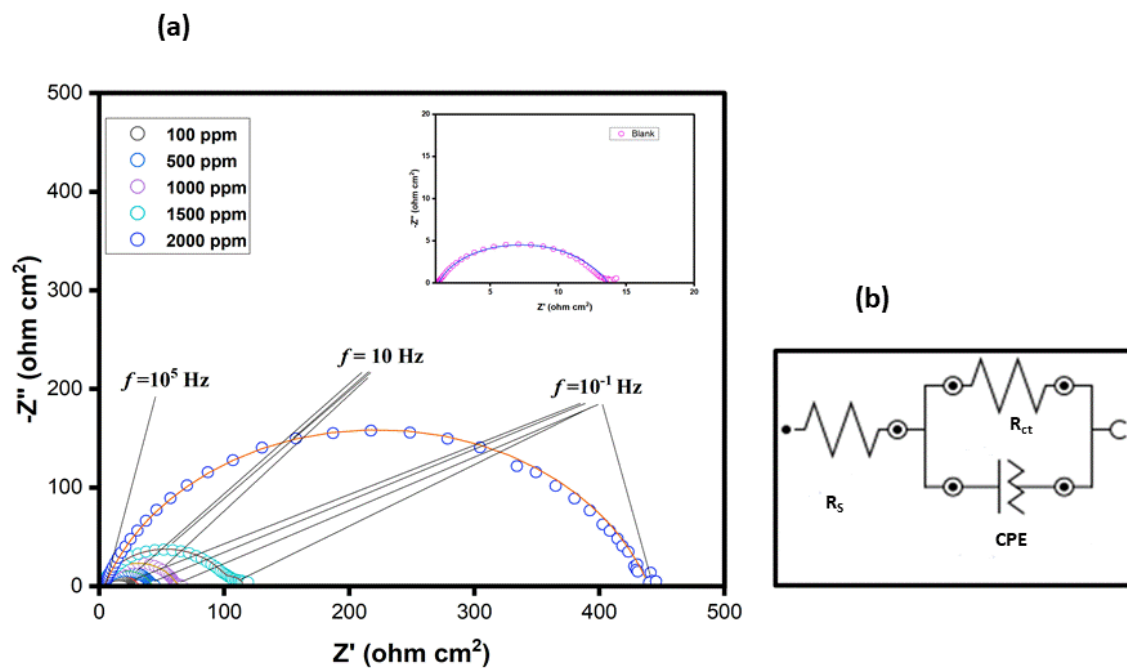


Figure 4.3.5 (a) Nyquist impedance diagram for metal in acid with different amount of Baclofen. (b) Electrical equivalent circuit.

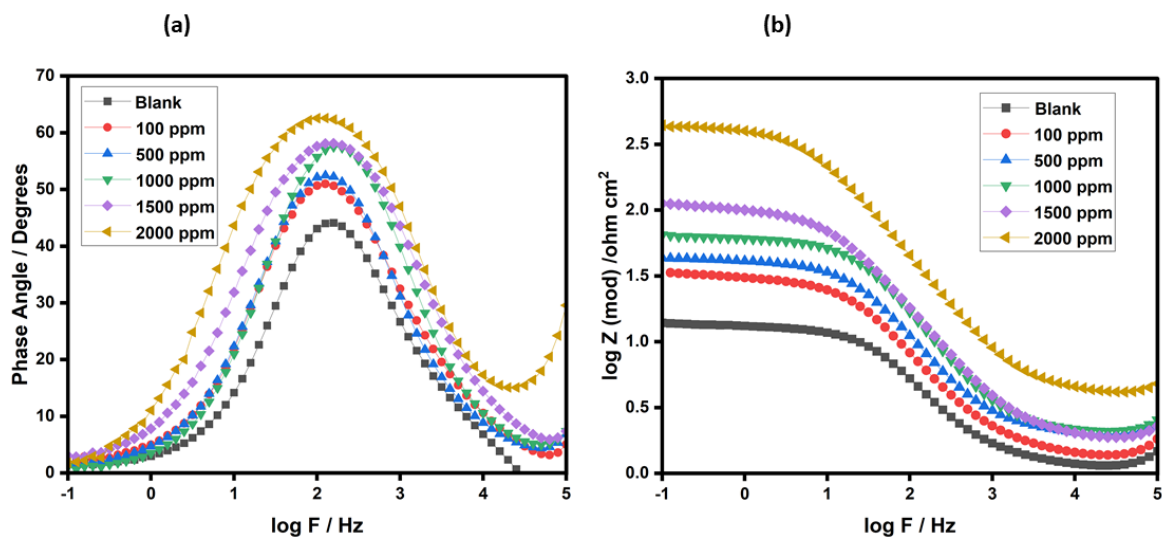


Figure 4.3.6 (a) Bode phase angle and (b) Bode modulus plots for metallic sample in acidic solution in the varied amount of Baclofen.

4.3.3 EIS investigations of corrosion inhibition properties of Betahistine dihydrochloride for MS in acidic medium

Semi-circular depressed circular loops resulted in the Nyquist plot (vide Figure 4.3.7a) confirmed the presence of charge transfer process and imperfection in the loops were resulted because of irregularity, inhomogeneity and roughness of electrodes surface (Dagdag et al., 2019; Fouda et al., 2017; Singh & Quraishi, 2011). Furthermore, with the increased amount of inhibitory drug Betahistine dihydrochloride, the increased loop size was confirmed (vide Figure 4.3.7a) and the maximum impedance value was confirmed at 1500 ppm of drug concentration (Dagdag et al., 2019; Singh & Quraishi, 2011). The Nyquist plots are then fitted in electrochemical circuit as indicated in Figure 4.3.7b. Multiple circuits can be used to fit Nyquist plots, hence no one circuit can be deemed the best match. A value of χ^2 indicates that the fitting deviation is derived from both the fitted and the actual data sets (Zhang et al., 2021). Resistance value showed a rise, C_{dl} levels dropped and the decrease in the constant phase element value was computed and summed up in Table 4.3.2 as a result of increasing concentration of drug from 50 to 1500 ppm. That was attributable to a decreased dielectric constant value, replacement of adsorbed water molecule with inhibitor molecules and increased width of double-layer, which proved the reduction of corrosion owing to the coverage of the metallic surface by a thin layer of drug molecules (Ashassi-Sorkhabi et al., 2005,2008; Ansari et al., 2016). The Bode curves are shown in Figure 4.3.8(a, b). Capacitive behaviour (vide Figure 4.3.8b) was explained in which the phase angle is smaller than 90° , which suggests that pure capacitive behaviour is lacking due to surface irregularity. However, when Betahistine concentration was increased, the value of phase angle rose, indicating that the creation of a layer of inhibitor molecules on the exposed electrode surface had successfully mitigated corrosion (Haque et al., 2017; Sundaram et al., 2021).

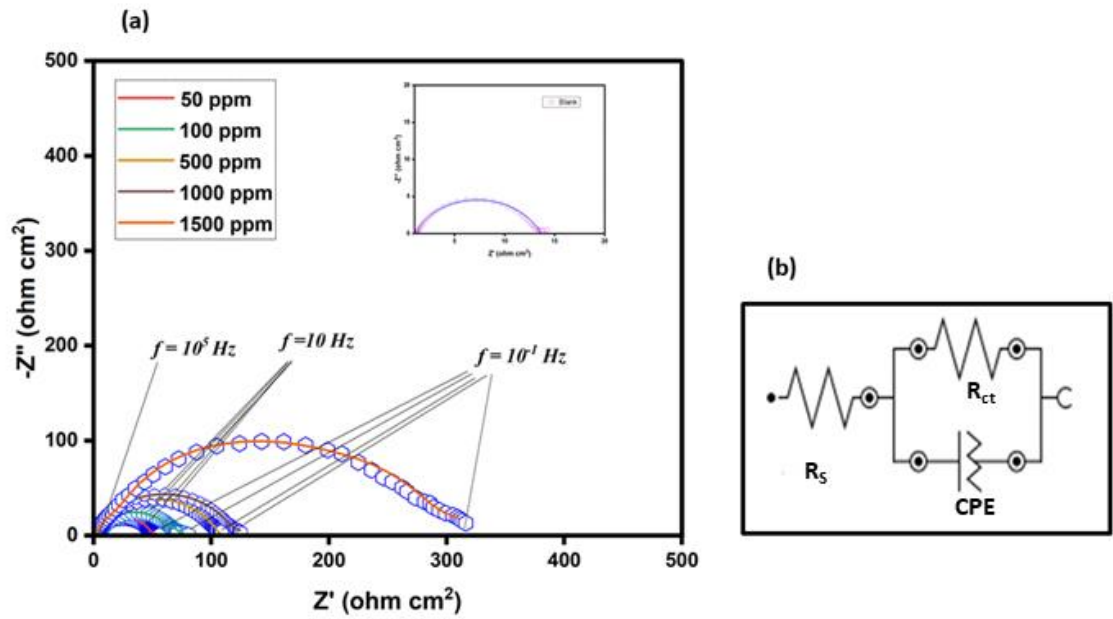


Figure 4.3.7 (a) Nyquist plots for metallic sample in acid solution with different amount of Betahistine dihydrochloride (b) Equivalent electrochemical circuit diagram.

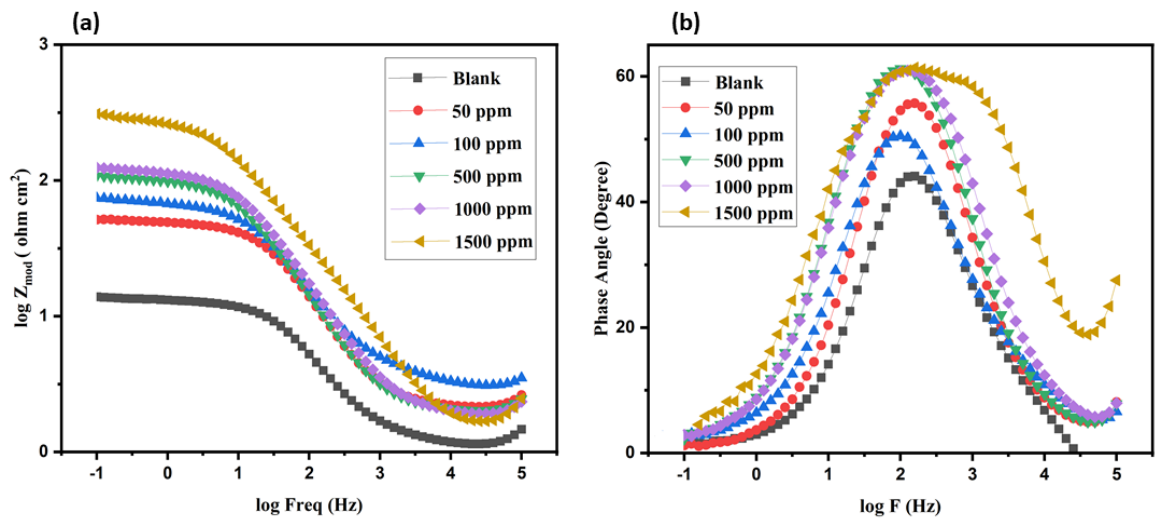


Figure 4.3.8 (a) Bode Phase angle and (b) Bode modulus plots for metallic sample in acidic solution in the varied amount of Betahistine dihydrochloride.

Table 4.3.2 Impedance parameters for mils steel soaked in varying amounts of Betahistine as an inhibitor.

Inhibitor	Inhibitor Concentration (ppm)	CPE.Y₀ (μF cm⁻²)	CPE, n	C_{dl} (μF cm⁻²)	R_{ct} (Ω cm²)	R_s (Ω cm²)	χ²	IE (%)
Betahistine	Blank	1010	0.80	390.35	12.77	1.18	0.18	
dihydrochloride	50	290	0.85	188.60	53.30	2.17	0.16	76.04
	100	470	0.76	130.03	77.31	3.16	0.19	83.48
	500	310	0.83	135.06	117.9	2.02	0.11	89.17
	1000	280	0.82	123.52	128.91	1.90	0.10	90.09
	1500	230	0.74	74.85	337.15	1.38	0.61	96.21

4.3.4 EIS investigations of corrosion inhibition properties of Isoxsuprine hydrochloride for MS in acidic medium

Nyquist vide Figure 4.3.9(a,b) and Bode plots vide Figure 4.3.10(a,b) were generated by immersing metal electrodes in an acidic solution containing Isoxsuprine hydrochloride (ranging from 0 to 2000 ppm) as an inhibitor. As the concentration of inhibitor was raised, the size of the semicircles grew (vide Figure 4.3.9a); the larger the semicircle's diameter, the more inhibition there was. However, these semicircles were imprecise because to the dispersed frequency and roughness of the exposed surface in Figure 4.3.9a (Cao et al., 2019; Tasic et al., 2021). Nyquist data was further fitted in to electric circuit shown in Figure 4.3.9b. Values incorporated in Table 4.3.3 depicted the increased value of R_{ct} with the concentration rise of Isoxsuprine hydrochloride from 0 to 2000 ppm and decreased CPE values verified the presence of an investigated drug molecule as a barrier on the surface of coupon (Hao et al., 2017; Khaled & Qahtani, 2009). On the basis of equation 4.3.5 and 4.3.6 the corrosion reducing efficiency along with double layer capacitance values were calculated and maximum efficiency depicted as 96.72% at 2000 ppm of inhibitor and also decreased C_{dl} confirmed the adsorption of Isoxsuprine hydrochloride on metal under investigation (Elkadi et al., 2000; Hameed et al., 2020).

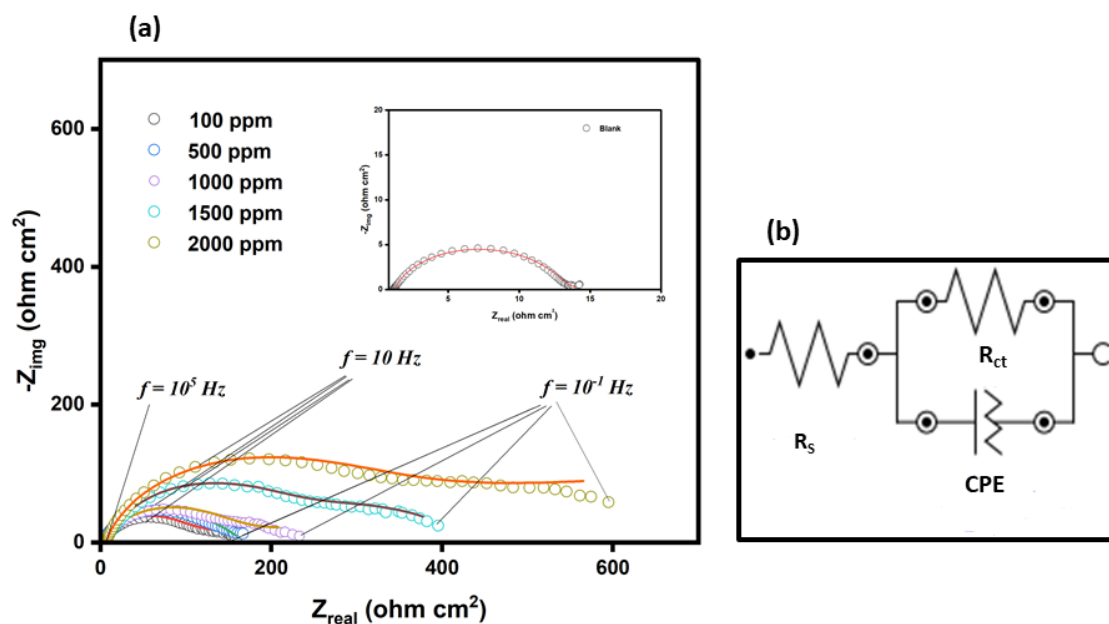


Figure 4.3.9 (a) Graphical presentation of Nyquist plot for MS with Isoxsuprine as corrosion inhibitor. (b) Equivalent circuit for electrochemical study.

Table 4.3.3 Parameters identified for varied concentration of Isoxsuprine hydrochloride with electrochemical analysis.

Inhibitor	Inhibitor Concentration (ppm)	CPE.Y ₀ (μF cm ⁻²)	CPE, n	C _{dl} (μF cm ⁻²)	R _{ct} (Ω cm ²)	R _s (Ω cm ²)	χ ²	IE (%)
Isoxsuprine hydrochloride	Acid without Inhibitor	1010	0.80	313.22	12.77	1.18	0.18	
	100	525	0.74	129.34	155.05	2.83	0.44	91.76
	500	379	0.77	122.23	164.07	2.20	0.19	92.22
	1000	469	0.72	87.41	229.42	2.96	0.60	94.43
	1500	320	0.73	64.78	389.54	5.38	0.56	96.72
	2000	259	0.75	54.05	588.03	6.11	0.89	97.83

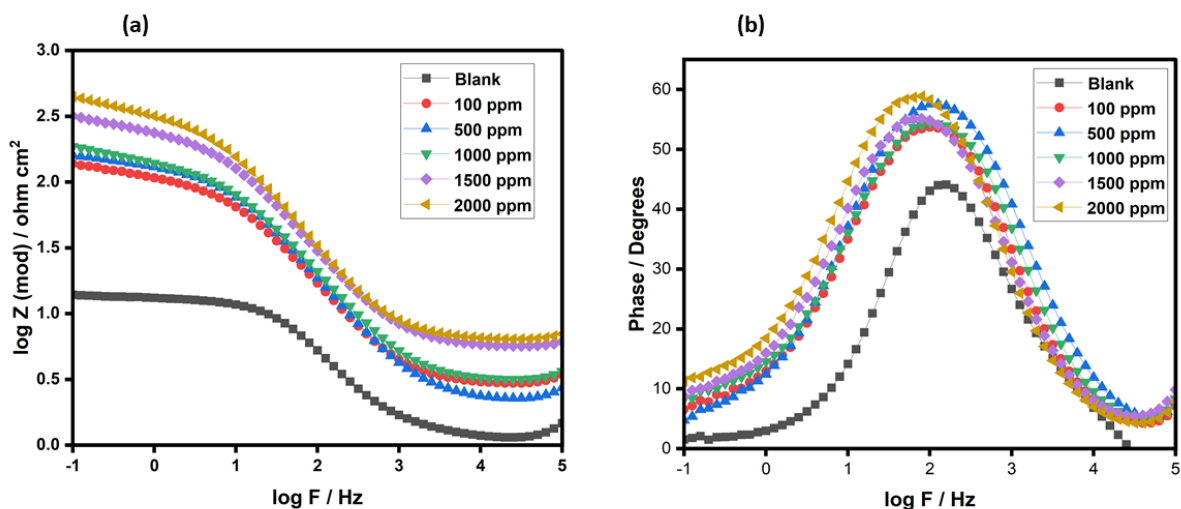


Figure 4.3.10 (a,b) Bode graphs for metal under study in HCl containing Isoxsuprine hydrochloride (0 to 2000 ppm) as inhibitor.

4.3.5 EIS investigations of corrosion inhibition properties of Panthenol for MS in acidic medium

EIS investigations were carried out to find out the inhibition efficacy of the Panthenol drug molecule, the equation 4.3.5 and 4.3.6 are employed to find out the values of inhibition efficiency and double layer capacitance. All the calculated variables are summed up in the Table 4.3.4 and Nyquist (vide Figure 4.3.11a, b) and Bode plots (vide Figure 4.3.12a, b) were also drawn with the help of data drawn from the measurements. Highest value of efficiency was 89.81% at 400 ppm of Panthenol. Also Figure 4.3.11a demonstrated the increase in the diameter of the semi-circular rings with the rise in concentration from 0 to 400 ppm, also the imperfection of these semi-circular rings was because of dispersed frequency and some surface roughness issues and because of that C_{dl} was replaced with CPE value in electric circuit drawn (Figure 4.3.11b) analogous to Nyquist data. Increased value of phase angle and impedance was also confirmed from Figure 4.3.12 (a, b) which further validated the protection of metal surface through the formation of defensive layer of drug molecules (Aslam et al., 2020; Berdimurodov et al., 2021; Xu et al., 2014).

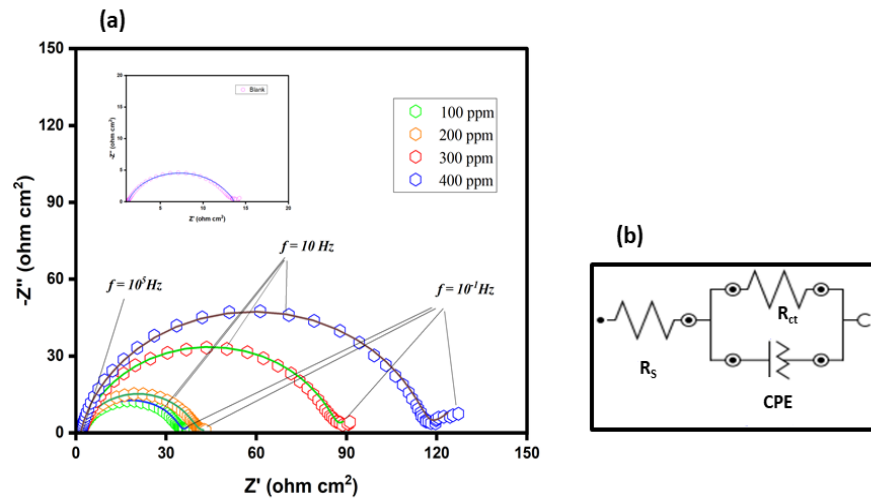


Figure 4.3.11 (a) Representation of Nyquist Plot with varied amount of Panthenol as inhibitor and **(b)** Equivalent circuit diagram.

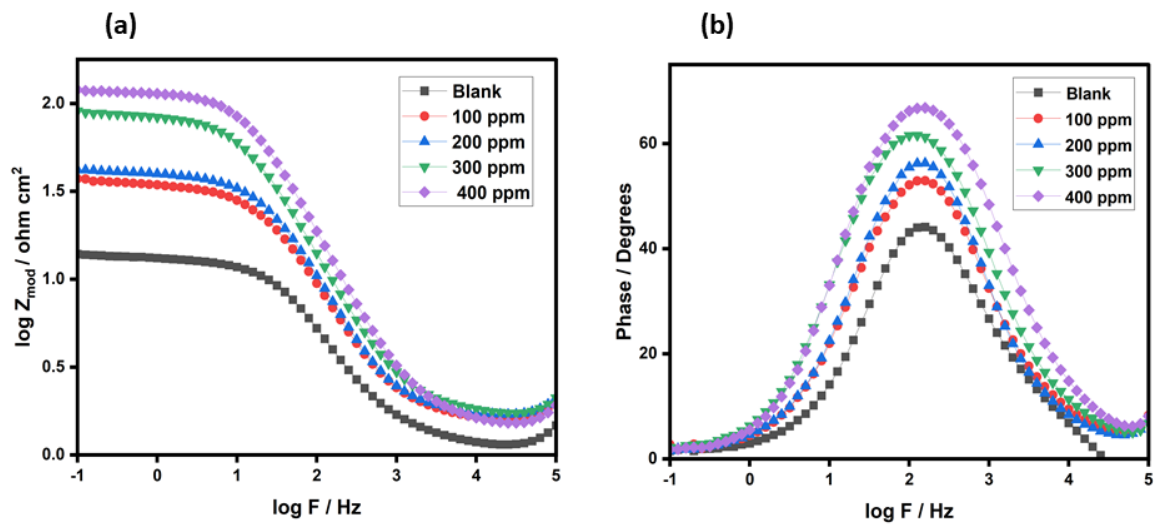


Figure 4.3.12 (a, b) Bode graphs for metal under study in HCl containing Panthenol (0 to 400 ppm) as inhibitor.

Table 4.3.4 Parameters calculated from EIS for MS sample and Panthenol as inhibiting molecule.

Inhibitor	Inhibitor Concentration (ppm)	CPE.Y₀ (μF cm⁻²)	CPE , n	C_{dl} (μF cm⁻²)	R_{ct} (Ω cm²)	R_s (Ω cm²)	χ²	IE (%)
Panthenol	Blank	1010	0.80	390.35	12.77	1.18	0.18	
	100	540	0.82	169.02	37.52	1.60	0.15	65.96
	200	380	0.86	154.48	41.05	1.72	0.12	68.89
	300	300	0.85	142.06	89.03	1.76	0.09	85.66
	400	190	0.87	100.92	125.32	1.55	0.15	89.81

4.3.6 EIS investigations of corrosion inhibition properties of Naphazoline for MS in acidic medium

As shown in Figure 4.3.13 (a, b), varying quantities of Naphazoline (0 -1500 ppm) in 1M HCl were used to generate the Nyquist plots and equivalent circuit diagram respectively at 298 K (Gao et al., 2020), Figure 4.3.14 (a, b) represented the bode plots and all the calculated parameters are summarized in Table 4.3.5. Trends of different variables like increased value of R_{ct} , decreased value of C_{dl} , decreased value of CPE confirmed the formation of thin layer of naphazoline on the metal surface, which protected it from corrosion (Goyal et al., 2020). Also, the size of the semi-circular rings formed in the Nyquist plot increased with increased amount of Naphazoline from 0 to 1500 ppm, which also confirmed the increased inhibition efficiency and was 89.10% at 1500 ppm. Increased phase angle value and increased impedance in the bode plots also verified the formation of protective naphazoline layer on the metal surface (Zhang et al., 2021).

Table 4.3.5 Parameters calculated from EIS for MS sample and Naphazoline as inhibiting molecule.

Inhibitor	Inhibitor Concentration (ppm)	CPE.Y ₀ (μF cm ⁻²)	CPE, n	C _{dl} (μF cm ⁻²)	R _{ct} (Ω cm ²)	R _s (Ω cm ²)	χ ²	IE (%)
Naphazoline	Blank	1010	0.80	390.35	12.77	1.18	0.17	
	100	664	0.82	191.45	41.69	1.44	0.11	69.37
	500	564	0.81	101.85	62.26	1.11	0.16	79.49
	1000	374	0.82	92.69	86.11	1.72	0.29	85.17
	1500	343	0.78	85.77	117.21	1.53	0.19	89.10

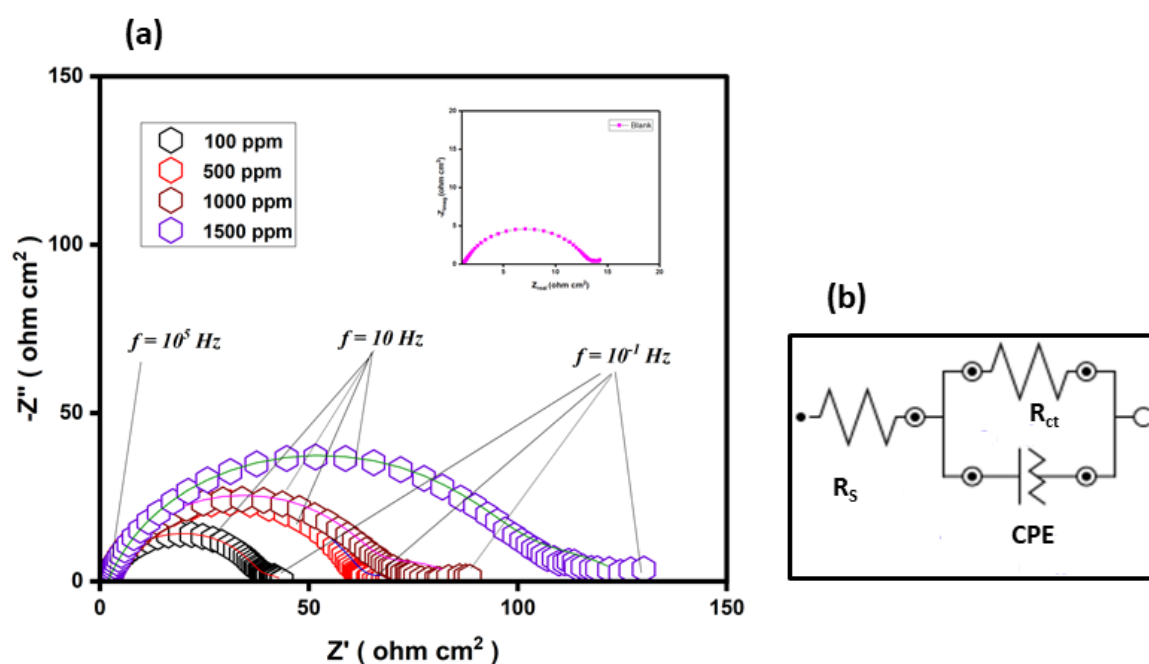


Figure 4.3.13 (a) Representation of Nyquist Plot with varied amount of Naphazoline as inhibitor and (b) Equivalent circuit diagram.

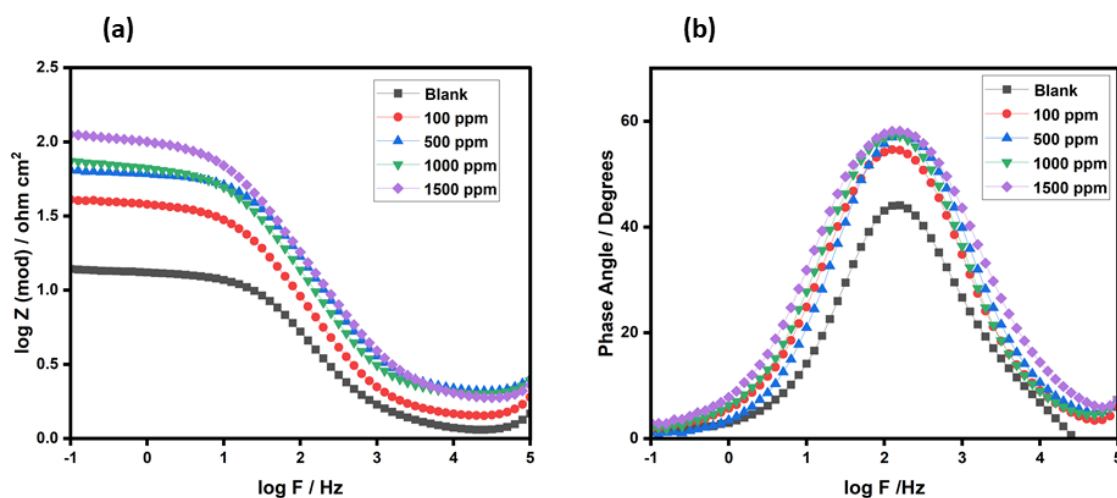


Figure 4.3.14 (a, b) Bode graphs for metal under study in HCl containing Naphazoline (0 - 1500 ppm) as inhibitor

4.3.7 EIS investigations of corrosion inhibition properties of Dicyclomine hydrochloride for MS in acidic medium

When varied amount Dicyclomine hydrochloride (0-800 ppm) in 1M HCl were investigated with EIS technique, the resulting Nyquist plots are shown in Figure 4.3.15a and the data of Nyquist was then fitted in to the simple Randel's circuit with the help of software (Figure 4.3.15b) (Liang et al., 2019). It was clear from the pictorial presentation that with the continuous increase in the concentration of dicyclomine hydrochloride, the size of the semi-circular rings (imperfect rings caused by frequency dispersion, inhomogeneity) were also increasing and further by employing the equations 4.3.5 and 4.3.6, the values of inhibition efficiency and C_{dl} were measured and IE was 95.70 % at 800 ppm of Dicyclomine hydrochloride (Dagdag et al., 2019; Sebhaoui et al., 2019). Figure 4.3.16 (a,b) depicted the bode plots, which shows increased phase angle and impedance values, which verified the corrosion mitigation. All the parameters measured from the study are tabulated in Table 4.3.6, the rise in the R_{ct} , dip in the C_{dl} , and decreased CPE values also confirmed the successful mitigation of corrosion by employing the Dicyclomine hydrochloride as inhibitor.

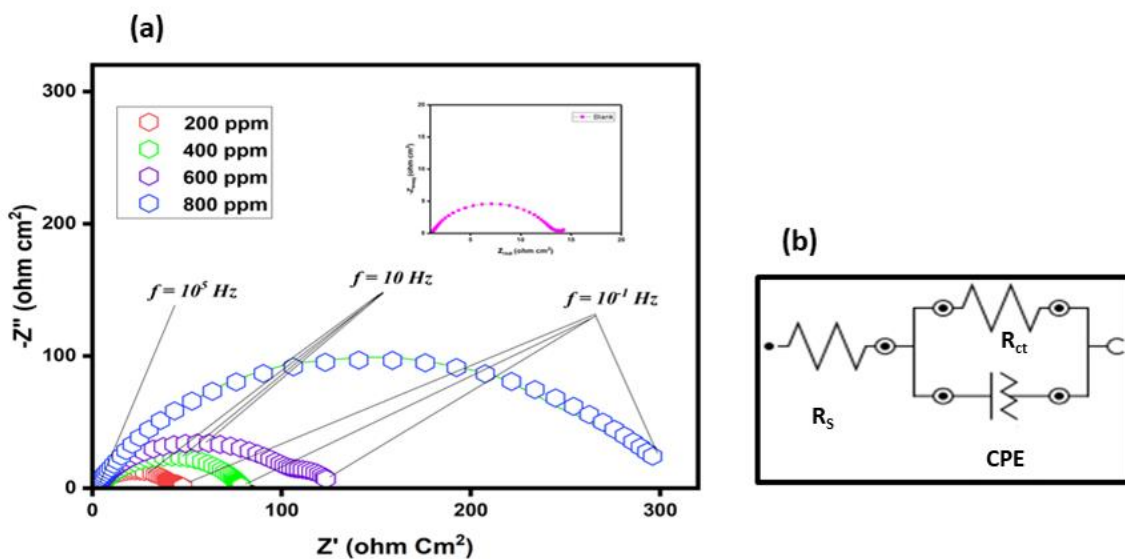


Figure 4.3.15 (a) Representation of Nyquist Plot with varied amount of Dicyclomine hydrochloride as inhibitor and (b) Equivalent circuit diagram.

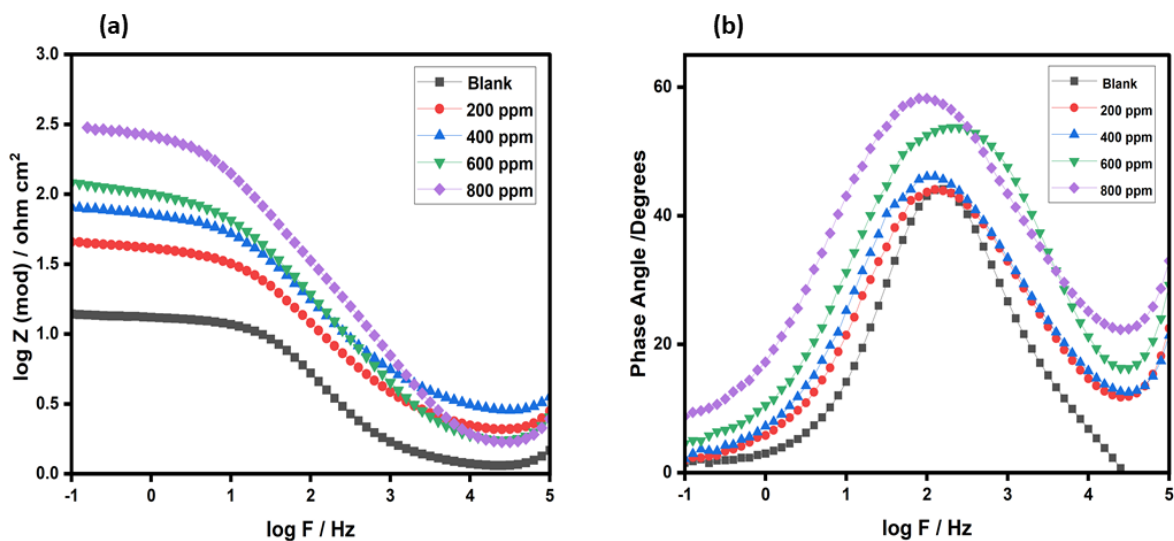


Figure 4.3.16 (a, b) Bode graphs for metal under study in HCl containing Dicyclomine hydrochloride (0 - 800 ppm) as inhibitor

Table 4.3.6 Parameters calculated from EIS for MS sample and Dicyclomine as inhibiting molecule.

Inhibitor	Inhibitor Concentrat ion (ppm)	CPE.Y₀ (μF cm⁻²)	CPE , n	C_{dl} (μF cm⁻²)	R_{ct} (Ω cm²)	R_s (Ω cm²)	χ²	IE (%)
Dicyclomine	Blank	1010	0.69	313.22	12.77	1.18	0.18	
hydrochloride	200	939	0.68	171.72	46.48	1.97	0.46	72.52
	400	657	0.71	127.33	78.9	2.70	0.38	83.81
	600	501	0.77	101.53	124.57	1.53	0.69	89.75
	800	229	0.75	84.94	297.09	1.35	0.44	95.70

4.3.8 Conclusions

Drugs (Baclofen, Betahistine dihydrochloride, Isoxsuprine hydrochloride, panthenol, Naphazoline, Dicyclomine hydrochloride) have been investigated for their corrosion mitigation tendencies for MS in 0.1M HCl by using EIS technique. Following are some conclusions drawn from the present study:

- The increased diameter of capacitive loops on addition of drug molecules as compared to blank solution confirms the effective inhibition of metal surface and rise in the inhibition efficiency value.
- The formation of a thicker monolayer by the inhibitor molecules is evidenced by a larger R_{ct} value.
- The decrease in C_{dl} values observed after the addition of the inhibitor, verifies the formation of a preventative layer of inhibitor on the metal surfaces
- The findings of the Bode plots demonstrated that the phase angle values significantly increased with the increased amount of inhibitor, which validated the reduction in roughness of metal surface due to the formation of inhibitor layer on the metallic surface.
- The general trend for the overall inhibitory efficacy of inhibitors on the MS in 1M HCl:
Isoxsuprine hydrochloride > Baclofen > Betahistine hydrochloride > Dicyclomine hydrochloride > Panthenol > Naphazoline.

4.4 Potentiodynamic Polarization technique

Potentiodynamic polarization measurement (PDP) is one of the most extensively used DC electrochemical approach in corrosion investigations. Potential is applied to the electrode and current is generated due to the reactions take place at cathode and anode. Here in this case the potential behaves as a function of log of current. Graphical presentation of potential and log I, called as Tafel plot or polarization plots as shown in Figure 4.4.1, from which the values of corrosion potential along with Tafel slopes (determination of corrosion rate) can be measured (Telegdi et al., 2018; Instrument, 2019). On applying the Potential, the current developed is a measure of rate of corrosion occurring on working electrode in calculated as current per unit area, known as current density (Keshavamurthy et al., 2021).

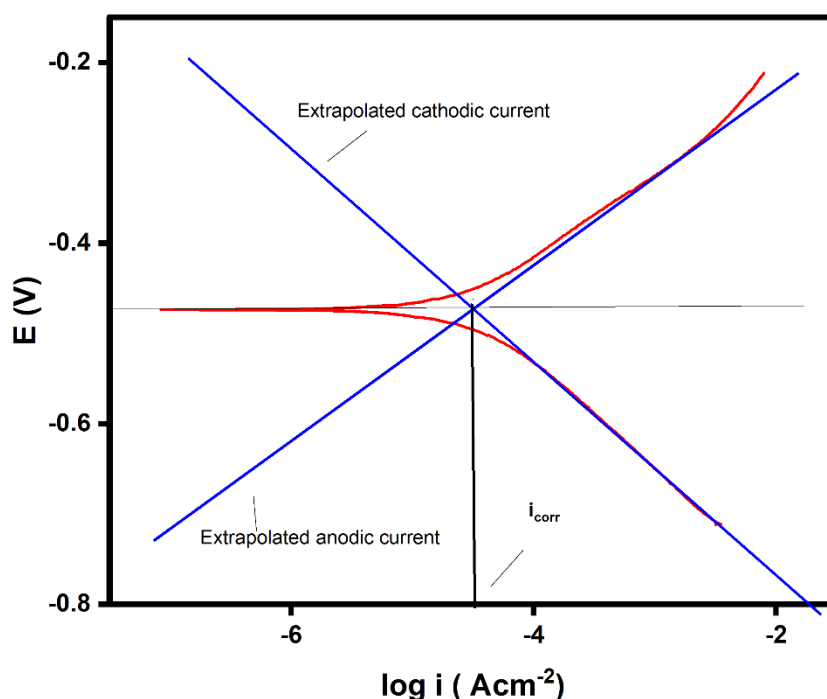


Figure 4.4.1 Tafel plot.

In order to study and measure the kinetics involved in the corrosion study, the most popular is the Butler–Volmer equation, written as follows (McCafferty, 2005; Okajima et al., 2010)

$$i = i_{\text{corr}} \left[e^{\alpha n F (E - E_{\text{corr}}) / RT} - e^{-(1-\alpha) n F (E - E_{\text{corr}}) / RT} \right] \quad (4.4.1)$$

Where, i specify the Current Density (A/m^2) at electrode, E and E_{corr} denote Applied Potential and Corrosion Potential respectively, η equal to $E - E_{\text{corr}}$, i_{corr} refers to Corrosion Current Density, β_a and β_c denotes Tafel Slope (anodic and Cathodic), F is Faraday's Constant (value 96580 C), R and T are Universal Gas Constant and Temperature respectively. Equation 4.4.1 is the basic behind the Tafel exploration. While studying *Butler-Volmer Equation* two conditions can arise first when potential on the electrode is more negative, that means rate of cathodic reaction has increased and anodic current showed a dip, therefore, the equation 4.4.1 has changed and the first part is removed from it, the new modified equation (known as cathodic Tafel equation) is as follows

$$\log(-I_c) = \log I_{\text{corr}} - (\beta_c n F \eta / 2.303 RT) \quad (4.4.2)$$

Second situation arises, when metal electrode potential is shifting towards positive, that is the situation when anodic reaction is faster as compare to cathodic reaction. At highly positive overpotential, anodic current rises and cathodic current showed a dip. In this case again, equation 4.4.1 is altered (known as anodic Tafel equation) by removing the second part and is as follows

$$\log(-I_a) = \log I_{\text{corr}} + (\beta_a n F \eta / 2.303 RT) \quad (4.4.3)$$

4.4.1 Potentiodynamic polarization investigation of MS in presence of 1M HCl

Potentiodynamic polarization technique was employed to investigate the corrosion behaviour of MS in 1 M HCl at 298K. Prior to this measurement, the open circuit potential was measured against the Ag/AgCl electrode. Further the current density values extracted from the PDP measurements, are substituted in the following equation to find out the inhibition efficiency (Farahati et al., 2020)

$$IE(\%) = \frac{j_{\text{corr}} - j_{\text{corr}}^{\text{inh}}}{j_{\text{corr}}} \times 100 \quad (4.4.4)$$

where j_{corr} and j_{corr}^{inh} are expressing the corrosion current densities in test solution and an acidic solution containing an inhibitor, respectively.

4.4.2 Potentiodynamic polarization study of corrosion reducing tendency for MS in 1M HCl by using Baclofen as inhibitor

Corrosion mitigation property of Baclofen drug molecule was also investigated for MS with potentiodynamic polarization method. In Figure 4.4.2 the Tafel curves produced without and with the different concentrations of Baclofen (0 to 2000 ppm) are shown and these plots are further used to extract corrosion parameters such as anodic (b_a) and cathodic (b_c) Tafel slopes, corrosion current density (j_{corr}), corrosion potential (E_{corr}), and all the calculated parameters are tabulated in Table 4.4.1. Baclofen's effect on both cathodic and anodic reactions can be detected by the change in b_a and b_c following the addition of the drug (El- Arrouji et al., 2020). Higher values of b_c validated that the inhibitor controlled the cathodic reaction more as compared to anodic reaction and negative shift in the E_{corr} values also confirmed the suppression of cathodic reaction (Soltaninejad & Shahidi, 2018). Decreased corrosion current density (j_{corr}) with the increased amount of Baclofen from 0 to 2000 ppm also confirmed the mitigation of corrosion. Further on substituting the j_{corr} values in equation 4.4.4, the inhibition efficacy was determined and was 92.65% at the 2000 ppm of Baclofen.

Table 4.4.1 Potentiodynamic parameters for MS when Baclofen was employed as inhibitor.

Inhibitor	Inhibitor Concentration(ppm)	b_a (V dec ⁻¹)	b_c (V dec ⁻¹)	E_{corr} (V)	j_{corr} (μ A cm ⁻²)	IE (%)
Baclofen	Blank	0.177	0.212	-0.436	1360	-
	100	0.119	0.140	-0.449	500	63.23
	500	0.100	0.158	-0.449	460	66.18
	1000	0.103	0.140	-0.451	220	83.82
	1500	0.104	0.140	-0.450	140	89.70
	2000	0.18	0.160	-0.673	100	92.65

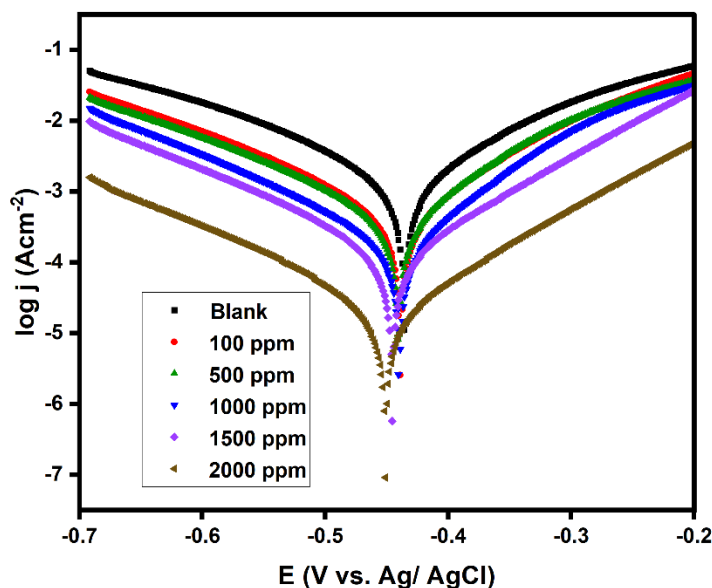


Figure 4.4.2 Tafel plots with varied concentration of Baclofen containing in acid solution.

4.4.3 Potentiodynamic polarization study of corrosion reducing tendency for MS in 1M HCl by using Betahistine dihydrochloride as inhibitor

Analysis was carried out in a test solution containing various concentrations of Betahistine dihydrochloride dissolved in an acidic solution and Figure 4.4.3 illustrated the polarisation curves that were produced and various polarization descriptors are compiled in Table 4.4.2. Illustrations in Figure 4.4.3 and tabulated values in Table 4.4.2 shown that at 1500 PPM, the inhibition efficiency is maximum. and j_{corr} decreased as inhibition efficiency rose. This study predicted the cathodic predominance because the inhibitor molecules alter the values of both b_a and b_c , but the changes in b_c are more prominent. (Haque et al., 2017). This has been stated in literature that both cathodic and anodic processes will be hindered if E_{corr} values are less than 85 mV as compared to the value of blank solution, and in the present investigation shift of the E_{corr} values came out to be 37 mV, therefore Betahistine dihydrochloride was depicted as a mixed type inhibitor, but with cathodic predominance due to the negative shift of E_{corr} (Farahati et al., 2019; Farahati et al., 2020; Haque et al., 2017; Kowsari et al., 2016, Yadav et al., 2013).

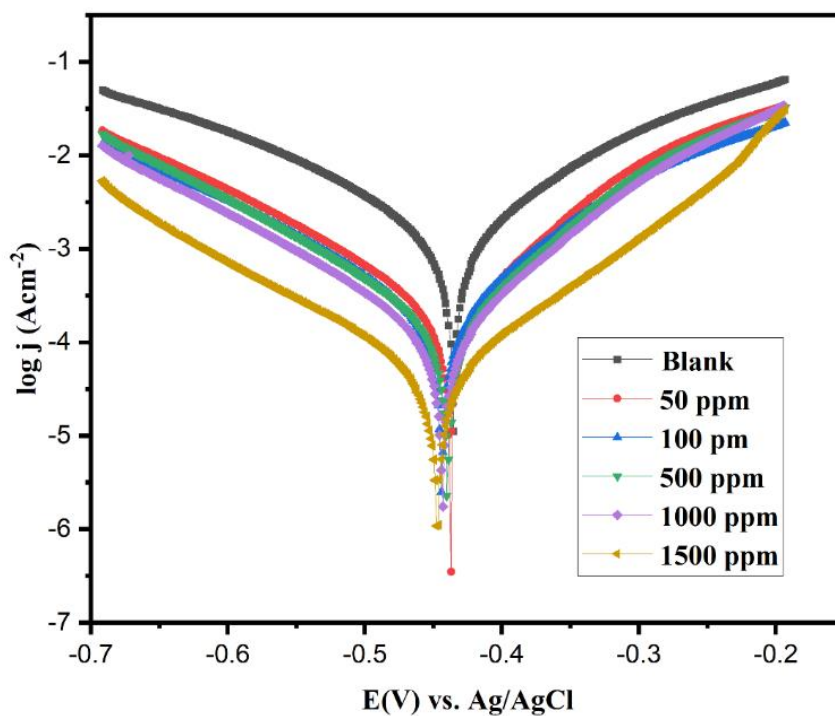


Figure 4.4.3 Representation of Tafel plot with varying concentrations of Betahistine dihydrochloride as inhibitor.

Table 4.4.2 Potentiodynamic parameters for MS using Betahistine dihydrochloride as a corrosion inhibiting molecule

Inhibiting Molecule	Concentration of Betahistine (ppm)	b_a (V/dec)	b_c (V/dec)	E_{corr} (V)	j_{corr} ($\mu\text{A cm}^{-2}$)	IE (%)
Betahistine dihydrochloride	Blank	0.177	0.212	-0.436	1360	-
	50	0.095	0.143	-0.449	260	80.88
	100	0.116	0.155	-0.456	220	83.82
	500	0.091	0.132	-0.452	198	85.44
	1000	0.088	0.128	-0.450	152	88.82
	1500	0.097	0.122	-0.473	50	96.32

4.4.4 Potentiodynamic polarization study of corrosion reducing tendency for MS in 1M HCl by using Isoxsuprine hydrochloride as inhibitor

In order to acquire insight into the electrochemical kinetics of the inhibitor, potentiodynamic polarisation (PDP) studies are needed and this study was carried out for MS samples and Isoxsuprine hydrochloride was considered as a new inhibitor. Varied concentrations ranging from 0 to 2000 ppm are considered for analysis and Tafel plots are illustrated in the Figure 4.4.4. E_{corr} and j_{corr} values, are determined by extrapolating the anodic and cathodic corrosion current curves, values extracted after the analysis of graphs are Tabulated in Table 4.4.3 (Chauhan et al., 2020). Results revealed dip in the j_{corr} with the rise in the concentration of Isoxsuprine hydrochloride (Feng et al., 2018). Results also revealed highest inhibition efficacy of 97.26 % at 2000 ppm of Isoxsuprine hydrochloride. In addition, the E_{corr} values in Figure 4.4.4 shift slightly toward the cathodic region, confirming that the inhibitor's principal role in affecting cathodic reaction, but the shift is 37mV towards cathodic region, which also confirmed the suppression of both cathodic and anodic reactions. It was already given in the previous studies that if the shift in the E_{corr} values is less than $\pm 85\text{mV}$, then the inhibitor will retard both cathodic and anodic reactions. (Bashir et al., 2018; Baig et al., 2019; Chauhan et al. 2018, Rahimi et al. 2021). Tafel slopes (b_c) values are high as compare to anodic Tafel slopes (b_a) in in Table 4.4.3, it revealed that the former was higher also confirmed the cathodic reaction reduction is higher as compare to anodic (Chauhan et al., 2018).

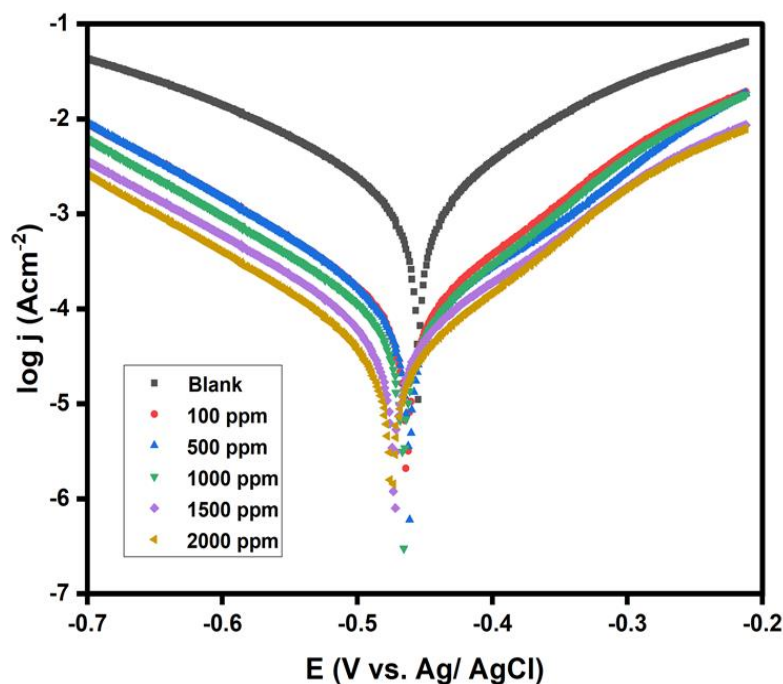


Figure 4.4.4 Potentiodynamic polarization plots for metallic samples submerged in the 1M HCl solution with the varied concentration of Isoxsuprine hydrochloride from 0 to 2000 ppm.

Table 4.4.3 Computed Tafel parameters for corrosion of MS when Isoxsuprine hydrochloride inhibitor is introduced.

Inhibitor Name	Concentration (ppm)	b_a (V dec ⁻¹)	b_c (V dec ⁻¹)	E_{corr} (V)	j_{corr} ($\mu\text{A cm}^{-2}$)	IE (%)
	Blank	0.177	0.212	-0.436	1360.00	-
Isoxsuprine hydrochloride	100	0.103	0.123	-0.462	120.38	91.15
	500	0.116	0.124	-0.477	104.74	92.30
	1000	0.097	0.123	-0.461	83.71	93.84
	1500	0.109	0.127	-0.475	55.35	95.93
	2000	0.096	0.122	-0.473	37.31	97.26

4.4.5 Potentiodynamic polarization study of corrosion reducing tendency for MS in 1M HCl by using Panthenol as inhibitor

Analysis was conducted in a test solution with varying amounts of Panthenol in ppm dissolved in acidic solution as a safe corrosion inhibiting substance. The polarization curves obtained are elaborated in Figure 4.4.5 and all the variables calculated are tabulated in the Table 4.4.4. It was clear from the tabulated results that with the rise in concentration of Panthenol, the j_{corr} values showed a decrease (Galai et al., 2021), on substituting the j_{corr} value in equation 4.4.4, the inhibition efficiency was calculated and at 400 ppm the efficacy value was maximum (89.41%). Graphical presentation (Figure 4.4.5) was showing the E_{corr} values change slightly toward the cathodic region, confirming that the inhibitor's primary role in affecting cathodic reaction, but the shift in the E_{corr} value with respect to the value of test solution was only 16 mV, which is less than ± 85 mV. Therefore, Panthenol behaved as mixed type of inhibitor but with slight cathodic predominance (Cahuhan et al. 2018; Rahimi et al., 2021; Galai et al., 2017).

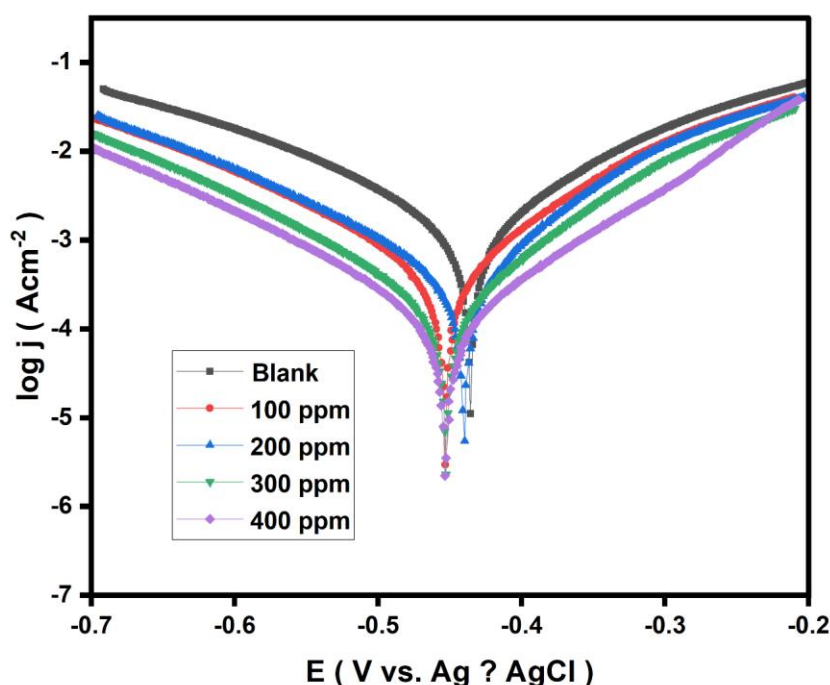


Figure 4.4.5 Potentiodynamic polarization plots for metallic samples submerged in the 1M HCl solution with the varied concentration of Panthenol.

Table 4.4.4 Computed Tafel parameters for corrosion of MS when Panthenol inhibitor is introduced.

Inhibitor Name	Concentration (ppm)	b_a (V dec ⁻¹)	b_c (V dec ⁻¹)	E_{corr} (V)	j_{corr} ($\mu\text{A cm}^{-2}$)	IE (%)
	Blank	0.177	0.212	-0.436	1360.00	-
Panthenol	100	0.130	0.140	-0.453	486.00	64.26
	200	0.110	0.162	-0.439	451.00	66.84
	300	0.120	0.146	-0.452	219.00	83.90
	400	0.092	0.127	-0.452	144	89.41

4.4.6 Potentiodynamic polarization study of corrosion reducing tendency for MS in 1M HCl by using Naphazoline as inhibitor

Using PDP experiments, we can learn more about the inhibitor's electrochemical kinetics. The PDP plots of drug Naphazoline obtained from the acidic solution with the different concentration of Naphazoline ranging from 0 to 1500 ppm are described in Figure 4.4.6 and various corrosion parameters derived from plot are tabulated in Table 4.4.5. Results revealed that with the rise in Naphazoline concentration, the j_{corr} values decreased and by using the current values the inhibition efficiency was calculated and was maximum (89.56%) at 1500 ppm. Shift of E_{corr} values towards the negative side depicted the cathodic suppression by inhibitor but as per the literature, the difference between E_{corr} values of blank and inhibited solution was less than $\pm 85\text{mV}$, therefore inhibition was of mixed nature but slightly cathodic predominance. These findings imply that the adsorption of inhibitor molecules on metal substrates takes up active sites, which can be interpreted as a process of substitution between the inhibitors and pre adsorbed H_2O molecules at the iron/solution interface (Deyab,2018; Tan et al., 2020a; Tan et al., 2020b).

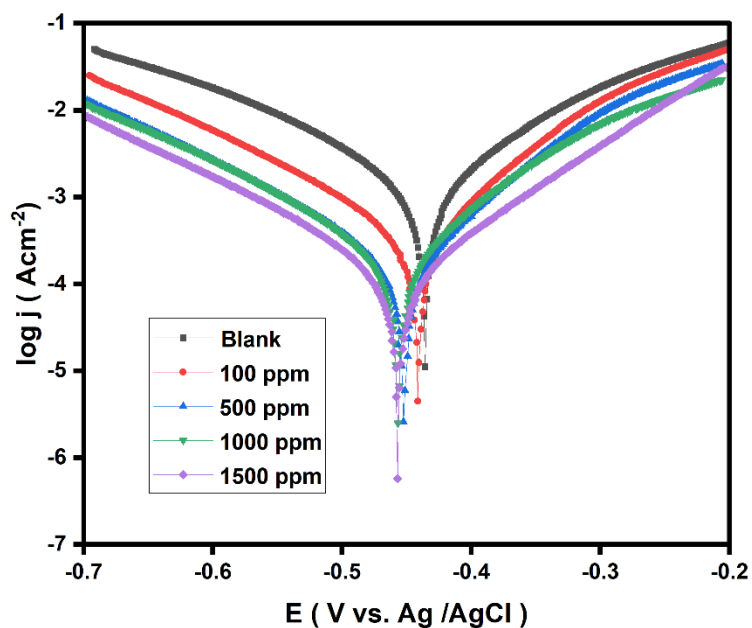


Figure 4.4.6 Potentiodynamic polarization plots for metallic samples submerged in the 1M HCl solution with the varied concentration of Naphazoline.

Table 4.4.5 Computed Tafel parameters for corrosion of MS when Naphazoline inhibitor is introduced.

Inhibitor Name	Concentration (ppm)	b_a (V dec⁻¹)	b_c (V dec⁻¹)	E_{corr} (V)	j_{corr} ($\mu\text{A cm}^{-2}$)	IE (%)
Blank	Blank	0.177	0.212	-0.436	1360.00	-
Naphazoline	100	0.100	0.151	-0.442	428.00	68.53
	500	0.110	0.147	-0.451	218.00	83.97
	1000	0.127	0.160	-0.452	198.00	85.44
	1500	0.109	0.156	-0.456	142	89.56

4.4.7 Potentiodynamic polarization study of corrosion reducing tendency for MS in 1M HCl by using Dicyclomine hydrochloride as inhibitor

Potentiodynamic polarisation (PDP) experiments are required to understand the detailed insight in to corrosion reactions and Tafel plots by utilizing the data obtained from PDP measurements are represented in Figure 4.4.7 and corrosion descriptors are tabulated in Table 4.4.6. Results from the calculations revealed that the inhibition efficacy was 95.37 % at 800 ppm of dicyclomine hydrochloride and current density values decreased with the rise in inhibitor's concentration. Also, the variation of E_{corr} values of inhibited solution to blank solution is less than $\pm 85\text{mV}$, therefore the inhibitor is successfully suppressing the cathodic and anodic reaction rates. This suppression of both the reactions may be attributed to the fact that dicyclomine hydrochloride molecules are attracted to the active sites of the sample (Ansari et al., 2017; Fouda et al., 2019; Saji et al., 2019).

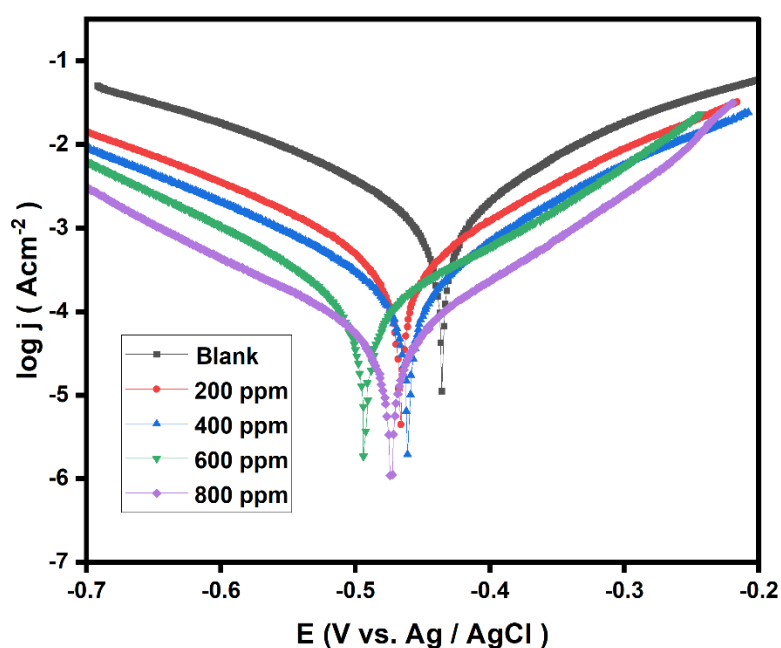


Figure 4.4.7 Potentiodynamic polarization plots for metallic samples submerged in the 1M HCl solution with the varied concentration of Dicyclomine hydrochloride from 0 to 800 ppm.

Table 4.4.6 Computed Tafel parameters for corrosion of MS when Dicyclomine hydrochloride inhibitor is introduced.

Inhibitor Name	Concentration (ppm)	b_a (V dec⁻¹)	b_c (V dec⁻¹)	E_{corr} (V)	j_{corr} ($\mu\text{A cm}^{-2}$)	IE (%)
	Blank	0.177	0.212	-0.436	1360.00	-
Dicyclomine	200	0.129	0.162	-0.466	374.00	72.5
hydrochloride	400	0.140	0.155	-0.460	209.00	84.63
	600	0.132	0.157	-0.492	133.00	90.22
	800	0.136	0.163	-0.472	63.00	95.37

4.4.8. Conclusions

Baclofen, Betahistine dihydrochloride, Isoxsuprine hydrochloride, Panthenol, Naphazoline Dicyclomine hydrochloride are the six drug molecules selected for the present study and potentiodynamic polarization study was also carried out. Different corrosion descriptors such as I_{corr} , E_{corr} , Tafel slopes were also determined.

- A rise in inhibition efficiency can be detected with an increase in the inhibitor concentration.
- E_{corr} value suggested the suppression of both cathodic and anodic reactions.
- The Tafel anodic and cathodic slopes changed irregularly, showing that the effect of corrosion abatement is not only due to the adsorption, but also because of the combined effect of blocking active sites on metals.
- The overall order of corrosion inhibition efficiency of inhibitors for MS is Isoxsuprine hydrochloride > Betahistine dihydrochloride > Baclofen > Dicyclomine hydrochloride > Naphazoline > Panthenol.

4.5 Scanning electron microscopy

In scanning electron microscopy (SEM), electron beam is allowed to fall on the particular area of sample under investigation, and is scanned across it, sometimes these electrons dissociate the atoms of sample, which cause the liberation of electrons from the sample. These electrons are called as secondary electrons. In SEM these secondary electrons are also studied to get the two- dimensional images of sample. SEM can even measure the surface topography of any sample up to < 1 nanometre spatial resolution. In the present SEM study is very useful to understand the surface changes that occurs when inhibitor being added in the test solution (Inkson,2016; Kuo, 2007; Stokes,2016).

4.5.1 Application of SEM in the present study

For the present study JEOL make SEM instrument was employed for surface study. Different mild steel coupons of the dimensions 1 c.m. X 1 c.m. X 0.1 mm were taken for analysis. Optimized time for exposure was two hours and chosen concentration of acid was 1 M HCl. Six drug molecules were considered for study, out of which maximum concentration of 2000 ppm was considered for Baclofen, and Isoxsuprine hydrochloride. For Betahistine dihydrochloride, Naphazoline, 1500 ppm of maximum concentration was selected. For Panthenol 400 ppm and for Dicyclomine hydrochloride 800 ppm concentration was selected for analysis. With the help of SEM analysis 2- dimensional images of the samples were obtained. For this analysis three type of samples were prepared, in the first type metallic coupons were cleaned sample without any external exposure, second samples were immersed in 1 M HCl acidic solution and third samples were immersed in acidic solution with optimized concentration of different drug molecules. The results are discussed as follows:

4.5.2 Scanning electron microscopy analysis for Baclofen as inhibitor

As shown in Figure 4.5.1(a–c), scanning electron microscopy pictures of the surface of MS after it has been subjected to the optimal acid solution (1 M HCl) and subsequently treated with 2000 ppm of Baclofen in acid for two hours are presented. Figure 4.5.1a presents the clear polished surface of the sample, MS is corroded on the surface in Figure 4.5.1b as a result of being immersed in 1 M HCl solution. This image shows more fractures and flaws because of the damage caused by the acid to metallic surface. Figure 4.5.1c shows the surface of MS dipped in the acid with 2000 ppm of Baclofen. Figure 4.5.1c shows a surface that seems cleaner and with less damage, which is quite similar to the clean surface shown in Figure 4.5.1 a, which verifies the presence of an inhibitor on the surface of the sample in the form of a thin layer that acts as a barrier between the MS sample and the acidic solution (Dhaundiya, 2019; Faradian et al., 2021; Parveen et al., 2019).

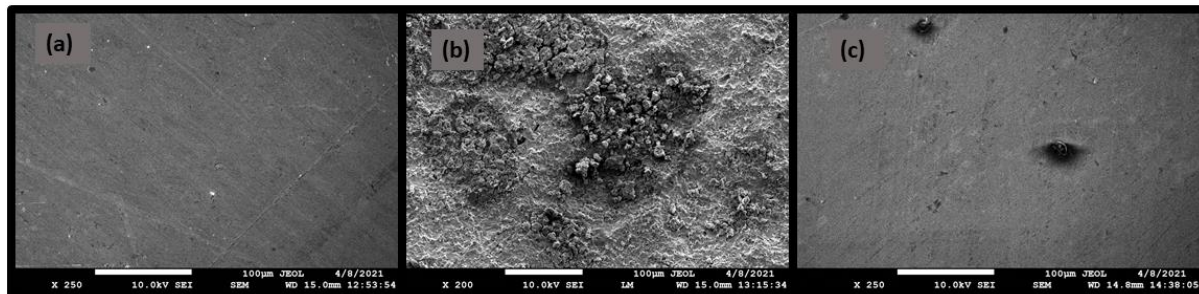


Figure 4.5.1 (a-c) SEM images of (a) polished metallic sample (b) sample submerged in 1M HCl (c) sample submerged in 1 M HCl with an optimized concentration of Baclofen.

4.5.3 Scanning electron microscopy analysis for Betahistine dihydrochloride as inhibitor

For two hours, the MS surface was subjected to the optimized acid solution (1 M HCL) and also treated to the solution with 1500 ppm of Betahistine dihydrochloride in acid. Figure 4.5.2a shows the polished surface of the sample in its natural state without any exposure. When MS is immersed in 1 M HCl solution, the outcome is a corroded surface as seen in Figure 4.5.2b. Because of the damage caused by the MS sample in the acid solution, there are more degradation of surface is evident in this photograph. Surface quality improved and damage is reduced in Figure 4.5.2c. SEM analysis reveals that inhibitor is available on the sample's surface as a fine layer, protecting it from corrosion (Kumar et al., 2013).

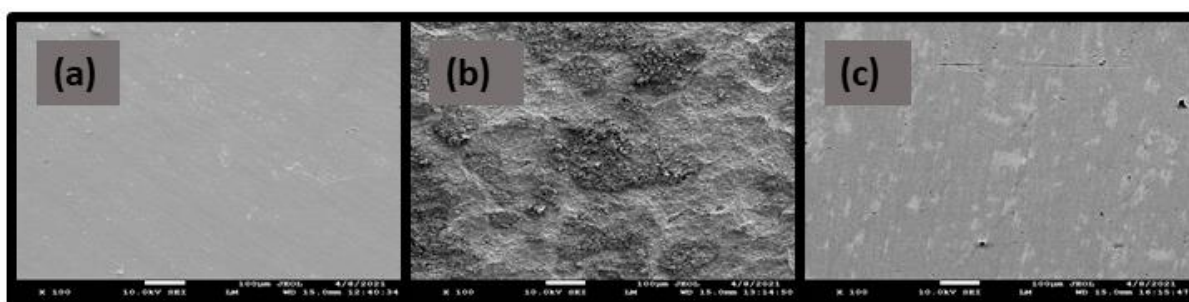


Figure 4.5.2 (a- c) SEM Micrograph: (a) Clear MS sample (b) Without Inhibitor (c) with Betahistine dihydrochloride as corrosion inhibitor.

4.5.4 Scanning electron microscopy analysis for Isoxsuprine hydrochloride as inhibitor

scanning electron microscopy images of MS surfaces subjected to different experimental conditions are shown in Figure 4.5.3 (a–c). These images include the unexposed sample given in Figure 4.5.3a, metal in acid solution without inhibitor shown in Figure 4.5.3b and metal in acid solution containing Isoxsuprine hydrochloride as an inhibitor presented in Figure 4.5.3c. Figure 4.5.3b shows the corroded surface with high level of roughness. Figure 4.5.3c shows a smooth finish with less breakage. It confirmed that the sample's surface is blanketed with a thin coating of corrosion inhibitor, preventing it from rusting (Guruprasad et al., 2020; ma et al., 2020; Palaniappam et al., 2019).

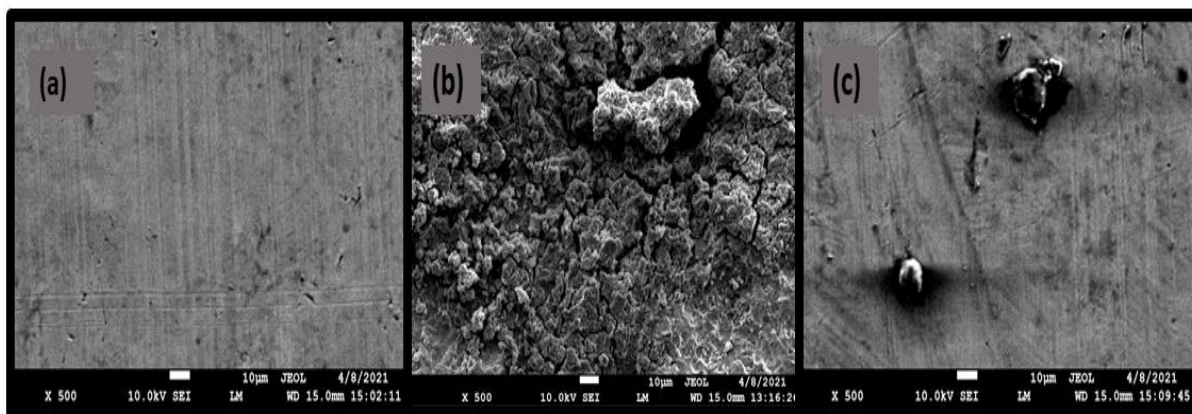


Figure 4.5.3 (a-c) SEM pictures of (a) steel sample without any exposure (b) sample treated with acidic solution (c) sample expose to acidic solution with 2000 ppm of Isoxsuprine hydrochloride.

4.5.5 Scanning electron microscopy analysis for Panthenol as inhibitor

Figure 4.5.4 (a–c) shows scanning electron microscopy images of MS exposed to optimised acid solution (1 M HCl) and then 400 ppm Panthenol drug as inhibitor in acid for two hours. Figure 4.5.4a depicts the sample's smooth polished surface. Figure 4.5.4b illustrates a corroded surface caused by acid attack on the metal surface and more damage is clearly evident in this image. Figure 4.5.4c depicts a surface that appears to be better and less deteriorated and was very much similar to the surface present in Figure 4.5.4a. Study verified the presence of Panthenol as inhibitor on top, preventing rust from forming on the sample's surface (Du et al., 2017; Derfouf et al.2019; Nasr et al.,2018).

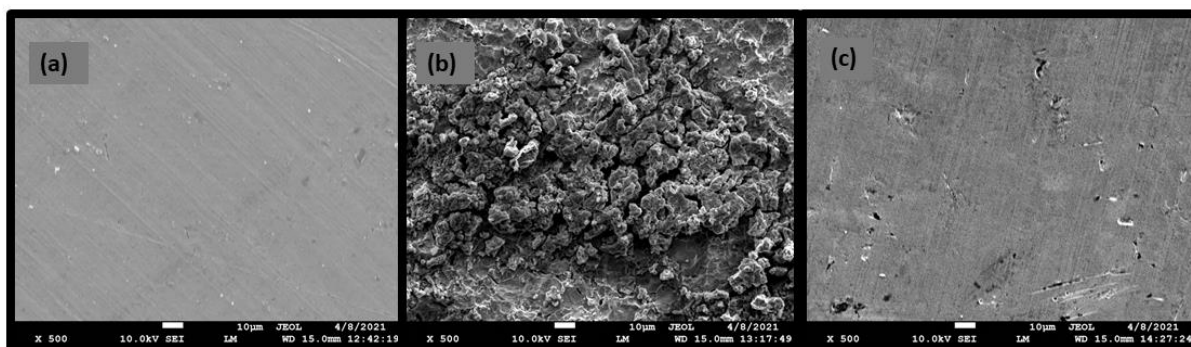


Figure 4.5.4 (a-c) SEM pictures of (a) steel sample without any exposure (b) sample treated with acidic solution (c) sample expose to acidic solution with 400 ppm of Panthenol.

4.5.6 Scanning electron microscopy analysis for Naphazoline as inhibitor

Figure 4.5.5 (a–c) shows scanning electron microscopy images of MS surfaces subjected to different experimental conditions including three different conditions unexposed sample, metal subjected to pure acid solution and metal kept in acid containing Naphazoline as inhibitor. Additional pits and cracks are evident in the Figure 4.5.5b as a result of the MS sample being damaged in the acid solution. Less damage and deterioration were there in Figure 4.5.5c, it established that the sample's surface is protected from oxidation by a thin layer of Naphazoline (El- Etre & Ali, 2017; Kumar et al., 2011; Ragul et al., 2018).

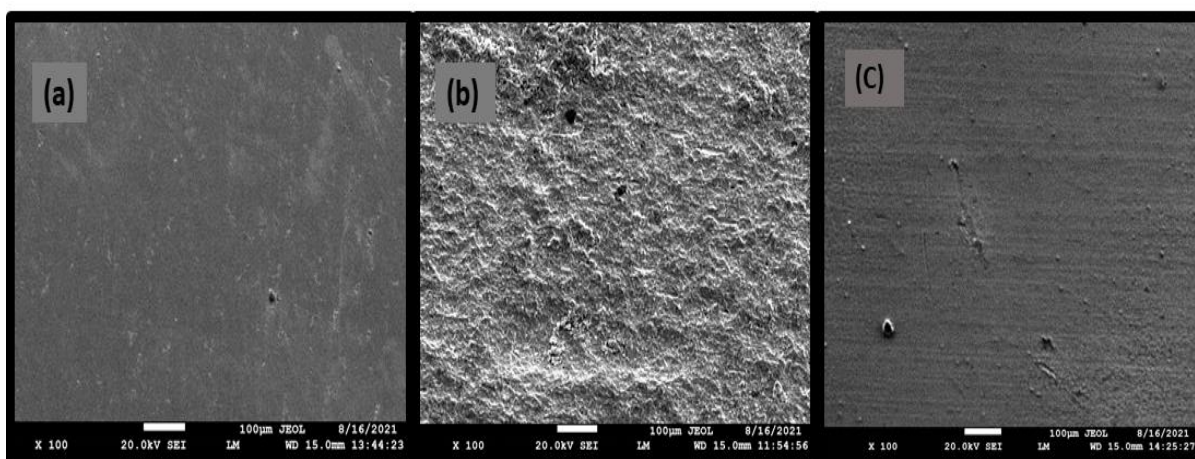


Figure 4.5.5 (a-c) SEM pictures of (a) steel sample without any exposure (b) sample treated with acidic solution (c) sample immersed in acidic solution with 1500 ppm of Naphazoline.

4.5.7 Scanning electron microscopy analysis for Dicyclomine hydrochloride as inhibitor

It is demonstrated in Figure 4.5.6 (a-c) that scanning electron microscopy pictures of MS that were subjected to the acid solution (1 M HCl) and subsequently to the Dicyclomine (800 ppm) in acid solution for two hours. the surface of the sample shown in Figure 4.5.6a is clear, unexposed and polished. Figure 4.5.6b displays a corroded MS surface after exposure in a 1 M HCl solution and more damage can be seen because the sample in the acid solution had been compromised. Figure 4.5.6c illustrates a surface that appeared cleaner and less degraded and is fairly comparable to the clean surface depicted in Figure 4.5.6a, it proved that the sample's surface is protected from rusting by the presence of Dicyclomine on the metal (Dhaundiyal, 2019; Faradian et al., 2021; Parveen et al., 2019).

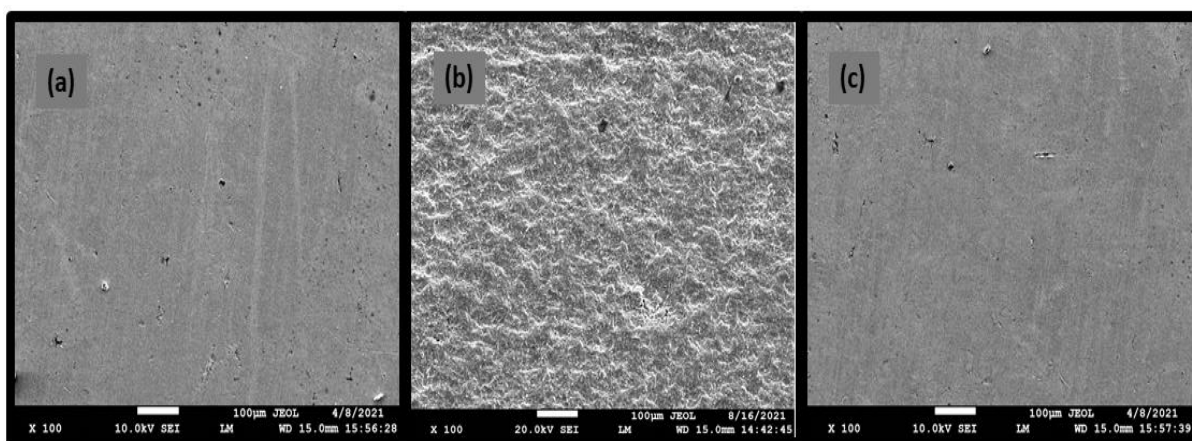


Figure 4.5.6 (a-c) SEM pictures of (a) steel sample without any exposure (b) sample treated with acidic solution (c) sample dipped in acid with 800 ppm of Dicyclomine hydrochloride.

4.5.8 Conclusions

SEM helped to investigate the surface of polished metals and by subjecting metal samples to acidic solutions and drug such as Baclofen, Betahistine dihydrochloride, Isoxsuprine hydrochloride, Panthenol, Naphazoline, and Dicyclomine hydrochloride containing acid solution. Three different samples were investigated: pure metal without any external treatments, pure metal exposed to acid, and finally pure metal exposed to acid with an optimal concentration of inhibiting molecule. The following are some of the conclusions that were made as a result of this research:

- According to the SEM experiments conducted for the corrosion MS, the highest roughness and deterioration were found in blank solution (In Fig.b of every drug molecule), indicating that the greatest amount of corrosion in blank solution.
- Optimized concentration of drug molecules was 2000 ppm for Betahistine dihydrochloride and Isoxsuprine hydrochloride. For Baclofen, Naphazoline the optimized concentration was 1500 ppm, for dicyclomine hydrochloride it was taken as 800 ppm and for Panthenol 400 ppm of drug was considered as optimized concentration. These were the concentrations on which maximum inhibition was reported in other experiments, hence same concentration of drug molecule was taken for SEM analysis.
- When selected drug molecules are added as corrosion inhibitors, the damage and roughness was compensated and the cracks and pits reduced extensively, which proved the formation of a preventative layer on the metal.

4.6 Atomic force microscopy

Atomic force microscopy (AFM) is a well-known and widely acknowledged method for studying inhibitor film development at the nano to microscale and for determining the roughness of metal surfaces (Chen et al., 2020; Sundaram et al., 2016). It is a type of scanning probe microscopy and was first used in 1985, mainly used to study surface topography (Shinato et al., 2020). The main advantages of using AFM technology is that it can be used in different environments like vacuum, liquid etc. Sample preparation is also not required as conducting and nonconducting, any type of the sample can be analyzed. But scanning speed and issue of unavoidable artifacts is also there (Shinato et al., 2020).

4.6.1 Principle

AFM is a specific form of SPM, with a proven resolution of the order nanometer (Shinato et al., 2020). A sharp cantilever tip connects with the sample surface, allowing the tip to sense the forces between the surface of metal and molecules of the tip. It is very much different from conventional microscope, as light is not being used but samples are being touched by cantilever and images are taken (Trache et al., 2018). The main parts of the commercial AFM instrumentation are AFM probe, optical lever, feedback loop, the piezoelectric scanner and a conversion system. The probe is a pointed tip set on a flexible cantilever. Optical lever that enables for the measurement of cantilever displacements, feedback loop monitored interaction forces, piezoelectric scanner is used moves the tip in 3-dimensional pattern and used to convert the data obtained in to images (Trache et al., 2018).

4.6.2 The AFM's operational modes

Following are the different modes of operations of AFM instrument (Jalili & Laxminarayana, 2004; vahabi et al., 2013; Yosakau, 2020).

4.6.2a Contact mode imaging

In this technique AFM tip has come into contact with the sample. This is also called repulsive mode and the interactions that are occurring between sample and tip of cantilever are repulsive in nature.

4.6.2b Lateral force microscopy

In this method the tip of the probe is tested over the sample in contact mode, a parallel deflection of the probe cantilever is measured. This mode measures the frictional force zones that are higher and the zones with lower frictional force.

4.6.2c Nanocontact mode

When operating in this mode, the cantilever tip is approximately 50–150 Å⁰ above the sample surface, allowing for the detection of the attractive van der Waals forces acting between the tip and the sample surface, respectively. Topographic images are created by scanning the tip of the instrument above the surface.

4.6.2.e Dynamic force\ intermitted contact

It is also commonly known as tapping mode. the AFM tip strikes or contacts the surface, and the tip is much closer as compare to nanocontact mode. In intermittent contact method the tip taps the surface and it sometimes have attractive and sometimes have repulsive interactions. This type of AFM investigation is bit advanced and even can be used for soft samples.

4.6.3 Application of AFM in the present study

For the present study different clean and polished MS coupons of the dimensions 1 c.m. X 1 c.m. X 0.1 mm were taken for analysis by employing atomic force microscopy. AFM with multimode 8, make Bruker was employed for analysis. The optimized time period for analysis was taken as 2 hours and selected concentration of acidic solution was 1 M HCl. Six drug molecules were considered for study, out of which maximum concentration of 2000 ppm was considered for Baclofen, Isoxsuprine hydrochloride. For Betahistine dihydrochloride, Naphazoline, 1500 ppm of maximum concentration was selected. For Panthenol 400 ppm and for Dicyclomine hydrochloride 800 ppm concentration was selected for analysis. With the help of AFM analysis along with 2-dimensional and 3-dimensional images, the quantitative roughness data was also obtained and is summed up in Table 4.6.1. For this analysis three type of samples were prepared, in the first type metallic coupons were cleaned sample without any external exposure, second samples were immersed in 1 M HCl acidic solution and third samples were immersed in acidic solution with optimized concentration of different drug molecules.

Table 4.6.1 Roughness data calculated from AFM investigation.

Name of the Inhibitor	Concentration (ppm)	Type of samples	Average roughness (Ra)	Root mean square roughness (Rq)
Baclofen	2000 ppm	Polished MS sample	16.1	24.4
		MS Immersed in 1M HCl	213	286
		MS Immersed in HCl and Baclofen	9.37	12.5
Betahistine dihydrochloride	1500 ppm	Polished MS sample	17.2	23.1
		MS Immersed in 1M HCl	357	454
		MS Immersed in HCl and Betahistine	15.9	24.2
Isoxsuprine hydrochloride	2000 ppm	Polished MS sample	22.6	28.6
		MS Immersed in 1M HCl	411	571
		MS Immersed in HCl and Baclofen	40.5	48.9
Panthenol	400 ppm	Polished MS sample	28.7	36.1
		MS Immersed in 1M HCl	401	518
		MS Immersed in HCl and Panthenol	56.9	82.5
Naphazoline	1500 ppm	Polished MS sample	14.8	19.1
		MS Immersed in 1M HCl	451	548
		MS Immersed in HCl and Naphazoline	23.8	31.2
Dicyclomine hydrochloride	1500 ppm	Polished MS sample	30.4	42.0
		MS Immersed in 1M HCl	547	768
		MS Immersed in HCl and Dicyclomine hydrochloride	32.3	43.4

4.6.4 AFM examinations evaluating the application of Baclofen for the reduction of corrosion of MS in 1 M HCl

The AFM technique was here employed to validate the conclusions of other experimental approaches (Verma et al., 2018). Figure 4.6.1 (a-c) are the pictorial representation of the unexposed sample, sample coupon exposed to optimized acid solution, and MS dipped in 1 M HCl containing 2000 ppm of Baclofen as an inhibitor for two hours. With the help of this technique, quantitative data like average roughness (R_a) and root mean square roughness (R_q) was also calculated and summed up in Table 4.6.1. Results revealed that R_a and R_q for MS sample dipped in 1 M HCl solution in absence and presence of 2000 ppm of Baclofen came out to be 16.1, 213, 9.37 nm and 24.4, 286, 12.5 nm respectively (Sharma et al., 2021). It is clear from the data that roughness values are maximum for metallic sample kept in pure acidic solution as compare to the calculated roughness values for sample kept in acid including Baclofen as inhibiting molecule, which confirmed the presence of Baclofen on the sample surface (Bashir et al., 2020).

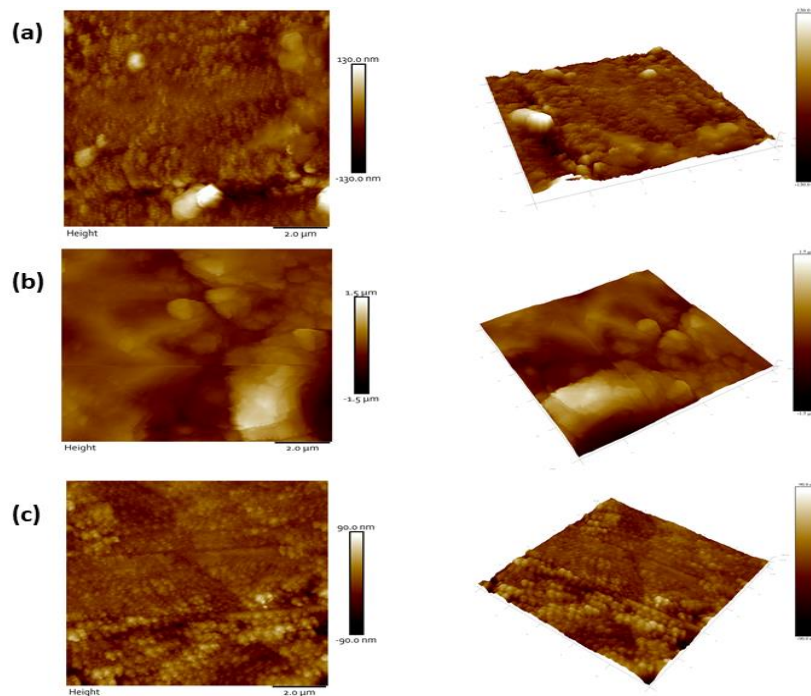


Figure 4.6.1 (a-c) Surface morphology (a) plain and unexposed metal sample (b) metal surface soaked in test solution (c) metal kept in acid with 2000 ppm Baclofen.

4.6.5 AFM examinations evaluating the application of Betahistine dihydrochloride for the mitigation of MS corrosion in 1 M HCl

The AFM micrographs and various parameters like average roughness (R_a), root mean square roughness (R_q) are given in Figure 4.6.2 (a-c) and in Table 4.6.1. The values of R_a and R_q came out to be 17.2 and 23.1 nm for clean surface, 357 and 454 nm for sample soaked in 1M HCl solution and 15.9 and 24.2 nm in test solution containing Betahistine as inhibitor. Higher values of roughness parameters confirmed the more damage caused by 1M HCl solution to sample as compared to polished and Betahistine dihydrochloride contained acid as given in Table 4.6.1. and in Figure 4.6.2 (a-c). Formation of thin layer of inhibitor molecules was also confirmed through the AFM, which protected the MS sample and resulted in the lower value of R_a and R_q values (Galai et al., 2021; Sharma et al., 2022).

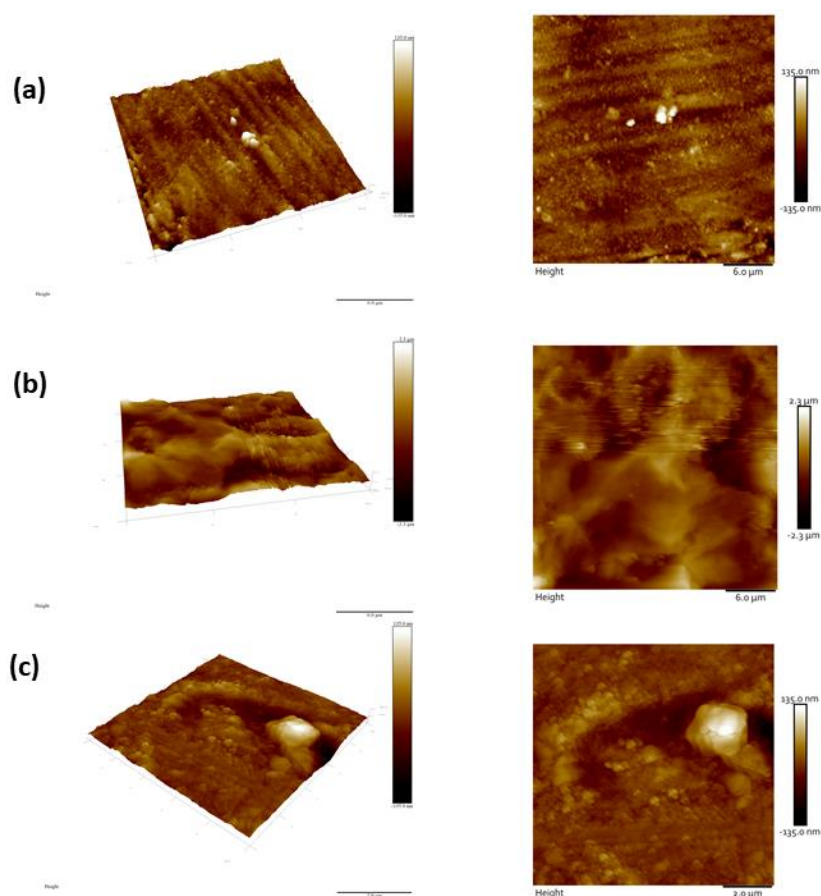


Figure 4.6.2 (a-c) Surface morphology (a) of polished sample surface (b) metal dipped in acid (c) metal in acidic with 1500 ppm Betahistine dihydrochloride.

4.6.6 AFM examinations evaluating the application of Isoxsuprine hydrochloride to prevent corrosion of MS in 1 M HCl

Figure 4.6.3 (a-c), illustrates the two- and three-dimensional presentation of a polished steel specimen, steel panel after being dipped in acid solution for 2 hours at room temperature (298 K) without and with 2000 ppm of Isoxsuprine hydrochloride drug respectively (El-Haddad & Fouda et al., 2021). Figure 4.6.3a strongly demonstrates that the specimen has a smooth finish, Figure 4.6.3b shows extremely high roughness on the metallic surface and Figure 4.6.3c demonstrated the lesser roughness as compare to the Figure 4.6.3b (Bashir et al., 2020). The R_a and R_q of steel panels came out to be 22.6, 411, 40.5 nm and 28.6, 571, 48.9 nm respectively and is summed up in Table 4.6.1. This pictorial presentation and obtained quantitative data validated the Isoxsuprine hydrochloride substance superficially on MS, which protected it from further corrosion.

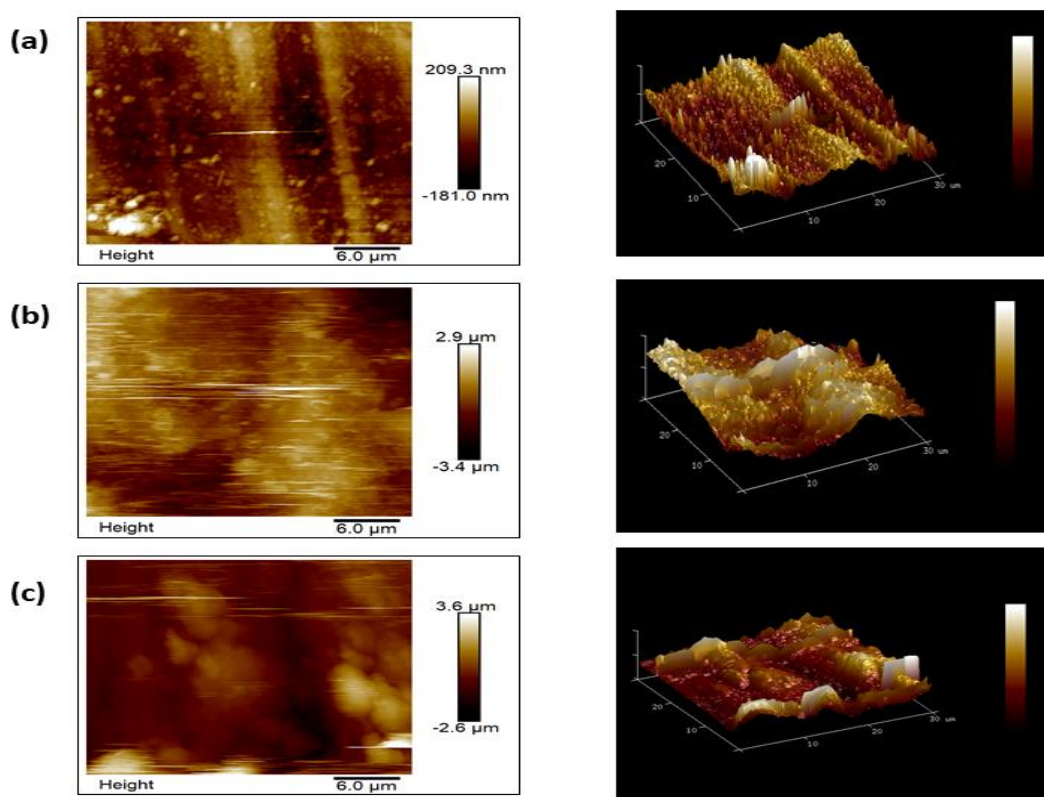


Figure 4.6.3 (a-c) Surface morphology (a) polished surface (b) metal submerged in acid (c) metal in acid containing 2000 ppm of ppm Isoxsuprine hydrochloride.

4.6.7 AFM examinations evaluating the application of Panthenol to prevent corrosion of MS in 1 M HCl

AFM images of cleaned metallic panels, metallic panels immersed in blank solution, and metallic samples soaked in 400 ppm Panthenol drug molecule containing acidic solution are given in Figure 4.6.4 (a-c). It is clearly mentioned in the quantitative data mentioned in Table 4.6.1 and also visible in the Figure 4.6.4(a-c) the roughness of sample b (specimen dipped in test solution) came out to be maximum. Average roughness (R_a) of sample b was 401 nm, which is higher than values of sample a (28.7 nm) and sample c (56.9 nm) and root mean square roughness (R_q) values of sample b was also highest (518 nm) as compare to the values of sample a (36.1 nm) and sample c (82.5 nm). Lowering in roughness values after the addition of Panthenol in the acid reduced the corrosion products, which ultimately confirmed the protection of metal panel (Goyal et al., 2020).

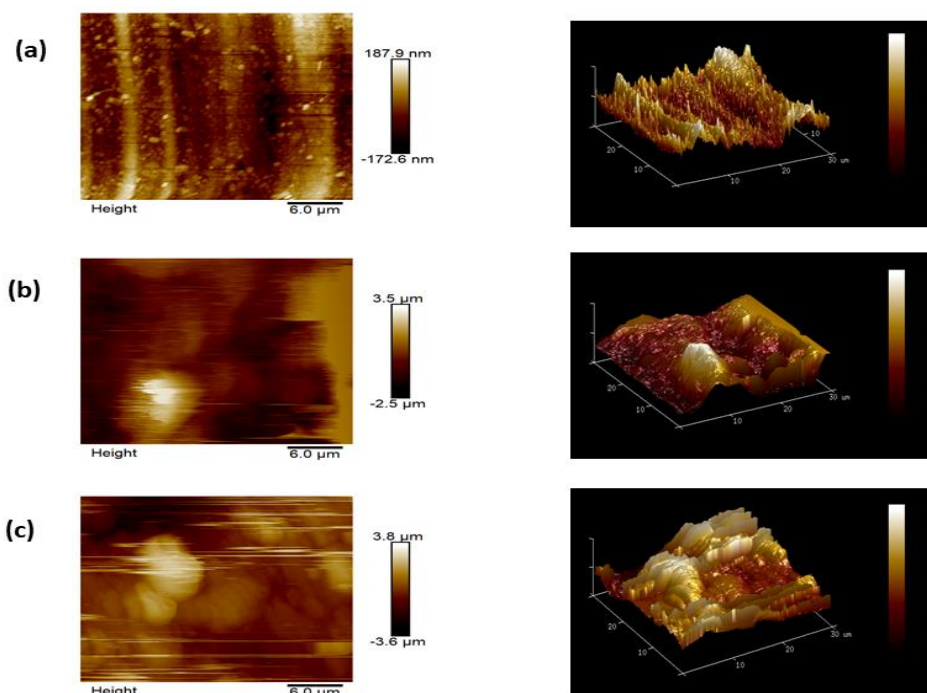


Figure 4.6.4 (a-c) Surface morphology of (a) clean metal (b) surface morphology of metal soaked in acid solution (c) surface morphology of metal soaked in Panthenol contained acid solution.

4.6.8 AFM examinations evaluating the application of Naphazoline to prevent corrosion of MS in 1 M HCl

By utilizing Naphazoline AFM experiments were conducted on metal under investigation for corrosion mitigation in acidic solution. Figure 4.6.5(a-c) and data summed up in Table 4.6.1 depicted the reduced roughness of sample c as compare to sample b. R_a (nm) of the samples came out to be 14.8, 451 and 23.8 nm respectively and R_q came out to be 19.1, 548, and 31.2 nm respectively. On the basis of these parameters, results depicted that the surface has become smoother in case of Naphazoline used with acid, in comparison to sample dipped in pure acid solution. Molecular clusters formed spontaneously on the steel surface by drug molecules in the test solution can be attributed to the decreased roughness values and protection of metal surface (Khan et al., 2016).

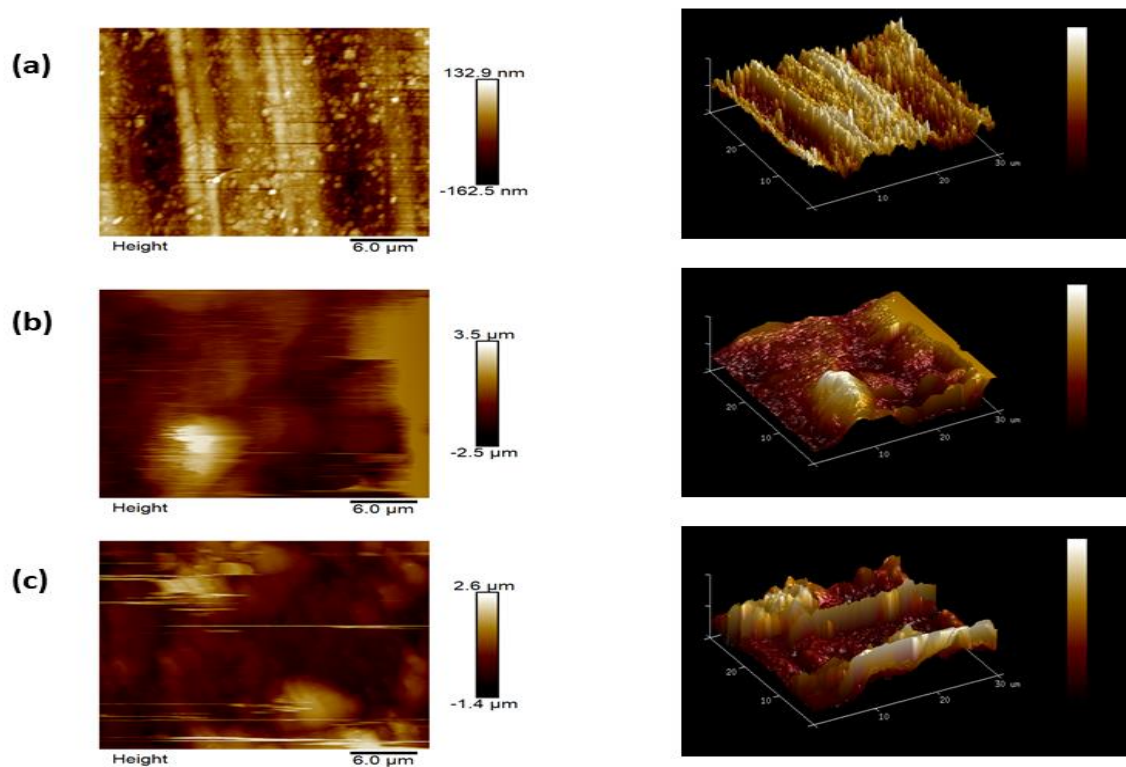


Figure 4.6.5 (a-c) Surface morphology of (a) clean metal (b) surface morphology of metal soaked in acid solution (c) surface morphology of metal soaked in Naphazoline contained acid solution.

4.6.9 AFM examinations evaluating the application of Dicyclomine hydrochloride to prevent corrosion of MS in 1 M HCl

Dicyclomine was used in AFM experiments for corrosion mitigation of MS in 1 M HCl. The end outcome was illustrated in Figure 4.6.6 (a-c) and Table 4.6.1 verified the maximum roughness in case of sample soaked in pure acid solution as compare to polished and the sample dipped in acid containing Dicyclomine hydrochloride as inhibiting molecule. Average Roughness values (nm) for sample a-c were 30.4, 547, 32.4 respectively and root mean square value (nm) for samples a-c were 42.0, 768 and 43.4 respectively. It was clear from the results that Figure 4.6.6b was with more cracked surface and higher roughness because of high rate of corrosion (Shukla & Quraishi, 2010).

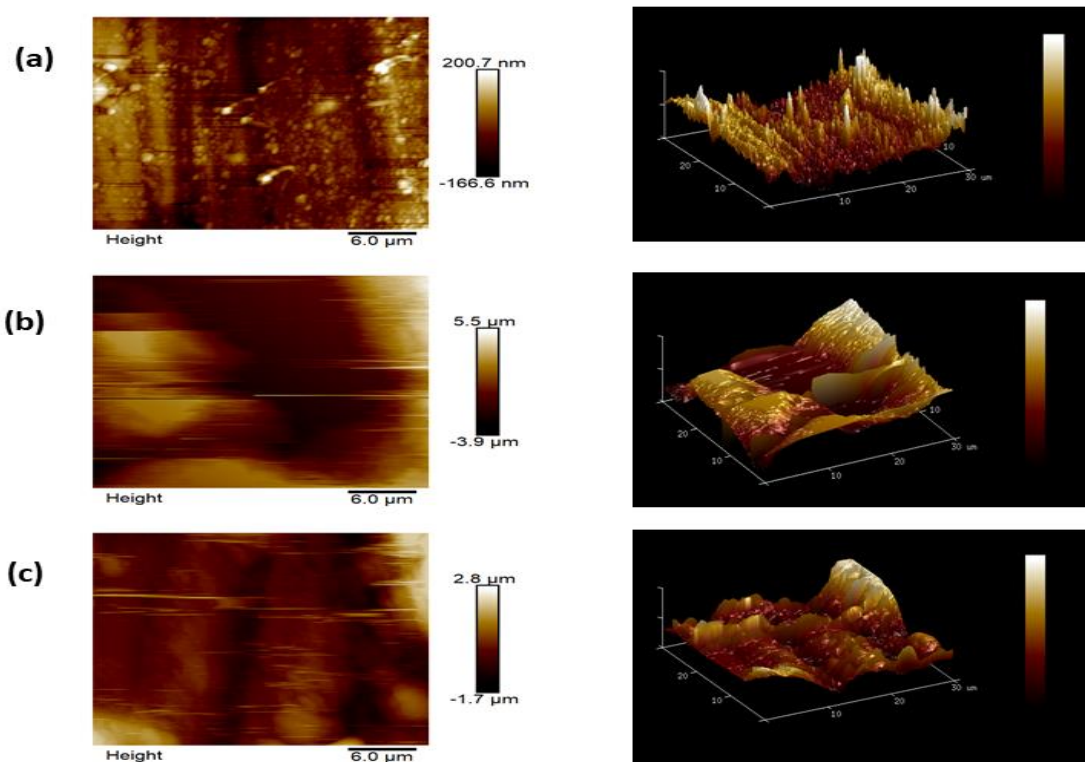


Figure 4.6.6 (a-c) Surface morphology of (a) clean metal (b) surface morphology of metal soaked in acid solution (c) surface morphology of metal soaked in Dicyclomine hydrochloride contained acid solution.

4.6.10 Conclusions

AFM investigated the topology of polished metals and by subjecting metal samples to acidic solutions and drug such as Baclofen, Betahistine dihydrochloride, Isoxsuprine hydrochloride, Panthenol, Naphazoline, and Dicyclomine hydrochloride containing acid solution. Average roughness (R_a) and root mean square roughness (R_q) were the parameters utilized to validate the corrosion retardation of the metal sample by employing various drug molecules. Three different samples were investigated: pure metal without any external treatments, pure metal exposed to acid, and finally pure metal exposed to acid with an optimal concentration of inhibiting molecule. The following are some of the conclusions that were made as a result of this research:

- According to the AFM experiments conducted for the corrosion MS, the highest average roughness value and root mean square values were found in blank solution, indicating that the greatest amount of corrosion in blank solution.
- When selected drug molecules are added as corrosion inhibitors, the values of average roughness and root mean square roughness drop, showing the formation of a preventative layer on the metal.
- Optimized concentration of drug molecules considered for study, was maximum concentration of 2000 ppm for Baclofen, Isoxsuprine hydrochloride. For Betahistine dihydrochloride, Naphazoline, 1500 ppm of maximum concentration was selected. For Panthenol 400 ppm and for Dicyclomine hydrochloride 800 ppm concentration was selected for analysis. These were the concentrations on which maximum inhibition was reported and roughness values were therefore compared by selecting these respective concentrations.
- The overall order of decrease in the average roughness values and root mean square values in the present study:

Average roughness and Root mean square roughness values decreased as follows:

Baclofen > Betahistne dihydrochloride > Naphazoline > Dicyclomine hydrochloride > Isoxsuprine hydrochloride > Panthenol.

4.7 Computational Study

The computational analyses in the present research work were conducted by incorporating the quantum chemical calculations and molecular dynamics simulation research. These theoretical studies are becoming extremely popular for modelling the corrosion inhibition performances of molecules because experimental approaches utilized to evaluate the anticorrosive properties and mechanism of compounds are overall pricey and laborious (Erdogan et al., 2017) Also, these theoretical studies validate the experimental work.

4.7.1 Quantum chemical analysis

Researchers use quantum chemical techniques to assess experimental findings and attempt to establish the anticorrosive capability of the inhibitors in a smaller duration of time. Calculations based on quantum chemical principles are extremely valuable in the study of corrosion inhibitors because they allow researchers to identify inhibitors with better degrees of corrosion resistance (Abd El-Raouf et al., 2018; Gece, 2008). In order to assert corrosion inhibiting potential, a corrosion inhibitor must typically be adsorbed onto the required metallic surface and electronic characteristics and molecular structure of compounds are what determine whether or not they will adhere to a given surface to behave as desired inhibitors (Singh et al., 2019). When it comes to optimizing the structure of inhibitors as well as determining their electronic characteristics, DFT has shown to be an invaluable tool (Yadav & Quraishi, 2012). The DFT study investigates all of the conceivable interaction between donor and acceptors. BIOVIA Material Studio software (version 7.0) was used for quantum chemical study. DMol³ module was employed for the quantum chemical calculations. DFT calculations were carried out using generalized gradient approximation (GGA) and Becke–Lee–Yang–Parr (BLYP) with double numeric polarization (DNP) basis set (including d as well as p orbital polarization functionals) in the COSMO implicit solvent model (Cao et al., 2014; Ciezak et al., 2006; Ndukwe et al., 2012). For these theoretical investigations, first and foremost, the geometry optimization of all of the

molecules by employing Computer simulations was achieved and after it was determined that the geometry was the most ideal, additional experiments were carried out in order to obtain more information about molecular orbitals.

The adsorption capacity of a molecule, which is closely related to its D–A capability, is significantly rely on the frontier molecular orbitals (FMOs) present in that molecule And, so far as orbitals are concerned, there are two major FMOs to take into consideration.: the highest-occupied molecular orbital (HOMO) and lowest-unoccupied molecular orbital (LUMO).

Following are the formulas to calculate the different parameters: (Abdallah et al., 2021; Hsissou, 2021).]

$$\Delta E = E_{LUMO} - E_{HOMO} \quad (4.7.1)$$

E_{LUMO} and E_{HOMO} are the energy levels values associated with the lowest unoccupied molecular orbital and the highest occupied molecular orbital respectively. E_{HOMO} and E_{LUMO} are attributed to the related electron's donating tendency and electron gaining tendency of the molecule. The following is how Koopman's theorem confirmed the relationship between HOMO and LUMO and the ionisation potential and electron affinity (Issa et al., 2008; Javadian et al., 2017; Murulana et al., 2012; Zhang et al., 2012)

$$IP = -E_{HOMO} \quad (4.7.2)$$

$$EA = -E_{LUMO} \quad (4.7.3)$$

Other important parameters such as electronegativity (χ), absolute hardness (η), and global softness (σ) can also be measured by utilizing the FMO's energy, as follows (El-Tabei et al., 2022; Lukovits, 2001):

$$\chi = \frac{IP+EA}{2} \quad (4.7.4)$$

$$\eta = \frac{IP-EA}{2} \quad (4.7.5)$$

$$\sigma = \frac{1}{\eta} \quad (4.7.6)$$

In order to determine the inhibitor-metal exterior interaction, one of the crucial characteristics is the quantity of electrons that are carried from the inhibitor

molecule to metallic surface and can be calculated as follows (Anupama et al., 2016):

$$\Delta N_{(FET)} = \frac{\chi_{Fe} - \chi_{inh}}{2(\eta_{Fe} + \eta_{inh})} \quad (4.7.7)$$

Here χ_{Fe} and χ_{inh} specifies the electronegativities of metal and inhibitor molecule under investigation, while η_{Fe} and η_{inh} denotes the hardness of the iron and inhibitor molecule, respectively. Theoretical values of $\chi_{Fe} = 7$ eV and $\eta_{Fe} = 0$ eV are generally used for the calculation of the ΔN value (John et al., 2013; Kovacevic & Kokalj, 2011).

Recent literature suggests the non-acceptance of $\chi_{Fe} = 7$ eV value, due to the improper consideration of electron-electron interactions, and is solely considered free electron gas Fermi energy of iron (Saha & Banerjee, 2015). Because of this, researchers are recently utilizing work function (ϕ) for relevant and true measure of electronegativity of iron (Obot et al., 2015; Saha, et al., 2015; Saha & Banerjee, 2018). Therefore, Equation 4.7.7 can be written in another way as follows:

$$\Delta N = \frac{\phi - \chi_{inh}}{2(\eta_{Fe} + \eta_{inh})} \quad (4.7.8)$$

In Density functional theory, the ϕ values for Fe (111), Fe (110) and Fe (100) surfaces are mentioned as 3.88, 4.82 and 3.91 eV, respectively (Obot et al., 2015; Saha, et al., 2015a; Saha & Banerjee, 2018). Fe (110) surface is the only surface that has been chosen for this work because of its densely packed surface and higher stabilization energy. Furthermore, electron transfer from the inhibitor to the metal surface will take place only if $\Delta N > 0$ and *vice versa* (Awad et al., 2010; Saha et al., 2015b; Saha, et al., 2016). Also, in one of the previous studies, it was mentioned that when the calculated ΔN value is less than 3.6, capacity to donate electron of inhibitor increased (Awad et al., 2010). For theoretical study six drug molecules Baclofen, Betahistine dihydrochloride, Isoxsuprine hydrochloride, Panthenol, Naphazoline and Dicyclomine hydrochloride are considered. All the parameters calculated for selected drug molecule by utilizing the above-mentioned equations are summed up in Table 4.7.1. When these

characteristics are considered together, it is possible to determine the effectiveness of inhibitor adsorption on metal surfaces.

Table 4.7.1. Quantum chemical parameters of the investigated drug molecules

Quantum chemical Parameters	Baclofen	Betahistine	Isoxsuprine	Panthenol	Naphazoline	Dicyclomine
$E_{HOMO} (eV)$	-5.698	-4.920	-4.989	-5.792	-4.918	-4.647
$E_{LUMO} (eV)$	-1.232	-1.345	-0.934	-0.694	-1.737	-0.798
$\Delta E (eV)$	4.466	3.575	4.055	5.098	3.181	3.849
$I = -E_{HOMO} (eV)$	5.698	4.920	4.989	5.792	4.918	4.647
$A = -E_{LUMO} (eV)$	1.232	1.345	0.934	0.694	1.737	0.798
$\chi (eV)$	3.46	3.132	2.96	3.24	3.33	2.72
$\eta (eV)$	2.23	1.79	2.02	2.54	1.59	1.92
$\sigma (eV^{-1})$	0.45	0.56	0.49	0.39	0.63	0.52
ΔN	0.79	0.47	0.46	0.31	0.46	0.55

Figure 4.7.1 to Figure 4.7.6 are demonstrating the optimized, HOMO and LUMO shapes of Baclofen, Betahistine, Isoxsuprine, Panthenol, Naphazoline and Dicyclomine respectively. The HOMO and LUMO of the inhibitor molecule provide information about the molecule's electron donating and electron - accepting sites, respectively. A larger value of HOMO indicates a greater potential that the inhibitor will be able to donate electrons to the metal surface, while a lower value of LUMO indicates a greater chance that the inhibitor will be able to accept electrons away from the filled d-orbitals of the metal under analysis. (Abdallah et al., 2021; Liangtian et al., 2020).

Higher inhibitory efficacy is generally related with lower energy gap (ΔE) and the obtained values as given in Table 4.7.1 are very good as compare to the other investigations present in literature (Matad et al., 2014; Obot et al., 2015; Sliem et al.,

2019). In all the selected drug molecules Baclofen has lowest ΔE value. Another key metric is electronegativity (χ), which describes the tendency of to attract electrons, and the high values of electronegativity (as mentioned in Table 4.7.1) confirms the tendency of the inhibitor molecule to accept the electron from the metallic sample under study. Further softness (σ) which is reciprocal to (η) another parameter explaining capacity of inhibitor to get adsorbed on the metallic surface. According to the Hard and Soft Acids Bases (HSAB) principle, metallic samples are regarded as soft acids, whereas inhibitor chemicals are regarded as soft bases in the current investigation. The tendency of the inhibitor to give electrons is represented by softness values, which confirm the adsorption. Further on calculating ΔN for different drug molecules by using equation 4.7.8 and value of ϕ for Fe (110) surface is 4.82 eV was substituted for the calculation. All the calculated values for drugs (Table 4.7.1) comes out to be greater than 0, which confirmed the donation of electrons from the inhibitor to metal, and proving the successful mitigation of corrosion from the selected drugs.

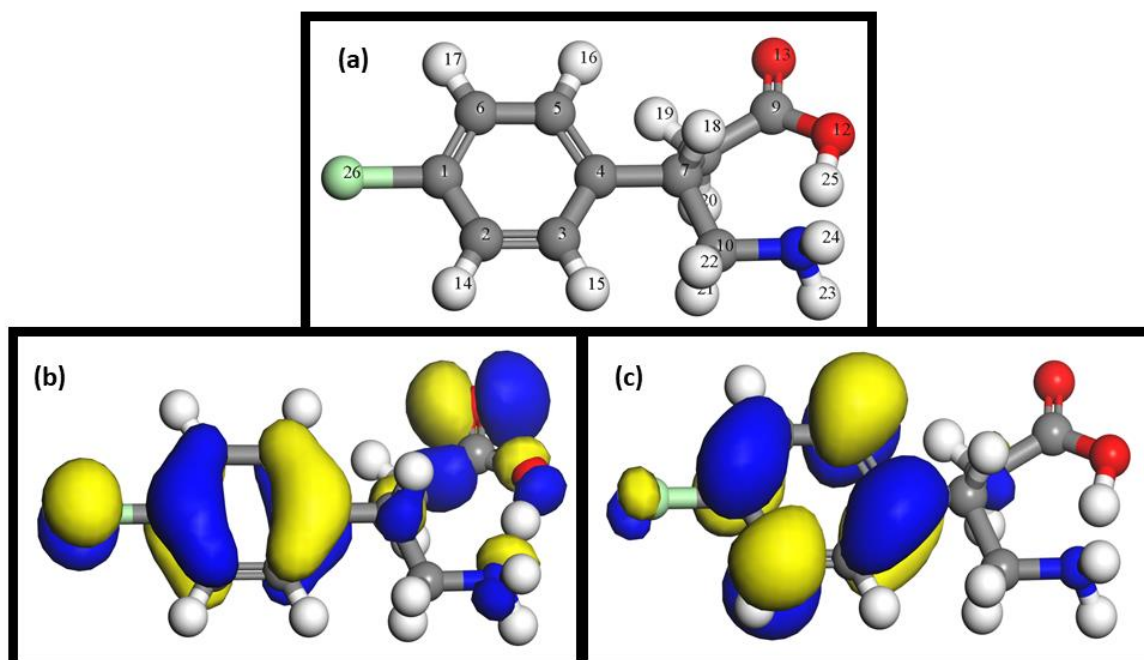


Figure 4.7.1(a-c) Pictorial presentation of (a) optimized structure, (b) HOMO and (c) LUMO of Baclofen.

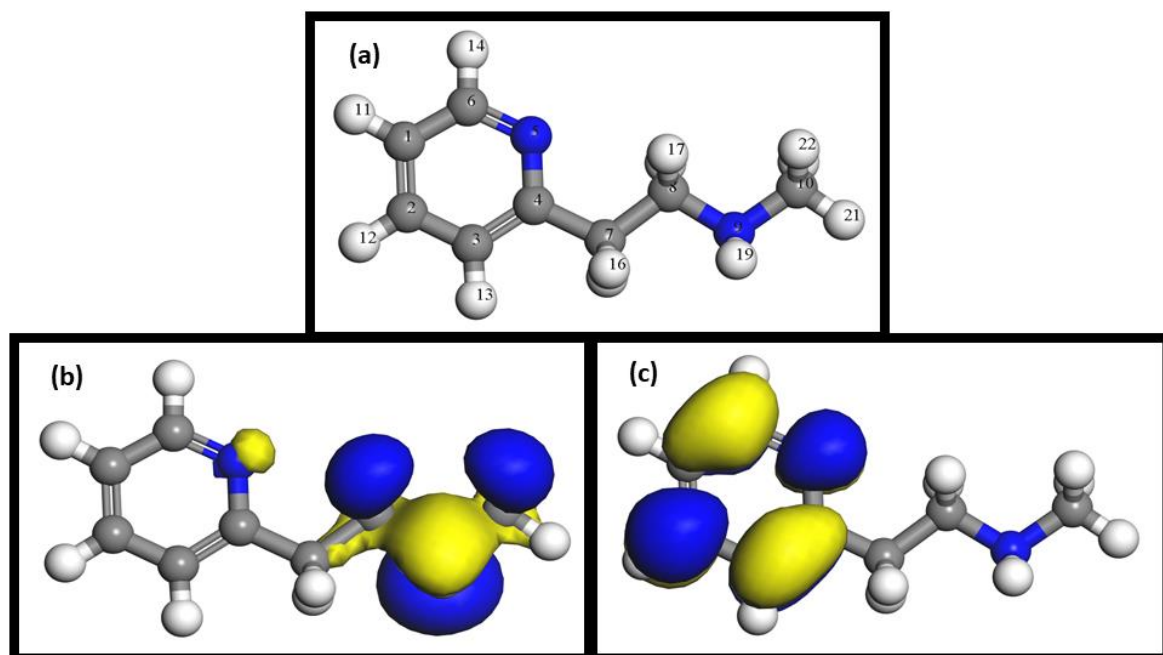


Figure 4.7.2 (a-c) Representation of (a) optimized geometry (b) HOMO and (c) LUMO of Betahistine.

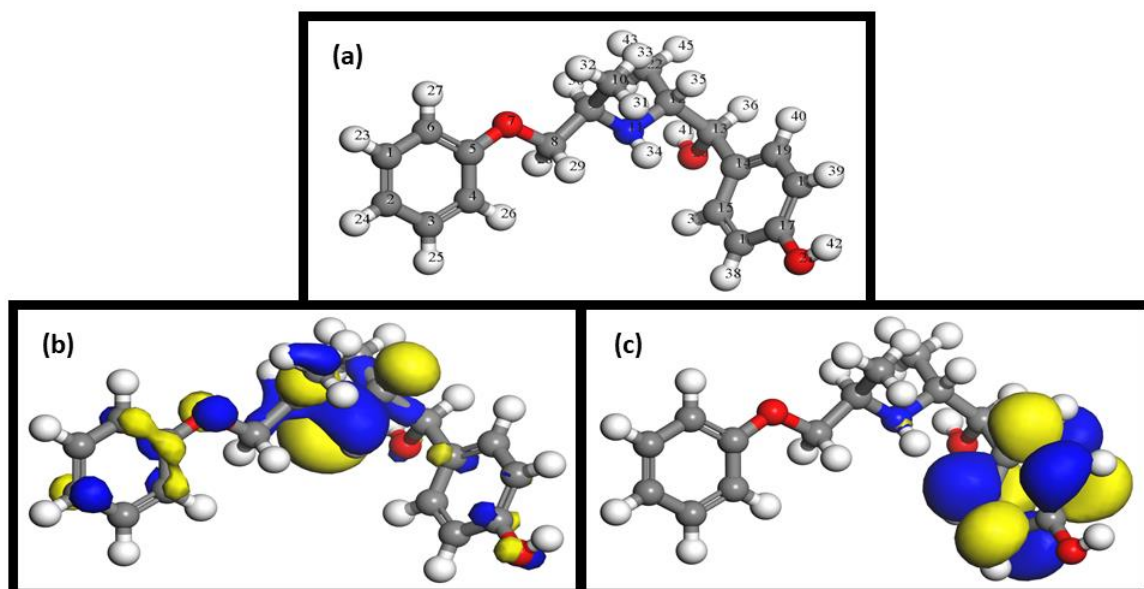


Figure 4.7.3 (a-c) Representation of (a) optimized structure, (b) HOMO and (c) LUMO of Isoxsuprine.

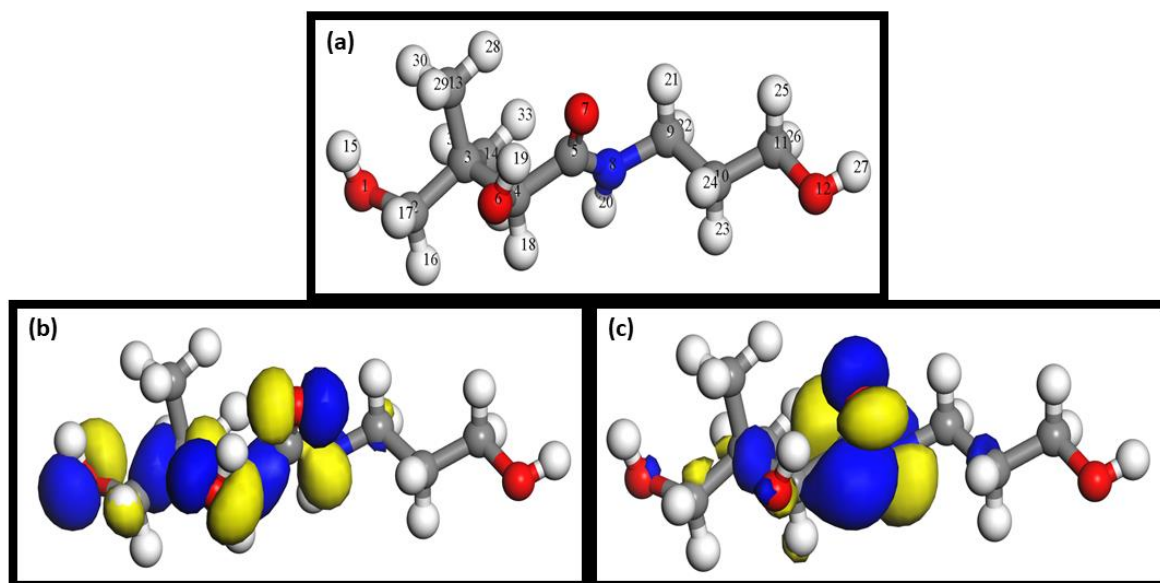


Figure 4.7.4 (a-c) Representation of (a) optimized structure, (b) HOMO and (c) LUMO of Panthenol.

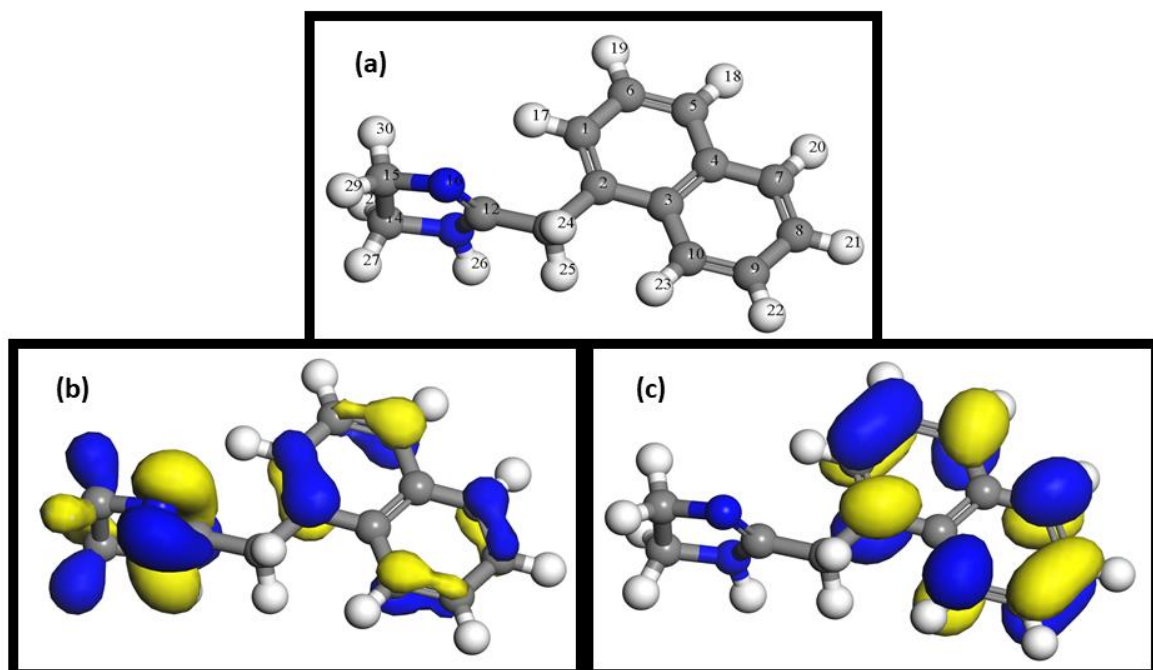


Figure 4.7.5 (a-c) Representation of (a) optimized structure, (b) HOMO and (c) LUMO of Naphazoline.

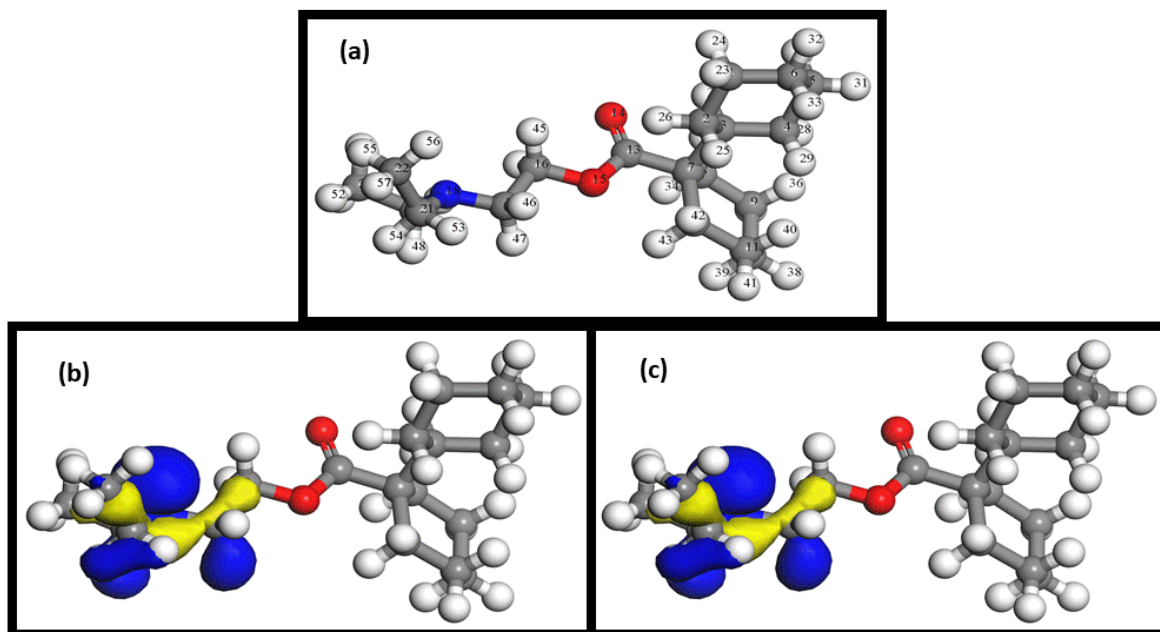


Figure 4.7.6 (a-c) Representation of (a) optimized structure, (b) HOMO and (c) LUMO of Dicyclomine.

4.7.2 Fukui functions

Fukui functions are estimated in order to gain an understanding of the nucleophilic and electrophilic adsorption sites available to the molecule under inquiry, and are calculated on the basis of Hirshfeld population analysis. In the present investigation the Fukui indices are summed up in the Table 4.7.2- 4.7.7. This is the most significant way to find out the behaviour of different sites, whether they are electron donating or behaving as electron acceptors. The highest value f_k^+ determining the appropriate sites for a nucleophilic attack, while the f_k^- highest value talks about ideal sites for an electrophilic attack (Masroor et al., 2017) and can be calculated as follows:

$$f_k^+ = q_k(N + 1) - q_k(N) \quad (4.7.8)$$

$$f_k^- = q_k(N) - q_k(N - 1) \quad (4.7.9)$$

Here q_k define to charge on the atoms, and (N), (N+1), (N-1) refers to total electrons in neutral, cationic, or anionic forms (Dagdag et al., 2020; Jafari et al., 2013; Zarrok et al., 2017). When electrons are taken or released by the inhibitor molecule, the electron density of the inhibitor molecule changes accordingly, and values of f_k^+ determines the

electron density on electron acceptance and f_k^- is the determines the electron density, when electrons are donated.

Table 4.7.2 depicted that the C(1), C(2), C(3), C(4), C(5), C(6), and Cl (26) atoms are the sites in Baclofen with electron accepting tendency as those atoms possess high values of f_k^+ . Similarly the high value of f_k^- are associated with C(1), C(2), C(3), C(4), C(5), C(6), C(9), O(12), O(13), Cl(26) atoms and which have the high electron donating tendency as compare to other atoms present in the molecule.

Table 4.7.3 explains that in Betahistine molecule, C (1), C (2), C (3), C (4), N (5) and C (6) atoms have comparatively higher f_k^+ values, therefore are suitable and for are most favoured places for the nucleophilic attack. On the contrary, C (8), N (9) and C (10) atoms are well- liked for electrophilic attack, because have the highest f_k^- values. It is now obvious from these FIs values that the inhibitor molecule's pyridine unit is responsible for electron intake, whereas the methylamine unit is incharge of electron donation.

Table 4.7.4 revealed C(1), C(3), C(4), C(6), C(15), C(16),C(17), C(18), C(19) have high values of f_k^+ and C(2), O(7), N(11), O(21) have the higher f_k^- values in Isoxsuprine molecule.

Table 4.7.5 for Panthenol explains that C(4), C(5), O(7), N(8), has high value of f_k^+ , therefore comparatively has higher chances of electron acceptance and O(1), C(2), O(6), O (7), O(12) has higher chances of electron donation because of larger highest f_k^- value.

Table 4.7.6 for Naphazoline illustrated that C(1) to C(10) has high f_k^+ values resulting in greater chances of electron acceptance at these sites and C(12), N(13), C(14), C(15), N(16) has highest f_k^- , resulted in higher probability of electron donation from these sites.

Table 4.7.7 for Dicyclomine C(3), C(7), C(8), C(9), C(13), O(14), O(15), C(16) with high f_k^+ values are more susceptible for electron acceptance and C(17), N(18), C(19), C(20), C(21), C(22) has more tendency to donate the electrons because of highest f_k^- .

The finding is in agreement with the electron density distribution on the HOMO and LUMO atoms.

Table 4.7.2 Calculated Fukui indices of the Baclofen inhibitor.

Atoms	f_k^+	f_k^-
C (1)	0.049	0.059
C (2)	0.121	0.049
C (3)	0.068	0.041
C (4)	0.058	0.059
C (5)	0.109	0.043
C (6)	0.079	0.042
C (7)	-0.013	0.016
C (8)	-0.007	0.023
C (9)	0.014	0.047
C (10)	-0.009	0.010
N (11)	0.000	0.028
O (12)	0.010	0.055
O (13)	0.017	0.173
Cl (26)	0.108	0.138

Table 4.7.3 Fukui indices of Betahistine as inhibiting molecule.

Atoms	f_k^+	f_k^-
C (1)	0.087	0.011
C (2)	0.153	0.010
C (3)	0.102	0.009
C (4)	0.077	0.006
N (5)	0.139	0.019
C (6)	0.119	0.010
C (7)	0.016	0.013
C (8)	0.006	0.051
N (9)	0.005	0.331
C (10)	0.003	0.067

Table 4.7.4 Fukui indices for Isoxsuprine hydrochloride.

Atoms of Isoxsuprine	f_k^+	f_k^-
C (1)	0.045	0.022
C (2)	0.028	0.045
C (3)	0.050	0.025
C (4)	0.041	0.029
C (5)	0.022	0.030
C (6)	0.049	0.032
O (7)	0.011	0.049
C (8)	0.004	0.013
C (9)	0.002	0.017
C (10)	0.001	0.018
N (11)	0.003	0.136
C (12)	0.002	0.018
C (13)	0.005	0.007
C (14)	0.032	0.020
C (15)	0.069	0.015
C (16)	0.082	0.026
C (17)	0.040	0.029
C (18)	0.077	0.024
C (19)	0.081	0.019
O (20)	0.008	0.015
O (21)	0.028	0.039
C (22)	0.003	0.010

Table 4.7.5 Fukui indices for Panthenol.

Atoms of Panthenol	f_k^+	f_k^-
O (1)	0.017	0.119
C (2)	0.011	0.028
C (3)	0.011	0.023
C (4)	0.031	0.028
C (5)	0.203	0.032
O (6)	0.044	0.112
O (7)	0.198	0.116
N (8)	0.104	0.055
C (9)	0.024	0.016
C (10)	0.013	0.009
C (11)	0.008	0.016
O (12)	0.007	0.064
C (13)	0.005	0.008
C (14)	0.004	0.009

Table 4.7.6 Fukui indices for Naphazoline.

Atoms	f_k^+	f_k^-
C (1)	0.064	0.032
C (2)	0.070	0.037
C (3)	0.030	0.014
C (4)	0.032	0.015
C (5)	0.086	0.048
C (6)	0.071	0.033
C (7)	0.088	0.039
C (8)	0.067	0.032
C (9)	0.073	0.032
C (10)	0.086	0.039
C (11)	0.014	0.014
C (12)	0.000	0.042
N (13)	0.003	0.116
C (14)	0.003	0.029
C (15)	0.003	0.027
N (16)	0.010	0.118

Table 4.7.7 Fukui indices for Dicyclomine hydrochloride.

Dicyclomine hydrochloride	f_k^+	f_k^-
C (1)	0.005	0.000
C (2)	0.004	0.000
C (3)	0.010	0.000
C (4)	0.009	0.000
C (5)	0.006	0.000
C (6)	0.003	0.000
C (7)	0.016	0.001
C (8)	0.015	0.001
C (9)	0.011	0.001
C (10)	0.004	0.000
C (11)	0.007	0.001
C (12)	0.005	0.000
C (13)	0.221	0.005
O (14)	0.233	0.011
O (15)	0.104	0.009
C (16)	0.023	0.018
C (17)	0.008	0.044
N (18)	0.004	0.265
C (19)	0.002	0.044
C (20)	0.001	0.020
C (21)	0.002	0.041
C (22)	0.001	0.030

4.7.3 Molecular dynamic simulation

MD simulation has been used to comprehend the inhibition of MS corrosion by using selected drug molecules as inhibitor molecules in a more realistic way. With the help of DFT, researchers only work upon the molecular properties of the inhibitor but interactions between metal and inhibitor were not taken into account. Every species (H_2O , H_3O^+ , Cl^- and iron surfaces) that were involved in the corrosion process were taken into consideration in the MD simulation. The MD simulation is conducted with the aid of the software BIOVIA Material Studio software (version 7.0), which is used to simulate and then explore the inhibitor's adsorption behavior. Metal surfaces with Fe crystal cleaved along the three planes (110), (100), and (111) were considered, but Fe (110) is believed to have a well-packed density surface and is the most stable, thus it is included in the analysis. Using a three-dimensional simulation box (39.64 39.64 75.63 nm) with periodic boundary conditions to avoid any arbitrary boundary effects, MD simulations of the inhibitor molecule are performed. The inhibitor molecule will only engage in non-bonding interactions with metal surfaces. therefore, only three layers are considered out of them the first layer contains Fe slab, consist of the eleven layers of iron and the second layer consisted of solution slab having water molecule along with molecular ions *like* H_3O^+ , Cl^- and the layer of vacuum is to be left within the box after these two layers. A dynamic simulation was conducted out once the simulation box was constructed by using COMPASS force field, which optimize the geometry to its most stable and low energy state (Saha et al., 2015) and by employing canonical ensemble (NVT) with a time step of 1.0 fs and a simulation time of 100 ps at 298 K.

MD simulation has been carried out to find out the equilibrium adsorption configuration of the inhibitor on the Fe surfaces as mentioned in Figure 4.7.7- Figure 4.7.12. Part a and c of every pictorial presentation depicts the side view and b part is illustrating the top view of the Equilibrium adsorption configurations of selected drug molecules on Fe (110) surface obtained by MD simulations. It can be understood from the diagrams that selected molecules adsorbs with planar orientation on the Fe (110) surfaces, and this parallel adsorption was shown by molecules because of formation of the coordinate as well as back bonding with surface atoms of metal under study. All the investigated drug molecules have π -electrons, heteroatoms and aromatic rings, because of which

molecules can easily donate electrons towards vacant d-orbital of Fe atom. On the other hand, π -antibonding orbitals of an aromatic ring (if present in the molecules) is capable to accept electrons coming from 4s or 3d orbitals of metal surface atoms. In this way, maximize contact between the inhibitor molecules and the iron surfaces was obtained, therefore, iron dissolution in the test solution is minimized. This could be one of the factors contributing to the remarkable corrosion inhibition efficacy achieved by the chosen inhibitor molecules, among other things. Further, interaction and binding energy between the Fe (110) surface and inhibitor molecules is also useful to analyze the adsorption ability of the studied inhibitor

Quantitatively the interaction energy has been calculated as follows (Berdimurodov et al., 2021) and summarized in Table 4.7.8.

$$E_{\text{interaction}} = E_{\text{total}} - (E_{\text{surface} + \text{H}_2\text{O} + \text{H}_3\text{O}^+ + \text{Cl}^-} + E_{\text{inhibitor}}) \quad (4.7.9)$$

Here E_{total} represents energy value which was related with concocted system, $E_{\text{surface} + \text{water} + \text{Cl}^-}$ the energy of the iron exterior containing H_2O , H_3O^+ , Cl^- and the energy value inhibitor drug molecule, which is adsorbed on the surface of the metal represented as $E_{\text{inhibitor}}$.

The binding energy of the studied inhibitor molecule is the negative of the interaction energy and presented as follows : (Guo et al., 2018; Kaya et al.,2016).

$$E_{\text{binding}} = - E_{\text{interaction}} \quad (4.7.10)$$

Negative value of interaction energy resulted in the spontaneous and strong adsorption of inhibitor molecule on the metal under study (Musa et al., 2012). A larger binding energy value validated the easy and strong capacity of the corrosion inhibitor to bond with the iron surfaces and facilitates excellent corrosion inhibitive performance. Strong interaction is validated by the high negative value of interaction energy.

Table 4.7.8 Energy values calculated from MD simulation on Fe (110) surface when different drug molecules are adsorbed.

Investigated Interaction	$E_{\text{interaction}}$ (kJ/mol)	E_{binding} (kJ/mol)
Fe- Baclofen	-365.95	365.95
Fe- Betahistine	-215.53	215.53
Fe-Isoxsuprine	-757.634	757.634
Fe- Panthenol	-557.078	557.078
Fe- Naphazoline	-535.485	535.485
Fe- Dicyclomine	-665.247	665.247

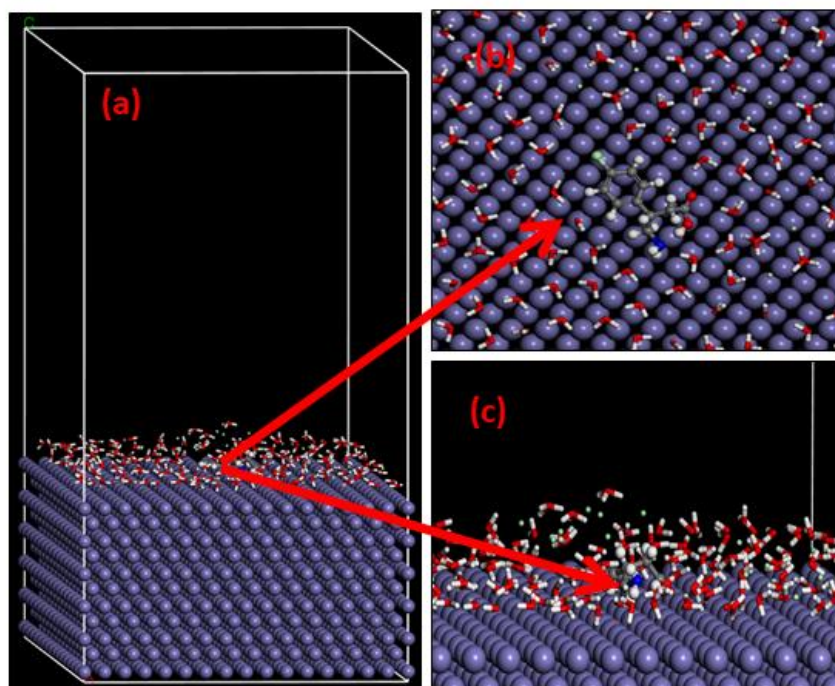


Figure 4.7.7(a-c) Equilibrium adsorption configuration of Baclofen inhibitor on the Fe (110) plane. (a,c) side view and (b) top view.

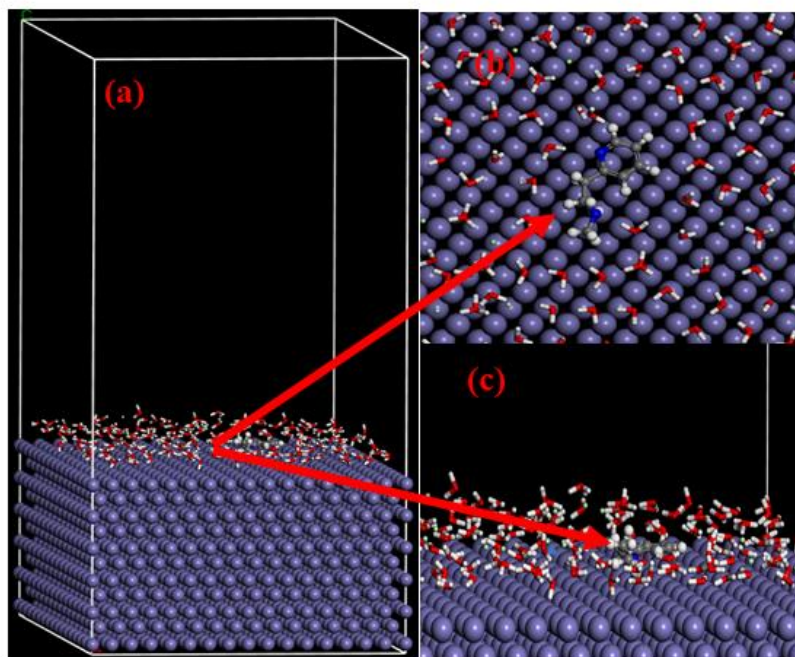


Figure 4.7.8(a-c) Stable low energy equilibrium configuration, (a and c) representing side view, (b) showing top view of Betahistine interacting on the surface of Fe (110).

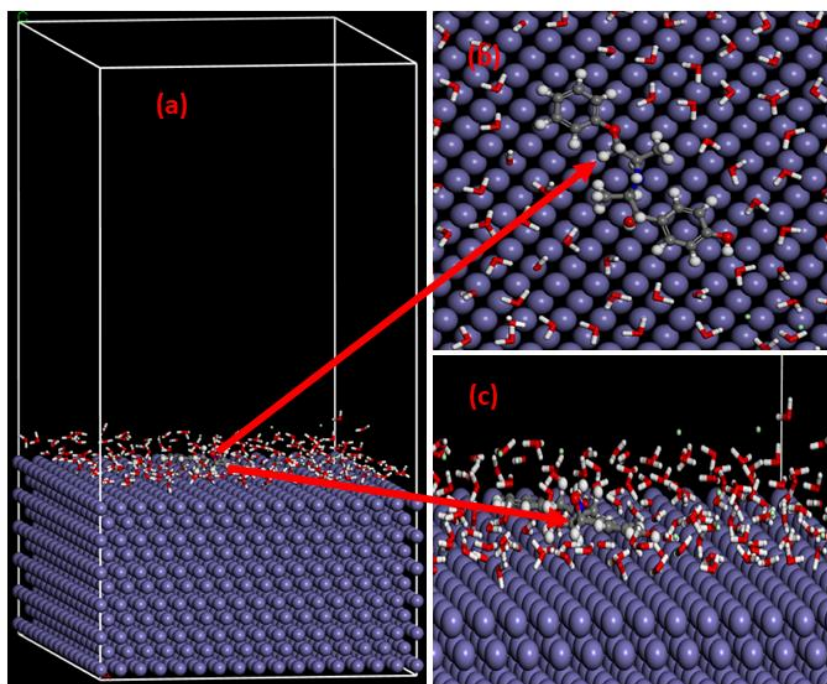


Figure 4.7.9(a-c) Low energy configurations of Isoxsuprine on Fe (110) surface obtained by MD simulations. (a & c) side view, (b) top view

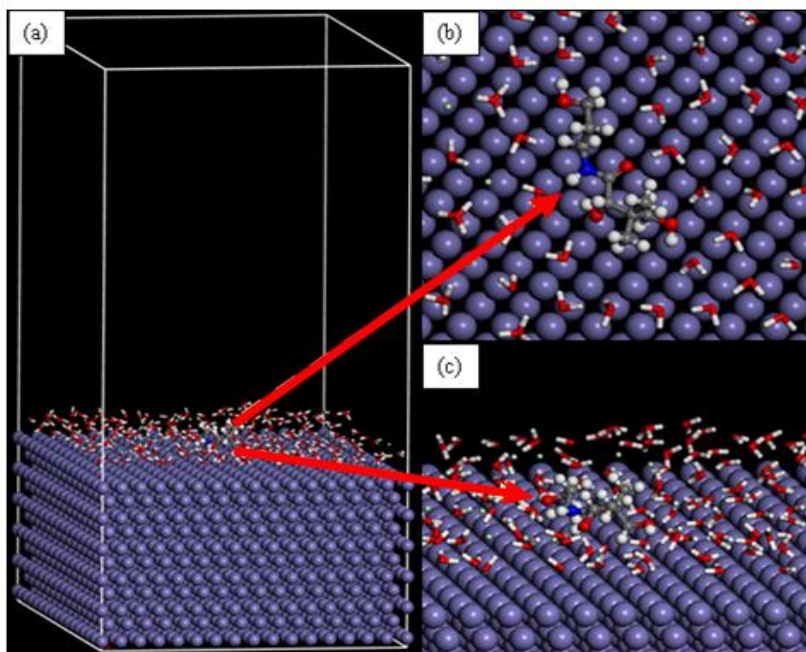


Figure 4.7.10(a-c) Low energy configurations of Panthenol on Fe (110) surface obtained by MD simulations. (a & c) side view, (b) top view.

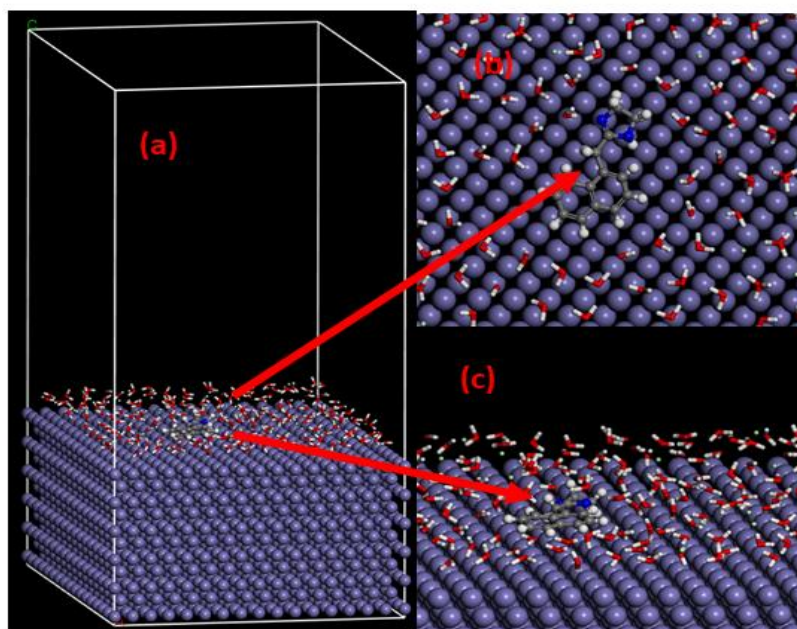


Figure 4.7.11(a-c) Low energy configurations of Naphazoline on Fe (110) surface obtained by MD simulations. (a & c) side view, (b) top view

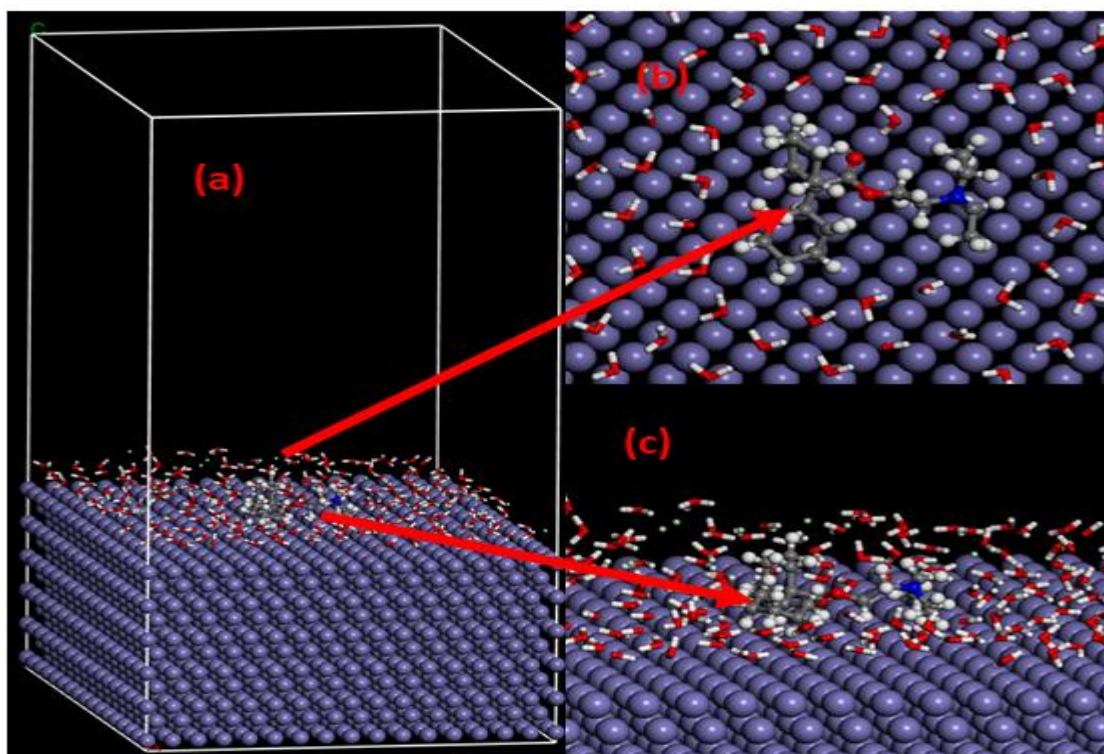


Figure 4.7.12(a-c) Adsorption configurations of Dicyclomine hydrochloride (low energy) on Fe (110) surface obtained by MD simulations. (a & c) side view, (b) top view.

4.7.4 Conclusions

To establish the relation between corrosion inhibition efficiency and structure of an inhibitor, computational studies were used. On the basis of molecular/electronic properties, we can predict the efficiency of an inhibitor molecule. Following conclusions that were drawn based on these computational methods:

- The negative value of interaction energies for all the six drug molecules suggested the stability of these drug molecules as inhibitors.
- The relationship between ΔE , and observed inhibition efficiency was complementing one another.
- Quantum chemical calculation showed that Panthenol has the lowest ΔN value, which means in comparison to other drug molecules Panthenol has least corrosion inhibition efficiency.

CHAPTER 5
SUMMARY AND CONCLUSIONS

5 Summary and Conclusions

In a wide range of applications, such as nuclear power plants, construction activities, the refineries and manufacture of petroleum products, transportation and marine equipment, MS alloys are quite useful. Owing to their prolonged exposure to an aggressive environment, the degradation of metal takes place and this deterioration or corrosion resulted in to a huge direct or indirect loss. As a result, it is critical to devise effective strategies for halting this corrosion. The various ways which can be employed to protect the metals and reduce the effects of corrosion include: design improvements, cathodic and anodic protection, coatings and modification in the properties of metals and utilizing corrosion inhibitors. The current research is concerned with the prevention of corrosion through the use of medicines as corrosion inhibitors.

The techniques that have been employed in the present work to complete the study are as follows:

- a. Weight loss measurements
- b. Electrochemical impedance spectroscopy
- c. Potentiodynamic polarization Study.
- d. Thermodynamics and kinetics studies.
- e. Computational studies.
- f. Surface studies (SEM and AFM)

The inhibitors used in the present work are:

- a. Baclofen
- b. Betahistine dihydrochloride
- c. Isoxsuprine hydrochloride
- d. Panthenol
- e. Naphazoline
- f. Dicyclomine hydrochloride

All the inhibitors were investigated for their corrosion inhibition performance at 298 K. Six drug molecules were considered for study, out of which maximum concentration of 2000 ppm was considered for Baclofen, Isoxsuprine hydrochloride. For Betahistine dihydrochloride, Naphazoline, 1500 ppm of maximum concentration was selected. For Panthenol 400 ppm and for Dicyclomine hydrochloride 800 ppm concentration was selected for analysis. All the drug molecules have either heteroatom, π electrons or ring structure, which were favouring the adsorption of drug on the metal surface and resulting in successful mitigation of corrosion. Literature also suggested the possibility of substitution process between the molecules of the inhibitor and the water molecules, which causes the adsorption of the inhibitor. Along with adsorption, other critical parameters that effect the corrosion inhibition process include a charge on the surface of the sample, temperature, the concentration of the inhibitor that is utilised, and the surrounding environment. When it comes to the process of physical adsorption, protonated inhibitors and other species that are already present on the surface of the sample are subject to weak electrostatic forces. Because of this, the inhibitor might slow down the cathodic as well as the anodic reactions. Physical adsorption requires the presence of charged species that can form complex structures. In case of chemical adsorption, formation of coordination bond is observed and sometimes reterodonation is also there. After investigating the drug molecules for anticorrosive properties by employing the above-mentioned techniques the following conclusions were drawn:

- All of the drug molecules were found to be efficient corrosion inhibitors for MS in acidic medium.
- Present study found the increase in inhibition efficiency with the rise in concentration of inhibitors and dip in the efficiency was there with the rise in temperature.
- As the quantity of inhibitor was raised, it was observed that the surface coverage increased as well.
- It was discovered that all dug molecules followed the Langmuir adsorption isotherm, which was supported by the values of the regression coefficient (R^2), which were close to one.
- Various calculated thermodynamic parameters were also supporting the fact

that drugs adsorbed on the metallic surface successfully. Negative value of free energy of adsorption, negative value of enthalpy, large values of activation energy etc. confirmed the spontaneous, exothermic nature of adsorption along with formation of preventive layer of inhibitor.

- Electrochemical impedance spectroscopy also proved the successful protection of metal by employing drug molecules as corrosion inhibitors, and it was proved with the increased values of R_{ct} and decreased value of C_{dl} with the rise in drug concentration.
- Potentiodynamic polarization techniques were in accordance to Electrochemical impedance spectroscopy measurements in terms of their outcomes. All the drugs were clearly shown mixed type of behaviour and that was proved by analysing the values of E_{corr} .
- Scanning electron microscopy prove the formation of thin layer of drug molecules on the metal under study, which reduce the corrosion effectively.
- When comparing the roughness values obtained for inhibitors from atomic force microscopy, the results revealed that the inhibitors were more successful at preventing metal corrosion.
- Theoretical investigations were complementing the experimental studies.
- The Tafel slopes that varied in an irregular way indicated that adsorption is not the only mechanism involved in inhibition but a combination of many mechanisms of the inhibitors and their anions presents in the corrosive medium.
- The decrease in C_{dl} values on addition of inhibitors is because of adsorption of inhibitors leading to the formation of a preventive film on the surface of metal.

Outcomes of the present work

- The inhibitors under investigation are effective corrosion inhibitors for MS, and their capabilities can be further studied and enhanced by applying them to other metals as well.
- Additional investigations can be carried out by evaluating binary combinations

of these drugs as inhibitors for different metals.

- At higher and extreme temperatures, these drugs could be tested for their effectiveness as corrosion inhibitors.
- The synergism, by combining the drug molecules with other compounds like with halides etc. can also be conducted to study the after effects on inhibition efficacy of these drugs.

REFERENCES

References

- Abd El Rehim, S. S., Hassan, H. H., & Amin, M. A. (2001). Corrosion inhibition of aluminum by 1, 1 (lauryl amido) propyl ammonium chloride in HCl solution. *Materials chemistry and physics*, 70(1), 64-72.
- Abd El-Raouf, M., Khamis, E. A., Abou Kana, M. T., & Negm, N. A. (2018). Electrochemical and quantum chemical evaluation of new bis (coumarins) derivatives as corrosion inhibitors for carbon steel corrosion in 0.5 M H₂SO₄. *Journal of Molecular Liquids*, 255, 341-353.
- Abd, E. A. F. S., & Ali, A. H. (2018). Egy-dronate drug as promising corrosion inhibitor of C-steel in aqueous medium. *Zaštita materijala*, 59(1), 126-140.
- Abdallah, M., Ahmed, S. A., Altass, H. M., Zaafarany, I. A., Salem, M., Aly, A. I., & Hussein, E. M. (2019). Competent inhibitor for the corrosion of zinc in hydrochloric acid based on 2, 6-bis-[1-(2-phenylhydrazono) ethyl] pyridine. *Chemical Engineering Communications*, 206(2), 137-148.
- Abdallah, M., Altass, H. M., Al-Gorair, A. S., Al-Fahemi, J. H., Jahdaly, B. A. A. L., & Soliman, K. A. (2021). Natural nutmeg oil as a green corrosion inhibitor for carbon steel in 1.0 M HCl solution: Chemical, electrochemical, and computational methods. *Journal of Molecular Liquids*, 323, 115036.
- Abdallah, M., Kamar, E. M., El-Etre, A. Y., & Eid, S. (2016). Gelatin as corrosion inhibitor for aluminum and aluminum silicon alloys in sodium hydroxide solutions. *Protection of Metals and Physical Chemistry of Surfaces*, 52, 140-148.
- Abdel-Gaber, A. M., Masoud, M. S., Khalil, E. A., & Shehata, E. E. (2009). Electrochemical study on the effect of Schiff base and its cobalt complex on the acid corrosion of steel. *Corrosion Science*, 51(12), 3021-3024.

Abeng, F. E., Ikpi, M. E., Ushie, O. A., Anadebe, V. C., Nyong, B. E., Obeten, M. E., ... & Nkom, P. Y. (2021). Insight into corrosion inhibition mechanism of carbon steel in 2 M HCl electrolyte by eco-friendly based pharmaceutical drugs. *Chemical Data Collections*, 34, 100722.

Addoun, A., Bouyegh, S., Dahmane, M., Ferroukhi, O., & Trari, M. (2019). Thermodynamic investigation on the adhesion and corrosion inhibition properties of a non-steroidal anti-inflammatory drug in HCl electrolyte applied on mild steel material. *Materials Today Communications*, 21, 100720.

Ahamad, I., & Quraishi, M. A. (2010). Mebendazole: new and efficient corrosion inhibitor for mild steel in acid medium. *Corrosion science*, 52(2), 651-656.

Ahmad, Z. (2006). *Principles of corrosion engineering and corrosion control*. Elsevier, pp. 1-7.

Ai, J. Z., Guo, X. P., Qu, J. E., Chen, Z. Y. and Zheng, J. S., "Adsorption behavior and synergistic mechanism of a cationic inhibitor and ki on the galvanic electrode", *Colloids and Surfaces A: Physicochemical and Engineering Aspects* 281, 147 (2006).

Akinbulumo, O. A., Odejobi, O. J., & Odekanle, E. L. (2020). Thermodynamics and adsorption study of the corrosion inhibition of mild steel by Euphorbia heterophylla L. extract in 1.5 M HCl. *Results in Materials*, 5, 100074..

Alibakhshi, E., Ramezanzadeh, M., Bahlakeh, G., Ramezanzadeh, B., Mahdavian, M., & Motamedi, M. (2018). Glycyrrhiza glabra leaves extract as a green corrosion inhibitor for mild steel in 1 M hydrochloric acid solution: experimental, molecular dynamics, Monte Carlo and quantum mechanics study. *Journal of Molecular Liquids*, 255, 185-198.

Al-Shafey, H. I., Hameed, R. A., Ali, F. A., Ae-AS, A. M., & Salah, M. (2014). Effect of expired drugs as corrosion inhibitors for carbon steel in 1M HCL solution. *Int J Pharm Sci Rev Res*, 27(1), 146-152.

Albrimi, Y. A., Addi, A. A., Douch, J., Souto, R. M., & Hamdani, M. (2015). Inhibition of the pitting corrosion of 304 stainless steel in 0.5 M hydrochloric acid solution by heptamolybdate ions. *Corrosion Science*, *90*, 522-528.

Ameh, P. O., & Sani, U. M. (2015). Cefuroxime Axetil: A Commercially Available Pro-Drug as Corrosion Inhibitor for Aluminum in Hydrochloric Acid Solution. *Journal of Heterocyclics*, *101*, 1-6.

Anadebe, V. C., Onukwuli, O. D., Abeng, F. E., Okafor, N. A., Ezeugo, J. O., & Okoye, C. C. (2020). Electrochemical-kinetics, MD-simulation and multi-input single-output (MISO) modeling using adaptive neuro-fuzzy inference system (ANFIS) prediction for dexamethasone drug as eco-friendly corrosion inhibitor for mild steel in 2 M HCl electrolyte. *Journal of the Taiwan Institute of Chemical Engineers*, *115*, 251-265.

Anaee, R. A., Tomi, I. H. R., Abdul majeed, M. H., Naser, S. A., & Kathem, M. M. (2019). Expired Etoricoxib as a corrosion inhibitor for steel in acidic solution. *Journal of Molecular Liquids*, *279*, 594-602.

Ansari, K. R., Quraishi, M. A., & Singh, A. (2017). Chromenopyridin derivatives as environmentally benign corrosion inhibitors for N80 steel in 15% HCl. *Journal of the Association of Arab Universities for Basic and Applied Sciences*, *22*(1), 45-54.

Ansari, K. R., Quraishi, M. A., Singh, A., Ramkumar, S., & Obote, I. B. (2016). Corrosion inhibition of N80 steel in 15% HCl by pyrazolone derivatives: electrochemical, surface and quantum chemical studies. *RSC advances*, *6*(29), 24130-24141.

Anupama, K. K., Ramya, K., & Joseph, A. (2016). Electrochemical and computational aspects of surface interaction and corrosion inhibition of mild steel in hydrochloric acid by *Phyllanthus amarus* leaf extract (PAE). *Journal of molecular liquids*, *216*, 146-155..

Arthur, D. E., Jonathan, A., Ameh, P. O., & Anya, C. (2013). A review on the assessment of polymeric materials used as corrosion inhibitor of metals and alloys. *International Journal of Industrial Chemistry*, *4*(1), 2.

Ashassi-Sorkhabi, H., Seifzadeh, D., & Hosseini, M. G. (2008). EN, EIS and polarization studies to evaluate the inhibition effect of 3H-phenothiazin-3-one, 7-dimethylamin on mild steel corrosion in 1 M HCl solution. *Corrosion Science*, 50(12), 3363-3370.

Ashassi-Sorkhabi, H., Shaabani, B., & Seifzadeh, D. (2005). Effect of some pyrimidinic Schiff bases on the corrosion of mild steel in hydrochloric acid solution. *Electrochimica Acta*, 50(16-17), 3446-3452.

Aslam, R., Mobin, M., Obot, I. B., & Alamri, A. H. (2020). Ionic liquids derived from α -amino acid ester salts as potent green corrosion inhibitors for mild steel in 1M HCl. *Journal of Molecular Liquids*, 318, 113982.

Ateya, B. G., El-Anadouli, B. E., & El-Nizamy, F. M. (1984). The adsorption of thiourea on mild steel. *Corrosion Science*, 24, 509-515.

Atkins, P., De Paula, J., & Keeler, J. (2018). *Atkins' physical chemistry*. Oxford university press

Attia, E. M. (2015). Expired Farcolin drugs as corrosion inhibitor for carbon steel in 1 M HCl solution. *Journal of Basic and Applied Chemistry*, 5(1), 1-15.

Awad, M. K., Mustafa, M. R., & Elnga, M. M. A. (2010). Computational simulation of the molecular structure of some triazoles as inhibitors for the corrosion of metal surface. *Journal of molecular structure: theochem*, 959(1-3), 66-74.

Awe, F. E., Idris, S. O., Abdulwahab, M., & Oguzie, E. E. (2015). Inhibitive and adsorptive effect of Parinari polyandra on mild steel corrosion in aqueous sulphuric acid. *African Journal of Pure and Applied Chemistry*, 9, 125-134.

Ayoola, A. A., Fayomi, O. S. I., & Ogunkanmbi, S. O. (2018). Data on inhibitive performance of chloraphenicol drug on A315 mild steel in acidic medium. *Data in Brief*, 19, 804-809.

Baig, N., Chauhan, D. S., Saleh, T. A., & Quraishi, M. A. (2019). Diethylenetriamine functionalized graphene oxide as a novel corrosion inhibitor for mild steel in hydrochloric acid solutions. *New Journal of Chemistry*, 43(5), 2328-2337.

Bansal, R. C., & Goyal, M. (2005). *Activated Carbon Adsorption*. CRC press.

Barsoukov, E., Macdonald, J. R. (Eds.) (2018). *Impedance Spectroscopy: Theory, Experiment, and Applications*. John Wiley & Sons.

Bashir, S., Lgaz, H., Chung, I. M., & Kumar, A. (2019). Potential of Venlafaxine in the inhibition of mild steel corrosion in HCl: insights from experimental and computational studies. *Chemical Papers*, 73(9), 2255-2264.

Bashir, S., Lgaz, H., Chung, I. M., & Kumar, A. (2020). Effective green corrosion inhibition of aluminium using analgin in acidic medium: an experimental and theoretical study. *Chemical Engineering Communications*, 1-10.

Bashir, S., Sharma, V., Lgaz, H., Chung, I. M., Singh, A., & Kumar, A. (2018). The inhibition action of analgin on the corrosion of mild steel in acidic medium: A combined theoretical and experimental approach. *Journal of Molecular Liquids*, 263, 454-462.

Bashir, S., Sharma, V., Singh, G., Lgaz, H., Salghi, R., Singh, A., & Kumar, A. (2019). Electrochemical behavior and computational analysis of phenylephrine for corrosion inhibition of aluminum in acidic medium. *Metallurgical and Materials Transactions A*, 50(1), 468-479.

Bashir, S., Singh, G., & Kumar, A. (2017). Shatavari (*Asparagus racemosus*) as green corrosion inhibitor of aluminium in acidic medium. *J Mater Environ Sci*, 8(12), 4284-4291.

Bashir, S., Singh, G., & Kumar, A. (2018). An investigation on mitigation of corrosion of aluminium by *Origanum vulgare* in acidic medium. *Protection of Metals and Physical Chemistry of Surfaces*, 54(1), 148-152.

Bashir, S., Thakur, A., Lgaz, H., Chung, I. M., & Kumar, A. (2019). Computational and experimental studies on Phenylephrine as anti-corrosion substance of mild steel in acidic medium. *Journal of Molecular Liquids*, 293, 111539.

Bashir, S., Thakur, A., Lgaz, H., Chung, I. M., & Kumar, A. (2020). Corrosion inhibition performance of acarbose on mild steel corrosion in acidic medium: an experimental and computational study. *Arabian Journal for Science and Engineering*, 45(6), 4773-4783.

Bashir, S., Thakur, A., Lgaz, H., Chung, I. M., & Kumar, A. (2020). Corrosion inhibition efficiency of bronopol on aluminium in 0.5 M HCl solution: Insights from experimental and quantum chemical studies. *Surfaces and Interfaces*, 20, 100542.

Bedir, A. G., Abd El-raouf, M., Abdel-Mawgoud, S., Negm, N. A., & El Basiony, N. M. (2021). Corrosion Inhibition of Carbon Steel in Hydrochloric Acid Solution Using Ethoxylated Nonionic Surfactants Based on Schiff Base: Electrochemical and Computational Investigations. *ACS omega*, 6(6), 4300-4312.

Behpour, M., Ghoreishi, S. M., Soltani, N., Salavati-Niasari, M., Hamadani, M., & Gandomi, A. (2008). Electrochemical and theoretical investigation on the corrosion inhibition of mild steel by thiosalicylaldehyde derivatives in hydrochloric acid solution. *Corrosion Science*, 50, 2172-2181.

Bentiss, F., Lebrini, M., & Lagrenee, M. (2005). Thermodynamic characterization of metal dissolution and inhibitor adsorption processes in mild steel/2, 5-bis (n-thienyl)-1, 3, 4-thiadiazoles/hydrochloric acid system. *Corrosion Science*, 47, 2915-2931.

Berdimurodov, E., Kholikov, A., Akbarov, K., & Guo, L. (2021). Experimental and theoretical assessment of new and eco-friendly thioglycoluril derivative as an effective corrosion inhibitor of St2 steel in the aggressive hydrochloric acid with sulfate ions. *Journal of Molecular Liquids*, 335, 116168.

Berdimurodov, E., Kholikov, A., Akbarov, K., Obot, I. B., & Guo, L. (2021). Thioglycoluril derivative as a new and effective corrosion inhibitor for low carbon steel

in a 1 M HCl medium: Experimental and theoretical investigation. *Journal of Molecular Structure*, 1234, 130165.

Bockris, J. M., & Yang, B. (1991). The mechanism of corrosion inhibition of iron in acid solution by acetylenic alcohols. *Journal of the Electrochemical Society*, 138, 2237-2252.

Bouklah, M., Hammouti, B., Lagrenee, M., & Bentiss, F. (2006). Thermodynamic properties of 2, 5-bis (4-methoxyphenyl)-1, 3, 4-oxadiazole as a corrosion inhibitor for mild steel in normal sulfuric acid medium. *Corrosion Science*, 48, 2831-2842.

Boulhaoua, M., El Hafi, M., Zehra, S., Eddaif, L., Alrashdi, A. A., Lahmidi, S., ... & Lgaz, H. (2021). Synthesis, structural analysis and corrosion inhibition application of a new indazole derivative on mild steel surface in acidic media complemented with DFT and MD studies. *Colloids and Surfaces A: Physicochemical and Engineering Aspects*, 617, 126373.

Broussard, G., Bramanti, O., & Marchese, F. M. (1997). Occupational risk and toxicology evaluations of industrial water conditioning. *Occupational medicine*, 47(6), 337-340.

Cao, S., Liu, D., Ding, H., Wang, J., Lu, H., & Gui, J. (2019). Task-specific ionic liquids as corrosion inhibitors on carbon steel in 0.5 M HCl solution: an experimental and theoretical study. *Corrosion Science*, 153, 301-313.

Cao, Z., Tang, Y., Cang, H., Xu, J., Lu, G., & Jing, W. (2014). Novel benzimidazole derivatives as corrosion inhibitors of mild steel in the acidic media. Part II: Theoretical studies. *Corrosion science*, 83, 292-298.

Chaubey, N., Savita, Singh, V. K., & Quraishi, M. A. (2017). Corrosion inhibition performance of different bark extracts on aluminium in alkaline solution. *Journal of the Association of Arab Universities for Basic and Applied Sciences*, 22(1), 38-44.

Chaudhari, L. P., & Patel, S. N. (2019). Corrosion inhibition study of expired acetazolamide on mild steel in dilute hydrochloric acid solution. *Journal of Bio-and Tribo-Corrosion*, 5(1), 1-13.

Chauhan, D. S., Mazumder, M. J., Quraishi, M. A., & Ansari, K. R. (2020). Chitosan-cinnamaldehyde Schiff base: A bioinspired macromolecule as corrosion inhibitor for oil and gas industry. *International Journal of Biological Macromolecules*, 158, 127-138.

Chauhan, D. S., Srivastava, V., Joshi, P. G., & Quraishi, M. A. (2018). PEG cross-linked chitosan: a biomacromolecule as corrosion inhibitor for sugar industry. *International Journal of Industrial Chemistry*, 9(4), 363-377.

Chauhan, L. R., & Gunasekaran, G. (2007). Corrosion inhibition of mild steel by plant extract in dilute HCl medium. *Corrosion Science*, 49, 1143-1161.

Chen, H., Qin, Z., He, M., Liu, Y., & Wu, Z. (2020). Application of electrochemical atomic force microscopy (EC-AFM) in the corrosion study of metallic materials. *Materials*, 13(3), 668.

Chen, Z., Fadhil, A. A., Chen, T., Khadom, A. A., Fu, C., & Fadhil, N. A. (2021). Green synthesis of corrosion inhibitor with biomass platform molecule: gravimetical, electrochemical, morphological, and theoretical investigations. *Journal of Molecular Liquids*, 332, 115852.196

Chetouani, A., Daoudi, M., Hammouti, B., Hadda, T. B. and Benkaddour, M., "Inhibition of pure iron by new synthesized tripyrazole derivatives in hcl solution", *Corrosion Science* 48, 2987 (2006).

Chitra, S., & Anand, B. (2017). Surface morphological and FTIR spectroscopic information on the corrosion inhibition of drugs on mild steel in chloride environment. *J. Chem. Pharm. Sci*, 10, 453-456.

Christov, M., & Popova, A. (2004). Adsorption characteristics of corrosion inhibitors

from corrosion rate measurements. *Corrosion science*, 46(7), 1613-1620.

Ciezak, J. A., & Trevino, S. F. (2006). Inelastic neutron scattering spectrum of cyclotrimethylenetrinitramine: a comparison with solid-state electronic structure calculations. *The Journal of Physical Chemistry A*, 110(15), 5149-5155.

Dąbrowski, A. (2001). Adsorption—from theory to practice. *Advances in colloid and interface science*, 93(1-3), 135-224.

Dagdag, O., Safi, Z., Erramli, H., Wazzan, N., Guo, L., Verma, C., ... & El Harfi, A. (2020). Epoxy prepolymer as a novel anti-corrosive material for carbon steel in acidic solution: electrochemical, surface and computational studies. *Materials Today Communications*, 22, 100800.

Dagdag, O., Safi, Z., Hsissou, R., Erramli, H., El Bouchti, M., Wazzan, N., ... & El Harfi, A. (2019). Epoxy pre-polymers as new and effective materials for corrosion inhibition of carbon steel in acidic medium: Computational and experimental studies. *Scientific reports*, 9(1), 1-14.

Dagdag, O., Safi, Z., Wazzan, N., Erramli, H., Guo, L., Mkadmh, A. M., ... & El Harfi, A. (2020). Highly functionalized epoxy macromolecule as an anti-corrosive material for carbon steel: Computational (DFT, MDS), surface (SEM-EDS) and electrochemical (OCP, PDP, EIS) studies. *Journal of Molecular Liquids*, 302, 112535.

Dariva, C. G., & Galio, A. F. (2014). Corrosion inhibitors—principles, mechanisms and applications. *Developments in corrosion protection*, 16, 365-378.

Dehghani, A., Bahlakeh, G., Ramezanzadeh, B., & Ramezanzadeh, M. (2019). A combined experimental and theoretical study of green corrosion inhibition of mild steel in HCl solution by aqueous Citrullus lanatus fruit (CLF) extract. *Journal of Molecular Liquids*, 279, 603-624.

Derfouf, H., Harek, Y., Larabi, L., Basirun, W. J., & Ladan, M. (2019). Corrosion inhibition activity of carbon steel in 1.0 M hydrochloric acid medium using Hammada

scoparia extract: gravimetric and electrochemical study. *Journal of Adhesion Science and Technology*, 33(8), 808-833.

Desai, P. S. (2015). Inhibitory action of extract of ankado (*calotropis gigantea*) leaves on mild steel corrosion in hydrochloric acid solution. *Int. J. Curr. Microbiol. App. Sci*, 4(1), 437-447.

Deyab, M. A. (2018). Corrosion inhibition of heat exchanger tubing material (titanium) in MSF desalination plants in acid cleaning solution using aromatic nitro compounds. *Desalination*, 439, 73-79.

Dhaundiyal, P., Bashir, S., Sharma, V., & Kumar, A. (2019). An investigation on mitigation of corrosion of mildsteel by *Origanum vulgare* in acidic medium. *Bulletin of the Chemical Society of Ethiopia*, 33(1), 159-168.

Diki, N. Y. S., Bohoussou, K. V., Kone, M. G. R., Ouedraogo, A., & Trokourey, A. (2018). Cefadroxil drug as corrosion inhibitor for aluminum in 1 M HCl medium: experimental and theoretical studies. *IOSR Journal of Applied Chemistry*, 11(4), 24-36.

Dohare, P., Chauhan, D. S., Sorour, A. A., & Quraishi, M. A. (2017). DFT and experimental studies on the inhibition potentials of expired Tramadol drug on mild steel corrosion in hydrochloric acid. *Materials discovery*, 9, 30-41.

Du, Y. T., Wang, H. L., Chen, Y. R., Qi, H. P., & Jiang, W. F. (2017). Synthesis of baicalin derivatives as eco-friendly green corrosion inhibitors for aluminum in hydrochloric acid solution. *Journal of environmental chemical engineering*, 5(6), 5891-5901.

Durnie, W. H., Kinsella, B. J., De Marco, R., & Jefferson, A. (2001). A study of the adsorption properties of commercial carbon dioxide corrosion inhibitor formulations. *Journal of Applied Electrochemistry*, 31(11), 1221-1226.

Dwivedi, D., Lepková, K., & Becker, T. (2017). Carbon steel corrosion: a review of key surface properties and characterization methods. *RSC advances*, 7(8), 4580-4610.

EC08, A. A. N. (2011). Basic overview of the working principle of a potentiostat/galvanostat (PGSTAT)–Electrochemical cell setup. *Metrohm Autolab. BV*, 1-3.

Eddy, N. O., & Ebenso, E. E. (2010). Adsorption and quantum chemical studies on cloxacillin and halides for the corrosion of mild steel in acidic medium. *International Journal of Electrochemical Science*, 5(6), 731-750.

Edison, T. N. J. I., Atchudan, R., Pugazhendhi, A., Lee, Y. R., & Sethuraman, M. G. (2018). Corrosion inhibition performance of spermidine on mild steel in acid media. *Journal of Molecular Liquids*, 264, 483-489.

El Arrouji, S., Karrouchi, K., Berisha, A., Alaoui, K. I., Warad, I., Rais, Z., ... & Zarrouk, A. (2020). New pyrazole derivatives as effective corrosion inhibitors on steel-electrolyte interface in 1 M HCl: Electrochemical, surface morphological (SEM) and computational analysis. *Colloids and Surfaces A: Physicochemical and Engineering Aspects*, 604, 125325.

Elabbasy, H. M., & Gadow, H. S. (2021). Study the effect of expired tenoxicam on the inhibition of carbon steel corrosion in a solution of hydrochloric acid. *Journal of Molecular Liquids*, 321, 114918.

El-Awady, A. A., Abd-El-Nabey, B. A., & Aziz, S. G. (1992). Kinetic-thermodynamic and adsorption isotherms analyses for the inhibition of the acid corrosion of steel by cyclic and open-chain amines. *Journal of the Electrochemical Society*, 139, 2149-2154.

Elayaperumal, K., & Raja, V. S. (2015). *Corrosion Failures: Theory, Case Studies, and Solutions*. John Wiley & Sons.

El-Deeb, M. M., Abdel-Shafi, N. S., & Shamroukh, A. H. (2018). Electrochemical, DFT and Mont Carlo simulations studies to evaluate the inhibition effect of novel pyridazine derivatives on iron pitting corrosion in 3.5% NaCl. *Int. J. Electrochem. Sci*, 13, 5352-5369.

El-Enin, S. A., & Amin, A. (2015). Review of corrosion inhibitors for industrial applications. *Int. J. Eng. Res. Rev*, 3(2), 127-145.

El-Etre, A. Y., & Ali, A. I. (2017). A novel green inhibitor for C-steel corrosion in 2.0 mol·L⁻¹ hydrochloric acid solution. *Chinese Journal of Chemical Engineering*, 25(3), 373-380.

El-Etre, A. Y., El Komy, M. A., Shohayed, S. M., & Abdelhamed, S. (2016). Inhibition of Aluminum Corrosion in Acid Medium by Cassia Acutifolia Extract. *Journal of Basic and Environmental Sciences*, 3, 37-46.

El-Haddad, M. N., & Fouda, A. E. A. S. (2021). Evaluation of Curam drug as an ecofriendly corrosion inhibitor for protection of stainless steel-304 in hydrochloric acid solution: Chemical, electrochemical, and surface morphology studies. *Journal of the Chinese Chemical Society*.

El-Haddad, M. N., Fouda, A. S., & Hassan, A. F. (2019). Data from Chemical, electrochemical and quantum chemical studies for interaction between Cephapirin drug as an eco-friendly corrosion inhibitor and carbon steel surface in acidic medium. *Chemical Data Collections*, 22, 100251.

Elkadi, L., Mernari, B., Traisnel, M., Bentiss, F., & Lagrenee, M. (2000). The inhibition action of 3, 6-bis (2-methoxyphenyl)-1, 2-dihydro-1, 2, 4, 5-tetrazine on the corrosion of mild steel in acidic media. *Corrosion Science*, 42(4), 703-719.

El-Tabei, A. S., Hegazy, M. A., Bedair, A. H., El Basiony, N. M., & Sadeq, M. A. (2022). Novel macrocyclic cationic surfactants: Synthesis, experimental and theoretical studies of their corrosion inhibition activity for carbon steel and their antimicrobial activities. *Journal of Molecular Liquids*, 345, 116990.

Emregul, K. C., & Hayvali, M. (2006). Studies on the effect of a newly synthesized Schiff base compound from phenazone and vanillin on the corrosion of steel in 2 M HCl. *Corrosion science*, 48, 797-812.

Erdogan, S., Safi, Z. S., Kaya, S., Işın, D. O., Guo, L., & Kaya, C. (2017). A computational study on corrosion inhibition performances of novel quinoline

derivatives against the corrosion of iron. *Journal of Molecular Structure*, 1134, 751-761.

Fajobi, M. A., Fayomi, O. S. I., Akande, I. G., & Odunlami, O. A. (2019). Inhibitive performance of ibuprofen drug on mild steel in 0.5 M of H₂SO₄ acid. *Journal of Bio- and Tribo-Corrosion*, 5(3), 1-5.

Faltermeier, R. B. (1999). A corrosion inhibitor test for copper-based artifacts. *Studies in conservation*, 44(2), 121-128.

Farahati, R., Ghaffarinejad, A., Mousavi-Khoshdel, S. M., Rezania, J., Behzadi, H., & Shockravi, A. (2019). Synthesis and potential applications of some thiazoles as corrosion inhibitor of copper in 1 M HCl: Experimental and theoretical studies. *Progress in Organic Coatings*, 132, 417-428.

Farahati, R., Mousavi-Khoshdel, S. M., Ghaffarinejad, A., & Behzadi, H. (2020). Experimental and computational study of penicillamine drug and cysteine as water-soluble green corrosion inhibitors of mild steel. *Progress in Organic Coatings*, 142, 105567.

Farhadian, A., Rahimi, A., Safaei, N., Shaabani, A., Sadeh, E., Abdouss, M., & Alavi, A. (2021). Exploration of sunflower oil as a renewable biomass source to develop scalable and highly effective corrosion inhibitors in a 15% HCl medium at high temperatures. *ACS Applied Materials & Interfaces*, 13(2), 3119-3138.

Feliu, S. (2020). Electrochemical impedance spectroscopy for the measurement of the corrosion rate of magnesium alloys: Brief review and challenges. *Metals*, 10(6), 775.

Feng, H., Singh, A., Wu, Y., & Lin, Y. (2018). SECM/SKP and SVET studies on mitigation of N80 steel corrosion by some polymers. *New Journal of Chemistry*, 42(14), 11404-11416.

Flis, J., & Zakroczymski, T. (1996). Impedance study of reinforcing steel in simulated pore solution with tannin. *Journal of the Electrochemical Society*, 143, 2458-2464.

Fouda, A. S., & Badawy, A. A. (2019). Adsorption and corrosion inhibition of Cu in nitric acid by expired simvastatin drug. *Protection of metals and physical chemistry of surfaces*, 55(3), 572-582.

Fouda, A. S., Abd El-Maksoud, S. A., El-Habab, A. T., & Ibrahim, A. R. (2021). Synthesis and characterization of novel fatty alcohol ethoxylate surfactants for corrosion inhibition of mild steel. *Journal of Bio-and Tribo-Corrosion*, 7(1), 1-14.

Fouda, A. S., Eissa, M., & El-Hossiany, A. (2018). Ciprofloxacin as eco-friendly corrosion inhibitor for carbon steel in hydrochloric acid solution. *Int. J. Electrochem. Sci*, 13, 11096-11112.

Fouda, A. S., El Morsi, M. A., & El Mogy, T. (2017). Studies on the inhibition of carbon steel corrosion in hydrochloric acid solution by expired Carvedilol drug. *Green Chemistry Letters and Reviews*, 10(4), 336-345.

Fouda, A. S., El-Desoky, H. S., Abdel-Galeil, M. A., & Mansour, D. (2021). Niclosamide and dichlorphenamide: New and effective corrosion inhibitors for carbon steel in 1M HCl solution. *SN Applied Sciences*, 3(3), 1-20.

Fouda, A. S., El-Ewady, G., & Ali, A. H. (2017). Modazar as promising corrosion inhibitor of carbon steel in hydrochloric acid solution. *Green chemistry letters and reviews*, 10(2), 88-100.

Fouda, A. S., Ibrahim, H., Rashwaan, S., El-Hossiany, A., & Ahmed, R. M. (2018). Expired drug (pantoprazole sodium) as a corrosion inhibitor for high carbon steel in hydrochloric acid solution. *Int. J. Electrochem. Sci*, 13, 6327-6346.

Fouda, A. S., Ismail, M. A., Al-Khamri, A. A., & Abousalem, A. S. (2019). Experimental, quantum chemical and molecular simulation studies on the action of arylthiophene derivatives as acid corrosion inhibitors. *Journal of Molecular Liquids*, 290, 111178.

Fouda, A. S., Motawee, M. S., Megahid, H. E., & Abdul Mageed, H. A. (2016). Evaluation of an expired non-toxic amlodipine besylatedrug as corrosion inhibitor for low carbon steel in hydrochloric acid solutions. *Benha Journal of Applied*

Sciences, 1(1), 1-13.

Fouda, A. S., Rashwan, S. M., Kamel, M., & Badawy, A. A. (2016). Unused meropenem drug as corrosion inhibitor for copper in acidic medium; experimental and theoretical studies. *Int. J. Electrochem. Sci, 11, 9745-9761.*

Galai, M., El Faydy, M., El Kacimi, Y., Dahmani, K., Alaoui, K., Tourir, R., ... & Ebn Touhami, M. (2017). Synthesis, characterization and anti-corrosion properties of novel quinolinol on C-steel in a molar hydrochloric acid solution. *Port Electrochim Acta, 35(4), 233-251.*

Galai, M., Rbaa, M., Ouakki, M., Guo, L., Dahmani, K., Nouneh, K., ... & Touhami, M. E. (2021). Effect of alkyl group position on adsorption behavior and corrosion inhibition of new naphthol based on 8-hydroxyquinoline: Electrochemical, surface, quantum calculations and dynamic simulations. *Journal of Molecular Liquids, 335, 116552.*

Gao, L., Peng, S., Huang, X., & Gong, Z. (2020). A combined experimental and theoretical study of papain as a biological eco-friendly inhibitor for copper corrosion in H₂SO₄ medium. *Applied Surface Science, 511, 145446.*

Garcia, S. J., Markley, T. A., Mol, J. M. C., & Hughes, A. E. (2013). Unravelling the corrosion inhibition mechanisms of bi-functional inhibitors by EIS and SEM-EDS. *Corrosion Science, 69, 346-358.*

Gece, G. (2008). The use of quantum chemical methods in corrosion inhibitor studies. *Corrosion science, 50(11), 2981-2992.*

Gece, G. (2011). Drugs: A review of promising novel corrosion inhibitors. *Corrosion Science, 53(12), 3873-3898.*

Geethamani, P., Narmatha, M., Dhanalakshmi, R., Aejitha, S., & Kasthuri, P. K. (2019). Corrosion Inhibition and Adsorption Properties of Mild Steel in 1M Hydrochloric Acid Medium by Expired Ambroxol Drug. *Journal of Bio-and Tribo-Corrosion, 5(1), 16.*

George, K. S., & Nestic, S. (2007). Investigation of carbon dioxide corrosion of mild steel in the presence of acetic acid—part 1: basic mechanisms. *Corrosion*, 63(2), 178-186.

Gholamhosseinzadeh, M. R., Aghaie, H., Zandi, M. S., & Giahi, M. (2019). Rosuvastatin drug as a green and effective inhibitor for corrosion of mild steel in HCl and H₂SO₄ solutions. *Journal of Materials Research and Technology*, 8(6), 5314-5324.

Glass, G. K., Page, C. L., & Short, N. R. (1991). Factors affecting the corrosion rate of steel in carbonated mortars. *Corrosion Science*, 32(12), 1283-1294.

Gouy, M. (1910). Sur la constitution de la charge électrique à la surface d'un électrolyte. *J. Phys. Theor. Appl.*, 9, 457-468.

Goyal, M., Vashisht, H., Kumar, A., Kumar, S., Bahadur, I., Benhiba, F., & Zarrouk, A. (2020). Isopentyltriphenylphosphonium bromide ionic liquid as a newly effective corrosion inhibitor on metal-electrolyte interface in acidic medium: Experimental, surface morphological (SEM-EDX & AFM) and computational analysis. *Journal of Molecular Liquids*, 316, 113838.

Guo, L., El Bakri, Y., Tan, J., Kaya, S., & Essassi, E. M. (2019). Multidimensional insights involving electrochemical and in silico investigation into the corrosion inhibition of newly synthesized pyrazolotriazole derivatives on carbon steel in a HCl solution. *RSC advances*, 9(60), 34761-34771.

Guo, L., Safi, Z. S., Kaya, S., Shi, W., Tüzün, B., Altunay, N., & Kaya, C. (2018). Anticorrosive effects of some thiophene derivatives against the corrosion of iron: a computational study. *Frontiers in chemistry*, 6, 155.

Gupta, N. K., Gopal, C. S. A., Srivastava, V., & Quraishi, M. A. (2017). Application of expired drugs in corrosion inhibition of mild steel. *Int. J. Pharm. Chem. Anal*, 4(1), 8-12.

Guruprasad, A. M., Sachin, H. P., Swetha, G. A., & Prasanna, B. M. (2020). Corrosion inhibition of zinc in 0.1 M hydrochloric acid medium with clotrimazole: Experimental, theoretical and quantum studies. *Surfaces and Interfaces*, 19, 100478.

Hackerman, N. (1948). Use of inhibitors in corrosion control. *Corrosion*, 4(2), 45-60.

Hameed, A., Ismail, E. A., Al-Shafey, H. I., & Abbas, M. A. (2020). Expired indomethacin therapeutics as corrosion inhibitors for carbon steel in 1.0 M hydrochloric acid media. *Journal of Bio-and Tribo-Corrosion*, 6(4), 1-10.

Hameed, R. A., Ismail, E. A., Abu-Nawwas, A. H., & Al-Shafey, H. I. (2015). Expired Voltaren drugs as corrosion inhibitor for aluminium in hydrochloric acid. *Int J Electrochem Sci*, 10, 2098-2109.

Hameed, R. S. A., Aljohani, M. M., Essa, A. B., Khaled, A., Nassar, A. M., Badr, M. M., ... & Soliman, M. S. (2021). Electrochemical Techniques for Evaluation of Expired Megavit Drugs as Corrosion Inhibitor for Steel in Hydrochloric Acid. *International Journal of Electrochemical Science*, 16(4).

Hao, Y., Sani, L. A., Ge, T., & Fang, Q. (2017). The synergistic inhibition behaviour of tannic acid and iodide ions on mild steel in H₂SO₄ solutions. *Corrosion Science*, 123, 158-169.

Haque, J., Srivastava, V., Verma, C., & Quraishi, M. A. (2017). Experimental and quantum chemical analysis of 2-amino-3-((4-((S)-2-amino-2-carboxyethyl)-1H-imidazol-2-yl) thio) propionic acid as new and green corrosion inhibitor for mild steel in 1 M hydrochloric acid solution. *Journal of Molecular Liquids*, 225, 848-855.

Hegazy, M. A., Badawi, A. M., El Rehim, S. A., & Kamel, W. M. (2013). Corrosion inhibition of carbon steel using novel N-(2-(2-mercaptoacetoxy) ethyl)-N, N-dimethyl dodecan-1-aminium bromide during acid pickling. *Corrosion Science*, 69, 110-122.

Hernández, H. H., Reynoso, A. M. R., González, J. C. T., Morán, C. O. G., Hernández, J. G. M., Ruiz, A. M., ... & Cruz, R. O. (2020). Electrochemical impedance spectroscopy (EIS): A review study of basic aspects of the corrosion mechanism applied to steels. *Electrochemical Impedance Spectroscopy*, 137-144.

Horsman, P., Conway, B. E., & Yeager, E. (Eds.). (2013). *Comprehensive Treatise of Electrochemistry: The Double Layer*. Springer Science & Business Media.

Hossam, K., Bouhlal, F., Hermouche, L., Merimi, I., Labjar, H., Chaouiki, A., ... & El Hajjaji, S. (2021). Understanding corrosion inhibition of C38 steel in HCl media by omeprazole: insights for experimental and computational studies. *Journal of Failure Analysis and Prevention*, 21(1), 213-227.

Hosseini, M., Mertens, S. F., Ghorbani, M., & Arshadi, M. R. (2003). Asymmetrical Schiff bases as inhibitors of mild steel corrosion in sulphuric acid media. *Materials Chemistry and Physics*, 78, 800-808.

Hsissou, R. (2021). Review on epoxy polymers and its composites as a potential anticorrosive coatings for carbon steel in 3.5% NaCl solution: Computational approaches. *Journal of Molecular Liquids*, 336, 116307.

Hussin, M. H., & Kassim, M. J. (2011). The corrosion inhibition and adsorption behavior of Uncaria gambir extract on mild steel in 1 M HCl. *Materials Chemistry and Physics*, 125(3), 461-468.

Idris, M. N., Daud, A. R., Othman, N. K., & Jalar, A. (2013). Corrosion control by benzyl triethylammonium chloride: effects of temperature and its concentration. *Int. J. Eng. Technol*, 13(03), 47-51.

Inkson, B. J. (2016). Scanning electron microscopy (SEM) and transmission electron microscopy (TEM) for materials characterization. In *Materials characterization using nondestructive evaluation (NDE) methods* (pp. 17-43). Woodhead Publishing.

Instruments, G. (2007). Basics of electrochemical impedance spectroscopy. *G. Instruments, Complex impedance in Corrosion*, 1-30.

Instruments, G. (2019). Potentiodynamic and Cyclic Polarization Scans. *Gamry Instruments*

Iskandar, I. K., & Selim, H. M. (1999). Fate and transport of heavy metals in the vadose zone. CRC Press.

Ismadji, S., Soetaredjo, F. E., & Ayucitra, A. (2015). *Clay Materials for Environmental Remediation*. 25, 1-124. Berlin: Springer.

Issa, R. M., Awad, M. K., & Atlam, F. M. (2008). Quantum chemical studies on the inhibition of corrosion of copper surface by substituted uracils. *Applied Surface Science*, 255(5), 2433-2441.

Iuen, E., Akaranta, O., & James, A. (2017). Evaluation of performance of corrosion inhibitors using adsorption isotherm models: an overview. *Chem. Sci. Int. J*, 18(1), 1-34.

Jafari, H., Danaee, I., Eskandari, H., & RashvandAvei, M. (2013). Electrochemical and theoretical studies of adsorption and corrosion inhibition of N, N'-bis (2-hydroxyethoxyacetophenone)-2, 2-dimethyl-1, 2-propanediimine on low carbon steel (API 5L Grade B) in acidic solution. *Industrial & Engineering Chemistry Research*, 52(20), 6617-6632.

Jalili, N., & Laxminarayana, K. (2004). A review of atomic force microscopy imaging systems: application to molecular metrology and biological sciences. *Mechatronics*, 14(8), 907-945.

Javadian, S., Darbasizadeh, B., Yousefi, A., Ektefa, F., Dalir, N., & Kakemam, J. (2017). Dye-surfactant aggregates as corrosion inhibitor for mild steel in NaCl medium: Experimental and theoretical studies. *Journal of the Taiwan Institute of Chemical Engineers*, 71, 344-354.

Ji, G., Anjum, S., Sundaram, S., & Prakash, R. (2015). Musa paradisica peel extract as green corrosion inhibitor for mild steel in HCl solution. *Corrosion Science*, 90, 107-117.

John, S., & Joseph, A. (2012). Electroanalytical studies of the corrosion-protection properties of 4-amino-4H-1, 2, 4-triazole-3, 5-dimethanol (ATD) on mild steel in 0.5 N sulfuric acid. *Research on Chemical Intermediates*, 38(7), 1359-1373.

John, S., Kuruvilla, M., & Joseph, A. (2013). Adsorption and inhibition effect of methyl carbamate on copper metal in 1 N HNO₃: an experimental and theoretical study. *RSC advances*, 3(23), 8929-8938.

Kadhim, A., Al-Amiery, A. A., Alazawi, R., Al-Ghezi, M. K. S., & Abass, R. H. (2021). Corrosion inhibitors. A review. *International Journal of Corrosion and Scale Inhibition*, 10(1), 54-67

Kanellopoulos, N. (2016). *Nanoporous materials: Advanced techniques for characterization, modeling, and processing*. CRC press.

Karthikaiselvi, R., & Subhashini, S. (2014). Study of adsorption properties and inhibition of mild steel corrosion in hydrochloric acid media by water soluble composite poly (vinyl alcohol-omethoxy aniline). *Journal of the Association of Arab Universities for Basic and Applied Sciences*, 16, 74-82.

Karthikeyan, S., & Jeeva, P. A. (2019). Corrosion studies of zinc coated steel parts in sea water. *Portugaliae Electrochimica Acta*, 37(5), 307-315.

Kaya, S., Guo, L., Kaya, C., Tüzün, B., Obot, I. B., Tour, R., & Islam, N. (2016). Quantum chemical and molecular dynamic simulation studies for the prediction of inhibition efficiencies of some piperidine derivatives on the corrosion of iron. *Journal of the Taiwan Institute of Chemical Engineers*, 65, 522-529.

Keshavamurthy, R., Ramesh, C. S., Kumar, G. P., & Tambrallimath, V. (2021). Experimental investigation of tribocorrosion. In *Tribocorrosion* (pp. 17-42). Academic Press.

Khaled, K. F. (2008). Application of electrochemical frequency modulation for monitoring corrosion and corrosion inhibition of iron by some indole derivatives in molar hydrochloric acid. *Materials Chemistry and Physics*, 112(1), 290-300.

Khaled, K. F., & Al-Qahtani, M. M. (2009). The inhibitive effect of some tetrazole derivatives towards Al corrosion in acid solution: Chemical, electrochemical and theoretical studies. *Materials Chemistry and Physics*, 113(1), 150-158.

Khaled, K. F., & Amin, M. A. (2009). Electrochemical and molecular dynamics simulation studies on the corrosion inhibition of aluminum in molar hydrochloric acid using some imidazole derivatives. *Journal of applied electrochemistry*, 39(12), 2553-2568.

Khamis, E., Bellucci, F., Latanision, R. M., & El-Ashry, E. S. H. (1991). Acid corrosion inhibition of nickel by 2-(triphenosporanylidene) succinic anhydride. *Corrosion*, 47, 677-686.

Khan, M. Z. H., Aziz, M. A., Hasan, M. R., & Al-Mamun, M. R. (2016). The role of drug as corrosion inhibitor for mild steel surface characterization by SEM, AFM, and FTIR. *Anti-Corrosion Methods and Materials*.

Kovacevic, N., & Kokalj, A. (2011). Analysis of molecular electronic structure of imidazole-and benzimidazole-based inhibitors: a simple recipe for qualitative estimation of chemical hardness. *Corrosion Science*, 53(3), 909-921.

Kowsari, E., Arman, S. Y., Shahini, M. H., Zandi, H., Ehsani, A., Naderi, R., ... & Mehdipour, M. (2016). In situ synthesis, electrochemical and quantum chemical analysis of an amino acid-derived ionic liquid inhibitor for corrosion protection of mild steel in 1M HCl solution. *Corrosion Science*, 112, 73-85.

Kruger, J. (2011). Cost of metallic corrosion. *Uhlig's Corrosion Handbook*, 3, 15-20.

Kumar, A., & Bashir, S. (2016). Ethambutol: A new and effective corrosion inhibitor of mild steel in acidic medium. *Russian Journal of Applied Chemistry*, 89(7), 1158-1163.

Kumar, H., Karthikeyan, S., Vivekanand, P. A., & Kamaraj, P. (2021). The inhibitive effect of cloxacillin on mild steel corrosion in 2 N sulphuric acid medium. *Materials Today: Proceedings*, 36, 898-902.

Kumar, K. V., Pillai, M. S. N., & Thusnavis, G. R. (2011). Seed extract of *Psidium guajava* as ecofriendly corrosion inhibitor for carbon steel in hydrochloric acid medium. *Journal of Materials Science & Technology*, 27(12), 1143-1149.

Kumar, P. E., Govindaraju, M., & Sivakumar, V. (2018). Experimental and theoretical studies on corrosion inhibition performance of an environmentally friendly drug on the corrosion of copper in acid media. *Anti-Corrosion Methods and Materials*.

Kumar, S., Sharma, D., Yadav, P., & Yadav, M. (2013). Experimental and quantum chemical studies on corrosion inhibition effect of synthesized organic compounds on N80 steel in hydrochloric acid. *Industrial & Engineering Chemistry Research*, 52(39), 14019-14029.

Kuo, J. (Ed.). (2007). *Electron microscopy: methods and protocols* (Vol. 369). Springer Science & Business Media.

Kutz, M. (2018). *Handbook of environmental degradation of materials*. William Andrew.

Landolt, D. (2007). *Corrosion and surface chemistry of metals*. EPFL press.

Lasia, A. (2002). Electrochemical impedance spectroscopy and its applications. In *Modern aspects of electrochemistry*. 143-248. Springer, Boston, MA.

Latanision, R. M. (1987). Current and projected impact of corrosion science and engineering. *Materials performance*, 26(10), 9-16.

Lece, H. D., Emregül, K. C., & Atakol, O. (2008). Difference in the inhibitive effect of some Schiff base compounds containing oxygen, nitrogen and sulfur donors. *Corrosion science*, 50(5), 1460-1468.

Liang, C., Liu, Z., Liang, Q., Han, G. C., Han, J., Zhang, S., & Feng, X. Z. (2019). Synthesis of 2-aminofluorene bis-Schiff base and corrosion inhibition performance for carbon steel in HCl. *Journal of Molecular Liquids*, 277, 330-340.

Liangtian, Y., Zhang, M., Shidong, C., Yunji, T., & Haixia, W. (2020). Investigation of Corrosion Inhibition Effect of Enprofylline Drug on Mild Steel Corrosion in Sulphuric Acid Solution. *Int. J. Electrochem. Sci*, 15, 5102-5114.

Liu, L., Luo, X. B., Ding, L., & Luo, S. L. (2019). Application of nanotechnology in the removal of heavy metal from water. In *Nanomaterials for the removal of pollutants and resource reutilization* (pp. 83-147). Elsevier.

Lukovits, I., Kalman, E., & Zucchi, F. (2001). Corrosion inhibitors—correlation between electronic structure and efficiency. *Corrosion*, 57(1), 3-8.

Ma, X., Dang, R., Kang, Y., Gong, Y., Luo, J., Zhang, Y., ..& Ma, Y. (2020). Electrochemical studies of expired drug (formoterol) as oilfield corrosion inhibitor for mild steel in H₂SO₄ media. *Int J Electrochem Sci*, 15, 1964-1981.

Maduelosi, N. J., & Iroha, N. B. (2021). Insight into the adsorption and inhibitive effect of spironolactone drug on C38 carbon steel corrosion in hydrochloric acid environment. *Journal of Bio-and Tribo-Corrosion*, 7(1), 1-14.

Magar, H. S., Hassan, R. Y., & Mulchandani, A. (2021). Electrochemical Impedance Spectroscopy (EIS): Principles, Construction, and Biosensing Applications. *Sensors*, 21(19), 6578.

Martinez, S., & Stern, I. (2002). Thermodynamic characterization of metal dissolution and inhibitor adsorption processes in the low carbon steel/mimosa tannin/sulfuric acid system. *Applied Surface Science*, 199, 83-89.

Masroor, S., Mobin, M., Alam, M. J., & Ahmad, S. (2017). The novel iminium surfactant p-benzylidene benzyl dodecyl iminium chloride as a corrosion inhibitor for plain carbon steel in 1 M HCl: electrochemical and DFT evaluation. *RSC advances*, 7(37), 23182-23196.

Matad, P. B., Mokshanatha, P. B., Hebbar, N., Venkatesha, V. T., & Tandon, H. C. (2014). Ketosulfone drug as a green corrosion inhibitor for mild steel in acidic medium. *Industrial & Engineering Chemistry Research*, 53(20), 8436-8444.

McCafferty, E. (2005). Validation of corrosion rates measured by the Tafel extrapolation method. *Corrosion Science*, 47, 3202-3215.

Mohammadinejad, F., Zandi, M. S., Bahrami, M. J., & Golshani, Z. (2020). Metoprolol: New and Efficient Corrosion Inhibitor for Mild Steel in Hydrochloric and Sulfuric Acid Solutions. *Acta Chimica Slovenica*, 67(3), 710-719.

Mohammed, K. Z., Hamdy, A., Abdel-Wahab, A., & Farid, N. A. (2012). Temperature effect on corrosion inhibition of carbon steel in formation water by non-ionic inhibitor and synergistic influence of halide ions. *Life Sci. J*, 9, 424-434.

Mortimer, R. J., Graham, K. R., Grenier, C. R., & Reynolds, J. R. (2009). Influence of the film thickness and morphology on the colorimetric properties of spray-coated electrochromic disubstituted 3, 4-propylenedioxythiophene polymers. *ACS Applied Materials & Interfaces*, 1, 2269-2276.

Murulana, L. C., Singh, A. K., Shukla, S. K., Kabanda, M. M., & Ebenso, E. E. (2012). Experimental and quantum chemical studies of some bis (trifluoromethyl-sulfonyl) imide imidazolium-based ionic liquids as corrosion inhibitors for mild steel in hydrochloric acid solution. *Industrial & Engineering Chemistry Research*, 51(40), 13282-13299.

Musa, A. Y., Jalgham, R. T., & Mohamad, A. B. (2012). Molecular dynamic and quantum chemical calculations for phthalazine derivatives as corrosion inhibitors of mild steel in 1 M HCl. *Corrosion Science*, 56, 176-183

Nasab, S. G., Yazd, M. J., Semnani, A., Kahkesh, H., Rabiee, N., Rabiee, M., & Bagherzadeh, M. (2019). Natural Corrosion Inhibitors. *Synthesis Lectures on Mechanical Engineering*, 14(1), 1-96.

Nasari, E., Hajisafari, M., Kosari, A., Talari, M., Hosseinpour, S., & Davoodi, A. (2018). Inhibitive effect of Clopidogrel as a green corrosion inhibitor for mild steel; statistical modeling and quantum Monte Carlo simulation studies. *Journal of molecular liquids*, 269, 193-202.

Nasr, K., Fedel, M., Essalah, K., Deflorian, F., & Souissi, N. (2018). Experimental and theoretical study of *Matricaria recutita* chamomile extract as corrosion inhibitor for steel in neutral chloride media. *Anti-Corrosion Methods and Materials*.

Ndukwe, A. I., & Anyakwo, C. N. (2017). Modelling of corrosion inhibition of mild steel in hydrochloric acid by crushed leaves of *Sida acuta* (Malvaceae). *Int. J. Eng. Sci*, 6, 22-33.

Negi, A. S., & Anand, S. C. (1985). *A textbook of physical chemistry*. New Age International.

Negm, N. A., Kandile, N. G., Badr, E. A., & Mohammed, M. A. (2012). Gravimetric and electrochemical evaluation of environmentally friendly nonionic corrosion inhibitors for carbon steel in 1 M HCl. *Corrosion science*, 65, 94-103.

Newman, D. J., & Cragg, G. M. (2007). Natural products as sources of new drugs over the last 25 years. *Journal of natural products*, 70(3), 461-477.

Nmai, C. K. (2004). Multi-functional organic corrosion inhibitor. *Cement and Concrete Composites*, 26(3), 199-207.

Noble, R. D., Noble, R. D., & Terry, P. A. (2004). *Principles of chemical separations with environmental applications*. Cambridge University Press.

Obot, I. B., Macdonald, D. D., & Gasem, Z. M. (2015). Density functional theory (DFT) as a powerful tool for designing new organic corrosion inhibitors. Part 1: an overview. *Corrosion Science*, 99, 1-30.

Obot, I. B., Obi-Egbedi, N. O., & Umoren, S. A. (2009a). Adsorption characteristics and corrosion inhibitive properties of clotrimazole for aluminium corrosion in hydrochloric acid. *Int. J. Electrochem. Sci*, 4(6), 863-877.

Obot, I. B., Obi-Egbedi, N. O., & Umoren, S. A. (2009b). Antifungal drugs as corrosion inhibitors for aluminium in 0.1 M HCl. *Corrosion Science*, 51(8), 1868-1875.

Obot, I. B., Umoren, S. A., Gasem, Z. M., Suleiman, R., & El Ali, B. (2015). Theoretical prediction and electrochemical evaluation of vinylimidazole and allylimidazole as corrosion inhibitors for mild steel in 1 M HCl. *Journal of Industrial and Engineering Chemistry*, 21, 1328-1339.

Obot, I. B., Obi-Egbedi, N. O., & Odozi, N. W. (2010). Acenaphtho [1, 2-b] quinoxaline as a novel corrosion inhibitor for mild steel in 0.5 M H₂SO₄. *Corrosion Science*, 52(3), 923-926.

Odewunmi, N. A., Umoren, S. A., & Gasem, Z. M. (2015). Utilization of watermelon rind extract as a green corrosion inhibitor for mild steel in acidic media. *Journal of Industrial and Engineering Chemistry*, 21, 239-247.

Odewunmi, N. A., Umoren, S. A., & Gasem, Z. M. (2015). Watermelon waste products as green corrosion inhibitors for mild steel in HCl solution. *Journal of Environmental Chemical Engineering*, 3(1), 286-296.

Oguzie Bockris, J. O. M., Reddy, A. K., Gamboa-Aldeco, M., & Gamboa-Aldeco, M. E. (1998). *Modern Electrochemistry 2B: Electrode Processes in Chemistry, Engineering, Biology and Environmental Science*. 2. Springer Science & Business Media.

Oguzie, E. E. (2006). Adsorption and corrosion inhibitive properties of Azadirachta indica in acid solutions. *Pigment & Resin Technology*..

Oguzie, E. E. (2007). Corrosion inhibition of aluminium in acidic and alkaline media by Sansevieria trifasciata extract. *Corrosion science*, 49(3), 1527-1539.

Oguzie, E. E., Unaegbu, C., Ogukwe, C. N., Okolue, B. N., & Onuchukwu, A. I. (2004). Inhibition of mild steel corrosion in sulphuric acid using indigo dye and synergistic halide additives. *Materials Chemistry and Physics*, *84*, 363-368.

Okajima, Y., Shibuta, Y., & Suzuki, T. (2010). A phase-field model for electrode reactions with Butler–Volmer kinetics. *Computational Materials Science*, *50*, 118-124.

Olasunkanmi, L. O. (2021). Corrosion: Favoured, Yet Undesirable-Its Kinetics and Thermodynamics.

Omotosho, O. A., Okeniyi, J. O., Oni, A. B., Makinwa, T. O., Ajibola, O. B., Fademi, E. O. J., ... & Popoola, A. P. I. (2016). Inhibition and mechanism of Terminalia catappa on mild-steel corrosion in sulphuric-acid environment. *Progress in Industrial Ecology, an International Journal*, *10*(4), 398-413.

Palaniappan, N., Alphonsa, J., Cole, I. S., Balasubramanian, K., & Bosco, I. G. (2019). Rapid investigation expiry drug green corrosion inhibitor on mild steel in NaCl medium. *Materials Science and Engineering: B*, *249*, 114423.

Palanisamy, G. (2019). Corrosion inhibitors. *Corrosion inhibitors*, *24*.

Parveen, G., Bashir, S., Thakur, A., Saha, S. K., Banerjee, P., & Kumar, A. (2019). Experimental and computational studies of imidazolium based ionic liquid 1-methyl-3-propylimidazolium iodide on mild steel corrosion in acidic solution. *Materials Research Express*, *7*(1), 016510..

Peme, T., Olasunkanmi, L. O., Bahadur, I., Adekunle, A. S., Kabanda, M. M., & Ebenso, E. E. (2015). Adsorption and corrosion inhibition studies of some selected dyes as corrosion inhibitors for mild steel in acidic medium: gravimetric, electrochemical, quantum chemical studies and synergistic effect with iodide ions. *Molecules*, *20*, 16004-16029.

Petchiammal, A., Rani, P. D., Selvaraj, S., & Kalirajan, K. (2012). Corrosion protection of zinc in natural sea water using Citrullus vulgaris peel as an inhibitor. *Research Journal of Chemical Sciences*, *2*(4), 24-34.

Popova, A. (2007). Temperature effect on mild steel corrosion in acid media in presence of azoles. *Corrosion Science*, 49(5), 2144-2158.

Popova, A., Christov, M., & Zwetanova, A. (2007). Effect of the molecular structure on the inhibitor properties of azoles on mild steel corrosion in 1 M hydrochloric acid. *Corrosion Science*, 49(5), 2131-2143.

Popova, A., Sokolova, E., Raicheva, S. and Christov, M. (2003). "Ac and dc study of the temperature effect on mild steel corrosion in acid media in the presence of benzimidazole derivatives", *Corrosion Science* 45, 33.

Prabhu, R. A., Venkatesha, T. V., Shanbhag, A. V., Praveen, B. M., Kulkarni, G. M., & Kalkhambkar, R. G. (2008). Quinol-2-thione compounds as corrosion inhibitors for mild steel in acid solution. *Materials Chemistry and Physics*, 108, 283-289.

Prakash, S., Yeom, J., Jin, N., Adesida, I., & Shannon, M. A. (2006). Characterization of ionic transport at the nanoscale. *Proceedings of the Institution of Mechanical Engineers, Part N: Journal of Nanoengineering and Nanosystems*, 220, 45-52.

Qiang, Y., Guo, L., Li, H., & Lan, X. (2021). Fabrication of environmentally friendly Losartan potassium film for corrosion inhibition of mild steel in HCl medium. *Chemical Engineering Journal*, 406, 126863.

Qiu, L. G., Wu, Y., Wang, Y. M., & Jiang, X. (2008). Synergistic effect between cationic gemini surfactant and chloride ion for the corrosion inhibition of steel in sulphuric acid. *Corrosion Science*, 50(2), 576-582.

Quraishi, M. A., Singh, A., Singh, V. K., Yadav, D. K., & Singh, A. K. (2010). Green approach to corrosion inhibition of mild steel in hydrochloric acid and sulphuric acid solutions by the extract of *Murraya koenigii* leaves. *Materials Chemistry and Physics*, 122, 114-122.

Raghavendra, N. (2019a). Expired Amitriptyline Drug as a New Nontoxic Inhibitor Protecting Mild Steel Corrosion in HCl Solution. *Science Letters*, 7(1), 26-31.

Raghavendra, N. (2019b). Expired Lorazepam Drug: A Medicinal Compound as Green Corrosion Inhibitor for Mild Steel in Hydrochloric Acid System. *Chemistry Africa*, 1-8.

Ragul, R., Kathiravan, S., Muruges, A., & Ravichandran, J. (2018). Anticorrosion performance of *Mitracarpus hirtus* extract on mild steel in 1 M HCl. *Journal of Bio-and Tribo-Corrosion*, 4(4), 1-11.

Rahimi, A., Abdouss, M., Farhadian, A., Guo, L., & Neshati, J. (2021). Development of a novel thermally stable inhibitor based on furfuryl alcohol for mild steel corrosion in a 15% HCl medium for acidizing application. *Industrial & Engineering Chemistry Research*, 60(30), 11030-11044..

Raja, P. B., & Sethuraman, M. G. (2008). Natural products as corrosion inhibitor for metals in corrosive media—a review. *Materials letters*, 62(1), 113-116.

Raja, P. B., Ismail, M., Ghoreishiamiri, S., Mirza, J., Ismail, M. C., Kakooei, S., & Rahim, A. A. (2016). Reviews on corrosion inhibitors: a short view. *Chemical Engineering Communications*, 203(9), 1145-1156.

Rajeswari, V., Devarayan, K., & Viswanathamurthi, P. (2017). Expired pharmaceutical compounds as potential inhibitors for cast iron corrosion in acidic medium. *Research on Chemical Intermediates*, 43(7), 3893-3913.

Roberge, P. R., & Eng, P. (2005). Corrosion engineering. *Principles and Practice*, 1.

Saha, S. K., & Banerjee, P. (2018). Introduction of newly synthesized Schiff base molecules as efficient corrosion inhibitors for mild steel in 1 M HCl medium: an experimental, density functional theory and molecular dynamics simulation study. *Materials Chemistry Frontiers*, 2(9), 1674-1691.

Saha, S. K., & Banerjee, P. (2015). A theoretical approach to understand the inhibition mechanism of steel corrosion with two aminobenzonitrile inhibitors. *RSC advances*, 5(87), 71120-71130.

Saha, S. K., Dutta, A., Ghosh, P., Sukul, D., & Banerjee, P. (2015). Adsorption and corrosion inhibition effect of Schiff base molecules on the mild steel surface in 1 M HCl medium: a combined experimental and theoretical approach. *Physical Chemistry Chemical Physics*, 17(8), 5679-5690.

Saha, S. K., Dutta, A., Ghosh, P., Sukul, D., & Banerjee, P. (2016). Novel Schiff-base molecules as efficient corrosion inhibitors for mild steel surface in 1 M HCl medium: experimental and theoretical approach. *Physical Chemistry Chemical Physics*, 18(27), 17898-17911..

Saha, S. K., Ghosh, P., Hens, A., Murmu, N. C., & Banerjee, P. (2015). Density functional theory and molecular dynamics simulation study on corrosion inhibition performance of mild steel by mercapto-quinoline Schiff base corrosion inhibitor. *Physica E: Low-dimensional systems and nanostructures*, 66, 332-341.

Saji, V. S. (2019). Supramolecular concepts and approaches in corrosion and biofouling prevention. *Corrosion Reviews*, 37(3), 187-230.

Samiento-Bustos, E., Rodriguez, J. G., Uruchurtu, J., Dominguez-Patiño, G., & Salinas-Bravo, V. M. (2008). Effect of inorganic inhibitors on the corrosion behavior of 1018 carbon steel in the LiBr+ ethylene glycol+ H₂O mixture. *Corrosion Science*, 50(8), 2296-2303.

Sayin, K., & Karakaş, D. (2013). Quantum chemical studies on the some inorganic corrosion inhibitors. *Corrosion Science*, 77, 37-45

Sebhaoui, J., El Bakri, Y., El Aoufir, Y., Guenbour, A., Nasser, A. A., & Essassi, E. M. (2019). Synthesis, NMR characterization, DFT and anti-corrosion on carbon steel

in 1M HCl of two novel 1, 5-benzodiazepines. *Journal of Molecular Structure*, 1182, 123-130.

Shalabi, K., Fouda, A. S., Elewady, G. Y., & Elaskalany, A. (2014). Protection of Metals and Phys. *Chem. Surfs*, 50(3).

Shamnamol, G. K., Sreelakshmi, K. P., Ajith, G., & Jacob, J. M. (2020, March). Effective utilization of drugs as green corrosion inhibitor—A review. In *AIP Conference Proceedings* (Vol. 2225, No. 1, p. 070006). AIP Publishing LLC.

Sharma, S., & Kumar, A. (2021). Recent advances in metallic corrosion inhibition: A review. *Journal of Molecular Liquids*, 322, 114862.

Sharma, S., Ganjoo, R., Kr. Saha, S., Kang, N., Thakur, A., Assad, H., ... & Kumar, A. (2021). Experimental and theoretical analysis of baclofen as a potential corrosion inhibitor for mild steel surface in HCl medium. *Journal of Adhesion Science and Technology*, 1-26.

Sharma, S., Ganjoo, R., Saha, S. K., Kang, N., Thakur, A., Assad, H., & Kumar, A. (2022). Investigation of inhibitive performance of Betahistine dihydrochloride on mild steel in 1 M HCl solution. *Journal of Molecular Liquids*, 347, 118383.

Shinato, K. W., Huang, F., & Jin, Y. (2020). Principle and application of atomic force microscopy (AFM) for nanoscale investigation of metal corrosion. *Corrosion Reviews*, 38(5), 423-432.

Shivakumar, S. S., & Mohana, K. N. (2012). Ziziphus mauritiana leaves extracts as corrosion inhibitor for mild steel in H₂SO₄ and HCl solutions. *European Journal of Chemistry*, 3, 426-432.

Shriver, D. F., Atkins, P. W., & Langford, C. H. Inorganic Chemistry, 1994. *Oxford University Press, Oxford*.

Shukla, S. K., & Quraishi, M. A. (2010). Cefalexin drug: A new and efficient corrosion inhibitor for mild steel in hydrochloric acid solution. *Materials Chemistry and Physics*, 120(1), 142-147.

Shukla, S. K., Singh, A. K., Ahamad, I., & Quraishi, M. A. (2009). Streptomycin: A commercially available drug as corrosion inhibitor for mild steel in hydrochloric acid solution. *Materials Letters*, 63(9-10), 819-822.

Singh, A. K., & Quraishi, M. A. (2011). Investigation of the effect of disulfiram on corrosion of mild steel in hydrochloric acid solution. *Corrosion Science*, 53(4), 1288-1297.

Singh, A. K., Chugh, B., Saha, S. K., Banerjee, P., Ebenso, E. E., Thakur, S., & Pani, B. (2019). Evaluation of anti-corrosion performance of an expired semi synthetic antibiotic cefdinir for mild steel in 1 M HCl medium: An experimental and theoretical study. *Results in Physics*, 14, 102383.

Singh, A., Ansari, K. R., Chauhan, D. S., Quraishi, M. A., Lgaz, H., & Chung, I. M. (2020). Comprehensive investigation of steel corrosion inhibition at macro/micro level by ecofriendly green corrosion inhibitor in 15% HCl medium. *Journal of colloid and interface science*, 560, 225-236.

Singh, A., Ansari, K. R., Quraishi, M. A., & Kaya, S. (2020). Theoretically and experimentally exploring the corrosion inhibition of N80 steel by pyrazol derivatives in simulated acidizing environment. *Journal of Molecular Structure*, 1206, 127685.

Singh, A., Ebenso, E. E., & Quraishi, M. A. (2012). Corrosion inhibition of carbon steel in HCl solution by some plant extracts. *International Journal of corrosion*, 2012.

Singh, A., Pramanik, T., Kumar, A., & Gupta, M. (2013). Phenobarbital: a new and effective corrosion inhibitor for mild steel in 1 M HCl solution. *Asian Journal of Chemistry*, 25(17), 9808.

Singh, A., Soni, N., Deyuan, Y., & Kumar, A. (2019). A combined electrochemical and theoretical analysis of environmentally benign polymer for corrosion protection of N80 steel in sweet corrosive environment. *Results in Physics*, 13, 102116.

Singh, P., Chauhan, D. S., Chauhan, S. S., Singh, G., & Quraishi, M. A. (2019). Chemically modified expired Dapsone drug as environmentally benign corrosion

inhibitor for mild steel in sulphuric acid useful for industrial pickling process. *Journal of Molecular liquids*, 286, 110903.

Singh, P., Chauhan, D. S., Srivastava, K., Srivastava, V., & Quraishi, M. A. (2017). Expired atorvastatin drug as corrosion inhibitor for mild steel in hydrochloric acid solution. *International Journal of Industrial Chemistry*, 8(4), 363-372.

Sliem, M. H., Afifi, M., Bahgat Radwan, A., Fayyad, E. M., Shibl, M. F., Heikal, F. E. T., & Abdullah, A. M. (2019). AEO7 surfactant as an eco-friendly corrosion inhibitor for carbon steel in HCl solution. *Scientific reports*, 9(1), 1-16.

Soltaninejad, F., & Shahidi, M. (2018). Investigating the effect of penicillin G as environment-friendly corrosion inhibitor for mild steel in H₃PO₄ solution. *Progress in Color, Colorants and Coatings*, 11(3), 137-147.

Sovizi, M. R., & Abbasi, R. (2020). Effect of carboxymethyl cellulose on the corrosion behavior of aluminum in H₂SO₄ solution and synergistic effect of potassium iodide. *Journal of Adhesion Science and Technology*, 34(15), 1664-1678.

Srivastava, M., Tiwari, P., Srivastava, S. K., Prakash, R., & Ji, G. (2017). Electrochemical investigation of Irbesartan drug molecules as an inhibitor of mild steel corrosion in 1 M HCl and 0.5 M H₂SO₄ solutions. *Journal of Molecular Liquids*, 236, 184-197.

Stansbury, E. E., & Buchanan, R. A. (2000). *Fundamentals of electrochemical corrosion*. ASM international.

Stokes, D. (2008). *Principles and practice of variable pressure/environmental scanning electron microscopy (VP-ESEM)*. John Wiley & Sons.

Struck, S., Schmidt, U., Gruening, B., Jaeger, I. S., Hossbach, J., & Preissner, R. (2008). Toxicity versus potency: elucidation of toxicity properties discriminating between toxins, drugs, and natural compounds. In *Genome Informatics 2008: Genome Informatics Series Vol. 20* (pp. 231-242).

Sundaram, R. G., Vengatesh, G., & Sundaravadivelu, M. (2016). Effect of pharmaceutically active compound nitroxoline on the corrosion of mild steel in an acidic environment. *Adv. Chem*, 1, 1-9.

Sundaram, R. G., Vengatesh, G., & Sundaravadivelu, M. (2021). Surface morphological and quantum chemical studies of some expired drug molecules as potential corrosion inhibitors for mild steel in chloride medium. *Surfaces and Interfaces*, 22, 100841.

Tait, W. S. (2018). Electrochemical corrosion basics. In *Handbook of Environmental Degradation of Materials* (pp. 97-115). William Andrew Publishing.

Tan, J., Guo, L., Wu, D., Duan, X., Leng, S., Obot, I. B., & Kaya, S. (2020). Electrochemical and Computational Investigations on the Corrosion Inhibition of X65 Steel by 2-Phenylbenzimidazole in H₂SO₄ Solution. *Int. J. Electrochem. Sci*, 15, 8837-8848.

Tan, J., Guo, L., Wu, D., Yu, R., Zhang, F., & Kaya, S. (2020). Electrochemical and computational studies on the corrosion inhibition of mild steel by 1-hexadecyl-3-methylimidazolium bromide in HCl medium. *Int. J. Electrochem. Sci*, 15, 1893-1903.

Tan, J., Guo, L., Yang, H., Zhang, F., & El Bakri, Y. (2020). Synergistic effect of potassium iodide and sodium dodecyl sulfonate on the corrosion inhibition of carbon steel in HCl medium: a combined experimental and theoretical investigation. *RSC Advances*, 10(26), 15163-15170.

Tasic, Z. Z., Mihajlović, M. B. P., Radovanovic, M. B., Simonović, A. T., & Antonijević, M. M. (2021). Experimental and theoretical studies of paracetamol as a copper corrosion inhibitor. *Journal of Molecular Liquids*, 327, 114817.

Tebbjji, K., Oudda, H., Hammouti, B., Benkaddour, M., El Kodadi, M. and Ramdani, A. (2005). "Inhibition effect of two organic compounds pyridine–pyrazole type in

acidic corrosion of steel", *Colloids and Surfaces A: Physicochemical and Engineering Aspects* 259, 143.

Telegdi, J., Shaban, A., & Vastag, G. (2018). Biocorrosion–Steel.

Timbola, A. K., Souza, C. D., Soldi, C., Pizzolatti, M. G., & Spinelli, A. (2007). Electro-oxidation of rutin in the presence of p-toluenesulfonic acid. *Journal of Applied Electrochemistry*, 37, 617-624.

Trache, A., Xie, L., Huang, H., Glinsky, V. V., & Meiningner, G. A. (2018). Applications of atomic force microscopy for adhesion force measurements in mechanotransduction. In *Nanoscale Imaging* (pp. 515-528). Humana Press, New York, NY.

Tran, T., Brown, B., Nestic, S., & Tribollet, B. (2014). Investigation of the electrochemical mechanisms for acetic acid corrosion of mild steel. *Corrosion*, 70(3), 223-229.

Umoren, S. A., Eduok, U. M., & Oguzie, E. E. (2008). Corrosion inhibition of mild steel in 1 M H₂SO₄ by polyvinyl pyrrolidone and synergistic iodide additives. *Portugaliae Electrochimica Acta*, 26(6), 533-546.

Umoren, S. A., Ogbobe, O., Okafor, P. C., & Ebenso, E. E. (2007). Polyethylene glycol and polyvinyl alcohol as corrosion inhibitors for aluminium in acidic medium. *Journal of Applied Polymer Science*, 105(6), 3363-3370.

Usman, A. D., & Okoro, L. N. (2015). A Review: Weight loss studies on the corrosion behavior of some metals in various media. *Chem Sci Rev Lett*, 4(13), 17-24.

Vahabi, S., Salman, B. N., & Javanmard, A. (2013). Atomic force microscopy application in biological research: a review study. *Iranian journal of medical sciences*, 38(2), 76

Valek, L., & Martinez, S. (2007). Copper corrosion inhibition by *Azadirachta indica*

leaves extract in 0.5M sulphuric acid. *Materials Letters*, 61, 148-151.

Vengatesh, G., & Sundaravadivelu, M. (2019). Non-toxic bisacodyl as an effective corrosion inhibitor for mild steel in 1 M HCl: thermodynamic, electrochemical, SEM, EDX, AFM, FT-IR, DFT and molecular dynamics simulation studies. *Journal of Molecular Liquids*, 287, 110906.

Vengatesh, G., Karthik, G., & Sundaravadivelu, M. (2017). A comprehensive study of ondansetron hydrochloride drug as a green corrosion inhibitor for mild steel in 1 M HCl medium. *Egyptian journal of petroleum*, 26(3), 705-719.

Verma, C., Olasunkanmi, L. O., Ebenso, E. E., & Quraishi, M. A. (2018). Adsorption characteristics of green 5-arylaminomethylene pyrimidine-2, 4, 6-triones on mild steel surface in acidic medium: Experimental and computational approach. *Results in physics*, 8, 657-670.

Verma, C., Quraishi, M. A., Ebenso, E. E., & Bahadur, I. (2018). A green and sustainable approach for mild steel acidic corrosion inhibition using leaves extract: experimental and DFT studies. *Journal of Bio-and Tribo-Corrosion*, 4(3), 1-12.

Vinutha, M. R., Venkatesha, T. V., & Nagaraja, C. (2018). Anticorrosive ability of electrochemically synthesized 2, 2'-disulfanediyldianiline for mild steel corrosion: electrochemical and thermodynamic studies. *International Journal of Industrial Chemistry*, 9(2), 185-197.

Volkova-Gugeshashvili, M. I., Volkov, A. G., & Markin, V. S. (2006). Adsorption at liquid interfaces: The generalized Frumkin isotherm and interfacial structure. *Russian Journal of Electrochemistry*, 42(10), 1073-1078.

Walsh, F., Ottewill, G., & Barker, D. (1993). Corrosion and protection of metals: II. Types of corrosion and protection methods. *Transactions of the IMF*, 71(3), 117-120.

Xu, B., Yang, W., Liu, Y., Yin, X., Gong, W., & Chen, Y. (2014). Experimental and theoretical evaluation of two pyridinecarboxaldehyde thiosemicarbazone compounds as corrosion inhibitors for mild steel in hydrochloric acid solution. *Corrosion Science*, 78, 260-268.

Xu, X., Singh, A., Sun, Z., Ansari, K. R., & Lin, Y. (2017). Theoretical, thermodynamic and electrochemical analysis of biotin drug as an impending corrosion inhibitor for mild steel in 15% hydrochloric acid. *Royal Society open science*, 4(12), 170933.

Yadav, D. K., & Quraishi, M. A. (2012). Electrochemical investigation of substituted pyranopyrazoles adsorption on mild steel in acid solution. *Industrial & engineering chemistry research*, 51(24), 8194-8210.

Yadav, D. K., Chauhan, D. S., Ahamad, I., & Quraishi, M. A. (2013). Electrochemical behavior of steel/acid interface: adsorption and inhibition effect of oligomeric aniline. *RSC advances*, 3(2), 632-646.

Yadav, M., Behera, D., & Sharma, U. (2016). Nontoxic corrosion inhibitors for N80 steel in hydrochloric acid. *Arabian Journal of Chemistry*, 9, S1487-S1495.

Yasakau, K. (2020). Application of AFM-Based Techniques in Studies of Corrosion and Corrosion Inhibition of Metallic Alloys. *Corrosion and Materials Degradation*, 1(3), 345-372.

Yurt, A., Balaban, A., Kandemir, S. U., Bereket, G., & Erk, B. (2004). Investigation on some Schiff bases as HCl corrosion inhibitors for carbon steel. *Materials Chemistry and Physics*, 85(2-3), 420-426.

Zaferani, S. H., Sharifi, M., Zaarei, D., & Shishesaz, M. R. (2013). Application of eco-friendly products as corrosion inhibitors for metals in acid pickling processes—A review. *Journal of Environmental Chemical Engineering*, 1(4), 652-657.

Zarras, P., & Stenger-Smith, J. D. (2015). Smart Inorganic and Organic Pretreatment Coatings for the Inhibition of Corrosion on Metals/Alloys. In *Intelligent Coatings for Corrosion Control* (pp. 59-91). Butterworth-Heinemann.

Zarrok, H., Oudda, H., Tourir, R., El M'Rabet, M., Warad, I., Guenbour, A., & Lakhrissi, B. (2017). Experimental and theoretical studies of 5-((4-phenyl-4, 5-dihydro-1H-tetrazol-1-yl) methyl) quinolin-8-ol quinoline derivative as effective corrosion inhibitor for mild steel in 1.0 M HCl.

Zhang, F., Tang, Y., Cao, Z., Jing, W., Wu, Z., & Chen, Y. (2012). Performance and theoretical study on corrosion inhibition of 2-(4-pyridyl)-benzimidazole for mild steel in hydrochloric acid. *Corrosion Science*, *61*, 1-9.

Zhang, Q. H., Hou, B. S., Li, Y. Y., Zhu, G. Y., Liu, H. F., & Zhang, G. A. (2020). Two novel chitosan derivatives as high efficient eco-friendly inhibitors for the corrosion of mild steel in acidic solution. *Corrosion Science*, *164*, 108346.

Zhang, Y., Zhang, S., Tan, B., Guo, L., & Li, H. (2021). Solvothermal synthesis of functionalized carbon dots from amino acid as an eco-friendly corrosion inhibitor for copper in sulfuric acid solution. *Journal of Colloid and Interface Science*, *604*, 1-14.

Zheng, X., Gong, M., Li, Q., & Guo, L. (2018). Corrosion inhibition of mild steel in sulfuric acid solution by loquat (*Eriobotrya japonica* Lindl.) leaves extract. *Scientific reports*, *8*(1), 1-15.

Zhu, Y., Free, M. L., Woollam, R., & Durnie, W. (2017). A review of surfactants as corrosion inhibitors and associated modeling. *Progress in Materials Science*, *90*, 159-223.

List of Publications


1. **Sharma, Shveta**, and Ashish Kumar. "Recent advances in metallic corrosion inhibition: A review." *Journal of Molecular Liquids* 322 (2021): 114862.
2. **Sharma, Shveta**, et al. "Experimental and theoretical analysis of baclofen as a potential corrosion inhibitor for mild steel surface in HCl medium." *Journal of Adhesion Science and Technology* (2021): 1-26.
3. **Sharma, Shveta**, et al. "Investigation of inhibitive performance of Betahistine dihydrochloride on mild steel in 1 M HCl solution." *Journal of Molecular Liquids* 347 (2022): 118383.
4. **Sharma, Shveta**, et al. "Electrochemical characterization and surface morphology techniques for corrosion inhibition—a review." *Chemical Engineering Communications* (2022): 1-36.
5. **Sharma, Shveta**, et al. "Multidimensional Analysis for Corrosion Inhibition by Isoxsuprine on Mild Steel in Acidic Environment: Experimental and Computational Approach." *Journal of Molecular Liquids* (2022): 119129.
6. **Sharma, Shveta**, et al. "Investigation of corrosion performance of expired Irnocam on the mild steel in acidic medium." *Materials Today: Proceedings* (2022).
7. **Sharma, Shveta**, et al. "Evaluation of Drugs as Corrosion Inhibitors for Metals: A Brief Review." *International Conference on Chemical, Bio and Environmental Engineering*. Springer, Cham, 2022.
8. Thakur, A., Kaya, S., Abousalem, A. S., **Sharma, S.**, Ganjoo, R., Assad, H., & Kumar, A. (2022). Computational and experimental studies on the corrosion inhibition performance of an aerial extract of Cnicus Benedictus weed on the acidic corrosion of mild steel. *Process Safety and Environmental Protection*, 161, 801-818.
9. Ganjoo, R., **Sharma, S.**, Thakur, A., Assad, H., Sharma, P. K., Dagdag, O., ... & Kumar, A. (2022). Experimental and Theoretical study of Sodium Cocoyl Glycinate as corrosion inhibitor for mild steel in hydrochloric acid medium. *Journal of Molecular Liquids*, 119988.

10. Thakur, A., Kumar, A., **Sharma, S.**, Ganjoo, R., & Assad, H. (2022). Computational and experimental studies on the efficiency of *Sonchus arvensis* as green corrosion inhibitor for mild steel in 0.5 M HCl solution. *Materials Today: Proceedings*.
11. Ganjoo, R., **Sharma, S.**, Thakur, A., & Kumar, A. (2022). Thermodynamic study of corrosion inhibition of Dioctylsulfosuccinate Sodium Salt as corrosion inhibitor against mild steel in 1 M HCl. *Materials Today: Proceedings*.
12. Thakur, A., **Sharma, S.**, Ganjoo, R., Assad, H., & Kumar, A. (2022, May). Anti-Corrosive Potential of the Sustainable Corrosion Inhibitors Based on Biomass Waste: A Review on Preceding and Perspective Research. In *Journal of Physics: Conference Series* (Vol. 2267, No. 1, p. 012079). IOP Publishing.
13. Ganjoo, R., Bharmal, A., **Sharma, S.**, Thakur, A., Assad, H., & Kumar, A. (2022, May). Imidazolium based ionic liquids as green corrosion inhibitors against corrosion of mild steel in acidic media. In *Journal of Physics: Conference Series* (Vol. 2267, No. 1, p. 012023). IOP Publishing.
14. Assad, H., Ganjoo, R., & **Sharma, S.** (2022, May). A theoretical insight to understand the structures and dynamics of thiazole derivatives. In *Journal of Physics: Conference Series* (Vol. 2267, No. 1, p. 012063). IOP Publishing.



Review

Recent advances in metallic corrosion inhibition: A review

Shveta Sharma, Ashish Kumar  

[Show more](#) 

[+](#) Add to Mendeley [🔗](#) Share [📄](#) Cite

<https://doi.org/10.1016/j.molliq.2020.114862>

[Get rights and content](#)

Recent Advances in Metallic Corrosion Inhibition: A Review

Shveta Sharma, Ashish Kumar*

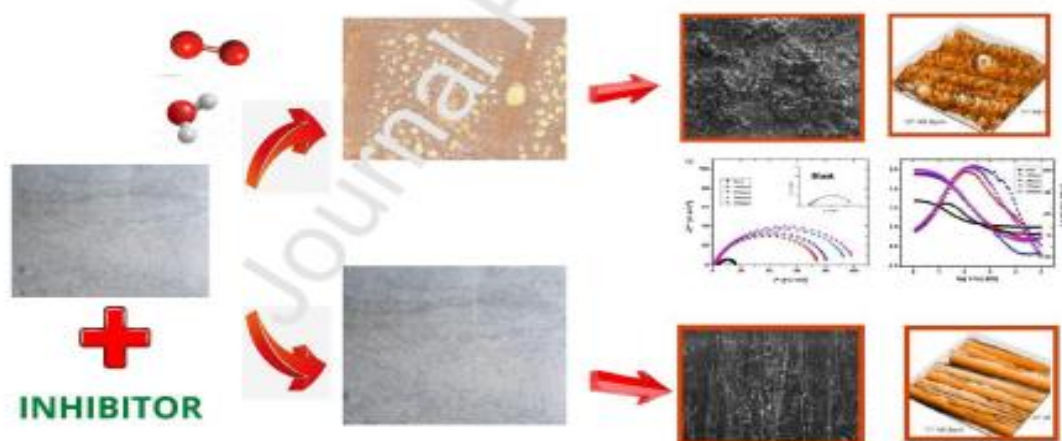
Department of Chemistry, School of Physical Sciences, Lovely Professional University, Punjab, India

*e-mail: drashishchemlpu@gmail.com

Abstract

This analysis includes studies targeting different compounds as inhibitors to corrosion for different metals in different solutions. The article tries to include various types of organic compounds like Drug molecules, Plant extracts and oils, surfactants, ionic liquids which had already been there in the literature. A brief about research methodology along with a literature review is also mentioned so the information will be beneficial to readers. The Experimental section includes the most frequently used techniques like weight loss, Electrochemical Impedance Study, Thermodynamic parameters, Adsorption isotherms. It was very much clear from the literature that due to the presence of heteroatoms and π electron cloud in conjugation, the inhibition efficiency of organic compounds came out to be exceptionally good.

Graphical Abstract



Keywords: Corrosion, Corrosion Inhibitors, Electrochemical Study, Adsorption Isotherm.



Experimental and theoretical analysis of baclofen as a potential corrosion inhibitor for mild steel surface in HCl medium

Shveta Sharma^a, Richika Ganjoo^a, Sourav Kr. Saha^b , Namhyun Kang^b ,
Abhinay Thakur^a, Humira Assad^a, Vivek Sharma^c and Ashish Kumar^a 

^aDepartment of Chemistry, School of Chemical Engineering and Physical Sciences, Lovely Professional University, Punjab, India; ^bDepartment of Materials Science and Engineering, Pusan National University, Busan 46241, Republic of Korea; ^cAnalytical Development and Characterization Laboratory, PI Industries Ltd, Udaipur, India

ABSTRACT

The effect of Baclofen on the retardation of mild steel corrosion was examined by employing the weight loss, electrochemical techniques and theoretical calculations. Investigations depicted the increased inhibition efficiency with the increased amount of Baclofen as a corrosion inhibitor and maximum inhibition efficiency was obtained ~97% at the concentration of 2000 ppm of Baclofen. Potentiodynamic polarization study showed that Baclofen as an inhibitor controlled both the anodic and cathodic reactions but with cathodic predominance. Electrochemical analysis showed a clear decrease in the values of double layer capacitance. Adsorption of Baclofen on the surface of mild steel followed Langmuir adsorption isotherm. Experimental results were validated with the help of quantum chemical, molecular dynamic simulation, and surface morphological study.

ARTICLE HISTORY



Received 23 September 2021
Revised 18 October 2021
Accepted 26 October 2021

KEYWORDS

Baclofen; mild steel;
corrosion inhibition; HCl;
electrochemical techniques;
surface morphology

1. Introduction

In different sectors, there is extensive use of mild steel, for example in the oil and gas industry, downhole or tubing, flow lines, and transmission or distribution pipes. Scaling, oxidized film formation, and rusting are common concerns with mild steel. Utilizing corrosion inhibitors to resolve the problem of corrosion is a low-cost and efficient alternative in comparison to the uses of expensive hazardous protective measures [1–3]. Various kinds of organic molecules are now being employed as corrosion inhibitors. Literature reveals that organic inhibitors having hetero atoms, conjugated pi bonds, and aromatic rings behave as excellent corrosion inhibitors. Although, most of the organic molecules have a negative impact on the environment [4–9] whereas, pharmaceutical drugs are the substances that also comes under the general classification of organic compounds [10] and nowadays research is orienting towards the application of pharmaceutical

CONTACT Ashish Kumar  drashishchemlpu@gmail.com  Department of Chemistry, School of Physical Sciences, Lovely Professional University, Punjab, India

© 2021 Informa UK Limited, trading as Taylor & Francis Group



ELSEVIER

Contents lists available at ScienceDirect

Journal of Molecular Liquids

journal homepage: www.elsevier.com/locate/molliq



Investigation of inhibitive performance of Betahistine dihydrochloride on mild steel in 1 M HCl solution



Shveta Sharma^a, Richika Ganjoo^a, Sourav Kr. Saha^b, Namhyun Kang^b, Abhinay Thakur^a, Humira Assad^a, Ashish Kumar^{a,*}

^a Department of Chemistry, Lovely Professional University, Punjab, India

^b Department of Materials Science and Engineering, Pusan National University, Busan 46241, Republic of Korea

ARTICLE INFO

Article history:

Received 30 October 2021

Revised 15 December 2021

Accepted 19 December 2021

Available online 22 December 2021

Keywords:

Betahistine dihydrochloride

HCl

Corrosion Inhibition

SEM

MD Simulations

ABSTRACT

This study evaluated the corrosion retardation of mild steel with the use of Betahistine dihydrochloride drug as a sustainable inhibitor in HCl solution and various techniques like weight loss measurements, electrochemical analysis was used to understand the inhibition process. The thermodynamic and adsorption parameters were calculated and discussed on the inhibition behaviour. The corrosion inhibition (% IE) gave a sharp rise with the increased concentration of the Betahistine dihydrochloride drug and reduced efficiency was observed with increased temperature and increased immersion time. Approximately 96% corrosion inhibition efficiency was attained with optimized conditions of 1500 ppm of Betahistine dihydrochloride, 2 h, 1 M HCl at 298 K temperature. Inhibitor adsorption to mild steel abided by the Langmuir adsorption isotherm. Electrochemical impedance spectroscopy revealed the reduction in the value of constant phase element, dip in the values of double-layer capacitance and increase in the charge transfer resistance with increased concentration of Betahistine dihydrochloride drug. Furthermore, potentiodynamic polarization experiments substantiated the mixed type of behaviour. The techniques like scanning electron microscopy, atomic force microscopy, along with ultraviolet-visible spectroscopy, fourier transform infrared spectroscopy, were employed for surface morphology and theoretical models like quantum chemical and molecular dynamics simulations authenticated the experimental observation.

© 2021 Elsevier B.V. All rights reserved.

Electrochemical characterization and surface morphology techniques for corrosion inhibition—a review

Shveta Sharma, Richika Ganjoo, Abhinay Thakur, and Ashish Kumar

Department of Chemistry, School of Chemical Engineering and Physical Sciences, Lovely Professional University, Phagwara, Punjab, India

ABSTRACT

This review article outlines the set of observations and findings from some previous publications that addressed the different techniques used for understanding and evaluating metallic corrosion and its retardation by using different inhibitors. The main emphasis is on the different electrochemical characterization techniques and surface analysis methods used for studying corrosion inhibition. A brief about polarization, electrochemical noise, electrochemical frequency modulation, impedance study for electrochemical characterization techniques and contact angle, scanning electrochemical microscopy, atomic force microscopy, and scanning electron microscopy methods, x-ray photoelectron spectroscopy, etc. are included for a better understanding of corrosion inhibition phenomenon. The literature suggests that corrosion of metals and alloys is effectively controlled by the use of inhibitors having heteroatoms such as nitrogen, oxygen, or sulfur. In this article, the papers from the last sixteen years i.e., from 1996 to 2021 are considered to get an insight into current methods for retarding corrosion. General introduction, mechanisms of corrosion along with factors affecting corrosion has also been described in the present article. Data collected in this review will be advantageous for researchers to get an idea about the basics and the recent techniques used in corrosion study.

KEYWORDS

AFM; corrosion; electrochemical measurements; organic corrosion inhibitors; SEM; surface characterization techniques

Introduction

In our periodic table, we have about 80 metals that react with other metals to form a large number of alloys. These metals or alloys have different and specific functions, which depend upon their properties. But many times, because of deterioration by corrosion they fail to work appropriately (Verma et al. 2018a). The corrosion of metals is a major problem that adversely affects many fields. Long-term exposure to environmental actions (chemical, biological and physical environment), induces metal degradation and this malfunctioning on large scale compels the researchers to work in this field (Nwosu and Muzakir 2016). On exposure to the external environment, the rate of metal disintegration increases, and this deterioration is termed as corrosion. Corrosion may also be called as reverse process of the metallurgical extraction (Ahmad

2006; Palanisamy 2019). Corrosion is a spontaneous and thermodynamically stable process that involves anodic and cathodic reactions, at anode metal ions go into the test solution, and at the cathode, electrons come from the specimen therefore at cathode electron acceptor should be present (Raja and Sethuraman 2008; Devi et al. 2017). This inevitable loss related to corrosion can be either direct or indirect. Direct here means replacing the deteriorated machinery, protection cost. Indirect loss refers to wastage of energy, retardation in productivity, most dangerous is the unexpected cessation of plants. Even there can be a threat to human safety also. Figure 1 is illustrating some of the aftereffects of corrosion (Revie 2008; Khanari and Finsgar 2019). The effects of corrosion are so slow that they appear to be insignificant and unimportant, but in reality, they are as dangerous as natural disasters like earthquake, flood, etc. (Kesavan et al. 2012).



Multidimensional analysis for corrosion inhibition by Isoxsuprine on mild steel in acidic environment: Experimental and computational approach

Shveta Sharma ^a, Sourav Kr. Saha ^b, Namhyun Kang ^b, Richika Ganjoo ^a, Abhinay Thakur ^a, Humira Assad ^a, Ashish Kumar ^{a, c, *} 

Abstract

This study investigates the impact of Isoxsuprine hydrochloride drug on mild steel corrosion in a 1.0 M HCl solution by employing weight loss, electrochemical methods, surface morphological techniques, and finally validated with theoretical studies like quantum calculation and MD simulation. Inhibitory efficacy of Isoxsuprine hydrochloride came out to be ~ 97 % at 2000 ppm concentration. The analysis demonstrated the increase in the inhibition efficiency with the rising concentration of inhibitor and decreasing effectiveness with increased temperature. Thermodynamic parameters were also investigated by utilizing the data obtained from temperature. Potentiodynamic polarization validated that the Isoxsuprine hydrochloride retarded the cathodic as well as anodic reactions. During the adsorption process, the Isoxsuprine hydrochloride molecules followed the Langmuir adsorption isotherm. Theoretical calculations like quantum chemical calculation and molecular dynamics simulation also confirms excellent adsorption of Isoxsuprine hydrochloride on the metallic sample. The results from all of the different methods were consistent.



Evaluation of Drugs as Corrosion Inhibitors for Metals: A Brief Review

Shveta Sharma , Richika Ganjoo, Suresh Kumar & Ashish Kumar

Conference paper | [First Online: 12 May 2022](#)

Part of the [Environmental Science and Engineering](#) book series (ESE)

Abstract

The use of chemical inhibitors is crucial to keep corrosion in check. Various inorganic and organic compounds are used as inhibitors, although their usage is being phased out in favor of newer and less toxic inhibitor types that produce desired results. For this purpose, the drugs are considered an excellent alternative to the toxic inhibitors, as the drug molecules contain heteroatoms oxygen, nitrogen, and sulfur, and they are less hazardous to the environment. Drugs are successfully inhibiting the corrosion of various metals like Steel, Zn, Cu, Al, etc. and generally, their corrosion inhibition efficiency is verified by employing the Weight Loss Technique, Electrochemical Analysis, and surface morphology are investigated by Scanning Electron Microscopy, Atomic Force Microscopy, etc. In this review article majority of the literature's past studies on the usage of drugs as corrosion inhibitors for different metals like Steel, Zn, Cu, Al, etc. and generally, their corrosion inhibition efficiency is verified by employing the Weight Loss Technique, Electrochemical Analysis, and surface morphology are investigated by Scanning Electron Microscopy, Atomic Force Microscopy, etc. In this review article majority of the literature's past studies on the usage of drugs as corrosion inhibitors for different metals are summarized along with the main techniques used for corrosion inhibition study.

Keywords

Corrosion

Corrosion inhibitor

Drugs

Chapter

EUR 24.95

Price excludes VAT (India)

- DOI: 10.1007/978-3-030-96554-9_71
- Chapter length: 12 pages
- Instant PDF download
- Readable on all devices
- Own it forever
- Exclusive offer for individuals only
- Tax calculation will be finalised during checkout

[Buy Chapter](#)

Investigation of corrosion performance of expired Irnocam on the mild steel in acidic medium

Shveta Sharma ^a, Richika Ganjoo ^a, Abhinay Thakur ^a, Ashish Kumar ^{a, b}  

Show more 

+ Add to Mendeley  Share  Cite

<https://doi.org/10.1016/j.matpr.2022.05.595>

[Get rights and content](#)

Abstract

Drug molecule expired Irnocam was studied for its corrosion reducing tendency for mild steel in 1 M hydrochloric acid. Weight loss, electrochemical analysis, and scanning electron microscopy were used to investigate the alterations in the metallic samples, which revealed the successful mitigation of corrosion and maximum inhibition efficiency was 80% at 600 ppm of Expired Irnocam at 298 K. Corrosion mitigation efficiency of expired Irnocam increased with increasing concentration of inhibitor and the inhibitor Irnocam slows down cathodic as well as anodic processes. Scanning electron microscopy proved corrosion inhibition because of protection given by inhibiting molecule in the form of thin layer on the exterior of metallic surface.

Keywords

Corrosion Inhibitor; Irnocam; Weight Loss; Electrochemical Analysis; Scanning Electron Microscopy

Manuscripts under consideration

1. Study of inhibitive property of Pipotiazine drug for mild steel in acidic medium.

Conferences Attended

1. Presented Paper “**Experimental and Theoretical Investigation of Corrosion Inhibition of Stainless Steel by Pipotiazine Drug in Sulfuric Acid Solution**” in International Conference (Virtual) on Recent Advancements in Chemical Sciences - 2021 [ICRACS-2021] on July 14-16, 2021.
2. Presented a paper “**Evaluation of Drugs as corrosion inhibitors for Metals: A Brief Review**” in 2nd international conference on chemical, bio and environmental engineering (CHEMBIOEN-2021) on 20-22nd August 2021, NIT Jalandhar.
3. Presented Paper “**Investigation of Corrosion Performance of Expired Irnocam on the Mild Steel in Acidic Medium**” in International conference advance in materials processing (ICAMP-22) on 8th-9th January 2022, NIT Raipur.
4. Presented Paper “**Techniques Employed to Identify the Drugs as Corrosion Inhibitor: A review**” in International conference in advanced materials for energy and environment (AMEE-2022) on 10-11th January 2022. Mother Teresa Women’s University, Kodaikanal, India.
5. Presented Paper “**Study of inhibitive property of Pipotiazine drug for mild steel in acidic medium**” in an International conference, on 19th -20th February, LPU , Punjab.

Workshops

1. National workshop on Electrochemical Techniques: Theory and Practice. Organized by centre of chemical analysis and Testing, LPU on 14th -15th February,2020.
2. Advanced certificate course on Plagiarism on 11th to 13th June 2021.
3. Workshop on computational chemistry using Gaussian software organized by Centre for Advanced Computational Chemistry Studies (ACC), Delhi, India from 3rd -8th January 2022.
4. Participated in six days Faculty Development Programme on “E-Content Development and Delivery, Research Methodology and Autonomy” organised by Kamla Nehru Mahavidyalaya, Nagpur on dated 27th July to 1st Aug.2020.
5. Participated in six days Faculty Development Programme on G Chem Paint organised by G.C. Una in association with spoken Tutorial Bombay from 15th may to 20th may 2020.